DOE/RA/10157-1

Design, Construction and Testing of a DC Bioeffects Test Enclosure for Small Animals

Final Report

November 1980

Prepared for:
U.S. Department of Energy
Assistant Secretary for Resource Applications
Power Delivery Division
Under Contract No. FG01-78ET 10157-1

DISCLAIMER

Available from:

National Technical Information Service (NTIS)
U.S. Department of Commerce
5285 Port Royal Road
Springfield, Virginia 22161

Price: Printed Copy: $16.00
Microfiche: $4.00

DOE/RA/10157-1
Dist. Category UC-97a

Design, Construction and Testing of a DC Bioeffects Test Enclosure for Small Animals

Final Report

November 1980

Prepared by:
M. J. Frazier
M. M. Preache
IIT Research Institute
Chicago, IL 60616
Under Contract No. FG-78ET 10157-1

Prepared for:
U.S. Department of Energy
Assistant Secretary for Resource Applications
Power Delivery Division
Washington, D.C. 20585

FOREWORD

This Final Report has been prepared under Department of Energy Contract ET-78-C-01-3026, "Design, Construction, and Testing of a DC Bioeffects Test Enclosure for Small Animals." The report covers the period September 26, 1978 through June, 1980.

The Department of Energy, Division of Electrical Energy Systems Program Manager was Mr. Alec O. Bulawka. Quarterly reviews of the program progress were provided by Dr. William Wisecup of Aerospace Corporation.

The authors wish to express their appreciation for the efforts of many associates at IITRI in their contribution to this program. In connection with the engineering development, credit is given to Dr. Raymond Zalewski for his contribution to the basic simulator design and to Mr. Neil Robertson for analytical and testing contributions. Recognition is given to Mr. William Lancaster for the fabrication of all design and prototype model simulators as well as extensive testing of these units.

A number of IITRI's Life Sciences Research staff assisted in the development of the biological experimental design and we wish to acknowledge their assistance. They are Ms. Catherine Aranyi, Dr. John Burns, Dr. Ruth Fugmann, Dr. Barry Levine, Dr. Rajendra Mehta, and Dr. Leonard Schiff.

Assistance in preparation of the discussion concerning the measurement of 5-hydroxytryptamine was provided by Dr. Krishnaswamy S. Rajan of IITRI's Chemistry Research Division and the contribution concerning electrocortical recordings was by Dr. Ernest Kent, Department of Psychology, University of Illinois, Chicago, Illinois.

Respectfully submitted,

IIT RESEARCH INSTITUTE

M. J. Frazier
Senior Engineer

APPROVED:

J. J. Krstansky
Manager
Electromagnetic Effects

M. M. Preache
Head, Toxicology and Pharmacology

ABSTRACT

This Final Report describes both the engineering development of a DC bioeffects test enclosure for small laboratory animals, and the biological protocol for the use of such enclosures in the testing of animals to determine possible biological effects of the environment associated with HVDC transmission lines.

The test enclosure which has been designed is a modular unit, which will house up to eight rat-sized animals in individual compartments. Multiple test enclosures can be used to test larger numbers of animals. A prototype test enclosure has been fabricated and tested to characterize its electrical performance characteristics.

The test enclosure provides a simulation of the dominant environment associated with HVDC transmission lines; namely, a static electric field and an ion current density. The test enclosure provides quite uniform ion current density and electric field levels at all locations within each animal housing space. Either positive or negative fields and ion currents can be produced. Both the electric field and ion current density levels can be adjusted over ranges likely to be of interest for biological testing. The design provides for the use of a filtered air flow through the simulator in order to minimize particulates and animal waste effluents. Feeding and watering provisions are at ground potential to minimize animal shocks. The materials used for animal caging walls were chosen to minimize current drawn by an animal contacting the wall, and to minimize problems with ion charge trapping by the walls. Ozone levels within the animal caging area have been shown to be insiginificant.

A biological experimental design has been developed for assessing the effects of the dominant components of the HVDC transmission line environment. The design which was planned for a research effort of approximately 18 months includes the following major features:

- Rats and mice as test subjects
- Concurrent manipulation of the magnitude of positive and negative dc electric fields and ion current densities as test conditions.

- Sham-exposed and unexposed control groups
- Intensity - response determinations
- Control of nonexperimental environmental conditions
- Screening of a diverse set of biological parameters or response systems

TABLE OF CONTENTS

TABLE OF CONTENTS (Cont.)

TABLE OF CONTENTS (Cont.)

TABLE OF CONTENTS (Cont.)

LIST OF TABLES

LIST OF FIGURES

1. INTRODUCTION

1.1 Background and Objectives

The use of high voltage direct current (HVDC) transmission "is being considered more and more as a viable adjunct to AC for electric power transmission". (Hingorani, 1978).

The projected growth of HVDC facilities over the next few years, both worldwide and in the United States, is expected to almost double the HVDC power transmission which existed in the mid-seventies.

The growing awareness and concern of the public for their environment has extended to the unique environments associated with high voltage power transmission. The investigation into possible biological effects due to the 60 Hz electric fields associated with HVAC transmission lines is being extensively investigated in numerous studies sponsored by both the Department of Energy and the Electric Power Research Institute. However, the 60 Hz investigations are not directly applicable to the HVDC line situation.

With the growing use of HVDC transmission and the increasing environmental concerns, it can be anticipated that the same type of biological interaction questions will be posed to the potential users of this form of power transmission, as are now being asked in connection with the construction of AC EHV lines. However, compared with HVAC transmission lines, the state of the art in environmental effects of HVDC is primitive.

Several critical reviews of past investigations into the biological effects of electromagnetic environments (Bridges, 1975; National Academy of Sciences, 1977; and Sheppard and Eisenbud, 1977) have shown that extreme care must be exercised in the planning, conduct and interpretation results of electromagnetic biological interaction studies. The scientific community has become aware that such studies must begin with a carefully planned experimental design, requiring the close cooperation of both engineers and biologists. To circumvent the difficulties identified in some past studies, DOE and EPRI have taken steps to insure the quality of research results by requiring the development of a carefully formulated experimental design prior to the conduct of major experiments.

In anticipation of the need for information on both the nature of the HVDC environment and the possible biological effects for such an environment the DOE is sponsoring several complementary research programs. This final report documents the activities and results of one of these programs.

One of the objectives of this Phase I program was the development of the experimental design for the conduct of biological tests on small laboratory animals of the environment associated with HVDC transmission lines. The conduct of biological experiments to determine the effects of the electromagnetic environment of concern requires the availability of a suitable means for producing the desired environment in the laboratory, in an enclosure which is adequate for the housing of animals. Since no previous laboratory biological studies of animals in the HVDC environment had been conducted in this country, the design of such an HVDC test enclosure did not exist at the outset of this program. A second objective of this Phase I program, therefore, was to design, fabricate and test an enclosure which would be suitable for use in conducting the biological experiments which were being planned.

While the broad objectives of the program, in response to the needs of the community, are as stated above, the specific goals are as follows:

- To consider the properties of the HVDC environment that will be of importance in stimulating the environment and to delineate those properties which will be of lesser or no importance.

- To consider the types of potentially interfering factors which, though not characteristic of the environment of interest, may arise in a laboratory simulation and, where possible, to describe methods for eliminating or reducing these factors, or where this is not possible, to define the methods that will be used for experimentally evaluating the involvement of these secondary factors in producing any observed biological effects.

- To design, fabricate, and test an enclosure for housing the small laboratory animals during exposure to the HVDC environment which will provide known, controllable and relevant conditions.

- To select the appropriate instrumentation for measuring and monitoring the environment and develop the methodology for the use of the instrumentation in the laboratory setup.

- To define the biological parameters that should be given consideration.

- To work out the experimental plan that will best utilize the proposed exposure facilities and exposed animals to yield maximum information on diverse biological systems, and at the same time will be consistent with the experimental demands of the individual biological tests, and will avoid the risk of confounding the results of the individual biological tests by factors in the prior test history of the animals.

1.2 Report Organization

Section 2 of this report presents the results of the test enclosure or simulator development. The discussion is initiated by a brief review of the HVDC transmission line environment, from which the dominant components of the environment to be considered for simulation are identified. Many requirements are imposed on the simulator design. A review of the considerations which influence the design is presented in Section 2.2. The HVDC environment is quite complex relative to the dominant environment associated with HVAC transmission lines. Correspondingly, the HVDC test enclosure which has been designed is not as simple a structure as is typically used for animal testing to the HVAC environment. Section 2.3 presents a rather detailed description of the resulting test enclosure, along with supporting rationale for various features and functional components of the unit. Section 2.4 presents the results of testing which has been conducted to characterize the performance of the prototype test enclosure that has been fabricated.

The biological experimental design is presented in Section 3. The opening discussion concerns factors that were important in determining the scope of the experimental design (Section 3.1) and is followed by a review of background literature (Section 3.2). Section 3.3 gives an overview of the design, and rationales for selection of the biological parameters are discussed in Section 3.4. General and specific study methods are outlined in Sections 3.5 and 3.6, respectively, and the final section highlights suggested directions for future research.

2. SIMULATOR DEVELOPMENT

This section of the report describes the dc bioeffects test enclosure for small animals, which has been developed and tested under this contract. Throughout the discussion the test enclosure is referred to as a simulator or simulator module. The term simulator is used, since the enclosure simulates the dominant environments of HVDC transmission lines which are felt to be necessary for the biological testing of laboratory animals.

The overall discussion is topically divided into subsections for logical presentation. In the first section, the environment associated with HVDC transmission lines is reviewed and the dominant features of this environment that are considered important for simulation are identified. There are many factors which must be considered before embarking on the design of a simulator for electromagnetic bioeffects testing of small laboratory animals. The desire to simulate the HVDC environment complicates many of these considerations. Therefore, a review of basic HVDC simulator considerations is presented in the second section, to clarify the approach taken in the design. A description of the simulator which has resulted from the design efforts of this program is presented in the third section. Included in the description of the unit is the rationale for specific approaches where this is appropriate. The fourth section concludes with the presentation of key electrical performance characteristics for the simulator that has been fabricated and tested.

2.1 HVDC Environment Review

The primary electrical environment of an HVDC transmission line may be characterized by the electric field, ion current density, and charge density at ground level near the line. These quantities depend upon such factors as line voltage, line configuration, wind, humidity of the air, and pollutants. In efforts to estimate the environment, numerical methods have been developed which predict the ground level electrical effects based on the line configuration and voltage. One such method, which has been presented by Harrington,* allows the electrical quantities to be calculated by computer. Harrington's method is based on a corona-loss analysis presented by Sarma (1969).

---

*Bonneville Power Administration, Transmission Line Reference Book HVDC to ± 600 kV. Palo Alto, California: EPRI. Appendix to Chapter 7 by Harrington and Kelly.

Unfortunately, such methods do not account for effects due to wind, humidity, rain, or the different properties of positive and negative corona present on a bipolar line, and thus cannot give a sufficiently accurate or general description of the dc environment.

Because the complex dc environment has not allowed adequate mathematical description, direct measurement is commonly used to determine the electrical effects near the line. While none of the measurement work performed to date may be considered exhaustive with regard to the assessment of diverse line configurations and long-term weather effects, some existing reports are quite detailed and provide useful descriptions of the environment near a particular line, and comprehensive measurement programs such as that at Project UHV are still in progress.

Bracken et al. (1978) have reported measurements near the Celilo-Sylmar $\pm$ 400 kV dc Intertie. This paper contains a basic discussion of the dc environment as well as a report on the measurements which were made. The measurements were of electric field (E) and ion current density (j) at ground level, and these were obtained in fair weather with low wind. Charge density (ρ) at ground level was derived from the measured values of electric field and current density using the relationship $j = \rho k E$, where k is ion mobility. The negative and positive maxima of electric field, ion current density, and space charge density which were observed in the vicinity of the line are given in Table 2-1, which presents a summary of the electrical environment measured by various investigators. Bracken observed that the electric field and ion current density due to the negative conductor of the transmission line are of a greater magnitude than those due to the positive conductor. He presumed this predominance of negative ion effects to be due to the lower corona onset, the less sporadic corona of the negative conductor, and the higher mobility of negative ions. Bracken reported that wind has a strong influence on both electric field and ion current density. Even a low wind (0-4 m/s) was enough to cause large variations in measurements. In a more recent paper, Bracken and Furumasu (1978) observed the wind to have a strong effect on measurements made near a $\pm$ 600 kV line.

A paper by Comber et al. (1979) discusses preliminary ground level measurements of electric field and ion current density near a $\pm$ 600 kV dc test line at Project UHV. Positive and negative maximum values are given in Table 2-1. Comber observed no predominance of the negative electric field and no effect on the field due to winds of 0-3 m/s. In agreement with Bracken, the Project

Table 2-1

MEASUREMENTS OF THE HVDC ELECTRICAL ENVIRONMENT

Author	Line Voltage Pole Spacing x Height	Measurement Instruments Electric Field	Ion Current Density	Charge Density	Maximum Values Measured Electric Field (kV/m)	Ion Current Density (nA/m^2)	Charge Density (nC/m^3)
Bracken[3]	± 400 kV 11.6 x 12 m	Monroe #225 meter with #1007E probe	1 m^2 collecting plate with Keithly #610C electrometer	-	+13/-34	+14/-72	-
Bracken[4]	± 500 kV 12.2 x 12 m	Monroe #225 meter with #1007E probe	1 m^2 collecting plate with current integrator circuit	Klykon #901 volumetric ion counter with Keithly #610 electrometer	+33/-25	+90/-75	+9.6/-7.8
Comber[5]	± 600 kV 13.2 x 13.7 m	Monroe #225 Trek #48C	1 m^2 plate with guard ring	-	+25/-25	+200/-250 measured during rain	-
EPRI/BPA[6] "Green Book"	± 600 kV 11.2 x 13 m	Monroe #225	-	-	+25/-40	-	-
Maruvada[7]	± 750 kV 13.7 x 16.4 m	-	-	-	-	+280/-300	-

UHV data show measured negative ion current density which was somewhat greater than positive ion current density. Figure 2-1 shows an ion current density profile reported by Comber et al. Finally, Comber observed that rain or high humidity increased the ion current density. Rain was observed to increase ion current density by a factor of 2.5 to 4 over fair weather values. Other reportings of the HVDC environment include EPRI/BPA* and Maruvada et al. (1977) Measurements performed by these researchers are also summarized in Table 2-1.

The above discussion of the literature on measurements made on HVDC transmission line environments has noted that some investigators have observed wind influences on the electric field and ion current. Bracken (1978) presents significant variations in both field and current density with time. However, these reported variations are relatively slow, i.e., less than 1 Hz.

The temporal variations that are imposed on the ion current density, and possibly the electric field, due to wind effects can complicate the measurement of these parameters in the transmission line environment. The reported measurements typically use integrating instrumentation in order to provide average characterization of the environment. Thus, there appears to be no representative data base reported which provides information on the electric field or ionic variations in the 1-15 Hz range.

The variation in ion currents and fields in this low frequency or "brainwave" region may be a future consideration in simulation, particularly if measurements show significant spectral content in this frequency range. However, at this time, the level of the ionic currents and electric fields appear to be the dominant factors for consideration in simulation, with incidental variations due to the interaction with other environmental parameters being considered as undesirable.

In addition to the temporal variation of the dominant environmental parameters (electric field, ion current density and charge density) which may be related to the wind, the electric and magnetic fields also contain harmonics of 60 Hz, due to the conversion process. Frazier (1978) has reported limited measurement of the converter harmonic fields under the Celilo-Sylmar $\pm$ 400 kV dc line. A spectrum analysis of the displacement current shows that the 60-Hz

*Bonneville Power Administration, Transmission Line Reference Book HVDC to $\pm$ 600 kV. Palo Alto, California: EPRI. Chapter 7.

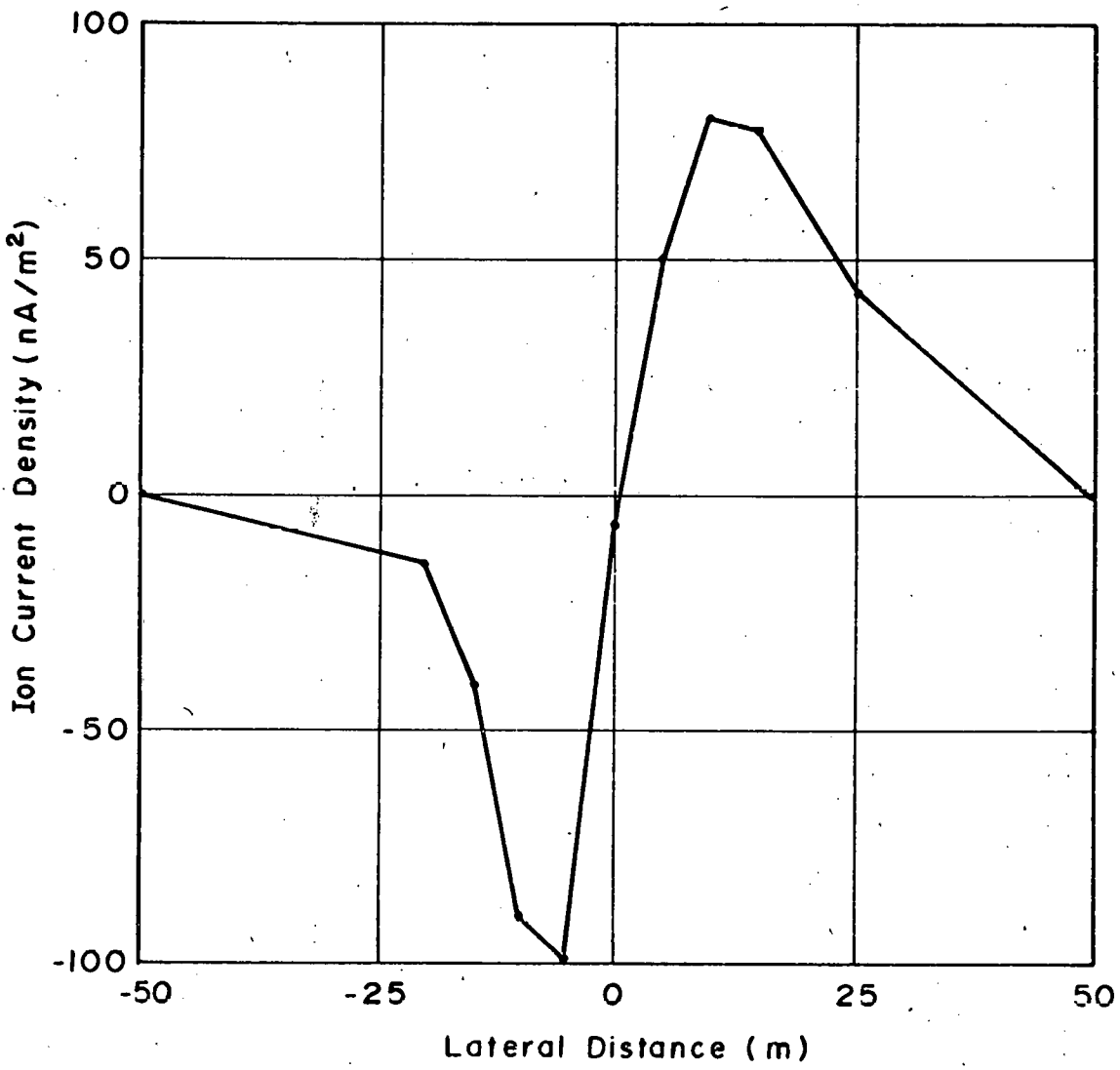

Figure 2-1 ION CURRENT DENSITY PROFILE MEASUREMENT FOR FAIR WEATHER (from Comber, 1979)

and several dominant harmonics are in the range of 65 nA/m^2. Thus, for a person with a collecting area of approximately 5 m^2, the total body current flow at each of the dominant harmonics will be in the range of 325 nA. The peak displacement current noted with an oscilloscope was approximately 600 nA/m^2, or about 3 μA total body current for a typical human. This peak current was nominally in the form of single cycle sine waves of about 0.4 ms period that occurred once per 60-Hz period.

The above displacement current density levels due to converter harmonics are in the range of the ionic conduction current density levels which have been measured by various investigators, as shown in Table 2-1. However, these levels are all significantly less than the displacement current density levels typically found under 60-Hz EHV lines.

Converter harmonic as well as 60-Hz displacement current flow to persons under typical HVDC lines is likely to be in the amplitude range of the dc conduction current flow. However, the simulation of such displacement currents for animal testing should be deferred until base line data is obtained with the dominant dc environment.

The dc magnetic field in the vicinity of an HVDC transmission line is contributed to by the line and by the earth's magnetic field. The published reportings of measurements near HVDC lines, that have been reviewed, have not included dc magnetic fields among the measured parameters. A sample calculation using the full rated current of the Celilo-Sylmar ± 400 kV line results in a magnetic field profile such as is shown in Figure 2-2. The magnetic field resulting from the line current is relatively small compared to the earth's magnetic field, which is in the range of 0.5 gauss. Thus, although an HVDC line contributes to the ground level magnetic field in its vicinity, the magnetic field is not considered to be one of the dominant components of the HVDC environment for consideration in simulation at this time. At some later date, if it is desired to include a magnetic field component in the simulation, such an addition should be relatively easy to implement, due to the low level of this field.

2.2 Basic Simulator Design Considerations

As evidenced in the discussions of the previous section, the electrical environment associated with an HVDC transmission line is quite complex. Animal testing to determine possible biological effects of such an environment

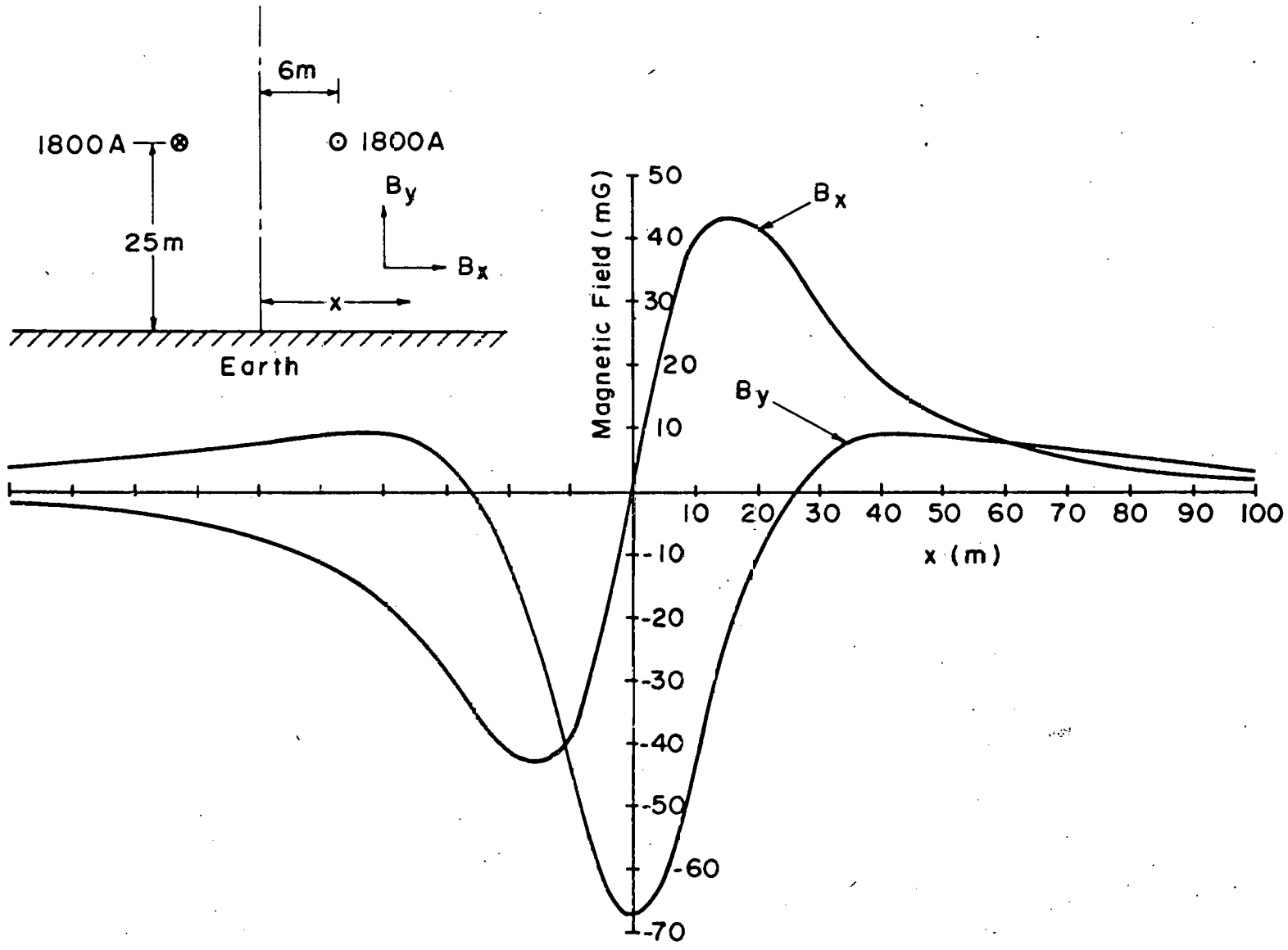

Figure 2-2 DC MAGNETIC FIELD AT EARTH'S SURFACE UNDER HYPOTHETICAL BIPOLAR TRANSMISSION LINE

must insure that the dominant aspects of this environment be simulated. This is particularly true for those components of the environment that are significantly different than normally encountered by the biological system, or for which past studies have shown potential biological interactions. On the other hand, a truly accurate simulation of the actual environment appears undesirable from the standpoint of controlling costs of the biological experiment and permitting a determination of cause-effect relationships or "dose" relationships, if biological interactions are observed.

The above considerations emphasize the need for a carefully controlled simulation of the dominant features of the environment for the first full-scale series of animal tests. Secondary or more subtle features of the environment may warrant simulation for a later series of tests, once a comprehensive evaluation of the dominant environments has been conducted.

The dominant environment as identified in Section 2.1 consists of a vertical electric field and a vertical component of ion current density. Under the condition of near zero wind, these components will be virtually time invariant. The simulation of these quantities for use on animal testing places a variety of constraints on the design of the simulator.

The following paragraphs of this section will discuss the various design considerations which must be addressed to insure:

- the adequate simulation of the desired environments
- the provision for adequate care and housing for the test animals
- the minimization of undesired collateral factors.

2.2.1 Ion and Field Uniformity

The electrical environment to be simulated consists of a vertical dc electric field and a vertical component of ion current density. In the immediate vicinity of a HVDC transmission line, these quantities vary as a function of spatial position, and may also vary with time due to wind effects.

An analogous situation exists in the vicinity of EHV ac transmission lines, where the electric field is also a function of spatial position. For laboratory testing of small animals, a test condition comprises a discrete setting of the ac electric field level; even though a person or animal under an actual transmission line would not likely be exposed to a fixed environment.

Thus, in an analogous manner, a test condition for HVDC simulation should consist of a discrete electric field and ion current density. Since for statistical evaluation of animal test results it is necessary for the exposure of multiple animals to a given test condition, the simulator must produce the desired test environment in the living space of all animals to be tested to a given environmental condition. In addition, the test environment within the area which can be occupied by an animal under test should be a constant; that is, the field and ion current density levels should not vary appreciably within the living space of an individual animal.

The desire to provide a discrete ion current density and electric field within an animal compartment, and from compartment to compartment, for all animals to be tested for a given condition, places significant demands on the simulator design. These considerations influence the means used to generate and control the ions and fields, the geometry of the simulator, and the materials used in fabricating the simulator.

The design of a simulator which has a uniform HVDC test environment is considerably more complex than is encountered in providing a uniform field for animal testing to the field environment of EHV ac transmission lines. For the ac case, individual animal units can be fabricated from low-loss, low-dielectric constant materials, which are readily available. However, the presence of free ions in the dc environment restricts the use of such materials for fabrication of animal enclosures for HVDC environment simulation. Low-loss dielectric materials whose resistivity is significantly greater than that of the ionized air can trap and retain ions. The trapping of ions by animal caging material has the effect of severely distorting both the electric field and the ion current density flow in the vicinity of such materials. Figure 2-3 pictorially depicts this situation.

In this figure, charges are shown trapped on a high resistivity material used as an animal containment wall. Once the charges are deposited onto the material, an electric field component which is normal to the wall surface is established. This electric field causes the air ions to be repelled from the wall, thus disturbing the desired vertical flow of ions and results in a lower than normal ion current density at the ground plane near the wall. Experiments have shown that charges trapped on high resistivity dielectrics can distort the ion current flow for long periods of time in the vicinity of the dielectric material.

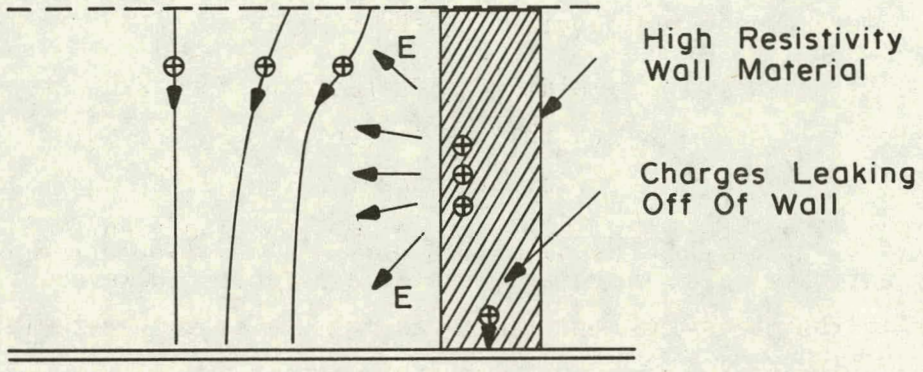

Figure 2-3 FIELD AND ION FLOW DISTORTION DUE TO TRAPPED CHARGE ON CAGE WALL

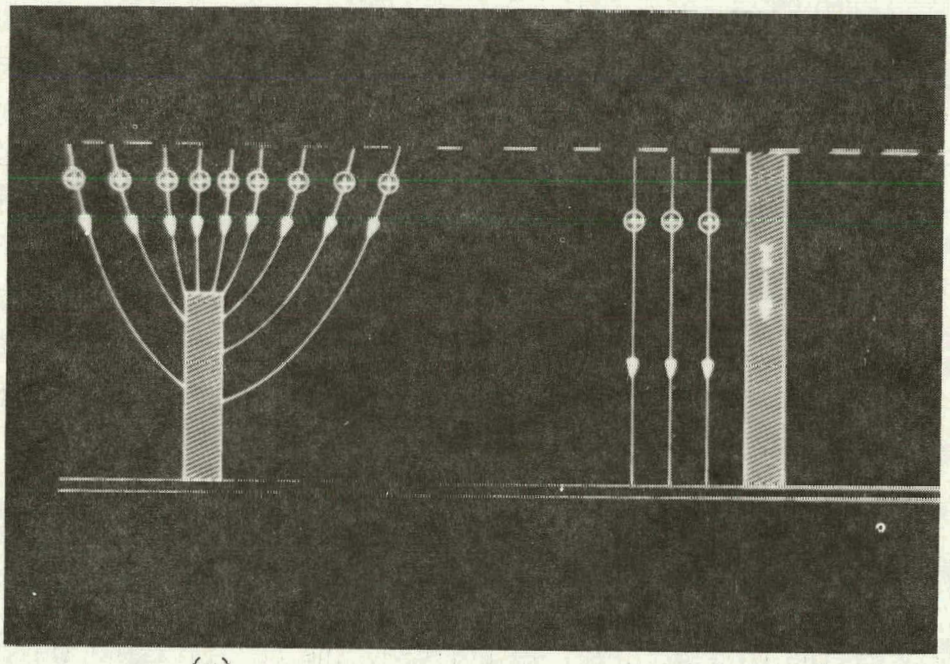

Figure 2-4 FIELD DISTORTION WITH PARTIAL WALL

The above suggests that materials to be considered for use in animal caging for the simulator should have a finite resistivity, which will allow charges to drain off in a reasonably short period of time. It also appears that there is no well-defined lower limit on an acceptable value for the material resistivity, although considerations of the current that can be drawn by an animal contacting the material (which will be discussed later) tend to provide a limit on the lower range of resistivity.

A well accepted arrangement for producing uniform electric fields for animal testing is with horizontal parallel plates. If the plates are sufficiently large relative to their separation, a region of very uniform field can be produced by applying a potential between the plates. If a means is provided to uniformly introduce ions into the interplate space, at the upper plate, then a uniform field and ion current environment can be produced. However, the ion and field uniformity can be severely distorted by the introduction of resistive materials which are used as animal constraining walls. Figure 2-4 illustrates both an unacceptable and an acceptable use of such constraining walls. In the illustration of Figure 2-4(a) the conductive wall material does not extend completely between the field producing plates. If the material resistivity is less than that of the ionized air, the field lines and ion flow will be distorted, as shown. The use of such "short walls" has been attempted in HVDC simulation, with poor success (Nakamura, 1979).

This illustration of Figure 2.4(b) shows the resistive material wall extending from the upper plate to the ground plate. If electrical contact is made at both plates, a current will flow through the wall material. If the resistivity of the wall material is uniform, the current flow through the wall will produce a tangential electric field component which is identical to the static electric field that exists in the absence of the wall.

Thus, animal caging walls must extend between the field-producing plates and be in electrical contact with these plates. If arranged in such a manner, the animal containment walls can serve as continuous grading rings, which force the electric fields to be uniform. Forcing the fields to be uniform by such means appears to be a good trade-off for the HVDC environment simulation, even though a slight variation of electric field with height is produced by the ion current flow in air.

An analysis of the effect of space charge on the electric field shows that for a space charge between two infinite parallel plates,

$$E_{oi}^2 - \frac{2jh}{k\varepsilon_o} = E_{hi}^2 \qquad (2\text{-}1)$$

where

E_{oi} = electric field at the lower or ground plate, with a space charge present

E_{hi} = electric field at the upper plate, with space charge present

j = ion current density

k = ion mobility (about 2×10^{-4} m^2/vs)

ε_o = free space permittivity

h = separation between plates.

Figure 2-5 shows the allowable current density to produce a 10% variation in field, from the top to bottom plate, due to space charge as a function of the electric field at the lower plate. For this figure, the plate separation (h) has been chosen to be 0.5 meter. Thus, for any desired electric field at the lower plate of the simulator, if the current density is less than the value shown in Figure 2-5 for the chosen field, the field variation over the simulator height at points remote from a wall will be less than 10 percent.

At points remote from a wall, the field at the bottom plate, E_{oi}, is enhanced (due to the presence of the ions) over the nominal electric field, or the field near a wall. For the values of enhanced field E_{oi} at the ground plane and the ion current density, j, shown in Figure 2-5, the field at the ground plane near a wall with uniform resistivity, will be less than E_{oi} by about 6 percent. Thus, the use of walls in the simulator, which force the potential gradient to be constant along the height of the wall, appears as an acceptable design approach if the ion current density does not significantly exceed the values shown in Figure 3-3 as a function of ground plane field level.

2.2.2 Ion and Field Control

It is necessary to provide a means for adjusting the field and ion current density levels, more or less independently of one another. Since consideration of "dose" related responses requires the use of different exposure levels, the simulator must be capable of providing reasonable combinations of field and ion current levels.

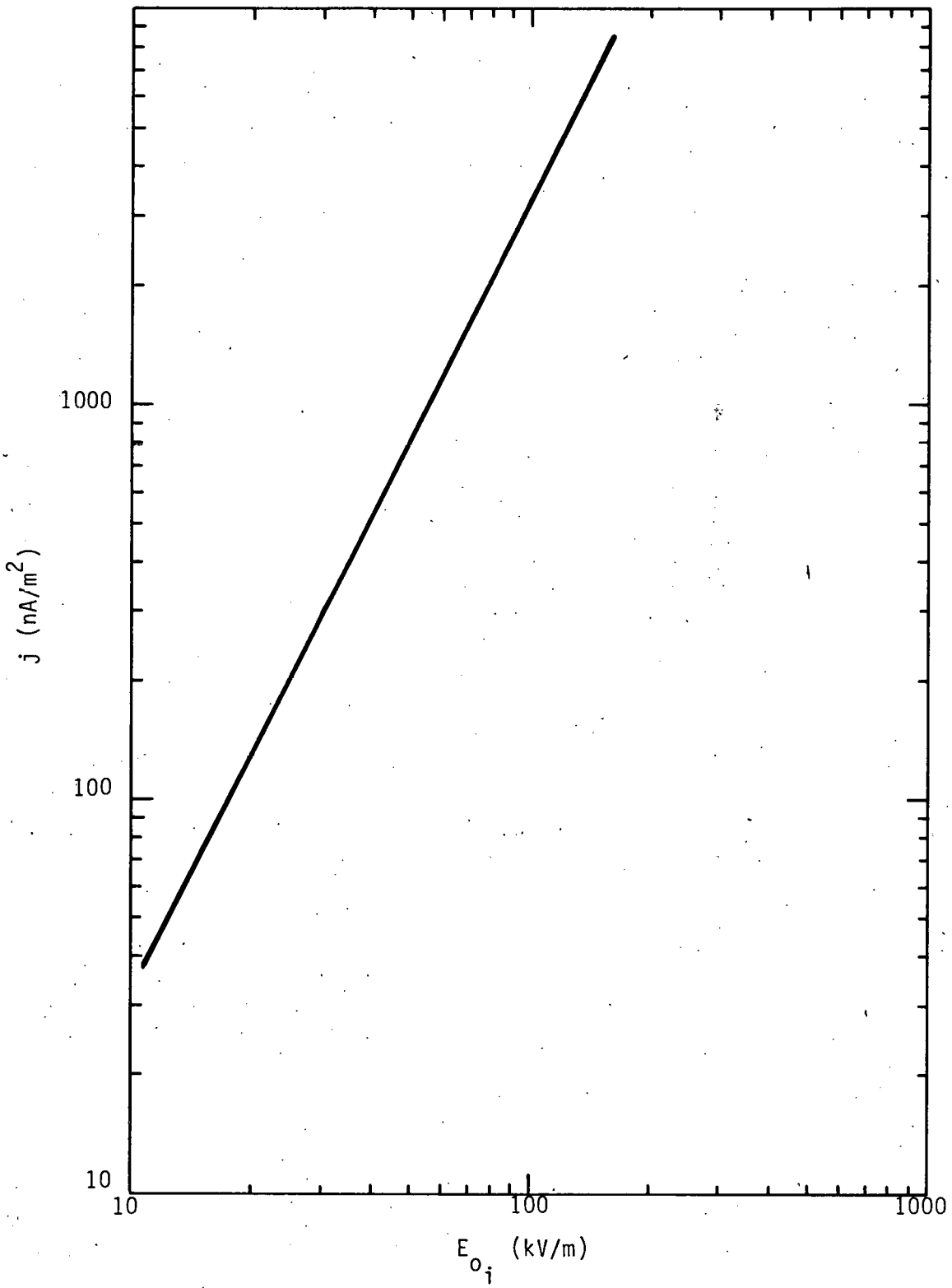

Figure 2-5 ION CURRENT DENSITY WHICH WILL PRODUCE A 10% ELECTRIC FIELD VARIATION BETWEEN 0.5 m SEPARATED PLATES VS. FIELD AT BOTTOM PLATE

The previous paragraphs have shown that field uniformity considerations provide a restriction on the ion current density range that can be considered for a chosen electric field level. The levels of both fields and ion currents typically measured beneath operating or test HVDC transmission lines provides guidance, as noted in Section 2.1, for the choice of a reasonable combination of these two parameters for use as one of the test conditions. However, the review of measurements that have been made on HVDC lines does not directly answer the question of the relation between field and ion current for higher or lower level exposure conditions. One approach which appears reasonable for providing guidance in the choice of field and ion current relations is to consider enhancement factors.

When a conducting object is placed in a field, the field at the surface of the object is changed from the field level which existed before the object was introduced. In general, the field at the top surface of the object is larger than the pre-existing field, and the larger the object the more the field is enhanced. For example, for a given ambient field, the field at the top of a man will be enhanced by a larger factor than will the field at the upper surface of a rat placed in the same pre-existing field.

Analysis of simple shaped objects, such as prolate spheroidal representations of man or rats show that for an ion current and electric field environment, the upper surface enhancement is the same for both field and ion current density. That is, if the pre-existing electric field and ion current density are denoted by E_o and j_o, respectively, then

$$F_e = \gamma F_o$$

and

$$j_e = \gamma j_o$$

where E_e and j_e are enhanced field and current density at the top of the object, and γ is a geometrically dependent enhancement factor which is larger than unity. The observation of importance is that both the field and ion current density are scaled up or enhanced by the same factor.

Thus, it appears reasonable to consider that for different exposure conditions, the ratio of electric field to ion current density might remain a constant. This is equivalent to maintaining the air resistivity or the ion charge density at a constant value for the various exposure conditions.

Thus, if a representative condition is for an electric field of 30 kV/m and ion current density of 200 nA/m^2, this results in an air resistivity of $\rho_a = 1.5 \times 10^{11}$ ohm·m = 1.5×10^{13} ohm·cm, and an ion density of $n = 2 \times 10^5$ ion/cm^3.

Figure 2-6 shows this current density-field relationship superimposed on the 10 percent field uniformity curve previously presented as Figure 2-5. It is seen that if a constant air resistivity relation between field and current density, such as is suggested above, is used for establishing different test environments, very little variation of field due to space charge should result over most of the range of field levels of interest.

The above noted desire to establish a particular ion current density level for a given electric field level necessitates that the simulator design provide the capability for setting the ion current density to the desired value. If a constant ion source is situated above a field-producing plate that has perforations, ions will be drawn into the exposure region between the plates when a potential is applied between the plates. Over a wide range of field levels, the ion current density level in the exposure region will be uniquely determined by the field level. However, the relation between ion current density and electric field will not follow the desired constant ratio noted above. Thus, an added means for controlling the ion current density is required.

The use of a corona source for generation of the required ions is attractive from two standpoints: (1) by use of a grid of wires in corona, a relatively uniform source of ions can be produced over a large area; and (2) the ion production mechanism is the same as for the HVDC environment being simulated. However, care must be exercised in the simulator design to control the ozone levels generated by the corona source to within acceptable limits. One factor influencing the ozone generated by the corona source is the corona current. Thus, control of the ion current level in the exposure chamber by controlling the drive to the corona source does not appear advisable, since this would make the ozone generated a variable with exposure level.

The simulator that has been designed operates with a fixed drive to the corona source, which results in acceptable levels of ozone in the exposure area. The control of the level of air ion current in the exposure chamber

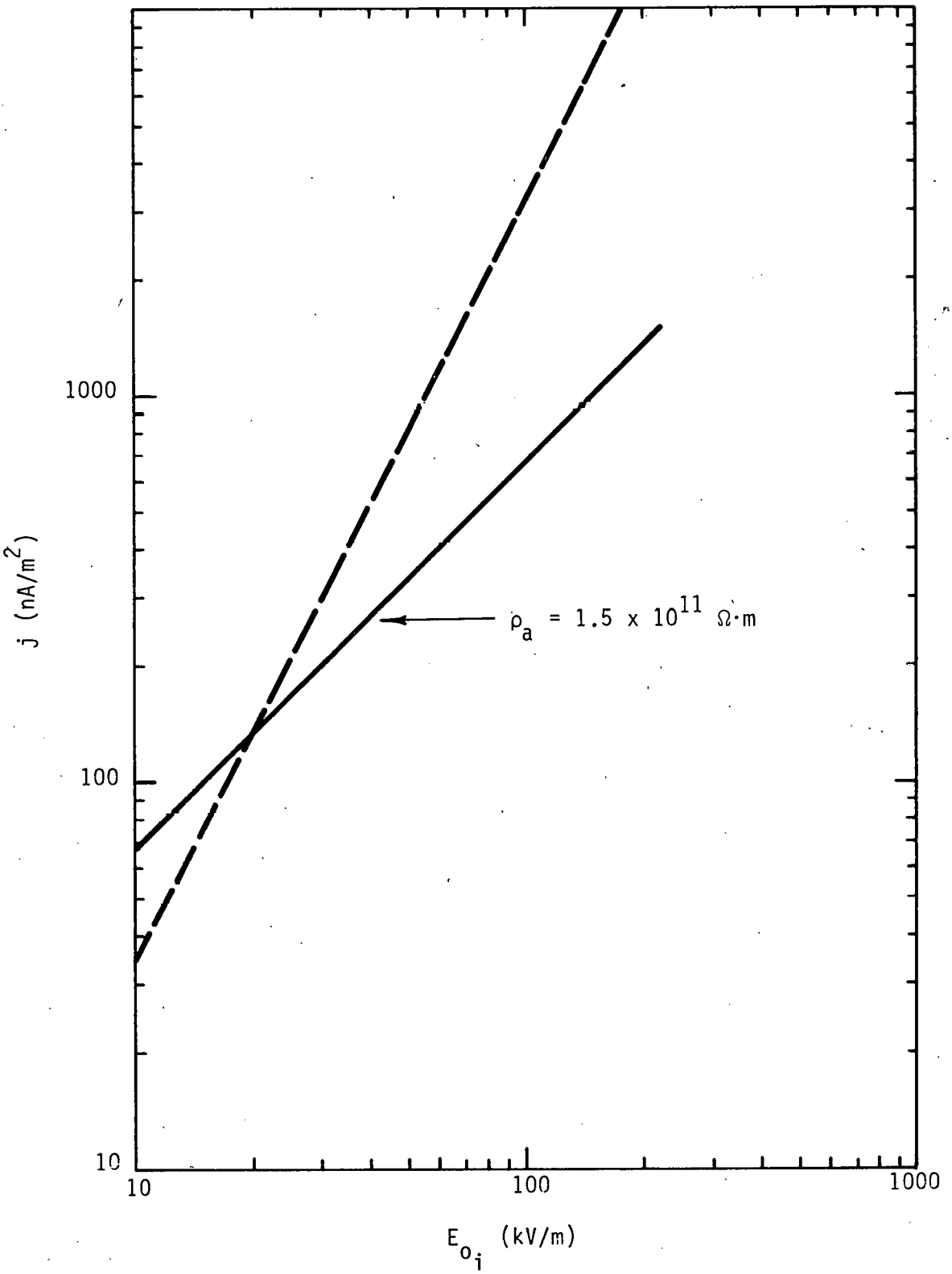

Figure 2-6 CONSTANT AIR RESISTIVITY RELATIONSHIP COMPARED TO FIELD UNIFORMITY RELATION

is effected by a grid arrangement which permits the adjustment of the ion current to any level within the desired range.

Significant care must be exercised in the design of the corona source to simultaneously meet the demands of (1) acceptable ozone levels, and (2) uniform ion generation and introduction into the exposure area to insure a relatively constant ion current density at all locations within the exposure chamber.

2.2.3 Animal Care and Housing

The simulator design must provide for the housing of rodents from the standpoint of acceptable animal care functions. Simultaneously, the design must insure that the animal care functions do not distort the desired electrical environment and that the animal is not subjected to undesired collateral environments or cues which may be different than experienced by control subjects. Thus, in addition to providing animal housing that meets the requirements for standard laboratory animal care, it must be ensured that the electrical environment under study is not distorted by the means used to provide these animal care functions.

Adequate provisions for animal care and maintenance that require consideration in simulator design include:

- adequate floor space for each animal (40 square inches recommended for individual rats)
- free access to food and water
- adequate ventilation to prevent exposure to waste effluents
- ready access to animals by maintenance personnel
- adequate light during light cycle
- thermal and humidity levels within recommended guidelines (This factor is generally a requirement on the laboratory space rather than on the individual caging units.)
- viewing of animals by maintenance and testing personnel.

Providing for the above functions in the simulator design must be accomplished without upsetting the environment that is to be simulated. Thus, for example, feeding and watering provisions should not distort the field and ion environment. The viewing and lighting requirement indicate the use of translucent or open-type structures. Many transparent materials are unacceptable since they will trap charge, thus distorting the ion environment.

2.2.4 Secondary Environments

The overall simulator design, including the provision for normal animal care functions, must ensure that the only difference between test and control units is the environment under study. The results of many biological experiments have been questioned because of undesired secondary environments which were not adequately considered or controlled. The lack of control of such environments may impose unintended stresses on the exposed animals, thus making it difficult to attribute any noted biological response solely to the exposure environment under study.

Secondary environmental factors which have a direct influence on the design and operation of an HVDC simulator include:

- Ozone - which may be produced by the ion generator. The ion generating corona source must be designed to result in acceptable levels of ozone in the exposure chamber. Acceptability appears to be a fraction of the EPA limit of 80 ppb.

- Shock - which may occur due to improper design of the animal feeding and watering systems. Elimination of this factor can be achieved by maintaining the animal, as well as the feeding and watering systems at ground potential. Shock or sub-perception animal current flow, which is significantly larger than that induced by the environment under study, due to animal contact with the caging material must be prevented. This requirement has a significant role in the selection of materials to be used in the fabrication of the animal housing structure.

- Noise - which may accompany the desired test environment should be minimal and must not provide cues to the animal.

- Particulates - may acquire a charge due to the ion environment in the exposure chambers. Such particulates may not be charged in the sham exposed controls. Since the particulates may be unique to the locale where the tests are being conducted, they do not represent a factor under study and should be deleted from the test environment. The simulator design, therefore, should provide for the low flow uniform velocity filtered air. The flow of this air must not distort the uniformity of the ion current flow.

2.3 Simulator Design, Rationale and Fabrication

2.3.1 Overview

This section presents a description of a prototype HVDC bioeffects simulator, which was developed by IITRI under Department of Energy Contract ET78-C-01-3026. It is felt that the simulator to be described in the following paragraphs meets the requirements of the Phase I design effort, and will be

satisfactory for use in the Phase II testing program. The development of the design and resulting prototype attempted to incorporate the wide range of considerations identified in the previous section, which are important for use of the simulator in animal studies.

The following paragraphs provide a description of the simulator, along with clarifying photographs, as well as the rationale for the design, where appropriate. A description of the important operating characteristics and performance is presented in the next section. Drawings of the simulator, in sufficient detail to allow fabrication of duplicate units, are provided in Appendix A. Appendix B presents a comprehensive overview of the program work efforts since the issuance of the Fourth Quarterly Report. During this period, three separate prototype units were tested. The appendix details the design modifications and testing which resulted in the final prototype simulator.

The basic simulator module will house up to eight separated rat-sized animals. As many of the basic simulator modules as necessary to house the total desired number of animals can be fabricated.

The simulator module is comprised of several functional sections which are stacked one on top of the other. Figure 2-7 presents a sketch which illustrates and identifies the various major components of a simulator. Figure 2-8 is a photograph of the prototype simulator.

The sketch of Figure 2-7 is the best starting point to provide a general description of the simulator and its various functional components. The five functional components are identified from top to bottom as:

- Plenum - where filtered, as well as temperature and humidity controlled air can be introduced into the simulator.
- Corona Section - where either positive or negative ions are produced by corona on a series of very fine parallel wires.
- Grid Section - which controls the amount of ions which pass into the caging area below it.
- Caging Area - where the desired electromagnetic test environment is established, and where the animals are individually housed.
- Base Section - which provides a support for the remainder of the simulator; serves as a ground plane through which the simulator air exits; and incorporates the feeding, watering and waste collection provisions.

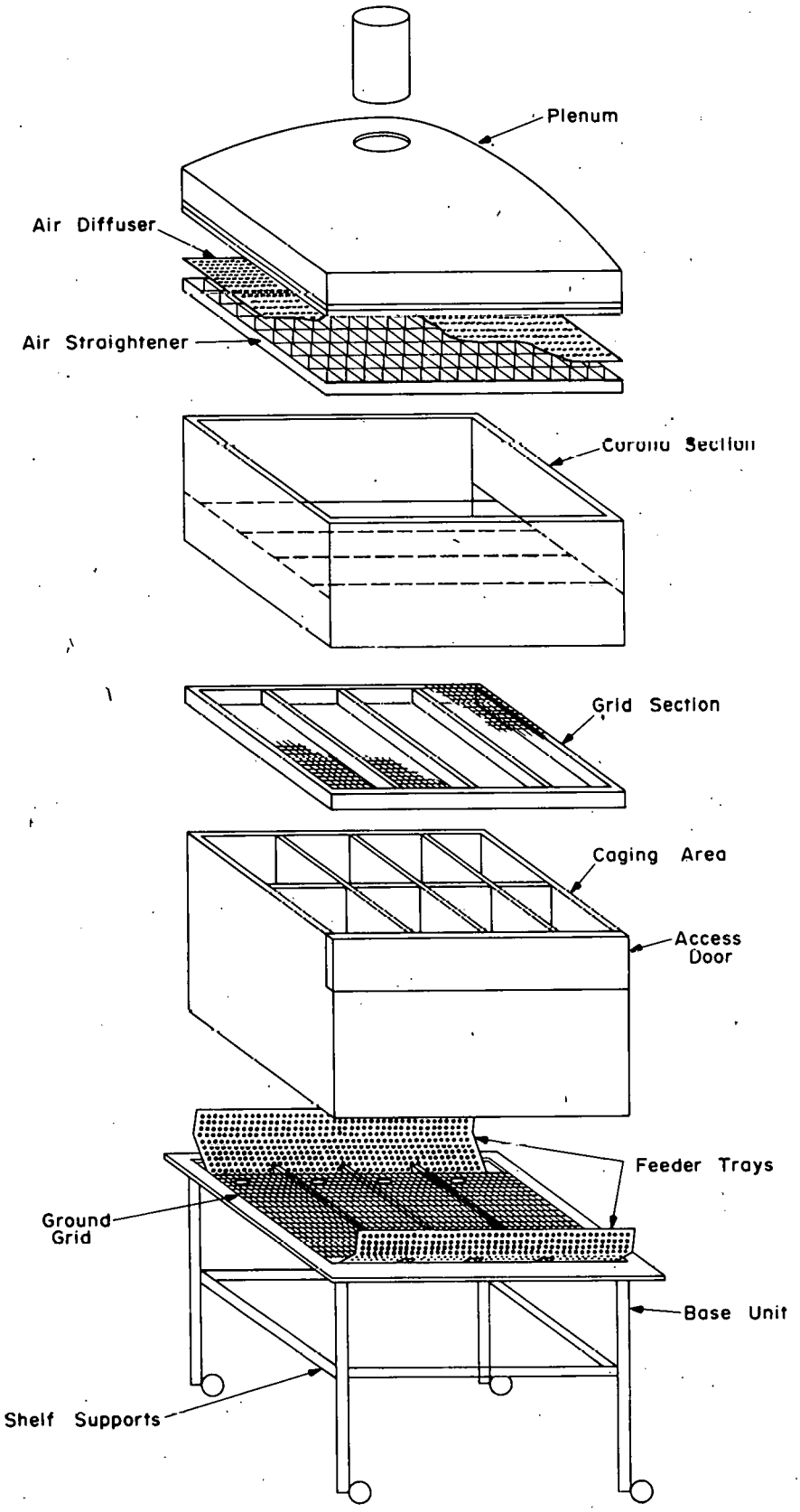

Figure 2-7 SKETCH OF PROTOTYPE SIMULATOR

Figure 2-8 FINAL PROTOTYPE SIMULATOR

The cross-sectional dimensions of the simulator are based on providing an adequate floor space area for each animal. The width dimension of the simulator accommodates two animal compartments. The width of two animal compartments was chosen to provide ready access to the animals by maintenance personnel via a door on each side, near the top of the animal caging section. The length dimension of the simulator accommodates four animal compartments. This dimension is not critical. Additional compartments could have been added by simply extending the structure. However, the four-compartment length was chosen for ease in handling, moving, and the ready availability of materials of this size.

It will be noted from the sketch of Figure 2-7 that the cross-sectional dimension of the top four sections of the simulator are the same. That is, the field and ion producing sections are the same cross-sectional dimensions as the caging section. This design provides a compact unit and simplifies the control of air flow uniformity through the structure.

The use of field-producing plates which are the same size as the exposure area is a departure from convention in electromagnetic bioeffects simulator design. Such a compact arrangement is not normally possible due to field non-uniformity near the edges of the field-producing plates. However, in this design, the conductive properties of the animal caging structure provides a natural field grading, which forces the fields to be uniform out to the edge of the field-producing plates.

While the attainment of quite uniform fields out to the periphery of the structure is a natural consequence of employing conductive walls (when these walls make electrical contact with both the field and ground plates), the attainment of uniform ion current density at the outer edges of the structure necessitated a significant empirical design effort for the corona chamber. The corona is produced on a horizontal series of wires, which are parallel planar to the corona grid. Establishing uniform ion flux near the feed-end walls involved different considerations than along the side walls, which are parallel to the wires.

The basic operation of the simulator for producing and controlling the desired ion and field environment in the animal exposure or caging area of the unit can be best explained with the help of the sketch presented in Figure 2-9. This figure depicts the three grids of the simulator (the ground

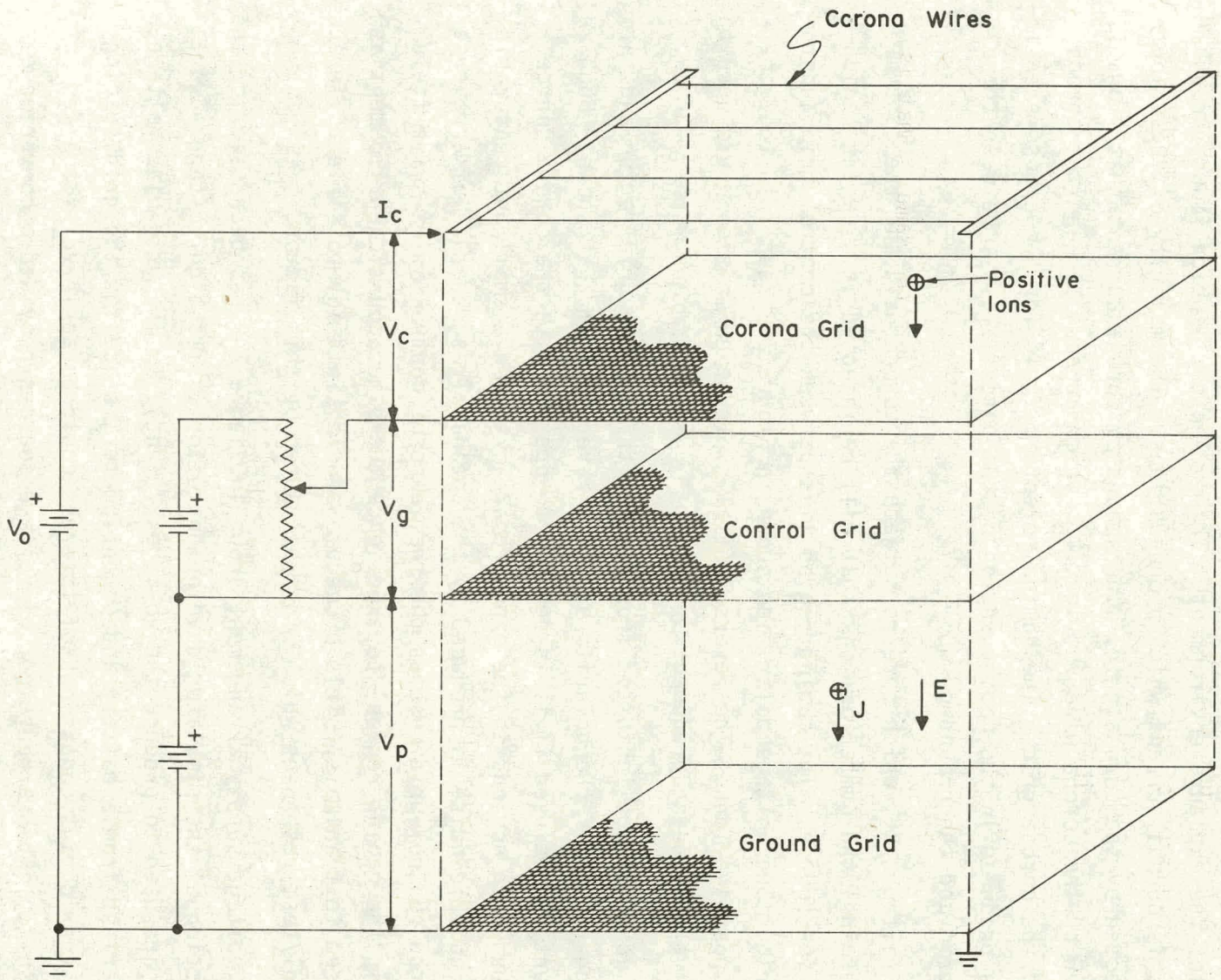

Figure 2-9 SKETCH OF ION AND FIELD GENERATION AND CONTROL ARRANGEMENT

grid, the control grid and the corona grid) and the corona wires. These elements are necessary for the basic generation and level control of the field and ion environment.

A series of parallel wires which are in corona provide the basic source of ions for the exposure environment. The current, I_c, which flows through the wires is corona current which produces ions. The majority of these ions are collected by the corona grid. The amount of corona current that flows is determined by the corona wire voltage, V_c, which appears between the corona wires and the corona grid. The nominal electric field for the exposure environment is produced in the caging region by the potential, V_p, between the control grid and the ground grid.

The voltage, V_g, which appears between the corona grid and the control grid determines the number of ions that will be injected into caging region from the ion source. The caging region lies between the control grid and the ground grid. The voltage polarities shown in Figure 2-9 result in the generation of positive ions. The reversal of all voltage polarities would result in negative ions being produced.

The ions will be inhibited from passing through the grid region and into the caging region if the polarity of V_g is reversed from that shown. Such an arrangement can be used if it is desired to operate with the corona source active, but with no ions in the exposure area. Since a small but measurable level of audible noise is produced by the corona wires, the use of a reverse bias on the control grid enables the sham exposed control animals (no field or ions in the caging region) to experience the same acoustic environment as the exposed test animals. This procedure should avoid any possible differences in control/test responses which might be caused by this factor.

The voltage supply arrangement shown in Figure 2-9 has been used for the major portion of the simulator development effort. Two high voltage power supplies are used to produce the voltages V_o and V_p. The grid bias voltage, V_g, is derived from a battery and potentiometer, since for the grid spacing used, most grid bias conditions of interest could be achieved with a few hundred volts. This arrangement of voltage sources provided a convenience during the developmental effort, since the field and ion levels could be readily adjusted. It should be noted that the indicated voltage connection is only one of several possible approaches to establishing the desired voltages on the simulator.

2.3.2 Functional Description of Simulator Components

The foregoing has presented a brief overview of the basic functioning of the simulator. The prototype simulator has been fabricated as several distinct components which, when assembled together, provide the desired environmental simulation capability. The functional components of the simulator were identified in Figure 2-7. The following paragraphs present a further description of each component of the simulator in order to clarify the overall design.

2.3.2.1 Air Plenum

As previously noted, it is desired to have air flow through the simulator. The principal reasons for air flow are:

- to minimize the aerosol content of the air which will be ionized
- to ensure that effluents from animal waste do not enter the animal housing area
- to prevent the buildup of ozone.

In addition to the above factors which can be effected if the simulator is designed to accommodate air flow, the air flow through the simulator can be thermally and humidity conditioned to minimize the influence of these variables on the experiment.

The plenum of the simulator is simply a transition for the input air stream from the geometry of the air duct to the geometry of the simulator. The plenum configuration is not highly critical, and two different plenums have been used in the simulator development. Both plenums have been made of plastic. The first plenum, which was illustrated in the third and fourth quarterly reports was pyramidal in shape and assembled from machined Plexiglas pieces. The fabrication expense of such units was quite high. Therefore, to minimize the cost associated with the fabrication of a large number of simulators, a modified plastic skylight was used as the plenum for the final prototype simulator.

It is necessary that the air flow past the corona wires and into the exposure chamber be relatively uniform throughout the cross section of the simulator. Thus, diffusers are employed to help in establishing velocity uniformity. A concentric ring diffuser is mounted just below the air inlet, as is shown in the plenum photographs of Figure 2-10. Additional air diffusion is provided by a sheet of perforated metal, which is physically located

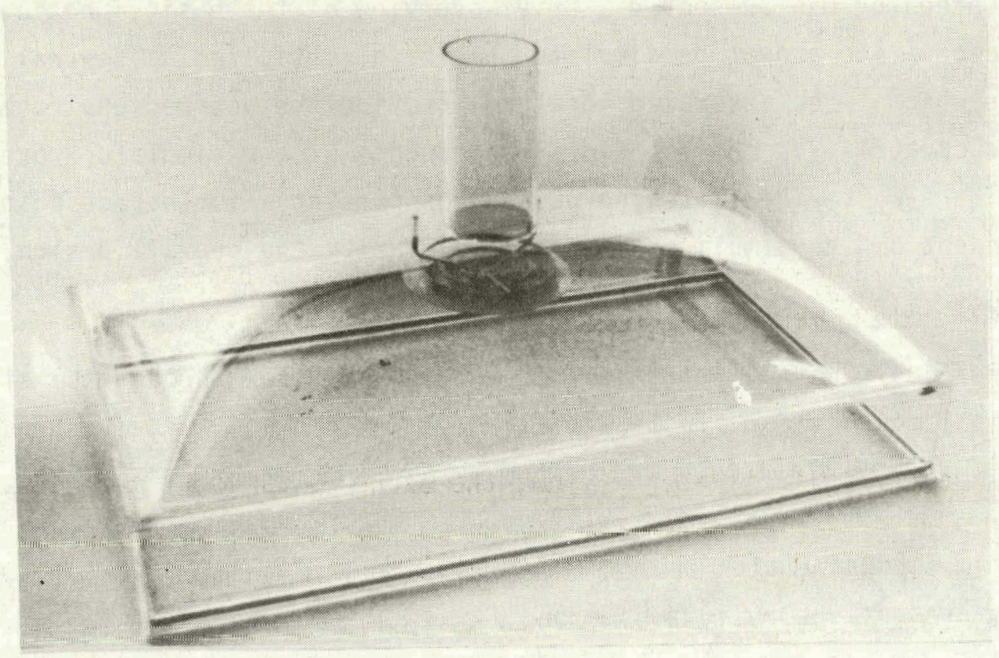

(a) Overall View of Plenum

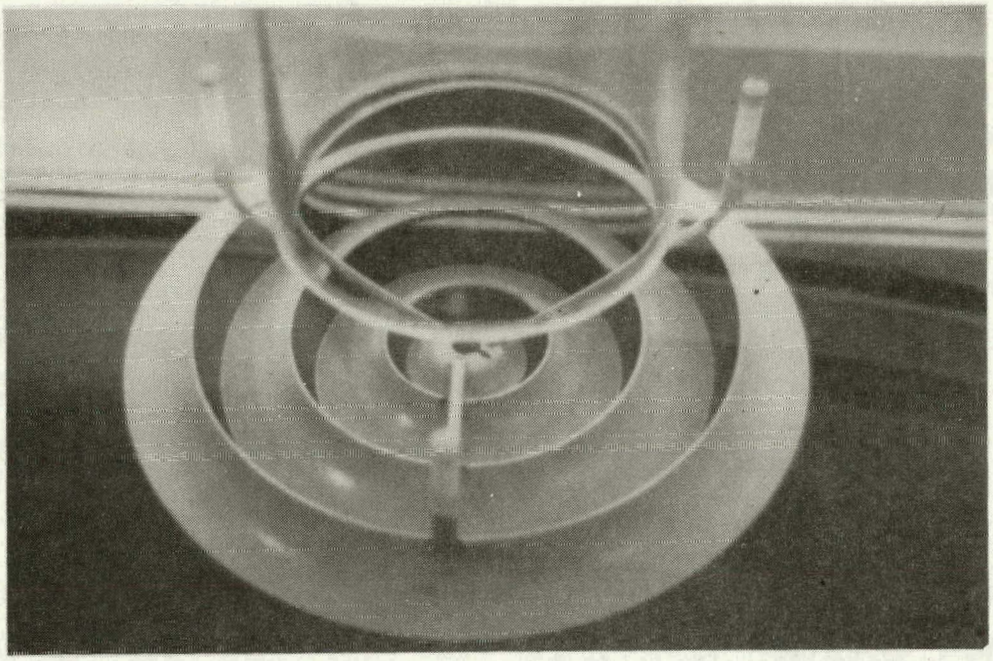

(b) Plenum Air Diffuser

Figure 2-10 Prototype Air Plenum

in the top of the corona section of the simulator, just below the plenum. This air diffusion grid has 0.033-inch diameter holes and is 21% open. The perforated metal air diffusion grid provides a restriction to the air flow, due to the small percentage of openness, thus causing a velocity equalization over the simulator cross section. The air diffusion grid is supported by, and lays on top of, a one-half inch thick plastic grid which serves to provide some straightening of the air flow. Figure 2-11 shows a photograph of the air-diffusing and straightening grids on top of the corona chamber. For this photograph, the diffusion grid has been moved somewhat to show the supporting straightening grid below it.

The air flow through the simulator results in lowered ozone levels in the exposure chamber. Without an air flow, the ozone level tends to build up. However, with air flow, the ozone stabilizes at an acceptably low level. The air flow rate which has been used with the prototype simulator is quite low (35 cfm or less) and does not appear to directly influence the ozone levels for rates between 15 and 35 cfm. At 35 cfm of air to the chamber, the measured air velocity within the chamber is within the range of 5-7 feet per minute. This air velocity is quite small compared to the ion velocity, which is in the range of 6 m/s ($\sim$ 20 ft/s) for a 30 kV/m field in the exposure section. However, it has been noted that the air flow has the effect of increasing the current density at the simulator ground plane by a few percent.

2.3.2.2 Corona Chamber

The corona chamber is where the ions are produced. The ion source is a series of parallel wires which are placed into corona by a voltage between the wires and the corona grid, which forms the top of the grid section. The prototype corona section was empirically designed, with a large number of variations being investigated. However, after initial investigation of needle-type corona ion sources, the wire sources were selected and subsequently exclusively employed.

Major considerations which influenced the corona chamber design included:

- the wall material;
- the number of wires;
- the spacing between wires;
- the height of the wires above the corona grid;
- the wire diameter;

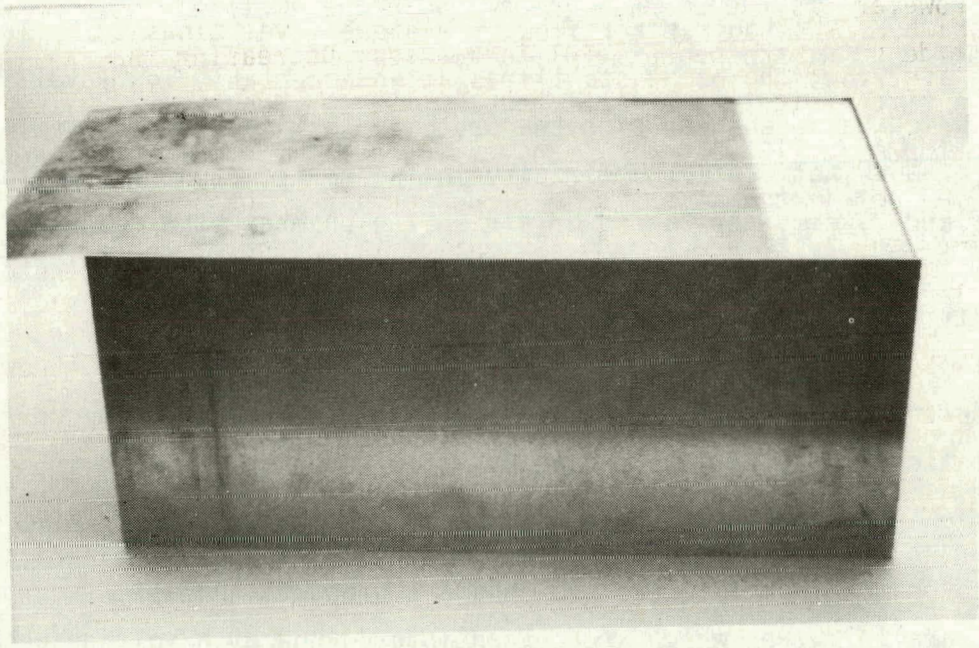

Figure 2-11 AIR DIFFUSING AND STRAIGHTENING GRIDS AT TOP OF CORONA SECTION

- the method of feeding and terminating the wire ends.

These factors have an influence on

- the uniformity of ion generation along the wire length;
- the ion density between wires relative to below a wire;
- the ion uniformity near the side and end walls;
- the ozone levels.

The wire diameter is a major factor in determining both the uniformity of ion generation along the length of the wire and the ozone generation, for a given wire corona current. For a given wire size and wire configuration, the ion current becomes more uniform as the corona current to the wires is increased. However, as the corona current is increased to effect a more uniform ion current density, the ozone level increases. Decreasing the spacing between wires, at a given height above the corona plate, produces more uniform current density in the central region for a given current per wire, but increases the ozone and may not improve the side wall performance. Decreasing the wire diameter improves both the ion density uniformity along the wire length and the ozone levels, for a given current per wire.

The corona wire configuration employed for the final prototype simulator appears to be a reasonable compromise between the above factors. Tests have shown quite uniform ion current densities in the exposure chamber, both in the central region and near the side and end walls. The ozone in the exposure chamber (animal caging section) is below detectability for the final prototype simulator.

The walls of the prototype corona chamber are aluminum. The use of conducting corona chamber walls prevents ion charging of the walls, which appeared as a potential problem when Plexiglas walls were used for an earlier simulator.

The corona wires are 1-mil diameter steel wires. There are seven wires which are equally spaced across the width of the chamber (approximately 2.5-inch spacing). The wires are at a height of 2.5 inches above the corona grid. The sketch of Figure 2-12 illustrates the manner in which the wires are terminated at the end wall of the corona chamber.

In order for the ion current density to be maintained near the end wall, it is necessary for the corona wires to extend nearly to the end walls, as is accomplished by the design shown in Figure 2-12. The arrangement shown allows

the wires to be fed without producing fields that upset the current density distribution near the wall. As shown, the wires are fed through grommets which are glued to a sheet of Plexiglas that is attached to the end wall of the chamber. The wires are kept in tension by the springs shown, which are attached to a metal feeder strip. The high voltage is applied to the feeder strip. The vertical run of the wires does not corona, after an initial brief period following turn-on, since the plastic becomes charged and inhibits further corona of these wire sections.

Figure 2-13 is a photograph of the corona section showing the end arrangement and feed. The high voltage is applied via an RG-8/u coaxial cable with the outer conductor stripped away. The cable is fed through the chamber side wall and is attached to the feeder strip by a mounting block and set screw. The corona wires cannot be seen in the photograph due to their small diameter.

2.3.2.3 Grid Section

The grid section of the simulator is mechanically quite simple, yet functionally very important. The grid section is shown in the photograph of Figure 2-14. The grids have been offset to show the silver-coated edges of the grid spacer. The section is comprised of two sheets of 51% open perforated steel. The perforated material is 0.06-inch thick with 3/16-inch holes, spaced on 1/4-inch centers. These two sheets are separated by a two-inch high frame of phenolic. A previous prototype grid section used 1/4-inch hardware cloth as the grids (see Figure 29 of Third Quarterly Report); however, internal spacers were required in the grid section to maintain flatness of the hardware cloth. Early experiments with a design model simulator indicated that only slight differences in ion current resulted from the use of different grids - the principal difference being in the percentage open area (see p 33, Third Quarterly Report). While the first prototype grid (using hardware cloth) performed well, it was much more complex to fabricate. Therefore, the grid section was simplified in later prototypes by using the perforated steel sheets as the grid material. These grids are sufficiently rigid to require no internal supports to maintain flatness.

The use of a phenolic frame as a grid spacer is likely to be somewhat arbitrary. The first prototype used phenolic material, and since this performed in an acceptable manner, the same material was used for later prototypes. The resistivity of the phenolic is in the range of 10^9 ohm-cm, which is adequate

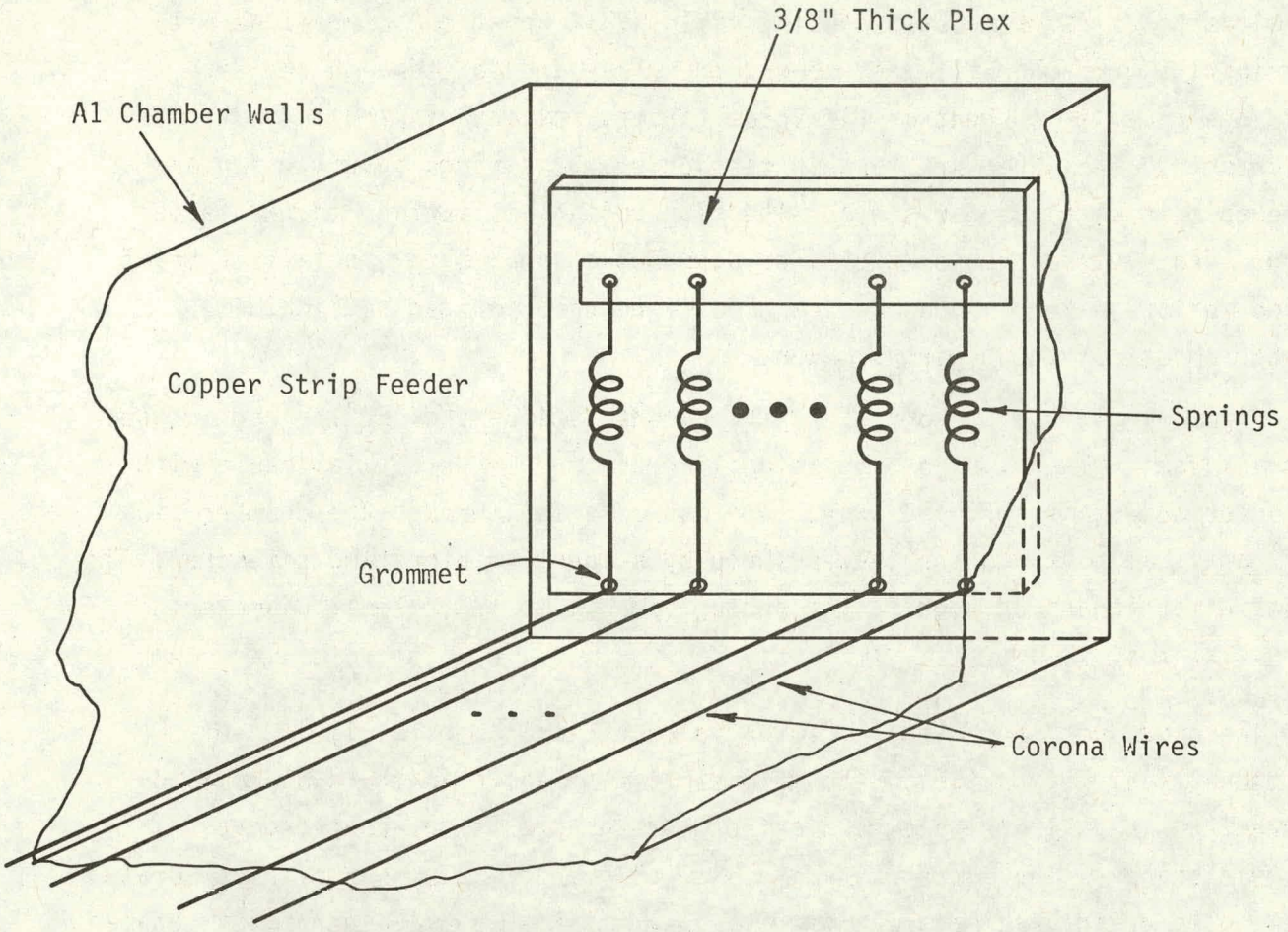

Figure 2-12 SKETCH OF CORONA WIRE TERMINATIONS AT END WALL OF CORONA CHAMBER

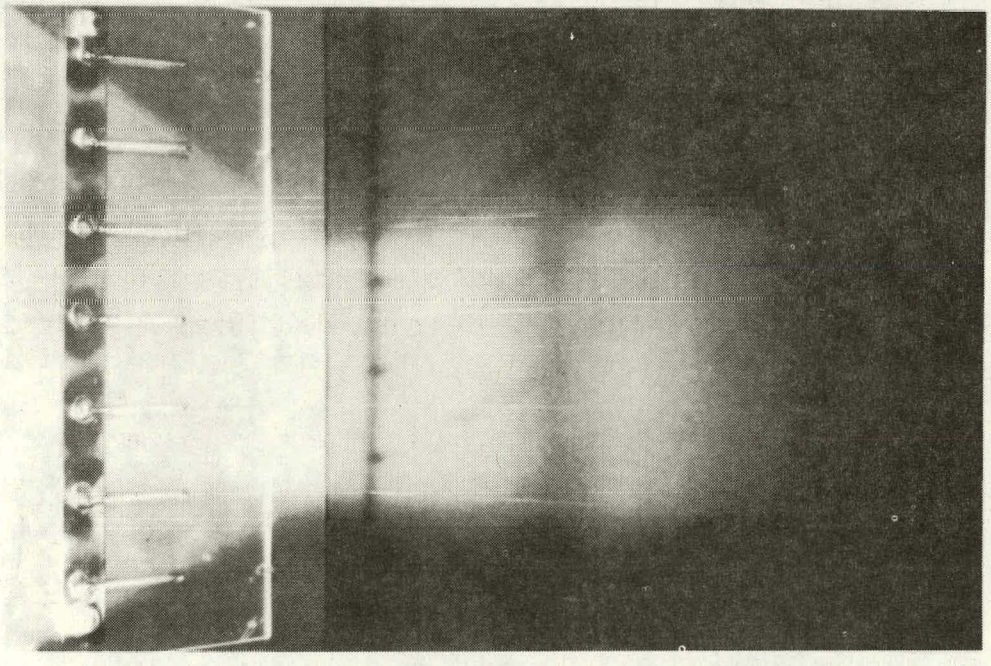

Figure 2-13 PHOTOGRAPH OF INSIDE END WALL OF CORONA CHAMBER

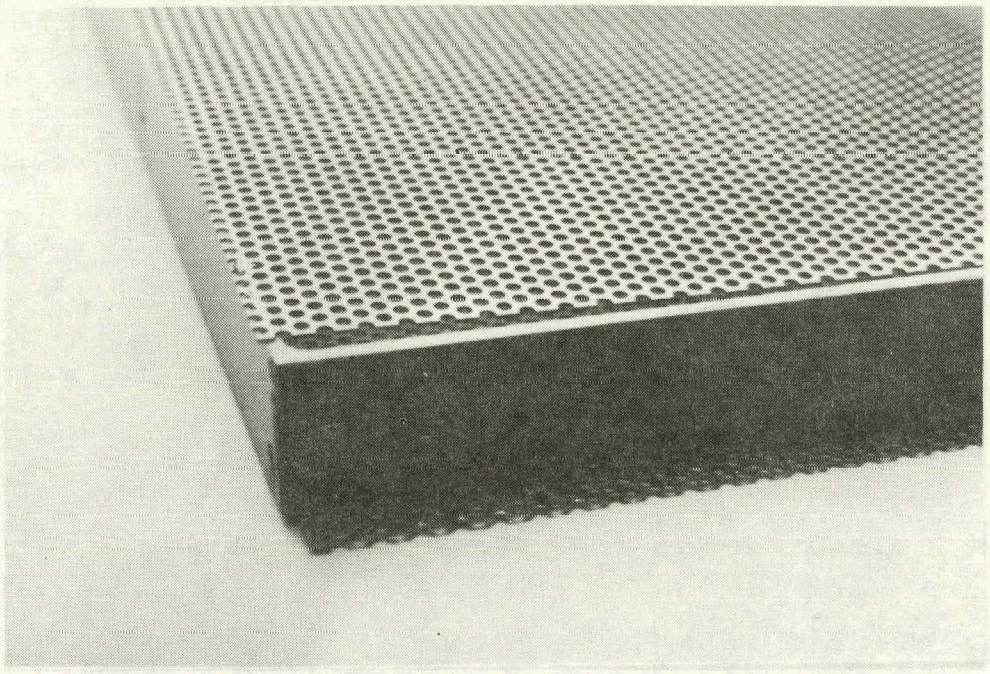

Figure 2–14 GRID SECTION

to prevent field fringing at the periphery of the grids. The edges of the grid spacer are coated with silver paint and overlayed with conductive adhesive copper tape, which provides a good conductive contact between the grid spacer and the two grids. The grid spacing has been found to not be a critical parameter. Initial experiments, with different grid spacings showed somewhat improved ion current density uniformity with larger grid spacings, for very low current densities. However, a brief experiment with a later prototype using a six-inch grid spacing showed no substantial improvement over a two-inch spacing. The samller spacing requires a smaller grid bias voltage for a given current density and, therefore, appears to be a reasonable choice.

2.3.2.4 Animal Caging Section

The animal caging section of the simulator is a very crucial component, which has required careful attention during the Phase I design and development effort. In addition to providing suitable housing for the animals, with observation and access by the biological staff, the caging area must maintain field and ion current uniformity, while ensuring that the animals do not encounter shock or current flows that are unique to the simulator implementation.

The basic concept for the caging area has been outlined in Section 2.2, where the use of conducting walls which extend between the control grid and the ground grid was described.

Caging area walls which have a finite bulk resistivity will permit current to flow through the walls if the top and bottom of the walls are in electrical contact with the control and ground grids. If the volume resistivity of the wall material is uniform, the potential gradient within the wall will be the same as the nominal electric field between theoretically infinite extent parallel plates. Thus, the use of conducting walls at the edge of finite-dimension parallel plates provides a convenient and simple means for eliminating fringing-field effects which are normally associated with finite-sized plates. When the ion current density produced in the simulator is restricted to values shown in Figure 2-5 or less, for a desired field level, the fields near the walls should not differ appreciably from the fields at locations remote from the walls.

The above considerations suggest finite conductivity walls, but do not provide guidance as to an acceptable conductivity range for the wall material. Two factors have been identified and used as guidance in the investigation for

suitable wall materials. One factor provides guidance on the upper range of resistivity, while the other provides guidance on the lower range of resistivity. Neither of these factors provides firm numbers for acceptability, but they have allowed the choice of a material to be made which appears to be a reasonable compromise.

The factors guiding wall material selection were:

- If the material has too high resistivity, any charge which may be deposited onto the wall surface will become trapped, thus distorting the field and ion current flow in its vicinity until the charge leaks off.

- If the material has too low resistivity, the current which may be drawn by an animal when in contact with the wall may be excessive. The current flow to the animal occurs because the animal is essentially a low impedance path to ground, while the wall is a current-carrying conductor with the upper surface at a high potential.

As an example to illustrate the first factor, i.e., the trapping and leak-off of charge, the results of a simple comparative test will be described. Samples of sheet glass (0.22-cm thick), canvas-reinforced phenolic (0.5-cm thick) and Plexiglas (0.5-cm thick) were cut into square, 4' x 4' samples. Conductive adhesive copper tape was applied to the peripheral edges of those samples. The samples were each placed on small 0.5-cm thick styrofoam supports so that they were parallel to a ground plane in which a Monroe 225 field meter was mounted. The sample was directly above the field meter aperture, a vertical electric field and ion flow was established so that the sample (which was insulated from ground by the styrofoam supports) accumulated ions. The field sensed by the field meter thus became very large due to the trapped charge and the test sample. After the test sample was charged, the field and ions were shut off. The peripheral edge copper strip on the sample was then grounded, allowing the charges to flow to the edge of the sample and thus to ground. As the sample discharged, the electric field beneath the sample decayed to zero. The field decay time for the different sample materials is a measure of the ability of the material to drain off charge. For the three materials tested in this manner, the times for the field to decay to 1/e of the initial value are shown in Table 2.2.

The specific discharge times shown are dependent on geometry factors associated with the experiment. However, the sample decay time relative to

the other samples provides some guidance on the material acceptability. It is obvious that the charge drain-off from the phenolic, with $\rho_b \sim 10^9$ ohm-cm, should be quite acceptable. It is also apparent that the decay for Plexiglas with $\rho_b > 10^{16}$ is too slow to be acceptable.

Table 2-2

CHARGE DECAY TIME FOR THREE MATERIAL SAMPLES

Material	Field Decay Time
Canvas Reinforced Phenolic	t < 1 sec
Glass	t = 15 sec
Plexiglas	t > 200 min

Early in the investigation, it became apparent that most common commercially available polymers and compounds were too high in resistivity to be useful for the application. This point was emphasized with the first prototype simulator which employed Plexiglas walls for the corona chamber. It was observed that the ion current density in the animal housing area could be significantly affected if a grounded object such as a person were to come near the corona chamber. The current density could remain disturbed for a considerable period of time, even though the person left the area. Figure 2-15 shows the results of a test that demonstrates this effect. For this test, the current density probe was placed on the ground plane near one of the side walls inside the animal exposure section. For a given condition of corona wire current, plate voltage, and grid bias voltage, a current density of 350 nA/m^2 was obtained. After this, a person held his hand approximately four inches from the the side of the corona chamber for a period of approximately ten seconds. Initially, the measured ion current density increased; however, when the person's hand was removed, the ion density went to near zero. Figure 2-15 shows the gradual increase in measured ion current density versus time after the person's hand was removed from near the side of the corona chamber. It is seen that a very long time is necessary in order for the equilibrium ion conditions to be re-established.

It was deduced that the presence of a person's hand near the side of the corona chamber caused a disturbance of the field lines in the corona chamber, with field lines going between the nearest corona wire and the person's hand. The ions were thus attracted in the direction of the person's hand and collected

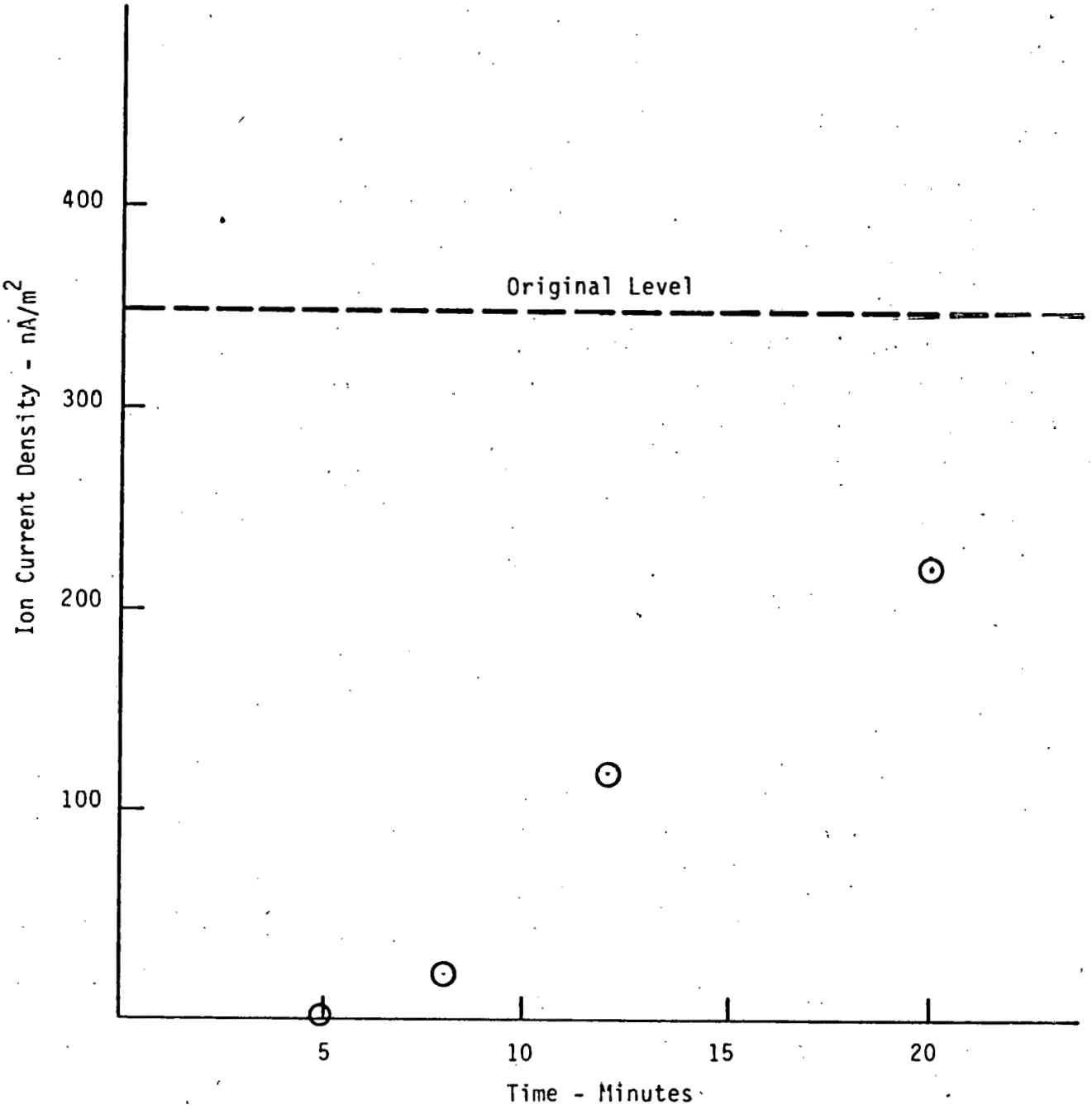

Figure 2-15 DEPRESSION OF ION CURRENT DENSITY NEAR WALL OF EXPOSURE CHAMBER - AFTER HAND HELD NEXT TO PLEX CORONA CHAMBER

on the side walls of the corona chamber. These ions were trapped on the wall by the Plexiglas material. When the person's hand was removed, the field of the trapped charges caused ions to be repelled from the general region of the wall. Thus, the observed effect was a reduction in ion current density near the wall. Due to the high resistivity of the Plexiglas material, a considerable time was necessary for these charges to drain off the wall, and for equilibrium conditions to be re-established. This test showed the desirability of using conducting material walls for the corona chamber and re-emphasized the care that must be exercised in the use of plastic materials in the simulator.

As noted above, many of the materials for which bulk resistivity tests have been performed evidenced resistivity values which would result in charge decay times which were considered to be too long. At the other end of the range, materials were eliminated from consideration due to the possibility of excessive current to an animal contacting a wall.

An approximate expression has been derived to determine the short circuit current drawn by a wall contact of diameter d at a height of h_2 from the ground plane, when the total wall height is h_T and the top of the wall is at a voltage V_o. The expression is

$$I_{sc} = \frac{2\pi t h_2 V_o \, (\ell n \, 4 \, h_1/d + \ell n \, 4 \, h_2/d)}{h_T \rho \, \ell n \, 4 \, h_1/d \, \ell n \, 4 \, h_2/d} \qquad (2\text{-}2)$$

where

h_2 = the height from the ground plane to the contact

h_T = the total height of the wall

h_1 = $h_T - h_2$

d = diameter of the contact

t = thickness of wall material

ρ = resistivity of wall material

V_o = voltage from top to bottom of wall

I_{sc} = short circuit current drawn from contact at height h_2 to ground.

As an example of the use of the above expression, Figure 2-15 shows the short circuit current anticipated for an 0.5 cm diameter wall contact as a function of height for a 50-cm high wall at a potential of 50 kV versus the wall material resistivity. For this example, a wall thickness of 0.4 cm has been assumed.

As a reference for comparison, the 50-kV wall potential will be associated with a 100-kV/m nominal field in the caging area. If a 900-nA/m^2 ion current density is associated with this field (about three times the field and ion current density typically reported under test and operating HVDC lines) and is collected by a test animal of base area of 0.013 m^2 with an enhancement factor of 3, the animal will receive about 35 nA. For the assumed contact area, such a wall current would be drawn by an animal making contact to the wall at a height of 20 cm for a material resistivity somewhat less than 10^{12} ohm cm. Thus, it appears that if the wall current which can be drawn by an animal is to not exceed the current normally collected by exposure to the ion current flow, the material resistivity should be in the range of 10^{12}-10^{13} ohm cm.

Material resistivity testing showed that very few materials possessed resistivities in the above range. When the desire for the material to be transparent (to permit animal viewing and adequate light levels within the animal housing area) was superimposed on the material resistivity considerations, only one tested material appeared to be suitable. Commercially available soda silicate plate glass has a bulk resisitivity of approximately 10^{13} ohm cm, and appears to possess the variety of other properties felt to be desirable for use in fabricating the animal caging section of the simulator.

The walls of the first prototype simulator were made of canvas reinforced phenolic which was felt to be too low in resistivity, was too hygroscopic, and was not transparent. Thus, this material was unsuitable for the final simulator design; however, it was felt to be suitable for the purpose of preliminary electrical investigations of the basic simulator geometry; and at that point in time, glass had not been identified as a candidate material.

After identification of glass as a candidate material, the first prototype simulator was modified to include one glass wall. A test was conducted to determine the current drawn from a known sized wall contact, for both the glass wall and one of the phenolic side walls. A 3/4-inch by one-inch piece of

conductive adhesive copper foil tape was placed on both the glass wall and on a phenolic wall at a height of nine inches above the ground plane. The voltage gradient in the wall material for this test was 30 kV/m.

The current measured from the phenolic and glass contacts are shown in Table 2-3. Shown also in the table are the measured values of bulk resistivity for samples of the glass and phenolic made at the time of these tests. When the geometry factors applicable for this test are substituted into the approximate expression given above as Equation 2-2 for the short circuit current, the expression for the current reduces to

$$I_{sc} = \frac{1.56\, t\, V_o}{\rho}$$

Substituting the material thickness, the measured resistivity of Table 2-3 and the voltage across the wall of 15 kV, gives the calculated values for current that are also listed in Table 2-3 for the two wall materials. A reasonable comparison between measured and calculated values is seen.

Table 2-3

CURRENT FROM 3/4" x 1" WALL CONTACT

Wall Material	Measured Current to Ground From Wall Contact	Calculated Current	Wall Resistivity
Phenolic	9 μA	1.9 μA	5×10^9 Ω-cm
Glass	0.8 μA	0.75 μA	10^{13} Ω-cm

Top of wall at 15 kV, contact height of 9".

The above tests illustrate that the current which can be drawn from materials with resistivity in the range of the phenolic might be excessive; and that the current drawn from a glass wall appears to be acceptable, in light of the discussion which was presented in association with Figure 2-16. The wall contact current question has been further assessed by tests with a rat contacting either a phenolic or glass wall.

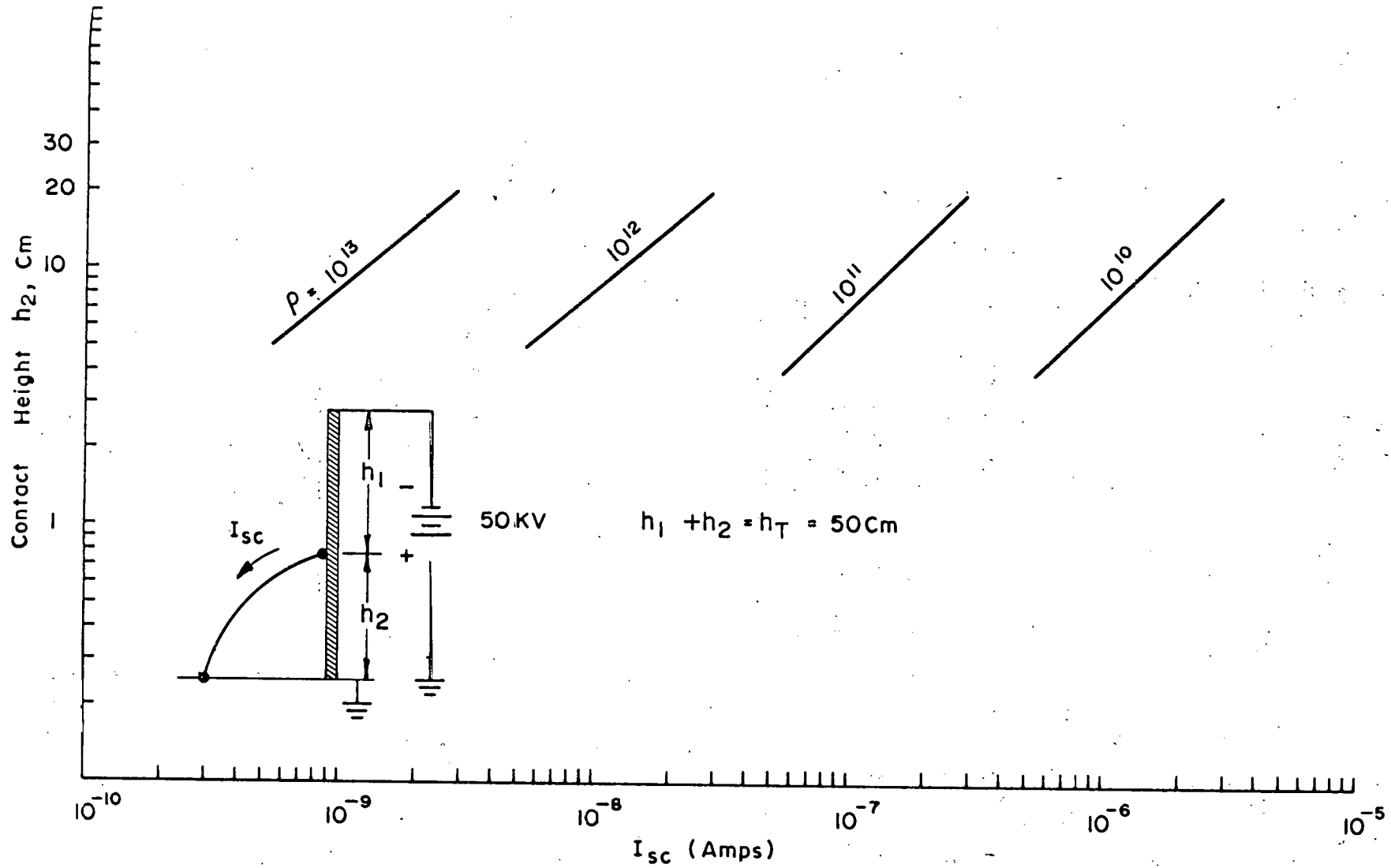

Figure 2-16 SHORT CIRCUIT CURRENT TO GROUND PREDICTED FOR 0.5 CM DIA. WALL CONTACT VS. CONTACT HEIGHT

For these tests, a rat was placed in a prone or upright position, either contacting one of the walls or in a region away from the walls. The anesthetized rat was tied to a metal support fixture which was insulated from ground so that the current collected by the rat could be measured with an electrometer. The modified first prototype simulator was used for these tests. Figure 2-17 shows the rat in position for one of the tests. The simulator plate voltage was set at 15 kV, thus producing a nominal 30-kV/m electric field for these tests. An ion environment was also used for some of the testing; in these cases, a current density of 400 nA/m^2 was used.

Table 2-4 summarizes the results of these tests. For the case shown, where the rat was in the upright position contacting the walls with only an electric field but no ions, it is seen that the current drawn by the rat due to the wall contact is very similar to that shown in Table 2-3 for a metallic spot contact to the wall. With the rat in the upright position and ions also in the chamber, it is seen that the current collected by the rat when in contact with the phenolic wall was the same as with no ions, thus indicating that the current drawn from the phenolic wall completely controlled the current collected by the rat. However, with the rat in the upright position and in contact with the glass wall,

Table 2-4

CURRENT COLLECTED BY RAT

	Position		
	1	2	3
Rat Prone With Ions	90 μA ? μA	14-16 nA	14-15 nA
Rat Upright With Ions	4 μA	24 nA	23 nA
Rat Upright Without Ions	4 μA		1 nA

Position 1 - Touching Phenolic Wall
" 2 - In Space Between Walls - Not Touching Wall
" 3 - Touching Glass Wall

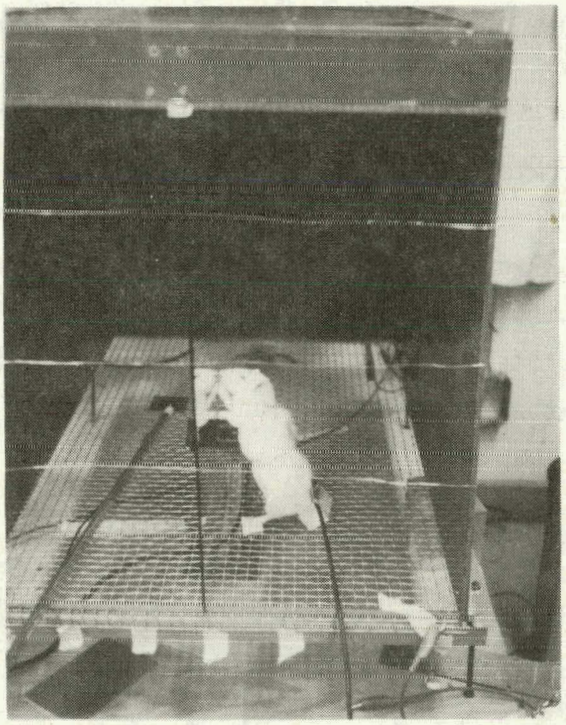

Figure 2-17 PHOTOGRAPH OF RAT IN UPRIGHT POSITION FOR TEST OF CURRENT FROM WALL

the current drawn by the rat was essentially the same as when the rat was in the space between the walls and only collecting ion current. Also, for the case where the rat was prone, the current drawn by the rat when in contact with the glass wall was essentially the same as when the rat was not in contact with either wall. However, when the prone rat contacted the phenolic wall, considerably more current flowed through the rat, the total current being dependent on how well the rat contacted the phenolic wall.

The results of the two above experiments indicate that the basic bulk resistivity of the glass wall material appears to be sufficiently high so that the current drawn by a rat test subject will be dominated by the current collected by the rat from the ion current density environment, and not by current drawn due to wall contact. Thus, from this standpoint, glass appeared to be an acceptable material for use in fabricating the animal caging section of the simulator.

Considering again the discharge characteristics illustrated previously by the data of Table 2-2, it is seen that while the phenolic resistivity results in a considerably faster discharge than glass, the glass discharge time is orders of magnitude better than for materials with resistivities in the range of Plexiglas. However, the animal current which can be drawn by an animal from phenolic range resistivity wall material appears excessive, while glass walls appear to result in an acceptable range of animal current. Thus, the use of glass as a caging area wall material appears to be a reasonable compromise when the high and low resistivity constraints identified above are considered.

The foregoing discussion on the conduction properties of glass has centered on the bulk properties of the material. For an application such as is envisioned for the simulator, the surface properties of the candidate wall material must also be considered. The surface conduction properties of the caging area wall material is important, since the surface conduction forms a shunt path with the bulk conduction of the material. Since the bulk properties of glass are determined by the glass composition, which is quite closely controlled during manufacture, the bulk properties are anticipated to vary negligibly over a sheet of dimensions necessary for the fabrication of a caging area wall. Thus, it is desired to insure that the dominant conduction is through the bulk, with a negligible or small conduction contribution due to the material surface properties. A considerable amount of investigation has

been performed in the study of the surface properties of glasses (Holland, 1964 and Koranyi, 1963). It is well documented in the literature that the surface conductivity of glasses is a strong function of relative humidity. Typically, the surface resistivity of glass shows a marked and rapid decrease in the range between 30-60 percent relative humidity. Figure 2-18, which was extracted from Holland (1964), illustrates this behavior for plate glass samples obtained by two different investigators. It is generally agreed that moisture which is adsorbed on the glass surface combines with the alkali in the glass to form a conducting electrolite. To circumvent these surface conductivity problems with glass, the surface is often treated with either wax or silicone compounds. The objective of either treatment is to prevent the moisture adsorption at the surface of the glass.

We prepared glass samples and coated them with various hygrophobic compounds for the purpose of increasing the surface resistivity of the glass. Compounds tested included organotitanate, chlorobenzotrifluoride, and dimethylsiloxane, as well as a commercially available hygroscopic agent. Of these, the dimethylsiloxane resulted in the largest surface resistivity, giving a surface resistivity of approximately 2×10^{14} ohms per square for both normal laboratory conditions, after exposure to a controlled 75 percent relative humidity, and after immersion in water. Also of significant importance is that a silicone treatment protects the glass surface from the degrading influence of common contaminants. For example, the surface resistivity of a clean glass sample decreases by several orders of magnitude after the glass has been fingerprinted. However, fingerprinting of a glass sample which had been treated with dimethylsiloxane had no apparent effect on the measured surface resistivity.

Three different glass prototype animal caging sections for the simulator have been fabricated and tested. Initial tests with the first glass prototype provided an indication that it is necessary to control the surface conduction properties. The final prototype has been coated with dimethylsiloxane, and the test results presented in the next section are for the coated condition.

Investigations have shown that the bulk resistance properties of available sodium silicate glass sheets is in an acceptable range relative to discharging trapped ions in a reasonable time, and preventing excessive current to be drawn by animals that will contact the walls. The surface conduction properties of the glass walls must be controlled to prevent wall gradient nonuniformities. The use of a silicone-derived compound such as dimethylsiloxane

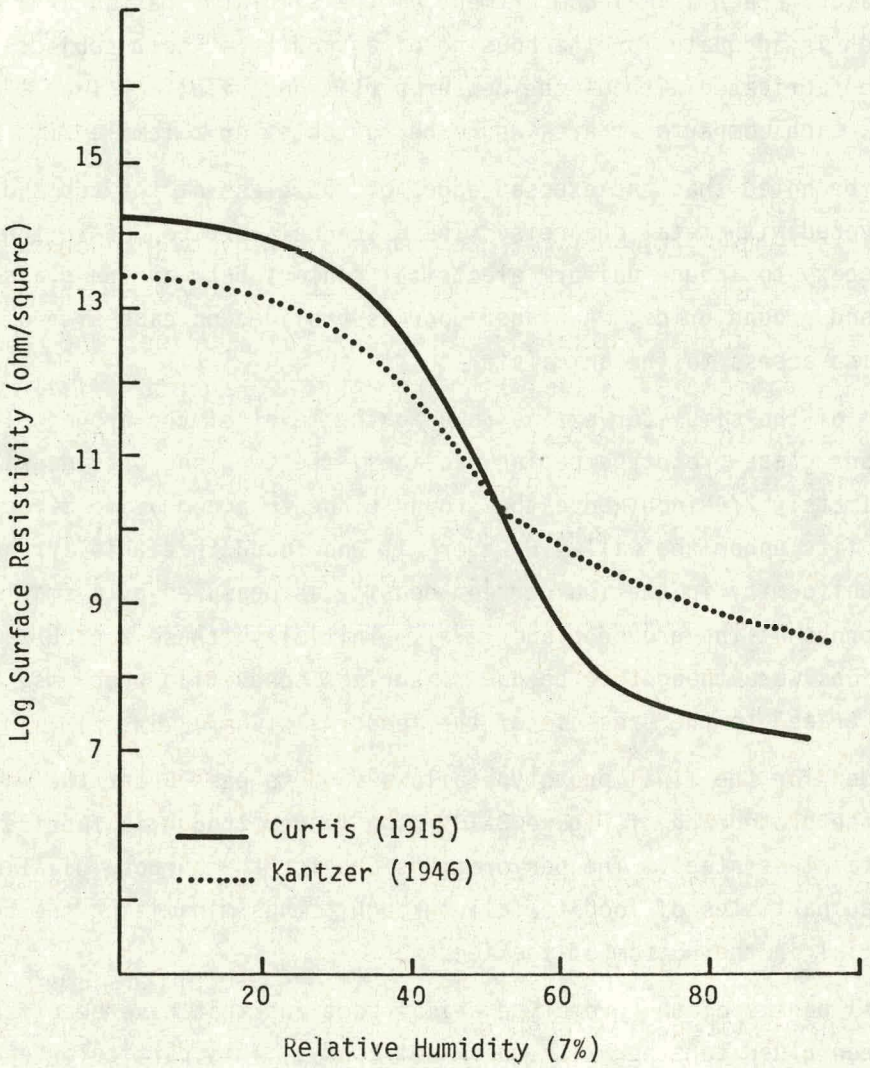

Figure 2-18 SURFACE RESISTIVITY OF PLATE GLASS AS A FUNCTION OF RELATIVE HUMIDITY

as a wall coating appears to stabilize the glass surface conduction properties and results in a conductivity that is sufficiently low to provide acceptable simulator performance.

Figure 2-19 is a photograph of the prototype glass animal caging section of the simulator. Each animal compartment of the simulator has an area of 8" x 10", which is adequate for the housing of an adult rat test subject. If the unit were fabricated without the center partitions, i.e., as four 8" x 20" compartments, each compartment area would be suitable for a female with litter.

It will be noted that the exposed edges of the glass at the top and bottom have been covered with metal channels. These channels are bonded to the glass with silver epoxy to insure uniform electrical contact between the glass and the control and ground grids. A hinged door is provided on each side of the unit to provide access to the animals.

All walls of the simulator extend down to the level of the ground plane. In the previous glass prototype caging sections, the two long outside walls ended approximately 3/4-inch above the ground plane to accommodate a feeder trough which fits under the wall. However, it was found that this arrangement caused a nonuniformity in the ion current density as measured by a small 10 cm^2 active area probe at the ground plane level. Initially, these ion current density distortions were thought to be due to surface conduction problems, but were finally traced to the presence of the feeder slot.

The feeder for the final prototype allows food to pass under the wall as is shown in the photograph of Figure 2-20. The feeder trough is fabricated of perforated stainless steel. The perforations are for the purpose of allowing the pulverized particles of food to fall through - thus minimizing the buildup of this material in the bottom of the feeder.

The glass panels of the prototype animal sections that have been fabricated have been glued together with quick-set epoxy. This particular epoxy has been used as a fabrication expedient, due to its rapid cure time. This epoxy does not possess adequate high temperature stability to withstand the rack washer temperatures. Therefore, for fabrication of the simulators for the Phase II effort, a higher temperature epoxy will be necessary. The use of such longer cure time epoxy will require the fabrication of suitable jigs to hold the glass assembly together until cured.

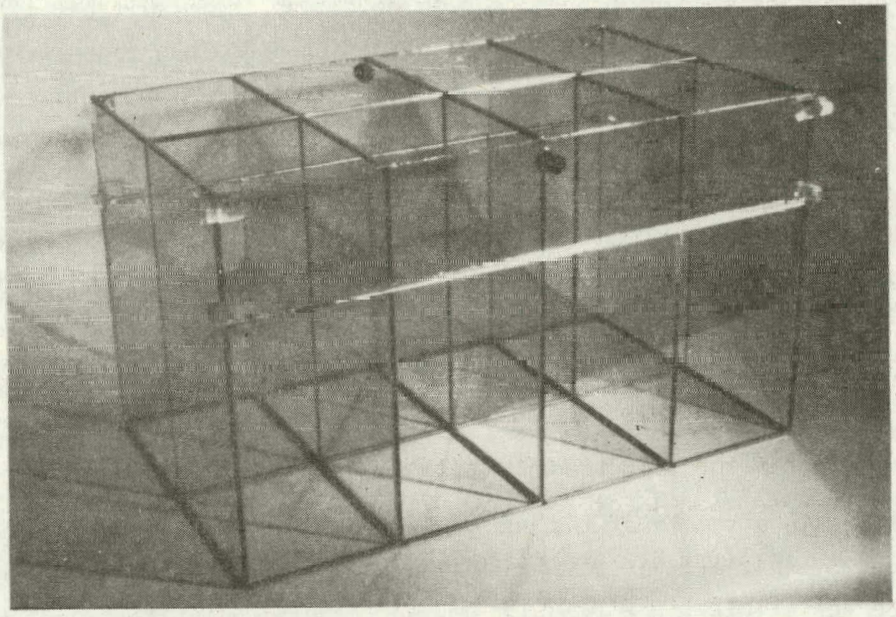

Figure 2-19 FINAL PROTOTYPE ANIMAL CAGING SECTION

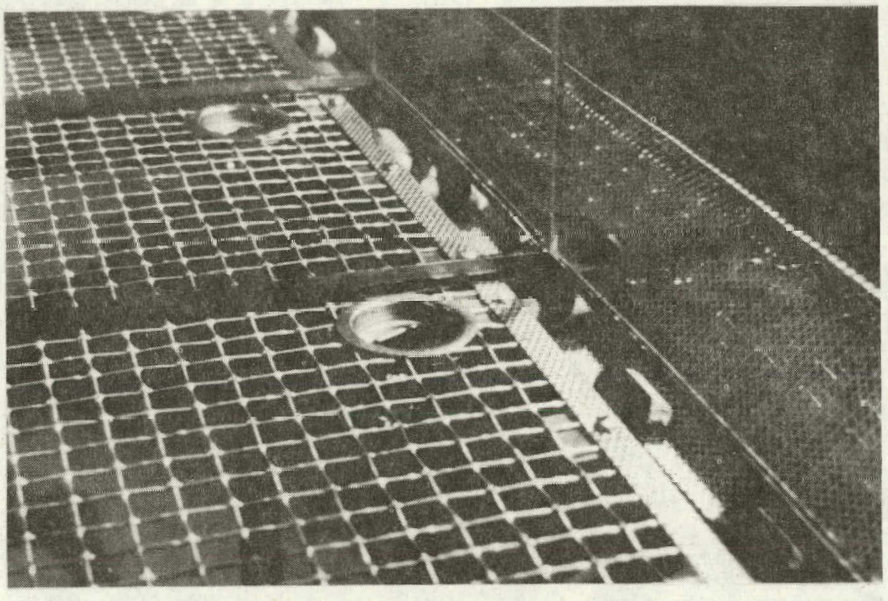

Figure 2-20 UNDER-THE-WALL FEEDER TROUGH VIEWED FROM INSIDE ANIMAL COMPARTMENT

Several epoxies have been tested to determine their suitability as an adhesive for assembling the glass caging section. Of importance was the ability of the epoxy to maintain its physical and electrical properties when subjected to high temperature water, which may be used in washing the cages.

A suitable epoxy is Epon 815 which is manufactured by the Shell Chemical Company. The viscosity of this epoxy was increased by adding 5% by weight of coloidal silica (Cabosil). It appears desirable to cure the epoxy for about two hours at a temperature in the range of 50°C.

Tests showed that glass samples which had been glued together as a butt joint with the above epoxy, then cured, remained physically strong after soaking in 85°C water for over twenty minutes.

Tests with a sample of the epoxy which was formed as a 10 cm x 10 cm x 0.2 cm sheet, suitable for testing in the H.P. 16008A resistivity cell, showed a surface resistivity $\rho_s > 10^{16}$ ohm cm, and a bulk resistivity $\rho > 10^{15}$ ohm cm, both before and after soaking for twenty minutes in 85°C water bath. Thus, this epoxy appears to be suitable for use in assembling the glass caging section of the simulator.

2.3.2.5 Base Section

The base section of the simulator places the remaining portion of the simulator at a convenient height for maintenance of the animals. The base section incorporates the ground grid, the watering manifold, the feeder trough, and the waste collection pan, which is located below the ground grid. The base section and the animal housing section can be wheeled as a unit to the washer. Figure 2-21 is a photograph of the base section.

The frame of the base section is made of steel angle for the prototype. The ground grid is made of steel hardware cloth. Both these components will be fabricated from stainless steel for the Phase II units to be built. The presently used materials were selected as an expediency. The ground grid of the base is 1/2" x 1/2" mesh. The feeder troughs are permanently-mounted stainless steel units as previously shown in Figure 2-20.

Water is provided to each animal compartment by Edstrom pivoting stem drinking valve units which are mounted in the ground mesh. Thus, both the water and feeders are at ground potential, the same as the animal that is in contact with the ground grid.

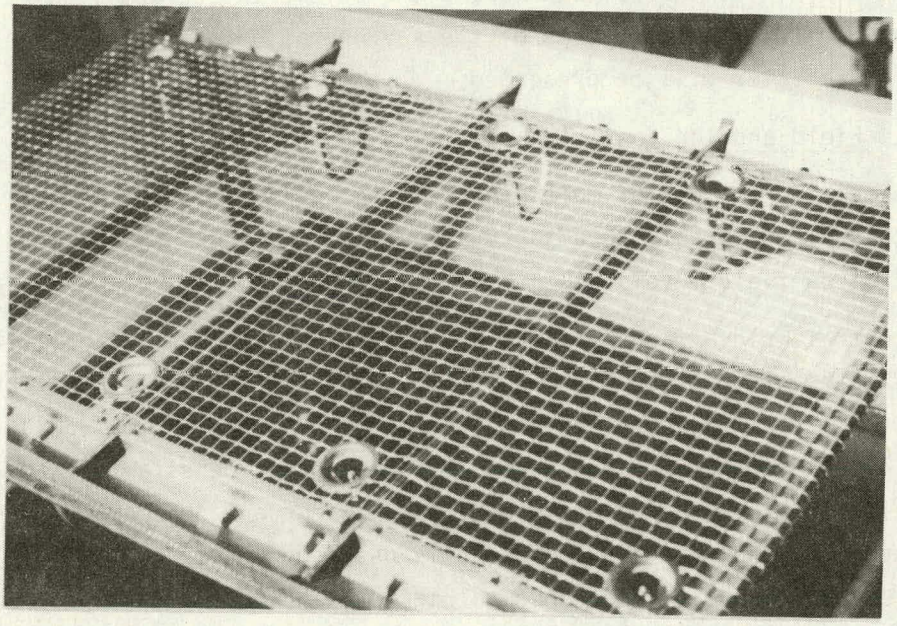

Figure 2-21 PHOTOGRAPH OF BASE SECTION

The animal waste is collected by the collection pan located below the ground grid. The air flow through the simulator exits through the ground mesh, thus inhibiting the waste effluents from rising into the animal caging area.

2.4 Prototype Simulator Electrical Performance and Operating Characteristics

Previous sections of this report have described the basic considerations thought to be important in simulator design. The influence of these considerations on the design of the simulator was also discussed. The prototype simulator which has resulted from this program has been described, both in terms of the function of various components and the physical description of these components. In this section, some of the key operating characteristics of the overall simulator will be presented.

2.4.1 Field and Ion Control

In describing the use of multiple grids in the design, it was noted that it was necessary to be able to adjust various combinations of ion current density and desired field levels.

The control grid arrangement was employed to provide this capability. Figure 2-22 presents curves which show the ion current density vs. electric field, parametric with control grid voltage. It can be seen that adjustment of the grid voltage provides wide range of ion current density for a given level of electric field. For example, if an ion current density vs. field relation such as was given in Figure 2-6 is desired for use in selecting different exposure levels, reference to Figure 2-22 indicates that such a relation can be obtained by appropriate grid voltage settings. The data of Figure 2-22 were obtained with a fixed value of corona current, I_c = 50 μA.

From Figure 2-22 it can be seen that the highest field level for this test was 100 kV/m. This limitation was due to the power supply available at the time of this test. The simulator can be operated at considerably higher field intensity. Appendix C describes the preference testing which used simulators of similar design. The highest field used for the preference tests was approximately 150 kV/m. It has been found that if voltages much above this are applied, corona will develop on the exterior of the simulator in the region of the grids. Such corona can be suppressed by the use of a corona ring around the chamber at the grid section. Including a corona ring as part of the design

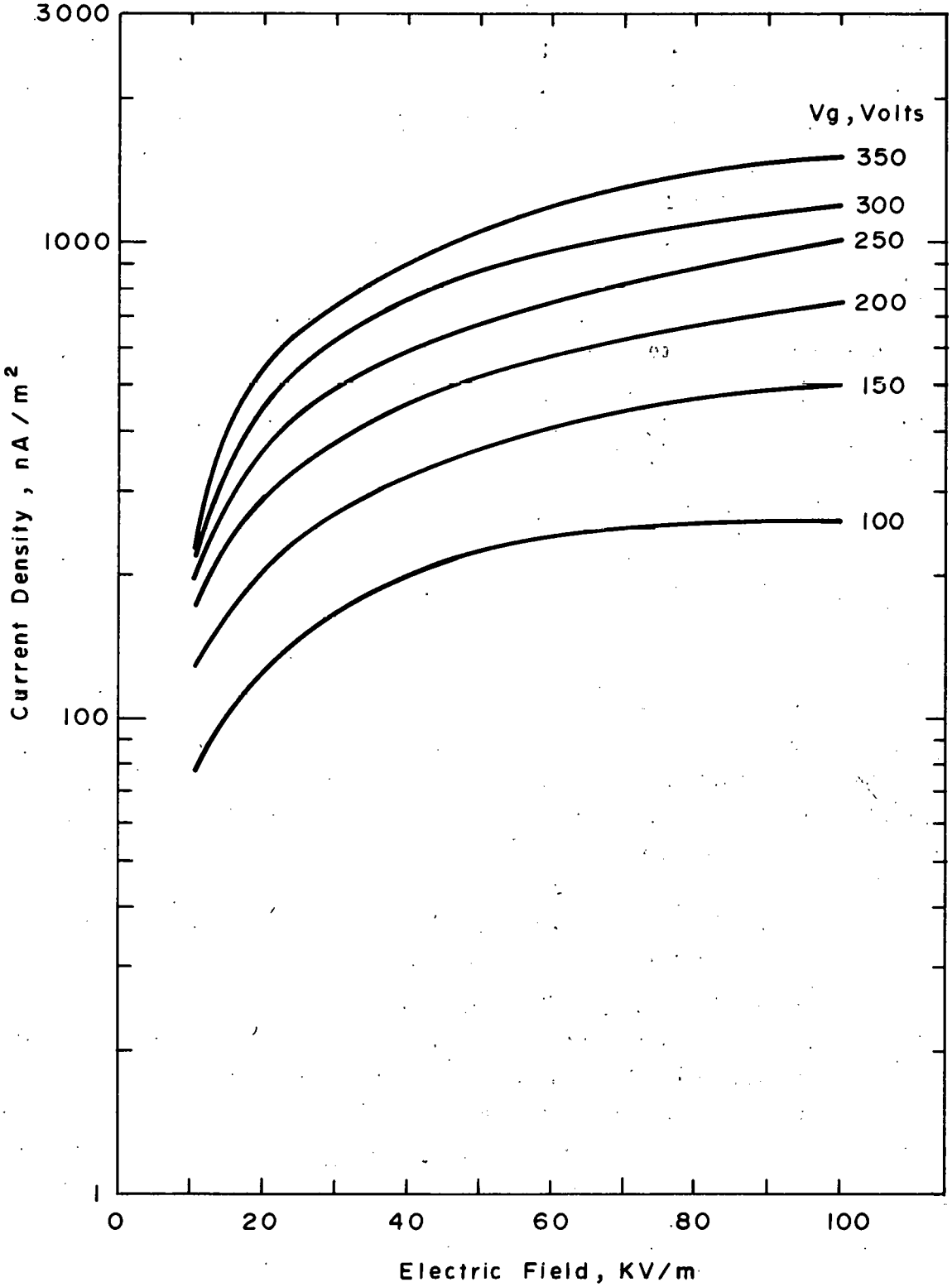

Figure 2-22 ION CURRENT DENSITY VS. ELECTRIC FIELD AS A FUNCTION OF GRID VOLTAGE

it is not felt to be necessary at this time. It is anticipated that the first series of animal tests will employ fields which are no higher than 150 kV/m.

Appendix C presents a method for biasing the simulator with a single power supply. For this bias arrangement, a resistance, R_g, is connected from the corona grid to the control grid, and a second resistance, R_f, is connected between the control grid and ground. The corona current flows through these two bias resistors. The corona current flowing through these resistors produces the bias potentials V_g and V_p, respectively. The nominal electric field in the exposure unit is produced by the voltage V_p between the control grid and the ground grid, while the ion current density is controlled by the grid bias potential V_g. The maximum grid bias potential which can be obtained by use of this bias arrangement is when the external grid bias resistor R_g is removed, thus forcing the corona current to flow through the resistance of the phenolic material which separates the grids. For this arrangement, the maximum ion current density was measured for two values of field resistance for a corona bias current of 50 μA. The two field resistance values were 320 MΩ and 800 MΩ, which correspond to plate voltages of 16 kV and 40 kV, respectively, i.e., nominal electric fields of 32 kV/m and 80 kV/m, for the 50 μA bias current. The ion current density levels at the exposure chamber ground plane were 2 $\mu A/m^2$ and 4 $\mu A/m^2$ for the 320 MΩ and 800 MΩ field bias resistors, respectively. These current density levels are considerably larger than are indicated by Figure 2-6 as desirable for maintaining a uniform field within the exposure chamber, or maintaining a constant air resistivity as a function of electric field. Thus, the simulator can provide current densities which are considerably higher than the levels which are likely to be used for the Phase II animal testing effort.

2.4.2 Field and Ion Uniformity

Previous sections have discussed the importance of ion density uniformity within the animal exposure section of the simulator. Also discussed were some of the difficulties associated with obtaining an ion current density which is acceptably uniform throughout the exposure area. Appendix B details the final evolution and design modifications which were required to obtain acceptable uniformity. The final prototype is considered very acceptable from the standpoint of ion current density uniformity.

Table 2-5 presents a summary of the data from a current density map of the final prototype simulator. The data were obtained with a 10-cm^2 current

probe which sampled the current density at twenty discrete locations on the ground grid within each 8"x 10" animal compartment. The nominal electric field for these data was 32 kV/m, and the ion current density was adjusted to be approximately 220 nA/m^2. Also, an air flow of approximately 35 cfm was supplied to the chamber.

The table shows the mean of the twenty current density values, and the standard deviation of these values as a percentage of the mean, for each of the eight compartments. Also shown are the current density extremes for each compartment as a percentage of the mean.

Table 2-5

FINAL PROTOTYPE CURRENT DENSITY UNIFORMITY

(Compartment Means, Standard Deviation and Extremes)

4	3	2	1
$\bar{j}$ = 220 σ = 3.3% -4.5% + 9%	$\bar{j}$ = 228 σ = 3.6% -8% + 7.5%	$\bar{j}$ = 228 σ = 2.6% -3.5% + 3%	$\bar{j}$ = 223 nA/m^2 σ = 5.4% -12.5% + 9%
$\bar{j}$ = 204 σ = 5.7% -9.3% + 10%	$\bar{j}$ = 221 σ = 4.6% -5% + 6.3%	$\bar{j}$ = 227 σ - 3.2% -5.3% + 8%	$\bar{j}$ = 226 nA/m^2 σ = 3.9% -7% + 6%
8	7	6	5

These measurements were made soon after the final prototype was fabricated and before animals had lived in the chamber. Thus, this data relates to a "clean" simulator.

A test was conducted to determine if the normal degradation in cleanliness of the chamber, which results from animal living in the chamber, would influence the uniformity of either the electric fields or the ion current density. Eight 21-week-old Fischer 344 male rats (CDF, Charles River Labs) were placed in the

simulator and lived there for a period of three weeks. No field or ions were produced in the simulator during this period, but filtered air was supplied at a rate of approximately 35 cfm. During this three-week period, the glass walls of the animal housing area were not cleaned.

After the animals were removed from the simulator, it was mapped to determine the field and ion current density uniformity. It was desired to perform the electric field measurements with the field probe flush with the ground plane, rather than with the probe on top of the ground plane. The Monroe 225 electric field probe only provides an accurate measure of the field when the probe is mounted so that the sensing aperture is in the plane of the ground. If the probe head is set on top of the ground plane, field distortions and enhanced readings will result.

It is difficult to mount the probe head so that the sensing aperture is flush with the ground plane, yet be able to move the probe from one location to another as is necessary for mapping the field distribution within the simulator. For fixed location measurements, the probe is generally mounted in a cut-out in the ground plane so that the sensing aperture is in the plane of the ground and the body of the probe is below the ground level. With the normal simulator arrangement, it is difficult to mount the flush mounted probe in a movable ground plate, since the weight of the simulator which is supported by the animal caging walls rests on the ground plane. Moving the simulator relative to a fixed probe is also not practical. Therefore, in order to accomplish the field mapping, the simulator unit was turned upside down for these tests.

The plenum was removed so that when upside down, the simulator weight rested on the top of the corona chamber. Since the corona chamber walls are at high voltage when the unit is excited, an insulating support was provided by placing several sheets of styrofoam on the floor. A sheet of plywood was placed on top of the styrofoam to provide a rigid base for supporting the simulator. The corona chamber was placed upside down on this base. The grid section was placed on top of the corona chamber, and the glass animal caging section was set, upside down, on top of the grid section. With this arrangement, the plane of the ground was at the top of the unit. The normal ground grid and base section were not used for these tests. Instead, several metal sheets, which could be moved around, were placed on top of the unit and served as the ground plane.

The Monroe 225 field probe head was mounted in a cutout in the center of a 16" x 20" metal plate, so that the sensing aperture was flush with the sheet. When set onto the simulator, the body of the field probe head was above the ground level, and thus not in the field. The 10 cm^2 current probe was mounted onto another plate, so that it could also be used to obtain current density readings at various locations with the simulator in this upside down position.

The field and ion current density mapping was made using a single power supply bias arrangement for the simulator. Appendix C includes a discussion of this method for exciting the simulator. A field bias resistor, R_f = 320 MΩ was used to establish the field, with a 50 μA total corona wire current. The grid bias potentiometer was adjusted to produce approximately 300 nA/m^2 of ion current density in the animal housing section. The field and current density data were taken at locations spaced every two inches, so that twenty readings were obtained in each 8" x 10" animal compartment.

Table 2-6 presents the electric field data obtained from this mapping. The data points appear on a plan view sketch of the simulator so that the data point location corresponds to the location in the simulator where the reading was taken. Table 2-7 summarizes these data in terms of the mean electric field within each individual animal compartment. The standard deviation and the maximum and minimum field levels are also shown and expressed as a percentage of the mean.

Table 2-8 presents the current density data for the simulator. These data, again, are arranged on a plan view sketch of the unit. The current density map data are summarized in terms of compartment means, standard deviation, highs and lows relative to the means in Table 2-9.

Comparison of the current density summary of Table 2-9 with the summary of Table 2-5, which was made before the three-week animal habitation shows that the uniformities are quite similar. The difference in the current density level between these two groups of data is of no consequence. The magnitude of the current density is controlled by the grid bias. No attempt was made to set the current density to be the same for these two tests.

The data presented above show what is felt to be acceptable uniformity for both the electric field and the ion current density, even after animals had lived in the chamber for a reasonable period of time. Cleaning the

TABLE 2.6

ELECTRIC FIELD MAP OF FINAL PROTOTYPE AFTER THREE WEEK ANIMAL HABITATION

(values in kV/m)

4				3				2				1			
30	32	32	31	31	33	33	32	32	32.5	33	32	32	33	33	32
32	33	33	32	33	34	34	32	32	34	34	33	33	34	33.5	33
32	33	33	31.5	32	33	34	31.5	32	34	34	32.5	32	34	33	34
32	33	32	31	31.5	33	33	32	32	34	34	32	32	34	33.5	33.5
29	31	31	29	30	31.5	32	30	31	32	32	30	33	32	32	33
30	31	32	29	29	30	31	30	30	31	32	31	30	32	32	31
32	33	33	31	31	33	32	31.5	31	34	33	32	31	34	34	33
33	34	34	32	31	33	33	32	31	34	34	32	32	34	34	33
32	33	34	32	31	34	33.5	32	32	34	34	32	32	34	34	33
29	31	33	31	30	32	32	31	31	33	33	30	31	32	33	31
8				7				6				5			

Table 2.7

ELECTRIC FIELD UNIFORMITY SUMMARY FOR FINAL PROTOTYPE
AFTER THREE WEEK ANIMAL HABITATION

4	3	2	1
$\overline{E}$ = 31.6 kV/m σ = 4% -9% +4%	$\overline{E}$ = 32.3 kV/m σ = 4% -8% +5%	$\overline{E}$ = 32.6 kV/m σ = 3% -9% +4%	$\overline{E}$ = 33 kV/m σ = 2% -3% +3%
$\overline{E}$ = 32 kV/m σ = 5% -10% +6%	$\overline{E}$ = 31.7 kV/m σ = 4% -9% +7%	$\overline{E}$ = 32.2 kV/m σ = 4% -7% +6T	$\overline{E}$ = 32.5 kV/m σ = 4% -8% +5%
8	7	6	5

TABLE 2-8

CURRENT DENSITY MAP OF FINAL PROTOTYPE AFTER THREE WEEK ANIMAL HABITATION

(values in nA/m^2)

4				3				2				1			
290	300	300	300	320	320	330	340	340	340	350	340	330	320	290	280
290	300	300	320	330	330	330	340	330	340	340	340	330	300	280	280
300	280	300	320	330	330	330	330	320	320	330	340	330	320	290	280
290	270	300	320	330	330	340	340	320	340	340	340	330	260	280	280
280	270	300	300	330	330	340	350	350	340	350	330	320	320	300	250
300	280	300	310	320	330	330	340	340	340	330	340	330	320	280	280
320	300	300	330	310	330	320	320	300	320	340	340	320	310	300	290
320	300	320	330	320	320	330	310	320	320	330	330	320	320	310	300
310	320	340	340	330	330	330	340	320	320	330	320	320	310	320	320
280	300	320	320	320	320	320	320	320	320	320	300	310	310	320	300
8				7				6				5			

Table 2-9

CURRENT DENSITY UNIFORMITY SUMMARY FOR FINAL PROTOTYPE
AFTER THREE WEEK ANIMAL HABITATION

4	3	2	1
$\overline{J}$ = 297 nA/m^2 σ = 4.8% -10% +1%	$\overline{J}$ = 333 nA/m^2 σ = 2% -4% +5%	$\overline{J}$ = 337 nA/m^2 σ = 2.7% -5% +4%	$\overline{J}$ = 300.5 nA/m^2 σ = 7.4% -16% +10%
$\overline{J}$ = 312 nA/m^2 σ = 5.5% -11% +9%	$\overline{J}$ = 324 nA/m^2 σ = 2.5% -4.5% +5%	$\overline{J}$ = 325 nA/m^2 σ = 4% -8.3% +4.6%	$\overline{J}$ = 309.5 nA/m^2 σ = 4.5% -10.5% +6.6%
8	7	6	5

animal caging area is not anticipated to cause any problems. Repeated washings may eventially require the recoating of the glass surface with the hydrophobic compound. However, a schedule for such recoating has not been established.

The discussion of Section 2.2.1 notes that the use of resistive material walls for the animal caging section should result in uniform fields even though the separation between field grids was large relative to the size of the grids. The reason for this is that current flows in the walls. The potential established along the walls by this current acts like a continuous grading structure between the plates or grids. Thus, the static field should be uniform out to the edge of the field plates, if a conducting wall is at the periphery. This factor permits a significant size reduction in the chamber, since the animal compartments need not be kept well inside the outer edge of the field producing plates. The electric field map presented in Table 2-6 substantiates that the glass walls of the animal housing section perform the function of a continuous grading structure, since the fields are essentially constant out to the periphery of the edges of the field-producing plates.

To further substantiate that the walls of the animal caging section perform as a continuous grading structure, the voltage division provided by a wall of the final prototype simulator was measured. The voltage division along the height of a wall must be uniform with distance in order to produce spatially uniform fields and ion current density within the enclosure.

To prevent current from being drawn by the measurement instrument, an electrostatic voltmeter (Model ESA, manufactured by the Sensitive Research Instrument Company) was used to sense the potential on the wall. For the measurement, a high voltage power supply was connected between the control grid and the ground grid of the simulator. The supply voltage was set to 20 kV. Measurements of the wall potential were made at nominal one-inch increments up the wall from the ground grid to the control grid. Marks were placed on the glass wall with a felt tip pen at these locations. Contact to the glass was made with a piece of 3/16-inch rectangular bar stock which was two inches long. The lead to the voltmeter was soldered to the bar stock contact and fed through a rigid plastic tube. The plastic tube was held by a test tube holder, which could be adjusted in height to press the bar stock contact against the glass surfaces at the marks.

After the voltage measurements were made, the location of the marks was measured. The total conduction distance in the glass wall is 19.75 inches. The ideal voltage at each mark location was calculated from the total voltage applied, the total glass distance, and the mark location. Table 2-10 presents the calculated or ideal voltage at the location and the measured voltages. In addition, the percent difference between the calculated and measured values is presented. It is seen that very good agreement between measured and calculated potentials was found. Only the lowest couple of readings have significant error, and this may have been contributed to by the difficulty in accurately reading the voltage on the lowest scale of the voltmeter, where compression of the scale exists.

Table 2-10

MEASURED AND CALCULATED SIMULATOR WALL POTENTIAL

Height Above Ground (in.)	Calculated Voltage (kV)	Measured Voltage (kV)	Percentage Difference
18.69	18.9	19.0	0.5
17.69	17.9	18.1	1
16.69	16.9	17.2	2
15.69	15.9	16.5	4
14.69	14.9	15.2	3
13.62	13.8	14.0	1
12.63	12.8	13.0	2
11.63	11.8	12.0	2
10.69	10.8	10.8	-
9.69	9.8	9.8	-
8.63	8.74	8.3	5
7.63	7.7	7.8	1
6.63	6.7	6.7	-
5.63	5.7	5.75	-
4.63	4.7	4.7	-
3.63	3.68	3.8	3
2.63	2.66	2.8	5
1.63	1.65	1.8	9

2.4.3 Ozone Measurements

Measurements have been made to assess the ozone levels within the simulator animal caging section. The measurements were made during a period when the ambient ozone level in the laboratory was below monitor detectability. A Dasibi Model 1003-AH ozone monitor was used for these measurements. This instrument has a quoted range of 0.000 to 1.000 PPM, an incremental sensitivity of 0.001 PPM, and an accuracy of 3%.

During the ozone measurements, the simulator was operated with a total corona current of 50 μA. The operating parameters were a nominal electric field of 32 kV/m, and a current density of 300 nA/m^2 of negative air ions. Filtered air was supplied to the simulator at approximately 35 cfm.

The air sample to the ozone monitor was obtained via a four-foot length of teflon tubing, which was positioned to sample the air in the simulator at a height of about one inch above the ground grid. No detectable level of ozone was recorded for a monitoring period of approximately 100 minutes during simulator operation at the above-noted conditions. Thus, a potential problem due to ozone related to the corona source does not appear to exist.

2.4.4 Acoustic Measurements

Measurements were also made of the acoustic noise attributable to the corona source of the final prototype simulator. The acoustic noise from the corona source is very low; however, it can be measured. Figure 2-23 compares the acoustic spectra within the animal caging area with and without 50 μA negative corona current from the corona wires. Air was being supplied to the simulator for both of the spectra shown. The spectrum with the corona source "off" is at the noise level of the measurement instrumentation. Thus any noise associated with the air flow was less than the instrument sensitivity.

To obtain these spectra, a B&K 4136 1/4-inch condenser microphone was inserted into the chamber through the ground grid. The microphone was pointed upward with the top of the microphone located approximately two inches above the ground grid. The microphone output was fed through a B&K 2209 sound level meter to a Spectral Dynamics Model 310C Real Time Analyzer and a Model 3026 Ensemble Averager. The processing bandwidth was 150 Hz, and the measurements were unweighted.

Although the acoustic noise due to the corona source is low, the fact that it can be measured suggests that the sham-exposed animals should also be exposed to this acoustic environment. These measurements prompted additional measurements to be made in preparation for the animal preference testing. The preparations for the animal preference tests are described in Appendix C.

The simulator can be biased so that the corona source operates normally, producing either positive or negative ions, while the field and ion environment in the animal exposure chamber is maintained at near ambient, i.e., a field of less than 0.1 kV/m and an ion density of a few hundred ions per cubic centimeter. This bias arrangement is described in Appendix C. Using this bias arrangement, acoustic measurements were made to determine the sound level within the animal exposure chamber for both positive and negative corona. These measurements have been compared to the acoustic levels within a chamber which was normally biased, to produce an ion and field environment in the animal exposure chamber. For these tests, the unweighted sound pressure levels in dB, r.e., 20 μPa in each octave band from 31 Hz to 31 kHz measured.

The results of the acoustic measurements in the preference test simulator show that if the corona source is operated normally, the sound level in the exposure chamber is the same for the simulator either biased to produce a field and ion environment or biased to inhibit the field and ions in the exposure chamber.

The test results show that the negative corona noise is stronger than when positive corona is produced. However, both conditions produce a measurable increase above the background noise. The positive corona noise was only observable above the background in the 16 kHz and above octave bands, while the negative corona was above the background in all bands above 2 kHz.

The acoustic measurements which have been made show that the corona source produces noise levels which can be measured. Thus, if efforts are to be made to keep all physical environments the same for test and control subjects, with the exception of the field and ion environment under study, then it will be necessary to produce the acoustic noise for both test and control subjects. The simulator can be biased to produce the corona acoustic noise in the "control" simulators. However, since the noise is different for positive and negative corona sources, it may be necessary to provide for both positive and negative "controls".

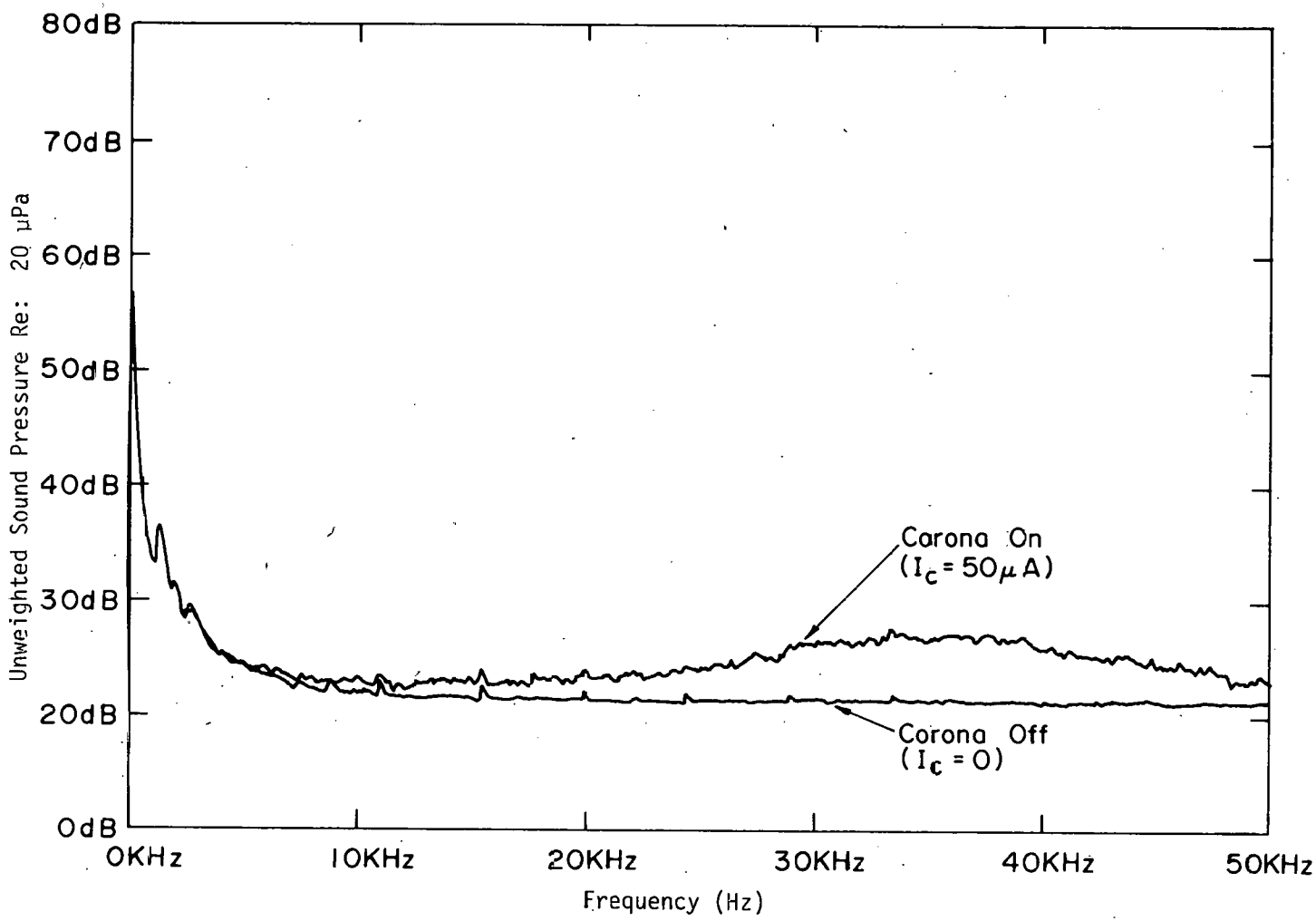

Figure 2-23 ACOUSTIC SPECTRUM WITH AND WITHOUT CORONA

2.5 Prototype Simulator Habitation Experiment

Two pilot experiments were conducted to evaluate the suitability of the simulator module as live-in quarters for adult male rats. The first experiment was terminated on the fifth day due to a burnt out motor in the air supply fan which resulted in smoke exposure of the animals housed in the simulator. Experiment 2 extended over a 19 day period. The measurements taken during experiments were body weight and food consumption.

2.5.1 Animals

The animals were male Fischer 344 rats (Charles River, Wilmington, MA) that had been used in the Control-Control condition of the preference testing experiment (Appendix C). During the period intervening between the preference testing and the experiments described here, the animals had been housed three/cage under the conditions described in Appendix C. The animals were 25 weeks old at the start of these first experiments and the second experiment was initiated one week later. For the first experiment, eight animals were randomly selected for assignment to the simulator module and eight for the laboratory control condition. The means and standard deviations of their body weights at that time were 360 ± 21 g and 354 ± 27 g for the simulator and control groups, respectively. When it became necessary to abort the first experiment due to smoke exposure of the animals in the simulator group, eight new animals were assigned to this group whereas the same control animals were continued into Experiment 2. This is of course not an ideal procedure as at the start of Experiment 2, the control animals had been handled more frequently in conjunction with daily weighings. At the start of Experiment 2 body weights for the simulator group averaged 351 ± 23 g and for the control group 340 ± 25 g. There were no statistically significant differences between the two groups in initial body weights for either experiment. Both groups were maintained on a 14 hr light: 10 hr dark cycle and on ad libitum food (Purina Lab Blocks) and water which were dispensed as described below.

2.5.2 Simulator Condition

The complete final prototype simulator was used for these experiments. An air flow of approximately 35 cfm was supplied to the simulator plenum. This air was filtered with a HEPA filter. No voltages were applied to the simulator for these tests; therefore, there were no field or ions generated by the simulator.

The water manifold was connected by rubber tubing to an Edstrom water filter No. WF470 and stainless steel float tank, No. FT452. The water tank and filter were mounted at a height of approximately 6 ft. above the floor to provide a pressure for the watering system. The food pellets were placed in the floor-level food troughs.

2.5.3 Control Condition

Control animals were housed in a separate room on the same corridor as the room in which the simulator module was located. For the control condition the rats were housed individually in solid-bottomed polycarbonate cages (10-1/2 x 9-1/2 x 8 in) on a bedding of Absorb-dri. Stainless steel wire-bar covers were employed as tops to the cages and food was dispensed through a well in the cage top. Water was dispensed through a sipper tube protruding through the top into the cage.

2.5.4 Measurements

Body weights were determined daily on Monday - Friday of each week of the studies and food consumption was measured four times each week. All determinations were made between 1:30 - 3:00 P.M. except those on the first day of Experiment 1 when the animals and food were weighed at approximately 10:30 A.M.

2.5.5 Results

Experiment 1: Considering body weight change from the preceding day, animals housed in the simulator did not significantly differ from the changes observed in the control group on either days 2, 3, or 4 of the experiment. The daily changes were -15±6g, 2±3 g, and -1±2 g for the control group and -15±7g, 1±9g, and -1±8 g for the group housed in the simulator. The initial 15 g weight loss seen in both groups is most likely due to a change between days 1 and 2 in the time of day at which the animals were weighed. This makes the values of cumulative weight change over the succeeding days misleading, however, it was clear that by day 4 the cumulative weight change was different for animals housed in the simulator as compared to those

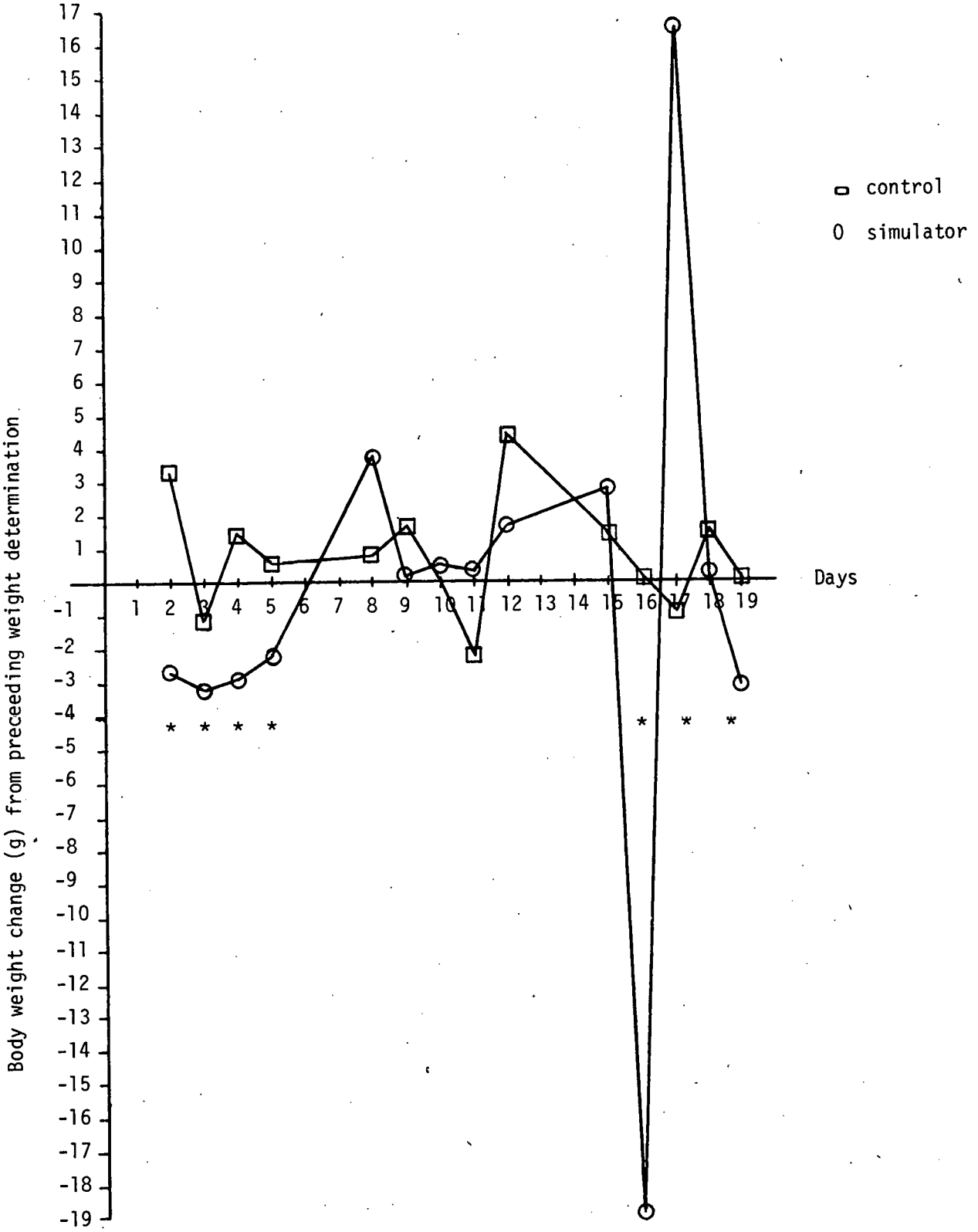

Figure 2.24 - Body weight change from preceeding measurement. The asterisks indicate days on which the control and simulator groups were significantly different as to weight change ($p<.05$).

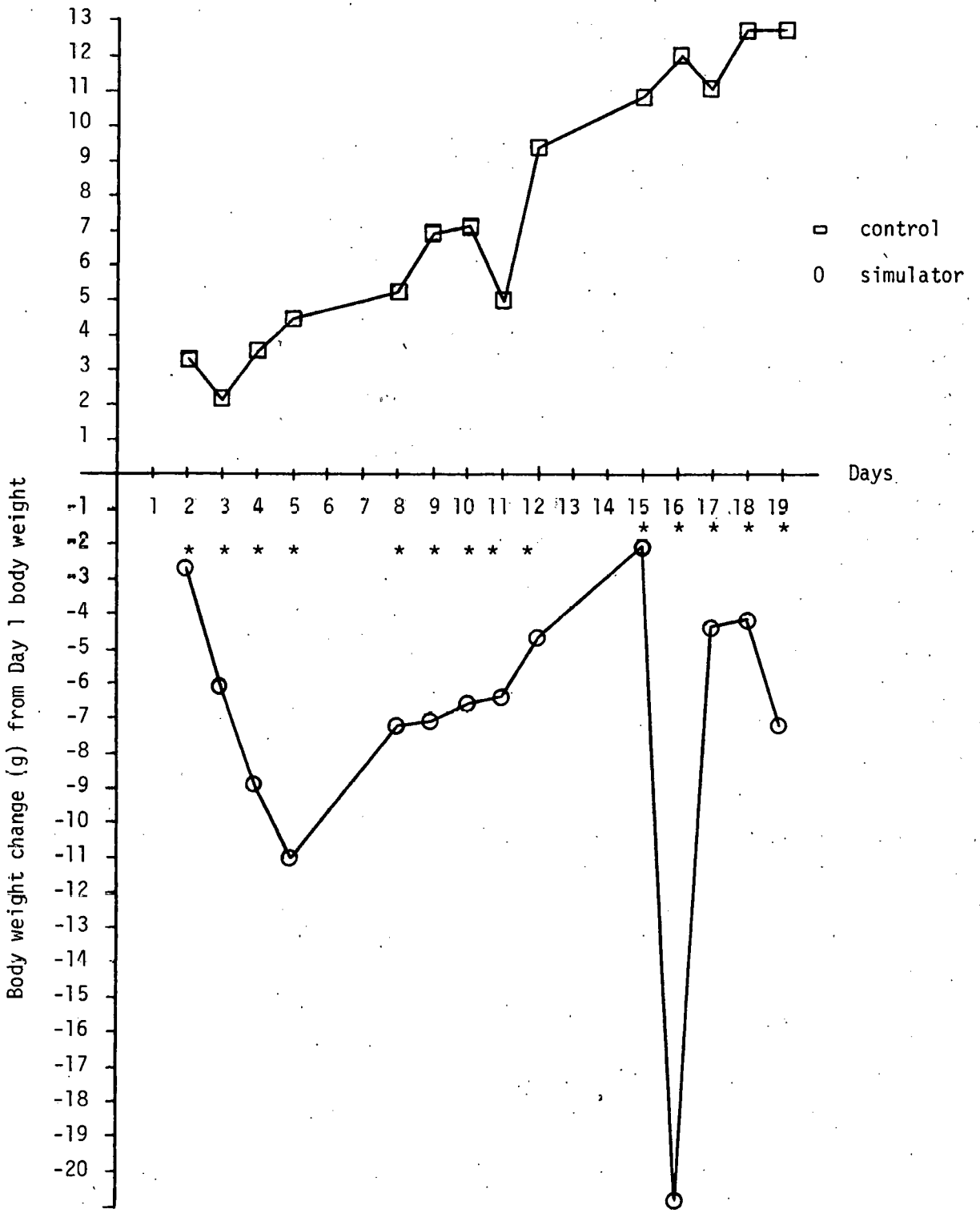

Figure 2.25 - Cumulative body weight change from day 1. The asterisks indicate days on which the control and simulator groups were significantly different as to cumulative weight change ($p<.05$).

maintained under control conditions. Food consumption averaged between 15 and 18 g per day and was statistically equivalent in both groups.

Experiment 2: The day to day body weight changes for animals housed in the simulator vs those maintained under control conditions in Experiment 2 are shown in Fig. 2.24 and cumulative body weight changes in Fig. 2.25. Fig. 2.24 indicates that during the first five days of the experiment animals housed in the simulator tended to lose weight and during this period their weight change was significantly different from that of the control animals ($p<.05$). Thereafter, except for days 16, 17, and 19 daily body weight changes for animals housed in the simulator were comparable for the two groups. The large weight loss seen in animals housed in the simulator on day 16 is attributable to a blockage in the water lines thus resulting in water deprivation of the animals and the day 17 data shows a recovery from this loss. Our records provide no information as to the basis for the 3 g loss seen on day 19 for the simulator group.

In terms of cumulative weight change, the animals housed in the simulator never fully recovered from the initial weight loss as is indicated by a negative weight change on the 19th day of the experiment and by the significant difference between control animals and the animals housed in the simulator on that day.

The food consumption data for Experiment 2 are summarized in Table 2-11. There were no significant differences in the consumption of animals maintained under control and simulator conditions for the first two days considered (Days 2 and 4). On Day 5 food consumption of animals housed in the simulator was less than that of control animals. Thereafter, except for Days 16 and 19 which are discussed below, animals in the simulator appeared to consume more food than control animals. This greater consumption by animals in the simulator most likely reflects an effort to recover initial body weight losses. The lower food consumption Day 16 of the experiment was due to a problem with the water supply, i.e., without water the animals would be expected to eat less. This may have also been the case for Day 19 as there is an unexplained weight loss on that day, however, this was not noted until after the apparatus was dismantled and there is no record of a problem with the water supply being recognized on that day.

TABLE 2-11

FOOD CONSUMPTION FOR ANIMALS MAINTAINED IN THE SIMULATOR OR UNDER LABORATORY CONTROL CONDITIONS

	Food Consumed Per Day (g, Mean ± SD)[a]									
	Day 2	Day 4	Day 5	Day 9	Day 10	Day 11	Day 16	Day 17	Day 18	Day 19
Control	20±1	16±2	20±1	16±1	16±1	19±2	19±2	18±1	17±1	20±1
Simulator	18±3	20±5	17±2^{S-}	20±3^{S+}	20±4^{S+}	20±3	12±3^{S-}	20±1^{S+}	19±1^{S+}	17±2^{S-}

a -- Data from Days 3 and 12 not available because food was added

S- -- Significantly less than control, $p < .05$

S+ -- Significantly greater than control, $p < .05$

2.5.6 Discussion

Most of the problems with the use of the simulator as living quarters for adult rats appeared to be related to the automatic watering devices. In addition to an air blockage noted on Day 16, there were repeated problems with leaks in the water devices and on Day 3 this was to the point of depleting the supply. This could have, of course, enhanced the trend toward weight loss during the first few days. Our test of the use of these watering devices could probably in many ways be considered a worst case test. Components were purchased and installed without being subjected to the extensive preflushing we later learned is recommended by the manufacturers. The supply to the drink valves was not a line supply but rather was from a suspended tank of approximately 1 liter volume which was filled with tap water Finally, the animals were placed individually in the apparatus without prior training on the use of the drinking valve whereas a better practice for initial training of rodents to automatic watering devices is multiple housing.

We suggest that a more extensive evaluation of the simulator module as living quarters for adult animals and evaluation of the module for use by young animals be conducted prior to initiating bioeffects research. These more extensive evaluations should, if possible, be conducted after the inclusion of the controls for air flow, temperature, humidity, and other environmental variables which are anticipated for use in the exposure facilities. However, provided that there are proper precautions relative to the use of the automatic watering devices, it is not anticipated that the simulator module per se will result in problems. It is suggested that during the quarantine period animals be multiple-housed in cages provided with automatic watering. This will facilitate adaptation to the use of the watering device and will allow discarding any animals that do not adapt at the end of quarantine.

3. BIOLOGICAL EXPERIMENTAL DESIGN

3.1 Objective and Scope

The overall objective for this experimental design is to obtain information that will aid in assessing the risks to humans, domestic animals, and wildlife from exposure to the environment that would potentially be created in the vicinity of overhead HVDC transmissions lines. The nature of this environment has been discussed in Section 2.1. With such a broad objective many approaches are possible. The particular approach outlined here is in part predicated on requirements specified in the initial request (RFP ET-78-R-01-3026) and in part on assumptions or decisions that have been made during development of the design. Some of the factors that were critical in shaping this experimental design should be mentioned.

One of the specifications was that the experimental approach be one suitable for execution in a laboratory simulation of the HVDC environment. Secondly, small laboratory animals were specified as the experimental test animals. The experimental design was planned with the understanding that the Phase II effort would be one feasible for completion in approximately 2 years. As it was anticipated that construction of suitable exposure facilities would require approximately 6 months, a biological research effort of approximately 18 months was planned.

The biological experimental design was planned under the assumption that the sponsor's objectives for the initial biological research would be best met by a broad screen for bioeffects rather than an in-depth evaluation of a more limited set of biological responses. An associated assumption is that the results of the initial screen will be used to identify those biological variables which should be examined more extensively or in greater detail in future research.

Very early in the planning it was decided that it would not be feasible in the first laboratory simulation to independently manipulate all properties of the environment of interest. The basis for section of three major properties, the dc electric field, ion current density, and the polarity of the field and ions, as having first priority is discussed Sections 2.1 and 2.2. A number of other important environmental conditions, some of which are

characteristic of the HVDC transmission line environment and some which are properties of the simulation, will be controlled and/or monitored (Sections 2.2.3 and 2.2.4). The point here is that in terms of experimental design, these conditions will not be subject to planned experimental manipulations during the initial research effort.

Similarly, it was decided that for the first approach to determining biological effects of the simulated environment, no attempts would be made to dissociate the effects of the dc electric field from the effects of air ions. Thus, in this design these two properties of the environment will be co-manipulated. That is, the highest levels of electric fields will be associated with the highest level of ion current density. Should effects that are considered of real biological significance be obtained, it could then become important to dissociate the sources of these effects.

The overall capacity and versatility of the exposure facilities of course has a major impact on the kinds of studies that can be planned. Similarly, the biological experimental design imposes some minimum requirements on the exposure facilities. For example, to perform lifetime rodent studies which include concurrent investigation of positive and negative polarities, three or more levels of dc electric fields and ion current densities at each polarity, concurrent sham-exposed control groups,and adequate group sizes, one should probably plan a facility capable of housing 350+ rodents. Alternatively, one can without great difficulty and within the bounds of good scientific practices conduct a variety of meaningful studies involving shorter term exposures to a more limited number of test environments in facilities of much more limited capacity. In arriving at recommendations for the Phase II effort, an attempt has been made to arrive at a good balance between the time and economic resource committments required for establishing exposure facilities vs those required for the biological research. Under this plan certain types of studies which we would propose for a long-range plan will be delayed. For example, no studies with exposure periods exceeding 13 weeks have been recommended for the Phase II effort. Similarly, full scale multi-generation reproduction studies in which both parents of succeeding generations are exposed to the test environments have not been suggested for the next phase of the program. To permit concurrent investigation of

positive and negative polarities, it is proposed that only two levels of test parameters be considered at each polarity.

The biological experimental design has been planned for exposure facilities with the following capacities:

- suitable live-in quarters for 115 individually housed rodents.
- flexibility to use the same facilities with minor revisions for rats and mice.
- capacity to simultaneously present sham-exposure conditions for control animals and four different test conditions which are represented by two levels of dc electric fields and ion current densities at each polarity.
- for each set of three modules of eight individual animal compartments, allocation of one of the 24 compartments for measurement of environmental, electrical, and ionic parameters.
- for each set of three modules, ability to operate at all possible on-off combinations, i.e., three off, two off - one on, one off - two on, or three on. (This feature is important to allow phasing in of the habituation and exposure initiation of part of the animals in each group over a period of several days. This practice will aid in limiting variability within a given experiment of the time lapsing between the end of an exposure interval and the performance of some specified biological assay.)

3.2 Background Literature

Several categories of literature were considered in developing the biological experimental design. Of primary interest were reports of investigations of the effects of dc electric fields and the effects of air ions and in particular those studies in which humans or other mammals were evaluated in a laboratory setting. Examples of such studies have been abstracted in tabular form and are discussed below. Non-mammalian test systems have also been considered at times but none of the plant research is discussed and only limited attention has been devoted to environmental studies.

Other sources of information that were considered in developing the experimental design were reports and reviews of investigations of the biological effects of other forms of electromagnetic energy at exposure levels greater than those inherent in the natural environment. The studies in this category with which we had greater familiarity and therefore considered more often were investigations of the effects of microwave

irradiation of humans and animals[a] and studies related to ELF electric fields (Bridges, Becker , and Preache, 1979 ; Bridges and Preache, 1980). This is not to suggest that the results of such studies have direct application to the problem at hand. First, coupling phenomena for microwave exposures would differ substantially from those in the environment to be simulated. Further, the greater than typical ambient air ion concentrations characteristic of the HVDC transmission Line environment add a dimension not associated with microwaves or ELF fields. However, when viewed as an added source of enlightment as to the kinds of environmental controls that are necessary for good laboratory simulations of EM test environments and as an aid to avoiding numerous methodological pitfalls which can cloud interpretation of such studies, the microwave and ELF bioeffects literature have a good deal of relevance.

Another body of literature which has potential relevance is that related to the use of dc currents for stimulation of bone growth and repair or stimulation of regeneration of tissues for which regeneration is not observed without intervention. Sheppard (1978) noted that it has now become reasonably well accepted that a few microamperes and possibly nanoamperes of current via closely spaced implanted electrodes can facilitate growth under controlled conditions. However, until there is clarification of the body currents, current densities, and current distribtuions which may be expected from the environment of interest, the implications of this literature in relation to effects that might be predicted for HVDC transmission line environment cannot be evaluated.

3.2.1 Bioeffects of DC Electric Fields

There have been a limited number of studies in which the biological effects of exposure to dc electric fields were explored. The fields for

---

[a] The microwave literature was reviewed as part of a grant proposal. Preache, M. Microwave Safety: Evaluations in Sensitive Models. Submitted to NIH, Dept. Health Education, and Welfare, 1976.

those in which humans or other mammals were studied have ranged from as low as 0.3 kV/m up to 225 kV/m. In a few studies repeated intervals of exposure over periods of 1 - 5 months were employed, however, the more frequent case was that exposure periods on the order of minutes, hours, or days were considered. Several investigators employed human subjects and aside from these the most common test species have been rats or mice. The biological parameters explored were varied. For the purpose of the tabular abstracts, these parameters have been somewhat loosely grouped as effects (or lack of effects) on the nervous system or behavior (Table 3-1); on metabolism, growth, reproduction or development (Table 3-2); on hematologic or blood chemistry parameters (Table 3-3); or on the heart or respiratory system (Table 3-4).

3.2.1.1 Nervous System and Behavior

If there has been an emphasis on parameters, it has been on those which could be categorized as investigations of effects on the nervous system and behavior (Table 3-1). Two of the studies reviewed were essentially behavioral evaluations of whether the dc field would be preferred over no field (Faraday condition). Altman and Lang (1974) reported that mice discriminated between the Faraday condition and ac or dc fields of 3.5 kV/m but whether the fields or the Faraday condition were preferred appeared to depend on the behavioral activity (nest building or play activity) being considered. Given a choice between the Faraday condition and a 177 kV/m dc (+) field in two arms of a maze, rats tended to choose the Faraday condition at a statistically significant greater frequency (Epstein and Ondra, 1976). Discrimination of the field might be expected under these conditions as preliminary tests indicate that the hair erection phenomenon probably occurs at substantially lower fields (Third Quarterly Report, p.46).

Alterations in brain activity during exposure to a 10 kV/m field were also interpreted by Lott and McCain (1973) as indicating an "awareness" of the field for the rats. These investigators used two preparations for studying brain activity, surface electrodes and electrodes implanted in the hypothalamic region. With surface recordings they observed bursts of activity at both the onset and offset of the fields as well as a sustained

Table 3-1

The Effects of DC Electric Fields
On The Nervous System and Behavior

Investigators	Subjects	Exposure		Results
Mayyasi & Terry, 1973	Rat	DC (-) 1.6 or 16 kV/m	5 Hr	*Maze Errors and Time Scores (DEC)
Lott & McCain, 1973	Rat	DC Continuous 10 kV/m	30 - 60 Min	*EEG Activity (INC) and Hypothalmic Activity (DEC)
		DC Pulsed 20 V (640 cps 100 msec)	30-60 Min	*EEG Activity(Erratic INC) and Hypothalmic Activity (DEC)
Altmann & Lang, 1974	Mouse	DC 3.5 kV/m Or 10 hz 0.18 Or 3.5 kV/m		*Choice of Nest or Playground Sites (Discriminated 3.5 But Not .18 KV/M)
Jones, 1975 (ABSTRACT)	Human Children	DC(+) 3000 V Potential		*Attention to Task (INC), Day Dreaming and Deviant Behavior (DEC) ●Arthemtic Speed and Accuracy
Epstein & Ondra, 197	Rat	DC (+) 177 kV/m		*Maze Choice (Faraday Chosen Over Field)
Nakamura, 1979 (UNPUBLISHED)	Cat	DC (+) 30 kV/m		*Aggressiveness (INC If Corona Present)
	Mouse	DC (+)10, 20, Or 30 kV/m	5 Mos (10 Hr/ Days)	*Maternal Cannabalism (INC at 30 KV/M)
Mose and Fischer, 1970	Mouse	DC 24 kV/m		*Running Activity (INC)
Petelina and Burdo, 1972	Rabbit	DC 130 kV/m		*EEG and Hypothalmic Activity

* Affected
● Not Affected

INC = Increased
DEC = Decreased

Table 3-2

The Effects of DC Electric Fields On
Metabolism, Growth, Reproduction, and Development

Investigators	Subjects	Exposure		Results
Anerson & Vad, 1965	Serrati Marcescens	DC(+,-) 94 kV/m 312 kV/m	46 Hr	*Colony Size (DEC + 94 kV/m only)
	E. Coli	DC(+,-) 312 kV/m	46 Hr	*Colony Size (DEC + Or -)
Bassett & Hermann, 1968	Fibroblast Cultures	DC(+,-) 100 kV/m Continuous Or Pulsed (1 hz)	14 Days	*DNA Synthesis (INC) *Collagen Synthesis (INC, More for Pulsed)
Marino et al, 1974.a	Rat	DC(+) Vertical .6-19.7 or Horiz. .3-9.8 kV/m	30 Days	•Body Weight *Glaucoma Incidence Rate (INC Vertical)
	Mouse	DC (+) Horiz. 8-16 kV/m	14 Days	*Chromosomal Abnormalities (INC)
Möse et al, 1971 Waibel, 1975	Mouse	DC 24 kV/m	8 Days	*Liver Oxygen Consumption
Nakamura, 1979 (UNPUBLISHED)	Mouse	DC(+) 10, 20, Or 30 kV/m	5 Mos (10 HR/ Day)	*F_1 Body Weight And Tail Length (DEC but not at 10 kV/m
Möse and Fischer, 1970	Mouse	DC 24 kV/m	Up to 4½ mos	*Food and Water Consumption (INC) *Progeny (DEC)

*Affected
• Not Affected

INC = Increase
DEC = Decrease

Table 3-3

The Effects of DC Electric Fields On
Hematologic and Blood Chemistry Parameters

Investigators	Subjects	Exposure		Results
Marino et al, 1974 a	Rat	DC(+) Vertical .6-19.7 kV/m	30 Days	*Relative Distribution of Serum Proteins (Inconsistent Across Exposure Levels)
Marino, et al, 1974 b	Mouse	DC Vertical 2.7-10.7 kV/m Or Horiz. 5.7 kV/m	7, 14, 21 Days	*Relative Distribution of Serum Proteins
Krievova et al, 1973 Cited by Sheppard, 1978	Human	DC 30 or 60 kV/m	2 hr/day for 2 mos	•Various Blood Composition Parameters WBC, RBC, Platelets and Others
	Human	DC 90 kV/m	2¼ hr/day for 30 days	*Platelets (DEC) •Others

* Affected
• Not Affected

INC = Increase
DEC = Decrease

Table 3-4

The Effects of DC Electric Fields On
Heart and Respiration

Investigators	Subjects	Exposure		Results
Hermer, 1971	Rat	DC 150-225 kV/m	30 Min	•Heart And Respiration Rates
Lott, 1973	Rat	DC Continuous 10 kV/m or Pulsed 20 V, 640 cps	30-60 Min	•Respiration Rate and Body Temperature
Nakamura, 1979	Cat	DC 45 kV/m		*EKG Spiking (INC If Corona)
Krievova et al, 1973 Cited by Sheppard, 1978	Human	DC 30 Or 60 kV/m	2 hr/day for 2 mos	*Blood Pressure and Heart Rate (DEC at 60 KV/m only) •EKG No Effect
	Human	DC 9C kV/m	2¼ hr/day, for 30 days	*Blood Pressure and Heart Rate (DEC)

* Affected
• Not Affected

INC = Increase
DEC = Decrease

increase in activity over baseline levels throughout the 30 - 60 min exposures to the field. In contrast, activity recorded from the hypothalmic region was less during periods of exposure to the field. Commenting on these results, Miller (1978) suggested that the bursts of activity at the onset and offset of the fields could possibly be explained by large current injections through the electrodes from transients associated with the switches (probably displacement current due to the time rate of change of the field). Alterations in brain activity were also observed for rabbits repeatedly exposed to a dc field of 130 kV/m for 2 hr intervals (Petelina and Burdo, 1972). Electrodes were chronically implanted in the cortex, hypothalamus, and operculum Brain activity was recorded immediately after exposure and again 1, 2, 3 and 4 hr later. Amplitude, frequency, and the ratio mean amplitude/ mean frequency (p factor) were analyzed. In addition correlation coefficients which appear to be an indication of the relationships between cortical activity and that in deeper structures were derived. They summarized their results as showing alterations in the EEG amplitude-frequency characteristics, the P parameter, and the correlation coefficients and interpreted the increase correlation between the hypothalmus and other brain areas as indicating an "elaboration of optimal level of activity of cerebral control systems under the SEF (static electric field) influence." Both the experiment and the interpretation are characteristic of Soviet investigators who throughout the spectrum of biological research place a large emphasis on the importance of the central nervous system in controlling and regulating other systems.

Investigating the effects of dc (-) fields on maze performance Mayyasi and Terry (1973) trained young and adult rats of both sexes to escape from a water maze following 5 hr exposures to 1.6 or 16 kV/m fields. For some groups white noise at 90 db was an added exposure condition, whereas for others the field exposure or corresponding control condition (generator off) was associated only with laboratory background noise (approximately 30 db). Their multifactor analytical design which might be represented as Electric Field x Noise x Sex x Age x Subjects considered the both main effects and interactions of the different factors. Of primary interest here is that the electric field significantly reduced error scores

and when time scores were considered significant interactions with other of the factors were shown. If however, we have understood their experimental design correctly, groups of animals undergoing different conditions of exposure were exposed and tested in the maze on different days, rather than a subset of animals from each group being processed through the procedures on a given day. While this practice does not invalidate the results, it does leave them open to questions.

Jones (1975) evaluated deviant behavior, daydreaming behavior, attention to task, and arithmetic rate and accuracy for ten emotionally disturbed children during periods of exposure to a dc field. The results during these periods were compared to results obtained for the same children during the periods when the field generator was off. The field had no effect on arithmetic rate or accuracy, however, deviant and daydreaming behaviors were decreased whereas attention to task was increased during the field exposures. The report (Dissertation Abstracts) gives the following description of the exposure setup "The bioelectric field generator produced a highly rectified, well filtered electrostatic field of 3000 volts DC potential. The field was invisible, inaudiable, and not detectable by touching the propogating grid that hung close to the ceiling." There were no indications of whether field measurements were made nor were a number of factors that could have affected the unformity of the field discussed. These details may have been provided in the complete report which was not reviewed.

In another study by Soviet investigators, human subjects were exposed to 30 or 60 kV/m dc fields for 2-hr intervals over a period of 2 months (Krievova et al , 1973). Neither reflexes nor reaction time were altered at either field strength, however, a lower threshold for neuromuscular excitation was associated with exposure to the 60 kV/m field. In a follow-up study, three subjects were given repeated intervals (approximately 2 hr) of exposure to a 90 kV/m field over a period of 30 days. Decreased neuomuscular control, evaluated by a task which required placing a stylus in a hole, was reported as an effect of the field exposure for two out the subjects.

Mice exposed to a 24 kV/m field for 15 days evidenced more running activity than control mice (Mose and Fischer, 1970). Activity was measured

daily. The largest difference between control and exposed mice was on the first day of exposure, however, substantial differences were recorded for each day and the increase averaged across all days was 51%. Nakamura (1979) exposed cats to a 30 kV/m dc (+) field and mice to positive fields of 10, 20, or 30 kV/m. The cats were more aggressive when the fields were on, however, this phenomenon appeared to be dependent upon the presence of corona. Maternal cannabilism, which may also be evidence of increased emotionality, was noted in mice exposed to the higher field (30 kV/m) over a period of several months.

3.2.1.2 Metabolism, Growth, Reproduction and Development (Table 3-2)

A variety of studies, some of which have little relevance to each other, have been tabulated under this rubric. The growth of bacterial colonies (S. Marcescens and E. Coli) cultured with no field present was compared to that of colonies cultured for 46 h in the presence of positive or negative fields of 94 or 312 kV/m (Anderson and Vad, 1965). Growth of the E. Coli colonies was inhibited by fields of $\pm$ 312 kV/m. The positive field of 94 kV/m inhibited growth for S. Marcescens whereas the high field strengths and -94 kV/m did not. In another in vitro study DNA and collagen synthesis of cultured fibroblasts were increased by about 20% over control values if the cultures were exposed to dc fields of $\pm$ 100 kV/m (Bassett and Hermann,1968). Pulsing the exposures at the rate of 1 Hz yielded about the same effects for DNA synthesis but resulted in even larger increases (100%) for collagen synthesis.

Growth effects in rodents exposed to dc fields have been considered in two studies. Final body weights of rats that been given 30-day exposures to dc vertical or horizontal fields of +20 kV/m or less from 3 weeks of age were not different from those of the control group (Marino et al 1974a). In this same study an overall glaucoma incidence rate of 17% was observed for groups exposed to the vertical fields. This condition, which was restricted to the right eye and was diagnosed as secondary to uveitis, was not observed in control animals or those exposed to the horizontally orientated fields. It has been noted that in general rats show spontaneous rates of glaucoma on the order of 1 - 2% (Committee, 1977). In the study under discussion there was no evidence of increased incidence

rates with increased field strengths, i.e., no intensity-response relationship.

Growth retardation was evidenced by mouse pups born in a +24 kV/m dc field by lower body weights and shorter tails whereas, a 10 kV/m field had no effect (Nakamura, 1979). The information on this study was obtained from informal discussions of the investigator's ongoing work at the Central Research Institute of Electric Power Institute, Tokyo, Japan and thus full details are not available. The exposures were for 10 hr/day over a period of 5 mo but whether they were initiated before conception or during pregnancy is not known by the reviewer. The maternal cannibalism mentioned earlier in connection with slightly higher fields in this study suggests that poor maternal care may have contributed to the growth retardation of the pups. Since conducting these studies in which plastic exposure cages were used and in which electric field intensities were found to vary widely with differences in humidity, the investigator has developed a new exposure cage which is constructed of metal.

Although no effects on growth were mentioned, Mose and Fischer (1970) noted increased food and water consumption in mice that were exposed to a 24 kV/m field over a period of 15 days. Compared to the control group the increases averaged over days were 19.4% for food consumption and 14.5% for water consumption. With extension of the exposure period to 4-12 monnths a failure to produce progeny was also noted in the exposed mice. In a later study, liver oxygen consumption of mice that had been maintained in the 24 kV/m field or in a Faraday cage for 8 days was compared to that of mice maintained in "normal" cages in a brick work building. The field exposure increased liver oxygen consumption whereas the Faraday condition was associated with decreased consumption. In reviewing the research by Mose and coworkers, Sheppard (1978) noted that they also reported effects of the same 24 kV/m field on 5-hyroxytryptamine levels (decreases for brain and uterine tissue, increases in the gut) and on susceptibility to infection. We have not, however, reviewed the original reports for these latter studies.

In a second study by Marino et al (1974a), mice were injected with tumor cells (Erhlich acsites) and were then continuously exposed to horizontally oriented dc (+) fields of 8 - 16 kV/m for 14 days. Cell division was arrested on the morning of the 14th day by treatment with

Colcemid and 4 hr after the treatment samples of the tumor cells were removed and prepared for examination of the chromosome. Compared to cells collected from host mice that had not been exposed to the fields, a greater percentage of the cells from the exposed host had chromosomal abnormalities and the percentage of abnormal chromosomes per cell was also higher.

3.2.1.3 Hematology and Blood Chemistry (Table 3-3)

The distribution of serum proteins was measured after exposure of rats (Marino et al, 1974a) or mice (Marino et al, 1974b) to dc fields for varying periods. Protein determinations were made for rats after 30 days. For all three field intensities studied the relative percentage of at least one of the protein fractions was reportedly significantly altered, however, the direction of effects was not the same across field intensities. For mice the determinations were made after 7, 14, and 21 days of exposure to one of two intensities of horizontal fields or to a vertical field. At 21 days the relative percentage of protein in the β fraction was greater than for controls under conditions of horizontal exposure whereas with exposure to the vertical field this percentage was decreased as compared to controls. The higher intensity (10.7 kV/m) horizontal field also increased the relative percentage of protein that was in the β fraction at 7 and 14 days. For both studies it appeared that sera from animals in each control or exposed group were pooled and the analysis performed on a given number of aliquots from each pool. This is not an uncommon practice as long there is a sufficient number of pools from each group to allow statistical evaluation. In this case it appeared that a single pool may have been used for each group and the statistics were then based on the number of aliquots. This then would inflate the value of n (number of samples) and make it easier to obtain significant effects as the variability across animals within a group is not considered.

Hematologic evaluations were performed on blood collected from human subjects after exposure to dc fields of 30 or 60 kV/m for 2 hr intervals over a period of 2 mo (Krievova et al, 1973). A number of the standard hematologic assays were performed and no significant effects observed. At 90 kV/m, however, the number of platelets found in blood of samples taken

from human subjects following the field exposure was greater than the comparable percentage after a period of non-exposure.

3.2.1.4 Heart and Respiration

No effects of heart or respiration rates were detected for rats exposed to dc fields as great as 225 kV/m for periods of 30 - 60 minutes (Hermer, 1971, Lott, 1973). Nakamura (1979) observed increased spiking in the EKG's of cats during exposure to a 45 kV/m field, however, as with the aggessive behavior noted earlier for this study, the EKG spiking appeared to be dependent upon the presence of corona.

Blood pressure and heart rate were decreased in human subjects exposed to a 60 or 90 kV/m field for 2 hr intervals (Krievova, 1973). Whereas normal rates were recovered within 24 h after the 60 kV/m exposure, decreases were sustained over 4 or 5 days following a 90 kV/m field exposure. A 30 kV/m field had no effects on heart rates or blood pressure.

3.2.1.5 DC Electric Fields Summary

The first and foremost impediment to drawing conclusions as to whether increased fields may represent a risk for mammalian systems is simply the lack of studies addressing this question. There is of course a practical reason for this. Stimulation of risk assessment research is most often predicated on the extent to which human exposure is expected. For many years the bulk of long distance power transmission as been handled via ac lines. However in recent years the use of dc transmission has been recognized as a more economic method so that its use has increased and further increases are planned. For example, as of 1954 dc power transmission was on the order of 20 megawatts whereas by 1985 it is expected to approach 25,000 megawatts/year (Shah, 1977).

The literature to date contains no strong and unequivocal bases for alarm concerning hazardous biological effects from exposure to dc electric fields. Scattered positive results have been reported. In several instances such results appeared to be in the direction of an ill-defined stimulatory effects of the exposure (better performance in a maze, lower time scores, increased EEG activity, increased attention to task, increases in metabolic activities). Some of these could be considered improvements if

they were replicable, however such qualitative judgements should not be made without a broader data base that permits consideration of the effects in the perspective of impact on the organism as a whole.

The question of whether some of these results could be replicated is a very real one. Many of the reports did not contain important methodological information or in some cases the reported methods could be questioned. It was not always clear whether the problem was the method or the reporting and admittedly some of the information was obtained from abstracts or preliminary reports where full discussions of methodology are usually not available. However, some of the problems that were recognized should be mentioned. The first of these was a failure to indicate whether or how the test fields were measured and to what extent the fields were uniformed. The details of the features of the space or enclosures used for field exposures were at times omitted. Efforts to assure that the appropriate sham-exposed condition was achieved for control subjects or control periods were often not described. Many reports made no mention of important nontest environmental variables such as light, temperature, noise, and humidity. These variables are important first from the standpoint of assuring that the subjects are maintained in a suitable environment and because these variables in and of themselves can have substantial effects on biological responses. Further, in relation to the test environments, if a noise of some kind was specific to the test situation, this could have provided cues to the presence of the field. Humidity is also a particularly important factor in the EM effects evaluations because of its effect on coupling phenomena. Finally, with certain exposure systems the question of the role of ion effects or ozone generation was not ruled out.

3.2.2 Air Ions

In contrast to the limited body of literature concerning dc electric fields bioeffects, investigation of the question of whether excess air ions, deprivation of air ions, or altered ratios of positive and negative ions have biological significance has a long and controversial history. Due to the volume of this literature, the number of original reports abstracted and tabulated for the present report represent only a small fraction

of the total literature. These have been supplemented to some extent by tabulating information from previous literature surveys and where this was the case the responsible reviewer has been cited. Preliminary to the discussion of air ions bioeffects, a brief discussion of the properties, sources, and behavior of air ions is given. This discussion was prepared almost exclusively from secondary reference sources rather than from original reports. The sources used were summary or review articles by Andersen (1971), Knoll et al (1964), Krueger (1972), Krueger and Reed (1976), and Swan (1961). Where statements were more or less directly attributable to one of these sources, that source has been cited. In their discussion of these subjects, the referenced sources cited a broad spectrum of original research reports. It was not considered necessary for the purpose of this rather simplistic discussion prepared as background for the discussion of the bioeffects literature to list these citations.

3.2.2.1 Definitions, Properties and Behavior of Air Ions

Recognition of the existence of air ions dates to the last decade of the 19th century when two scientists in Germany, Elster and Geitel, and Thomson in England apparently made this discovery independent of each other (Krueger and Reed, 1976). Air ions are formed when some agent causes separation of an electron or negatively charged particle from a neutral molecule of atmoshperic gas. The remainder of the molecule thus left with a net positive charge is called a positive ion. Within a very short time the electron attaches to a neutral molecule or group of molecules and thus a negative ion is formed.

The primary natural agents for air ionization in the lower atmosphere are radioactive radiations and cosmic radiatons passing through air. A small contribution to natural ion production is also made by radioactive gaseous enamations from the soil which contains radium and similar substances. Together these sources account for an ion production rate of about 10 ions/ cm^3/sec (Swan, 1961). Other natural sources of air ionization include corona from lightning, the friction of rapidly moving wind over land, and friction of water molecules in waterfalls.

By ionizing under relatively high pressure and separating the ions according to mass under low pressure conditions, it can be demonstrated

that air can be ionized into a number of monomolecular ions including O^+, N^+, H_2O^+, N_2^+, NO^+, O_2^+, $Ay2^+$, N_3^+, N_2O^+, O_3^+, N_4^+, O^-, O_2^-, NO_2^-, NO_3^-, OH^- (Knoll, 1964). However, in atmospheric air these monomolecular ions have a short life because within approximately 1 x 10^{-6} sec a number of other molecules cluster around them thus forming a multimolecular ion. In nature clusters of one of the following compositions predominate: $H^+(H_2O)n$, $H_3O^+(H_2O)_n$, $O_2^-(H_2O)_n$, $OH^-(H_2O)_n$ (Krueger, 1972).

Ions are frequently categorized according to the rate at which they move through air however both the terminology and the definitions are somewhat arbitrary and not universal. Andersen (1971) suggested that "light ions" are most frequently defined as those having mobilities greater than 1 cm^2/v. sec whereas heavy ions are those having lesser mobilities. The term "small ion" has been used to designate ions with mobility spectra centered around 1.5 cm/v. sec (Swan, 1961) or 2 cm^2/v.sec (Knoll et al, 1964). These light or small air ions are the ions to which proponents of ion bioeffects have typically attributed biological activity. Intermediate and large ions are formed by the attachment of positive or negative charges to neutral condensation nuclei of varying sizes. Mobilities on the order of 0.01 cm/v. sec (Swan, 1961) or 0.01 cm^2/v. sec (Knoll et al, 1964) have been denoted as intermediate ions and those with lesser mobilities as large ions. The term "secondary ions" has alo been used to collectively denote intermediate and large ions and to distinguish these species of ions, the composite of which includes condensation nuclei, from primary multimolecular ions which are smaller clusters of a only few molecules.

Due to continual ageing or decay processes, the life of the small air ion is short. Estimates on the order of seconds or minutes have been suggested and depend in part on the purity of the air (Knoll et al, 1964). Andersen (1971) lists the following mechanisms of decay for light ions.

> "(1) by recombination with a light ion of the opposite sign forming neutral molecules, (2) by combination with a heavy ion of the opposite sign forming a neutral nucleus and neutral molecules or (3) by combination with a neutral nucleus forming a heavy ion. The heavy ions decay by combination with a light ion of opposite sign or by combination with heavy ions of the opposite sign."

Due to recombinations with condensation nuclei, the concentration of air ions in regions where dust, smog, or high humditiy is prevalent tend

to be small. Typical ranges for ions of either polarity have been suggested as 100 to 2000 ions/cm^3 and a average values of 150, 500, and 600 have been cited for cities, open country, and over oceans, respectively (Knoll et al, 1964). Krueger and Reed (1976) noted that even in clean country air the total number of ions seldom exceeds 1×10^4 ions/cm^3.

In undisturbed weather conditions, positive species of small ions tend to be predominant with n^+/n^- ratios ranging from 1.0 to 1.4. However, during rainfall or thunderstorms ratios of less than one are observed (Knoll et al, 1964). Increased concentrations of negative air ions also appear to be characteristic of highly humid areas such as areas near waterfalls or the seashore. Shifts in the direction of atypically high concentrations of positive ions may also be observed under certain weather conditions. Most frequently mentioned is the warm, dry windstorms that sweep through certain regions (Sharav or Hamsin winds in the Middle East, the Foehn in Central Europe, and the Santa Ana in California). The attribution of causation for diverse illnesses, symptoms, and behaviors to these winds or to the ionic imbalance that precedes and accompanies them apparently rests partially on scientific evidence, partially on anecdotal reports, and to some extent on folklore. The range of such claims can be appreciated by reading a book called "The Ion Effect" which was seemingly written for popular consumption by Soyka (1977). It presents from the viewpoint of a self-claimed ion sensitive individual relatively uncritical descriptions of scientific investigations as well as discussions of both historical and contemporary anecdotes. Simplistically, the position being offered by Soyka is that deprivation of ions or overdoses of positive ions are detrimental and high concentrations of negative ions are beneficial.

The discussion thus far has been concerned primarily with natural sources of air ions and ions in the natural environment. However, much of the ion bioeffects research appears to have been stimulated by proposals that human health and well being could be improved not only by controlling the air ions in the environment but by controlling via artifical means the ion ratios in places of residence or work. The primary means proposed for maintaining the preferred ion balance through natural sources is a reduction in air pollution for which one result would be higher concentrations of small air ions in cities and adjacent areas. However, for a

more immediate approach to air ion control in buildings ion generators, presumably capable of creating higher densities of small ions and probably primarily negative ions, are being suggested. Such generators are commercially available and being sold as health assist devices in some countries. In the U.S. such devices are apparently also available commerically but regulations (FDA) limits the extent of their advertising claims to claims of effectiveness as air cleaning devices.

Even with artificial sources of small air ions, the maximum densities achievable are small compared to the total number of molecules in a given volume of air. Swan (1961) discussed this in terms of the time required for excess ions of one polarity to disappear when superimposed on a room filled with positive and negative ion pairs. If for example the initial excess density is on the order of $1 \times 10^4/cm^3$ and there is no mechanism for replenishment, the excess ion density would be reduced to about 90% of the initial value within 10 min. For very high excess densities ($> 1 \times 10^4/cm^3$), it may be meaningful to consider the disappearance rate in terms of $t_{\frac{1}{2}}$, i.e., time requried for 50% of the inital excess to disappear. Under the condition of very large excess densities, $t_{\frac{1}{2}}$ decreases as the initial excess density increases. In other words the more excess ions present, the faster half of them will disappear. Andersen (1971) describes the cases in which ions are delivered via a steady flow system such a tube with a stream of air outward from the ion source. Using curves derived from a report by Whitby and Jordan (1973), he calculated that regardless of the output of the source the maximum concentration of small uinpolar ions that could be obtained at a positon that could be reached in 1 sec of travel from the source would be 3×10^5 unipolar ions/cm^3. For a position 10 sec travel away from the source the maximum obtainable value would be lowered by one order of magnitude. When it is considered that one cubic centimeter of air contains about 2.7×10^{19} molecules, even at maximum concentrations small air ions make up only a small fraction of the air. It is consideration of this large dilution factor that has caused some scientist to be skeptical of biological effects reportedly associated with alterations in ambient ionic conditions. In response to this skepticism, proponents of ion bioeffects phenomena point to the extreme sensitivity of certain biological systems to physical or chemical stimuli. For example, Krueger and Reed(1976) mention the retinal response

which can be elicted by a single quantum of light and the extreme sensitivity indicated by responses to species specific phermones which for some organisms serve as sexual attractants or for communication of alarm. Evidence of effective pheromone concentrations as low as 200 molecules/cm^3 air and 1 molecule of pheromone in 1.5×10^{11} molecules of water were cited.

The preceding paragraph concerns maximum densities of unipolar ions achievable under optimal conditions. The actual densities achieved in a particular situation would of course depend on all the factors that affect ageing or decay of ions. Further, if the issue is whether the ions may affect a given biological system, the more critical questions become the ions available at the point of uptake into the system and the fate of the ions after uptake. Critical factors for determining the ions available at the point of uptake include the electric fields in the exposure area, the potential of the biological subject in relation to the potential of other objects in the room, and airflow within the room. Illustrating with a hypothetical situation in which a nozzle from an ion generator delivers unipolar ions to a room where a patient or subject is located, Swan (1961) described situations in which essentially no ions would reach the subject. This could be either because they were repulsed by like charges on the subject or because most of the ions would be attracted by other objects in the room that were of lower potential than the subject. Discussing the electrical fields and relative potentials and effects on ion availability he stated: "In order to get ions to the patient we must have the lines of electric force going to him in case of positive and away from him in the case of negative ions."

Another issue raised by skeptics of ion bioeffects is that of the means of interaction between biological systems and the ions. The points of contacts for humans and other mammals would be the skin, skin coverings, and the respiratory system. The latter has received a great deal more attention. Andersen (1971) reviewed several studies in which the distribution of inhaled air ions in the respiratory system was considered. He concluded that, "a considerable deposition of ions takes place on the mucosal surface of the respiratorytract and mainly in its upper part - the nasal cavity, nasopharynx and trachea. The physiological effects, if any, of inhaled gas

ions therefore must cause a local effect in these regions or there elicit reflex mechanisms or humoral mechanisms."

3.2.2.2 Air Ion Bioeffects

A major focus in this research has been the respiratory system (Table 3-5). Where effects in humans were reported they tended to be in the direction of improved or more economic functioning under conditions of excess negative ionization (Goldman and Rivolier, 1977; Wehner, 1961) or decreased capacity with excess positive ions (Winsor and Beckett, 1975). However, in several studies with human subjects there appeared to be little or no effect on respiratory measures even though the studies were conducted with ion concentrations in the same range or greater than those which yielded positive results (Goldman and Rivolier, 1977; Hamburger, 1962; Minkh, 1961; Sulman, et al, 1978)

The upper respiratory tract was of particular interest because of the evidence that if local effects were to obtain, it would be the most likely target. Krueger and his coworkers have led much of the air ion research in animal models including the studies of the upper respiratory tract (Table 3-5) as well studies tabulated in subsequent tables. Their studies of tracheal functioning involved both in vitro and in vivo preparations for a number of different mammalian species. The general pattern of their results is consistent with the hypothesis that excess positive ions impair tracheal functioning and that negative ion exposures reverse this effect or may even improve tracheal functioning over baseline conditions. In contrast, at least three investigators or groups have determined ciliary beat and mucous flow rates in the mammalian trachea and found no effects of either positive or negative ionization or ion deprivation (Andersen, 1971; Guillerm et al, 1966; Kensler and Bettista, 1966). Andersen (1971) reviewed the studies reported by Krueger and coworkers and suggested that due to the extreme sensitivity of tracheal preparations to temperature and humidity, these factors may have been involved in the positive results obtained. It was also suggested that in the earlier studies the electrophysical conditions may have been inadequately controlled. Krueger (1972) in responding to these comments acknowledged that these early studies may have had some methodological deficiencies but noted that on the positive side the studies

Table 3-5

The Effects of Air Ions On
The Heart and Respiration

Investigators Investigators	Subject Subject	Exposure		Results
Winsor & Beckett, 1957	Human	(+) and (-) 3.2×10^4/cc	20 min	*Breathing Capacity (DEC,+ Only) *Various Symptoms Reported by Subjects More Severe and More Persistent In Positive
Minkh, 1961	Human	(-) Ionizer Produced 1.5×10^6/cc	25 days 15 min/day	•Blood Pressure, Pulse, Respiration Rate
Hamburger	Human	(+) and (-) 4×10^6/cc	92 min	•O_2 Uptake During Exercise (Trends INC for + but not statistically significant)
Sulman et al, 1978	Human	(-) 10^4/cc	2 mos 16 hr/day	•Body Weight, Blood Pressure, Pulse, Respiration Rate, Oral Temperature
Bachman et al, 1965	Rat	(+) and (-)	30 min	•Heart Rate *Respiration Rate (+ INC, -DEC Then INC)
Bachman et al, 1966	Rat	(+) 61 - 4900 x 10^3/cc (-) 73 - 2080 x 10^3/cc	45 min	*Respiration (DEC)
Skorobogatova	Cat	(-) 10^6/cc to Donor Adrenalin to Receipient		*Reduced Adrenalin-Induced Rise in Blood Pressure

* Affected
• Not Affected

INC = Increased
DEC = Decreased

Table 3-5
The Effects of Air Ions on
The Heart and Respiration
Cont'd

Investigators	Subject	Exposure		Results
Krueger & Smith, 1957 Krueger & Smith, 1958a,b Krueger et al, 1959a,b Krueger & Smith, 1959 Krueger, 1962 Krueger et al, 1962	Tracheal Strips From Mouse, Rabbit, Guinea Pig, Monkey or In Vivo Through Tracheal Aperture	(+) and (-) Ranged From 10^3 - 10^9/cm^2/sec		*General Pattern Ciliary Rate (+ DEC, - INC) Mucous Flow Rate (+ DEC, - INC) Tracheal Appearance (+Contracted, -None) Vulnerability to Trauma (+ INC, - DEC) Some Effects at Concentrations on Order 2.5 x 10^3/cm^2. With (+) at 10^9 sometimes Obtained Complete Supression of Ciliary Beating and Mucous Flow. With In Vivo Preparation Respiration Rate (+ INC, -DEC) and Vasoconstriction (+INC) of Tracheal Wall also observed.
Kensler & Bettista, 1966 Cited by Andersen, 1971	(In Vitro)	Unipolar Ions		•Tracheal Mucous Flow and Ciliary Rate
Guillerm et al, 1966 Cited by Andersen, 1971	Rabbit (In Vitro)	Unipolar Ions		•Tracheal Mucous Flow and Ciliary Rate
Andersen, 1971 (Noted ion concentration in measuring tube given. Author notes at the preparation the concentrations were ^ twice these values)	Rabbit (In Vivo and In Vitro)	Bipolar ^ 2 x 10^5/cc (-) 1.9 x 10^5/cc (+) 2.0 x 10^5/cc Unionized 275/cc	90 min	•Tracheal Mucous Flow and Ciliary Rate

* Affected
• Not Affected

INC = Increased
DEC = Decreased

Table 3-5
The Effects of Air Ions on
The Heart and Respiration
Contd

Investigators	Subject	Exposure		Results
Goldman & Rivolier, 1977	Human (4 subjects)	(-) 5-6 x 10^4/cc	30-45 min intervals on-off measure-ments over 3-week period.	•Pulse, Rectal Temperature, Average Ventilation Rate, Maximum Volume Expired Air/Sec, Average Current Volume, Average Respiration Rate
	Human (19 subjects)	(-) 3-4 x 10^4/cc	20 min interval once/week for 4 weeks alternated with no excess ions for 4 weeks.	*Recovery of Respiration Rate After Exertion (INC) •Recovery of Heart Rate After Exertion
	Human (2 subjects)	(-) 5 x 10^4/cc	8 h/night, 5 nights/week, alter-nating weeks with-without excess ioni-zation. Measurements at beginning and end of 3 weeks.	*Repose ventilation, Respiratory Frequency at Rest and Under Exertion, Oxygen Consumption Under Exertion, Inefficient Fraction of External Ventilation, Cardiac Output at Rest all DEC *Respiratory Current Volume at Rest, Deep ventilatory Efficiency INC •Oxygen Consumption at Rest, Alveolar Ventilation.

* Affected INC = Increased
• Not Affected DEC = Decreased

Table 3-5
The Effects of Air Ions On
The Heart and Respiration
Contd

Investigators	Subject	Exposure	Results
Wehner, 1961	Several Thousand Human Patients (Adults & Children)	Electroaerosol Therapy (EAT)	*Author cites reports and communications from clinic directors and company physicians reporting success with EAT in respiratory illnesses. One source mentioned pneumoconiosis as not being affected but another indicated success. Other illnesses for which success was reported included pertussis, asthma, bronchitis, laryngitis, emphysema, plus reports of improvement of non-respiratory conditions such as migrains, eczema, rheumatism, cardiovascular diseases, as well as improved mood, sleep, and appetite. Author notes "findings...in some instances wre based on only limited number of cases, in others the indication is still controversial" however his overall interpretation was favorable to EAT.

* Affected
● Not Affected

INC = Increased
DEC = Decreased

were conducted in replicates and that all stroboscopic readings of ciliary beats were performed by one person thus providing for uniformity of counting techniques.

Krueger has also led the efforts in another approach to study of the respiratory system, that of susceptibility to respiratory infectious agents (Table 3-6). In a series of experiments with mice, he and his coworkers observed earlier or greater mortality for mice challenged with respiratory infectious agents when the mice were exposed to excess positive ion concentrations. In general negative ionization was associated with decreased mortality in challenged mice, however, in one study a negative ion density on the order of 10^3 ions/cm^3 resulted in increased mortality. There were indications that intranasal challenge was necessary for the effects to obtain and that challenge after exposure to the ionic test conditions did not show the ion effects.

Several investigators have considered cardiovascular functioning in human subjects exposed to different ion ratios (Table 3-5). Considering clinical evidence, cardiovascular diseases were reportedly improved by electroaerosol therapy (Wehner, 1961). However for laboratory studies in humans there appeared to be little evidence of effect on the normal functioning of the cardiovascular system (Goldman and Rivolier, 1977; Hamburger 1962; Minkh, 1961; Sulman et al, 1978). Similarly, heart rate was not affected in rats that were given brief periods of exposure to increased concentrations of positive or negative ions (Bachman et al, 1965).

Hematologic parameters explored have failed to show any strong trends for ion bioeffects (Table 3-7), however, effects on blood sedimentation rates, pH and CO_2 combining power have been reported (Kusima, 1967; Worden, 1961).

A major hypothesis offered by proponents of air ion bioeffects is that certain of the effects are mediated via alterations in metabolism of 5-hydroxytryptamine (5-HT or serotonin). There is considerable evidence that 5-HT is a neurotransmitter although evidence of its being the sole mediator at specific synaptic connections is lacking in mammals (Cooper et al, 1970). In the nervous system the highest concentrations of 5-HT are found in the hypothalamus, limbic structures, and basal ganglia (Bogdanski et al, 1957; Maickel et al, 1968), however, about 90% of the 5-HT present in mammals is located in the gastrointestinal tract (Goodman and Gilman (1975).

Table 3-6

The Effects of Air Ions on Resistance to Infection

Investigators	Subjects	Exposure (Ions/cc of Air)		Results
Krueger & Levine 1967	Mouse	(+) 3-4 x 10^5/cc Controls: Room air or positive electric field comparable to that in the ion exposure chamber. The two control groups gave comparable results	Up to 30+ days beginning immediately after infection	*Course of Coccidioidomycosis (Death rate and cumulative mortality at 30 days INC)
			7 days beginning 47 days after infectior or 7 days (only) prior to infection	•Course of Coccidioidomycosis
Krueger et al, 1970	Mouse	(+) 1.0-4.1 x 10^5/cc Controls: Room air or electric field	48 hr prior to and up to 16 days after infection	*Death rates following challenge with Klebsiella Pneumoniae or PR8 influenza virus (INC)
Krueger, Kotka, & Reed, 1971	Mouse	(-) 2.5 x 10^5/cc Controls: Pollutant-free air with ≃ 1 x 10^2 ions of each polarity	48 hr prior to and up to 10 days after infection	•Death rates following challenge with PR8 influenza virus
Krueger & Reed, 1972, 1973	Mouse	Low (-): 3.0-3.5 x 10^3/cc Low (+): 2.7 x 10^3/cc Mid (-): 2.0 x 10^4/cc Mid (+): 1.7 x 10^4/cc High (-): 2.2-3.0 x 10^5/cc Ion depleted air Controls:Bipolar with 2.0-3.5 x 10^3/cc and n+/n- ratio of 1.2/1	48-72 hr prior to and up to 12-13 days after infection	*Death rates following challenge with influenza virus (INC by all levels of +, by low level of -, and by ion depletion. DEC by high level -)
Krueger et al 1974	Mouse	Low (+ or -): 2.7-5 x 10^3/cc High (+ or -):2.3-5 x 10^3/cc Ion depleted air with low (1.0 v/cm) or high (40-60 v/cm) positive or negative field. Control: Bipolar as above.	72 hr prior to and up to 11 days after infection	•Death rates following aerosol challenge with influenza virus. Results suggested effects may be dependent on the method of delivery of the infectious challenge as intranasal instillation used in above studies.

* Affected o Not affected INC - Increased DEC - Decreased

Table 3-7

The Effects of Air Ions On
Hematologic And Clinical Chemistry Parameters

Investigators	Subjects	Exposure		Results
Krueger et al, 1966	Mouse	Nonionized Vs. Ionized (+) (1.3×10^4/cc (CO_2^+)	5 Hr	*Blood Levels Serotonin (Nonionized DEC, + Ionized INC)
Krueger et al, 1968	Mouse	(+) And (-) 4 - 5 X 10^5/cc	Intervals Up to 7 Days	*Blood Levels Serotonin (+INC, -DEC) Hypothesized that Active + Ions were Oxonium and Hydronium Ions and - Ions were $O_2^-(H_2O)_n$ and $OH^-(H_2O)$. Experiments in which CO_2, O_2, and N_2 were added to Exposure Chamber Supported Hypothesis
Krueger & Smith, 1960	Guinea Pig	(-)	24 Hr	*5-Hydroxyindoleacetic Acid in Urine (INC)
Kusmina, 1967	Cat	(+) 1.0×10^6/cc (-) 1.2×10^6/cc	6 - 10 Min	•Electrophoretic Mobility of Erythrocytes, Serum Protein Fractions, Stability of Serum Proteins *Blood Sedimentation Rate (Slight INC + And -), Blood PH, Blood Pressure (- DEC Effects of Exsanguination)
Sulman et al, 1978	Human (10 Ss, 5 were weather sensitive)	(-) 1×10^4/cc	2 Months (16 Hr/Day)	*Serotonin, 5-HIAA, Histamine Thyroxine Urinary Excretion DEC if initial elevation. •Excretion of 17-Ketosteroids, 17-Hydroxy-steroids, Adrenaline, Noradrenaline

* Affected
• Not Affected

INC = Increase
DEC = Decrease

Table 3-7

The Effects of Air Ions on
Hematologic And Clinical Chemistry Parameters
Contd

Investigators	Subject	Exposure		Results
Goldman & Riovlier, 1977	Human (2 Subjects)	(-) 5 x 10^4/cc	8 h/night, 5 nights/week, alternating weeks with and without excess ions. Measurements at the beginning and end of each week	*Arterous-venous Difference in Oxygen Content at Rest and Under Exertion. •Hemotocrit, Hemoglobin
Worden, 1961	Hamsters	Biopolar with $n^-:n^+$ or $n^+:n^-$ ion ratios ^ 200-2500 ions/cc	24-96 h	*Blood pH and CO_2 combining power.

* Affected
• Not Affected

INC = Increased
DEC = Decreased

Another major locus of 5-HT is the blood platelets.

Diverse pharmacological actions can be shown with administration of exogenous 5-HT. Prominent among these are stimulation of smooth muscle, bronchoconstriction in some mammals but uncommonly in humans other than asthmatics, dose-dependent effects on respiratory rate, vasoconstriction in smooth muscle, and vasodilatation in skeletal muscle and skin.

Possible involvement of 5-HT has been proposed for varied physiological processes including sleep (Jouvet, 1968), temperature regulation (Fedberg and Myers, 1964), hormonal release (Wurtman, 1971), sensory perception, and mood and affect (Bogdanski and Udenfriend, 1956). Discussing the possible role of raphe tryptaminergic or 5-HT-releasing neurons, Goodman and Gilman (1975) concluded that one important function "may be to dampen overreactiveness to various stimuli (external and internal) involving, for example, auditory, visual, olfactory, nociceptive, and other signals affecting social and adaptive behavior (including learning) and involving such parameters as sleep, sexual behavior, aggressiveness, motor activity, perception (including pain), and mood."

Relevant to air ions, the serotonin hypothesis is that positive ions cause accumulation of 5-HT in blood and tissues, whereas, negative ions have the opposite effect (Krueger and Reed, 1976). The proposed mechanism is inhibition (positive ions) or stimulation (negative ions) of monoanmine oxidase activity, the enzyme by which 5-HT is oxidatively deaminated to 5-hydroxyindoleacetaldehyde and immediately thereafter converted to one of three metabolites of which 5-hydroxyindoleacetic acid (5-HIAA) is primary. Further extensions of the hypothesis have suggested that excess positive ions would adversely affect the processes mentioned above and that negative ions would, by depleting excess 5-HT, ameliorate these conditions. Although it is clear that proponents of air ion bioeffects consider ion depletion an adverse condition, we are not clear how or whether it is postulated that ion depletion effects are mediated via alterations in 5-HT metabolism. It should be noted however when considering the air ion bioeffects literature that two issues are involved. One has to do with the total density of ions of either sign and the other with excess ions of one sign or the other.

A variety of evidence has been cited by proponents of the serotonin hypothesis as supportive of the susceptibility of 5-HT pathways to air

ion effects. This includes alterations in circulating and tissue levels of 5-HT and in the excretion of 5-HT or its major metabolite 5-HIAA (Table 3-7, 3-8). It also includes behavioral studies such as those of Frey (1967), Nazzaro et al (1967), and Gilbert (1973) in which the general trend was toward a reduction in emotional reactivity with high concentrations of negative ions and in some studies an increase in indications of emotionality with excess positive ions. The symptomatology and increased 5-HT release reported aasociated with the ionic imbalance that precedes Sharave or similar weather conditions has also been cited as supporting this hypothesis (Krueger and Reed, 1976; Sulman et al, 1978). Krueger (1961) reported pharmacological studies in which reserpine, a known depleter of 5-HT from certain tissues mimicked the effects of negative ions and blocked the effects of CO_2^+ in the mammalian trachea. Conversely, treatment with iproiazid which results in tissue accumulation of 5-HT produced effects on the trachea similar to those observed with CO_2^+. Frey (1961) also obtained parallel results for reserpine treatment and treatment with excess negative ions with rats evaluated in the conditioned emotional response paradigm mentioned above. Relevant to these findings it should be noted that reserpine also depletes catecholamine stores in both the brain and adrenal medulla (Goodman and Gilman, 1975), however, there was no evidence of increased excretion of adrenaline or noradrenaline following human exposure to protracted negative ion exposures (Sulman et al, 1978). As a final commment with respect to the serotonin hypothesis, it might be noted that two investigators (Assel et al, 1974; Sulman et al, 1978) observed increased synchronization and amplitude in EEG recordings under conditions of negative ion exposure. Such recordings could be considered as supportive of the hypothesis as they might be expected in subjects that were in a calm or undisturbed state.

Table 3-9 lists a series of studies on endocrine glands that were performed or cited by Gualtierotti(1968). Among the effects reported were accelerated maturation of gonadal cells in animals exposed to negative air ions. In the face of clinical reports and anecdotal claims concerning the effects of air ions on sexual drive or behavior, it is surprising that there appears to have been so little laboratory research into air ion effects on sexual behavior and reproduction. Several investigators have considered effects on growth processes including embryonic growth, neonatal

Table 3-8

The Effects of Air Ions On the Nervous System and Behavior

Investigators	Subject	Exposure		Results
Knoll et al, 1961 Rheinstein, 1961	Human	(+) And (-) 2 X 10^3-10^6/cc Directed at Face or Leg	30 Min Alternating Periods	*Reaction Time (Changes Bidirectional for Both + and -; Not Observed when Ions Directed at Leg) •Visual Moment
Minkh, 1961	Human	(-) Ionizer Produced 1.5 X 10^6/cc	25 Days, 15 Min/ Day	*Reports of Improved Mood, Sleep, Appetite *Improved Endurance, Muscular Strength, Reaction to Visual Irritation, Equilibrium In Test Situations
Slote, 1961	Human	(+) And (-) 2 X 10^4/cc	15 Min Periods + Test Period	•Finger Tapping for 10 Sec. *Finger Tapping for 60 Sec. (Speed +DEC,-INC) *Visual Reaction Time (+INC, -DEC) *Flicker Fusion Threshold (+DEC, -INC)
Assel et al, 1974	Human	(-) 3.5 X 10^5/cc	45 Min Periods	*EEG (DEC.Alpha Activity, INC. Amplitude, Sychronization)
Sulman et al, 1978	Human	(-) 10^4/cc	2 Mo,16 Hr/ Day	*EEG (Stabilized Frequency, INC. Amplitude, Synchronization)
Bachman et al, 1966	Rat	(+) 61-4900 X 10^3/cc (-) 73-2080 X 10^3/cc	45 Min	*Motor Activity (+DEC then INC, -INC then DEC). *Reported Effects on Urination, Defecation, Sleep
Nazzaro et al, 1967	Rat	(+) 3 X 10^4/cc (-) 2.5 X 10^4/cc	8 Days	*CER (+INC Anxiety, More Variable; Anxiety, More Stable Behavior, not consistent throughout

* Affected
• Not Affected

INC = Increase
DEC = Decrease

Table 3-8

The Effects of Air Ions on The Nervous System and Behavior
Cont'd

Investigators	Subject	Exposure		Results
Terry et al, 1969	Rat	(-) 7 X 10^6 - 7 X 10^7/cc	5 Hr	*Maze Learning Improved (Males Only)
Skorobogatova	Rabbit	(-) 10^6/cc		*Air Ions Used as UCS to Obtain Body Temperature INC to Conditioned (Bell)
Krueger & Kotka, 1969	Mouse	(+) And (-)		Brain Seretonin
		Low: 2 - 4 X 10^3/cc	12 Hr	*DEC But Mid Levels No Effect
		Mid: 3 - 4 X 10^4/cc	24 Hr	*DEC Only Mid Level +
		High:3.5-5 X 10^5/cc	48 Hr	•All Levels
			72 Hr	*DEC All But Mid Level +
Gilbert, 1973	Rat	(-) 3 X 10^3/cc	17 Days, 8 Hr/Day or Continuous	*Brain Seretonin (DEC, Continuous Only) *Reaction to Handling (Counteracted Effects of Isolation) •Body Weight Change, Emergence Latency, Avoidance Responding, Runway Activity
Frey, 1967 Cited by Krueger, 1972	Rat	Negative ions		*Conditioned Emotional Response Suppressed. Same effects observed with Reserpine treatment
Felici et al, 1977	Mice	50% Depletion of small ions and depletion of large ions to ^ 10% vs background of 100-400 ions/cc		•Activity Appeared Normal, No Deaths
	Mice	3-6 Small ions/cc vs background	3-6 weeks	•"No Visible effects"

* Affected
• Not Affected
INC = Increased
DEC = Decreased

Table 3-9

The Effects of Air Ions on Endocrine Glands

Investigators	Subject	Exposure		Results
Gualtierotti, 1968	Guinea Pigs	Negative Ions	63-207 h	*Width and Volume of Adrenal Cortical Cells (INC)
	Mice	Negative Ions	2-8 days	*Thyroid Gland Colloid Production (INC)
	Mice	Negative Ions	96 h	* Maturation of Testicular and Ovarian Cells (INC)
Oliverau Cited by Gualtierotti, 1968	Rat	Negative Ions		*Adrenal Gland Weight (INC)

* Affected
● Not Affected

INC = Increased
DEC = Decreased

development, and regeneration of nervous or other tissue after experimental injury (Table 3-10). If there is a trend for these studies, it is in the direction of facilitation of growth by exposure to excess negative ionization, however, the models cited are so diverse that it may be an over simplification to consider them as supportive of each other.

3.2.2.3 Methodological Problems in Air Ion Bioeffects Research

Some of the methodological problems in air ion research have been mentioned above and previously discussed by other reviewers (Andersen, 1971; Frey, 1961; Krueger, 1968; Krueger and Reed, 1976; Sheppard, 1978), however, they merit restatement here.

Some of the problems are more or less uniquely or directly related to air ion research. For example, Krueger and Reed (1976) listed the following as being major factors contributing to errors in observation in air ion research:

- "Neglect of ozone and oxides of nitrogen produced by corona discharge ion sources."
- "Failure to monitor and control ion densities, temperature, and humidity."
- "Use of air containing particulates and gaseous pollutants which combine with air ions and lead to widely fluctuating small ion densities."
- "Failure to hold the experimental subjects at ground potential, so that their surfaces developed high electrostatic charges and repelled approaching air ions."

Sheppard (1978) also noted that in some studies in which ion densities were measured, the points (in relation to the source, subject, or part of the body) were not reported and that in others there was no separation of positive and negative ions.

Although not specific to the air ion problems, we would also mention that in some studies, particularly those with human subjects, the sample size was extremely small (two subjects in one cases) and method of selection and assignment of subjects was not indicated. Further, the statistical approaches

Table 3-10

The Effects of Air Ions
On Growth, Development and Healing Process

Investigators	Subjects	Exposure		Results
Worden, 1961	Newborn Hamsters	Excess ratios of (+) or (-) ions		*(-) Body Weight and Proportional Weight of Heart, Adrenals, Kidney, Testis Seminal Vesicles, and Epididymis (INC). Testicular Fat Mass ●(+) Above Values lower in Positive than Controls but Difference Not Significant. (-) Proportional Liver and Spleen Weights
	Chick Embryo Explants in Culture	Excess ratios of (+) or (-) ions	72 h	* Growth of Cultured Explants Increased to 1½ Times Control, Positive Ion Culture 9/10 Size of Control
	Hamster	Excess ratios of (+) or (-) ions		*(-)Regeneration of Several Femural Nerve (INC). (-)No Effect
	Hamster	Excess ratios of (+) or (-) ions		*Healing of Skin Lesions (-) Accelerated, (+) Slowed Healing

* Affected
● Not Affected

INC = Increased
DEC = Decreased

were not always clear and in some cases interpretations appeared to have been based solely on visual inspection of the data. In general reporting of the biological assay methodology appeared to be somewhat better than in some of the dc electric field studies but here again it would often be difficult to approach replication of specific experiments from the details given.

3.2.2.4 Air Ion Summary

In summary, the questions of bioactivity of small air ions and the role of 5-HT methabolism in such effects are still controversial issues. Interpretations based on comparisons of results obtained from different laboratories are hampered by methodological questions. Seemingly some of the evidence fits together rather well and offers some support for the serotonin hypothesis. However, some caution is indicated. One of the problems with a putative mediator like 5-HT is that its actions are so diverse and some of them not well understood so that it can be used to explain effects in seemingly opposite directions. The complex feedback and interactive roles characteristic of neurohormones in general, and of 5-HT specifically, often make it difficult to rule out even inconsistent evidence as supportive of the hypothesis.

In any event, given the reports of adverse effects of sometimes relatively short exposures to environments containing excess positive ions, (some of which are based on ion densities that occur in nature in unusual weather conditions and will almost certainly occur in the vicinity of HVDC transmission lines), it is important for the objectives of the proposed experimental design that some of the lines of investigation suggested by the air ion literature be pursued.

3.3 Methodological Approach to Biological Tests

Based on the foregoing analysis of available literature the biologic tests that should be employed should include those which can reliably detect changes in different physical, physiological, and behavioral responses. The rationale for their selection should be based on the background literature, the reproducibility they offer, the state of the art developed, and upon sound toxicologic principles.

3.4 Behavioral Tests

The design should include a fairly strong emphasis on behavioral testing. This is compatible with the literature for both electric fields and air ion bioeffects as well as with the new emphasis being placed on behavioral evaluations in many areas of risk assessment. Emotional reactivity is a predominent component considered in several of the behavioral tests and this is also consistent with the background literature. Feasibility in terms of the overall experimental design must also be considered in selection of behavioral tests. Tests which require extensive preliminary training of animals should not be planned for the first screen.

Concerning specific tests, the open field is one that is easily administered and has been shown to be sensitive to a variety of genetic, experimental, physiological, and pharmacological manipulations. Even for such a simple test the interpretations are not always straight forward. Procedures for this vary widely as do the measures or responses considered. There appears to be reasonable agreement that at least for the two measures (ambulation and defecation) that will be considered in the open field tests for this program, that a large component of the determinants of the behaviors is some nonspecific affective state which for want of a better term is called emotionality (Walsh and Cummins, 1976). A tendency to explore has also been suggested as a component in determining the extent of ambulation in the field.

The skeletal motor startle response to an auditory stimulus is easily obtainable and shows some habituation with repeated presentations of the stimulus. The most common measure used is either occurrence or nonoccurrence of the response or the magnitude of the response. The

latter is preferred as it provides quantitative information. Connor et al (1970) found transitory decreases in the rate of habituation of this response in rats for which brain 5-HT had been almost completely depleted by treatment with paracholoro-pheylalanine. In the current program the effect of the test environments on the magnitude of the startle response for sequential trials should be considered.

Irritability upon presentation of a painful stimulus should be evaluated in terms of aggressive responses in male animals. The one-way avoidance task is also a test in which emotional reactivity may play an important role, however, the test also probes ability to acquire and retain a response to a specific set of stimuli.

3.4.1 Electrocortical Measures

Since procedures involving EEG measurements could be expensive and time consuming with little value unless properly done, a rather extensive discussion recommending a sound approach follows.

Potential effects of exposure to electric fields include CNS effects which may involve both acute and chronic changes of either physiological or functional presentation. Although histological and neurochemical analyses may detect many sorts of CNS damage, it is well known that a variety of functional deficits of a pronounced nature may be present without any obvious chemical or anatomical lesion. While functional impairments undoubtedly stem from underlying physiological damage, such damage may be distributed or be of an unrecognized nature.

For this reason, it is necessary to perform tests of adequate CNS function in exposed animals. These tests may include neurological examination, behavioral tests, and electrophysiological assessment. Neurological examinations are an excellent indication of certain types of CNS disorder, but they are generally insensitive to impairments of such "higher functions" of the CNS as learning ability, perceptual discrimination, memory, and the like. Moreover, neurological examination is frequently a weak measure of adequate function of forebrain structures in general, except where definite sensory and motor mechanisms are in question. Behavioral tests by contrast are very sensitive and discriminating measures of specific CNS functions when applied with the proper controls.

A drawback of behavioral tests in the present context, however, lies in their very specificity. Such tests are difficult and time consuming, and it is frequently impractical to employ them unless there is some specific hypothesis regarding the nature of the effect resulting from the experimental manipulation. In the absence of any such hypothesis, much experimental effort could be expanded on behavioral testing while missing some relatively gross effect which did not happen to fall within the purview of the test battery.

Electrophysiological measures, and particularly electrocortical measures present a reasonable compromise among these problems. They are thus desirable as an adjunct to neurological and behavioral tests of CNS function. Among the electrophysiological measures, the electroencephalogram (EEG) and the closely related electrocorticogram have a long history of employment in the detection of CNS abnormalities. They are sensitive measures for many kinds of functional disorder, and are particularly sensitive to forebrain and cortical abnormalities. In addition, they are the subject of a large experimental literature which relates EEG phenomena not only to experimentally produced pathology, but to a variety of normal functional states of the CNS. In the present context, it is only necessary that this relation exists in order to make a case for the value of electrocortical measures as a technique for the assessment of CNS function. In the absence of any specific hypothesis concerning the nature of the deficits to be expected, <u>any</u> change in electrocortical activity is of interest, irrespective of ability to identify it with a particular functional impairment. Given this, the chief advantage of the electrocortical measure is seen in its sensitivity to a very broad spectrum of potential abnormalities. The chief disadvantage, the difficulty of specifying the precise functional effect of an observed anomaly in electrocortical activity, is not of paramount importance in a preliminary investigation having the objective of establishing the existence or non-existence of <u>any</u> evidence of change in CNS function. Finally, electroencephalographic effects have been documented in response to exposure to electromagnetic fields of other types than those under study in this investigation (Adey and Bawin, 1977).

3.4.1.1 Rationale for a Power Spectrum Approach in EEG

Despite the desirability of the EEG as a general index of forebrain function, certain difficulties occur with this measure which are particularly problematical in the present experiment. The raw EEG waveform, as usually obtained for clinical assessment, is particularly useful in the instance of marked abnormalities of brief duration, such as seizure spikes. It is difficult however to detect more subtle changes that may manifest themselves in alterations of the frequency content of the EEG waveform. Such changes might be introduced by a change in the activity of some particular cortical generating area which contributes, together with others, to the overall waveform. Such small changes in the steady state activity are best detected by statistical techniques which are exceedingly difficult to apply to the raw EEG waveform. In addition, the present situation demands optimal sensitivity of detection, which implies the necessity of averaging results from a number of subjects. This is not possible with the raw EEG waveform. In normal clinical assessment the concern would be with detection of abnormalities in a particular subject and averaging would be inappropriate, but this is of no consequence in the current context.

A measure which is more suitable than the raw EEG waveform in regard to the above considerations is the EEG power spectrum. This measure is obtained by taking the Fourier transform of samples of the EEG waveform and then obtaining the root mean square amplitude of the sine and cosine components for each frequency component. This results in a power spectrum in which each spectral component represents a measure of the amount of activity present in a particular frequency range of the raw EEG. The advantage of this procedure is that it eliminates phase relations in the EEG frequency components and thus permits averaging of the power spectra. This makes possible the application of statistical procedures to the spectral components and the averaging together of data from many subjects. With these techniques in hand, it becomes possible to detect small changes in restricted portions of the EEG frequency spectrum which would be impossible to detect by simple inspection of the raw EEG waveform. This procedure is thus well suited to obtaining a quantitative measure of differences in the EEG activity of experimental and control

groups of animals subjected to procedures such as those proposed in the present investigation.

A drawback of the power spectral measure is its relative insensitivity to brief events such as seizure spikes which are better detected in some instances by standard clinical evaluation of individual EEG records. However, since the EEG records are obtained as a preliminary to the construction of power spectra, the employment of a power spectral measure does not preclude a visual inspection of the normalcy of the raw waveform.

Thus, the power spectral measure is markedly superior to the standard clinical techniques of EEG analysis for this application, in that it provides an objectivity and quantificability which is lacking in the most skilled subjective evaluation, and it is particularly well suited to the detection of small changes in specific EEG components such as might result from distributed CNS damage. Its inferiority at detecting isolated activity of the type frequently resulting from focal lesions is not a serious handicap in view of the type of damage which might be expected from wholebody exposure to electric fields, and in any event, the data required to supplement the power spectral measure are available.

3.4.1.2 Potential Problems and Artifacts

The recording of EEG activity is a standard technique, and is widely available with standard apparatus. The technique of Fourier analysis as applied to EEG waveforms are similarly well documented. Standard procedures are available for dealing with such potential difficulties as the effects frequency truncation by filtering, "aliasing," sampling rate, and the like.

One potential problem unique to the proposed experimental situation is the possibility of interaction between the applied electromagnetic field and the metallic conductors implanted for recording purposes in the animal's skull. There are two conceivable forms of artifact. The conductors might serve to distort the field in some fashion, or they might act to generate currents in the neural tissue. The possibility of distortion of the field is minimied by the small mass of the conductor involved. It should consist of under 1 cm of stainless steel wire of less than 64 micron diamter, plus one 0-0-0 x 1/16 stainless

steel skull screw plus one 2H4 socket tab per recording lead. Further, a distortion or deflection of the field will be compensated by varying orientations of the animals (and consequently the electrode assembly) during the course of exposure. The possibility of any substantial currents being generated by the interaction of the field and the wire seems remote since (a) the field is a dc field so that any generator effects would have to be provided by induction consequent upon the movements of the animal carrying the wire through the field, and the relatively slow motions so produced should generate negligible potentials, and (b) since the animal will not be connected to the recording apparatus during exposure, the electrode will present an open circuit to any induced currents except for the very low capacitance and leakage resistance of the acrylic and bakelite insulators. The leakage resistance must be very high for successful EEG recording, and is typically in excess of 10 megohms at least. It seems unlikely therefore that the presence of the conductors of such an electrode assembly will materially alter the effects of exposure to the field.

The only possible interaction between the electrodes and air ions generated by the field would seem to be the chance that the electrodes might offer ohmic conduction paths for ion currents to ground. This possibility can be eliminated by preventing ion contact with the electrodes during exposure through the use of a suitable seal over the top of the animal's connector socket. All other conductive elements in the electrode assembly are encased in insulating materials.

A final possible problem emerges from the fact that the study is examining the animals with chronically implanted indwelling electrodes. It is possible that the electrodes themselves might over time cause degenerative changes in the surrounding tissue which could produce results having the appearance of changes due to exposure. Although the stainless steel electrode is reasonably stable and is frequently used in experiments lasting for substantial periods, the design of the study should be such as to control for such effects in two ways. First, the experimental comparison should be made between an experimental group exposed to the field and a set of yoked controls operated on the same days but not exposed to the field, so that any changes not due to the exposure should appear in both groups and thus be factored out of the analysis. However, this might cause one to fail to detect an effect of the field on normal tissue which is not manifested in damaged tissue. To insure that the

preparation is normal and not undergoing substantial changes due to the presence of the electrodes, a comparison of the control animals' records should be made with an additional set of records taken from these same animals prior to exposure. (A similar set of pre-exposure records should be taken from the animals of the experimental group to ensure equal degrees of habituation to the test environment and to serve as a basis for constructing the percentile transformation loc. cit.). Finally, all brains should be examined for infection and electrode damage after the experiment.

3.4.2 5-HT and 5-HIAA Levels in Blood and Brain

Considering the emphasis placed on the serotonin (5-hydroxytryptamine) hypothesis in ion bioeffects research, the extent of inclusion of direct measurements of 5-HT and its metabolities in a study design should be considered rather important however the proposed design does not reflect this view. There are several reasons for this. First, it is not considered appropriate to weight the design, which is to consider effects of both dc fields and air ions, too heavily in one direction. Secondly, though they are indirect measures other evaluations in the design would offer potential for correlation with 5-HT measures and thus could strengthen the evaluation of the serotonin hypothesis. Finally, when costs for different measurements are considered the 5-HT and 5-HIAA measurements are relatively more expensive. Their usages in the initial screen should probably be limited. However, if initial results for these measurements were positive a more extensive exploration of 5-HT metabolism and possible other neurohormones could be included.

3.4.3 Evaluations of the Reproduction System

Unless they can be excluded on the basis that they are not relevant to the populations that will be exposed to a specific environment or event, evaluations of reproduction and development processes should be considered as fundamental in any broad-range program designed to aid in risk assessment. This is based not only on the importance of these processes for the integrity of future generations, but also on the evidence that reproduction and development may be disrupted by diverse physical or chemical exposure conditions (see, for example, Archer and Blackman, 1971; Selye, 1950; Wilson and Fraser, 1977).

Further, in situations in which humans are exposed to environments that they may consider hazardous for one reason or another effects on sexual drive or claims of impotence frequently appear in the general patterns of symptoms. For example, Soyka (1977) includes anecdotal reports of effects of ion imbalance on sexual drive. In fact one of the promotional blurbs on the cover reads, "How ions may change your sex life - and your health" and a chapter entitled "Ions and Sex" is included. Regardless of what one concludes concerning the scientific basis for such statements, some assessment of the questionable reports on reproduction should be included in a program such as the one being planned. Ultimately multi-generation studies should be included. However, for the first approach the male reproductive system should be considered by mating test animals to unexposed female animals and by determination of sperm counts and motilities. Potential effects on female reproduction should be considered in verifications of estrus cycling, in a teratology study, and in the hormonal assays discussed below. For both sexes, gonodal weights should also be determined.

3.4.4 Hormonal Assays

The current interest in prolactin is due in part to the recognition that it has multitudinous functions in both mammalian and submammalian species, and that it can be measured quantitatively in the blood by specific radioimmunoassays (RIA). Thus, alterations in the levels of circulating prolactin levels could account for alteration in a physiologic function in the animal. There are several agents which are known to increase or decrease the levels of serum prolactin. For example, stress, fall in blood glucose, renal failures, thyrotrophic releasing hormone, a number of pharmacological drugs, and increased catocholamines all tend to increase the prolactin secretion, whereas L-DOPA, ergocrytin, and other ergot-derivates decrease the level of prolactin. Thus, the measurements of levels of prolactin under the planned experimental conditions could provide important information on alterations in normal physiology of the animals.

The principle of RIA for protein and sterioid hormones is the same. It is of importance to measure corticoids and sex steroids quantitatively following exposure to the dc electric fields as earlier reports, in fact, have indicated significant decreases in the levels of gamma globulins and serum corticoids with a simultaneous elevation in the serum albumin level as a result of exposure to such fields. Moreover, if there is any reproductive alterations to be expected in the female rodent,

this effect may be reflected by alterations in the levels of sex steroids. Thus, measurements of estradiol and progesterone concentrations in addition to corticoids in certain experiments could substantiate the grossly observed effects on reproductiv functioning biochemically.

Endocrine organ weights and their relationship to body weight should also be considered. Special attention should be given to male rats in all studies to detect any gynecomastia.

3.4.5 Hematology and Blood Biochemistry

Hematological evaluations and measures of levels of certain serum chemicals has become a relatively standard practice in chemical toxicity evaluations. Alterations in certain of these parameters is also a predicted response to a number of nonspecific stressors (Selye, 1950). And although a critical evaluation raises some questions about the methodology used, a recent review of studies concerned with bioeffects of exposure to ELF fields identified several in which the assessment of hematological parameters or of certain serum chemical yielded positive results (Bridges et al, 1979). The hematologic and blood chemistry parameters which should be considered for inclusion in this program are listed in Tables 3-11 and 3-12.

3.4.6 Respiratory System

The respiratory tract has been suggested as the primary means of uptake for air ions and has been a focus for much of the research. In the current program, assays of tracheal and ciliary and broncho-pulmonary functioning are recommended to be performed after varying periods of exposure to the test environments. Resistance to a respiratory infectious agent should probably also be considered, but special thought should be given to avoid risks of contamination of a large facility with an infection for which the test species is known to have susceptibility.

3.5 Basic Guidelines

3.5.1 Exposure Facilities

In the first experiments determining biological effects of the simulated environment, we recommend no attempts to dissociate the effects of the dc electric field from the effects of air ions. Thus, in this design these two properties of the environment will be co-manipulated. That is, the highest levels of electric fields will be associated with the highest level of ion current density. Should effects

TABLE 3-11

HEMATOLOGY METHODS

Parameter	Method or Procedure	Counter System or Method Reference
Hemoglobin	Cyanmethemoglobin method	Coulter Counter Model S System
Hematocrit	Indirect method; calculated value based on erythrocyte count and mean corpuscular volume	Coulter Counter Model S System
Erythrocycte Count	Electronic Counting Procedure	Coulter Counter Model S System
Leukocyte Count	Electronic Counting Procedure	Coulter Counter Model S System
Leukocyte Differential Count (Neutrophils-Immature, Neutrophils-Mature, Monocytes, Basophils, Lymphocytes, Eosinophils)	Wright stain procedure	Schalm, O.W., Jain, N.C. and Carroll, E.J. Veterinary Hematology, Color Plates Chapter, 3rd Edition, Lea & Febiger, 1975
Nucleated RBCs	Wright stain procedure	Schalm, O.W., Jain, N.C. and Carroll, E.J. Veterinary Hematology Color Plates Chapter, 3rd Edition, Lea & Febiger, 1975
Platelet Count	Direct method	Schalm, O.W., Jain, N.C. and Carroll, E. J. Veterinary Hematology, p. 69, 3rd Edition Lea & Febiger, 1975
Reticulocyte Count	New methylene blue staining procedure	Brecher, G. Am. J. Clin. Path. 19, 895, 1949.
Clotting Time	Capillary tube method	Schalm, O.W., Jain, N.C. and Carroll, E.J. Veterinary Hematology, p. 291, 3rd Edition, Lea & Febiger, 1975

TABLE 3-11
HEMATOLOGY METHODS
continued

Parameter	Method or Procedure	Counter System or Method Reference
Prothrombin Time	Quick One-Step method	Fibrometer precision coagulation timer (Fibrosystem: Bio-quest Lab)
Sedimentation Rate	Wintrobe method	Schalm, O.W., Jain, N.C. and Carroll, E.J. Veterinary Hematology, pp 40-42, 3rd Edition, Lea & Febiger, 1975

TABLE 3-12

CLINICAL CHEMISTRY METHODS
(SERUM)

Parameter	Method or Procedure	Counter System or Method Reference
Glucose	Hexokinase method	Centrifichem Centrifugal Analyzer System Neeley, W.E. Clin. Chem. 18, 509, 1972
Urea Nitrogen (BUN)	Modified urease technique	Centrifichem Centrifugal Analyzer System Karmen, A. J. Clin. Invest. 34, 131, 1955
Glutamic-Oxaloacetic Transaminase (SGOT)	Modified Karmen technique	Centrifichem Centrifual Analyzer System Henry, R.J., Chiamori, N., Golub, O.J. and Berkman, S. Am. J. Clin Path. 34, 381, 1960
Glutamic-Pyruvic Transaminase (SGPT)	Modified Wroblewski and LaDue technique	Centrifichem Centrifugal Analyzer System Henry, R.J., Chiamori, N., Golub, O.J. and Berkman, S. Am J. Clin. Path. 34, 381, 1960
Alkaline Phosphatase	Modified Bessey-Lowry technique	Neumann, H. and Van Vreedendall, M. Clin. Chem. Acta. 17, 183, 1967
Inorganic Phosphate	Daly and Ertingshausen technique	Centrifichem Centrifugal Analyzer System Daly, J.A. and Ertingshausen, G. Clin. Chem. 18, 263, 1972
Chloride	Silver chloride precipitation method	Chloride Meter (Corning Medical Co.) Catlove, E., Trantham, V. and Bowman, R.L. J. Lab. Clin. Med. 50, 358, 1958

TABLE 3-12
CLINICAL CHEMISTRY METHODS
continued

Parameter	Method or Procedure	Counter System or Method Reference
Sodium	Flame photometry	Klina Flame Photometer (Beckman)
Potassium	Flame photometry	Klina Flame Photometer (Beckman)
Total Protein	Biuret technique	Centrifichem Centrifugal Analyzer System Failing, I.F., Jr., Buckley, M.W. and Zak, B. Am. J. Clin. Path. 33, 83, 1960
Electrophoresis of Serum Proteins (Albumin, α_1 Globulin, α_2 Globulin, β Globulin, γ Globulin)	Microzone Electrophoresis Cell and Densitometer	Chin, H.P. Cellulose Acetate Electrophoresis Techniques and Applications. Ann Arbor Science Publisher, 1970
Lactic Dehydrogenase (LDH)	Lactate → Phruvate technique	Centrifichem Centrifugal Analyzer System Henry, R.J., Chiamori, N., Golub, O.J. and Berkman, S. Am. J. Clin, Path. 34, 381, 1960
Creatine Phosphokinase (CPK)	Modified Oliver method	Centrifichem Centrifugal Analyzer System Oliver, I.T. Biochem. J. 61, 116, 1955
Cholestrol	Cholesterol esterase-cholesterol oxidase method	Centrifichem Centrifugal Analyzer System Roseschlaw, P., Bernt, E. Gruber, W. Z.f. Klin. Chem. u. Klin. Biochem. J. 12, 226, 1974

TABLE 3-12
CLINICAL CHEMISTRY METHODS
continued

Parameter	Method or Procedure	Counter System or Method Reference
Calicum	Alizarin method	Centrifichem Centrifugal Analyzer System Connerty, H.V. and Briggs, A.R. Clin. Chem. 11, 716, 1965
Bilirubin, Total	Modified Walters and Gerarde method	Centrifichem Centrifugal Analyzer System Walters, M. and Gerarde, H. Microchem. J. 15, 231, 1970
Bilirubin, Direct	Modified Walters and Gerarde method	Centrifichem Centrifugal Analyzer System Walters, M. and Gerarde, H. Microchem. J. 15, 231, 1970
Hemoglobin	Tetramethylbenzidine method	Centrifichem Centrifugal Analyzer System Chin, B.H., Kozbelt, S.J. and Mudry, L.L. Toxicol. Path. 6, 18, 1978

that are considered of real biological significance be obtained, it could then become important to dissociate the sources of these effects.

The exposure facilities employed for the biological experiments shall have the following capacities:

- suitable live-in quarters for 138 individually housed rodents.
- flexibility to use the same facilities with minor revisions for rats and mice.
- capacity to simultaneously present sham-exposure conditions for control animals for positive and negative polarities and four different test conditions which are represented by two levels of dc electric fields and ion current densities at each polarity.
- for each set of three modules of eight individual animal compartments, allocation of one of the 24 compartments for measurement of environmental, electrical, and ionic parameters.
- for each set of three modules, ability to operate at all possible on-off combinations, i.e., three off, two off - one on, one off - two on, or three on. (This feature is important to allow phasing in of the habituation and exposure initiation of part of the animals in each group over a period of several days. This practice will aid in limiting variability in the time between the end of an exposure interval and the performance of some specified biological assay.)

3.5.2 Exposure Parameters

The following is a general design, which takes into account the manipulative HVDC variables previously discussed.

TYPICAL DESIGN FOR EXPOSURE GROUPS

Sham-exposed Control Group (Positive Polarity)	n animals
Sham-exposed Control Group (Negative Polarity)	n animals
Unmanipulated Control Group (if appropriate)	n animals
Positive Electric Fields and Air Ions	
High electric field, high ion current density	n animals
Low electric field, low ion current density	n animals
Negative Electric Fields and Air Ions	
High electric field, high ion current density	n animals
Low electric field, low ion current density	n animals

As a means of planning utilization of the exposure facilities, the studies should be organized into series that in total will require approximately 54 weeks utilization of the exposure facilities when acclimation times and time in some experiments to phase in animals over several days are included. This assumes that for each successive series acclimation would begin immediately following the last exposure interval for the previous series. The schedules should be flexible enough to fit in a few extra experiments if along the way results that are of immediate interest are obtained.

3.5.3 General Biological Methods

3.5.3.1 Animals

Rats are recommended as the species of small laboratory animals for which, considering the overall design, most background or historical control data are available. Mice have been used more frequently when testing for the susceptibility to infectious challenge and their low initial and maintenance costs make it feasible to employ the large numbers required. Justification for the selection of species and strain should be given.

Quarantine procedures and procedures to exclude unsuitable animals should be provided. For animals which will be used in the longer term studies a random sample should be selected for parasitology evaluations during the quarantine period. After quarantine, the animals should be given a one-week acclimation period in the exposure facilities prior to starting exposures to the test environments. The exception might be the pregnant female rats if a teratology study is used. These animals should be obtained by breeding from a larger population and should be placed on test shortly after it is determined that copulation has taken place.

For periods of acclimation or exposure, the facilities should serve as a residence for test and sham-exposed animals. During quarantine and for housing of unmanipulated control animals, breeders, and male rats that will be used for opponents in aggression testing, other caging appropriated for the species should be used. The size of the cages, the number of animals housed in each cage, and the feeding and watering devices should be described for each set of animals. These animals should be maintained on a 12-hour light/12-hour dark cycle and at room temperatures and relative humidities of approximately 22-24° and 40-60%, respectively.

Each animal in a test series should be uniquely identified by an accepted method. All data should be recorded under the identification number. Assignment of the animals to test and control groups should be by random selection procedures.

3.5.3.2 Control Conditions

The sham-exposed control condition should be applicable to all studies. Every effort should be made in planning the exposure facilities to assure that this condition is equivalent to the test conditions with the exception of the electrical field and ion environments. The nature of these efforts has been discussed in Section 2. Due to the different auditory noise spectra produced in generation of positive and negative ions, separate sham exposed control groups should be provided for each polarity. It might be noted here that the sham-exposed control environment is one essentially depleted of ions. Animals in the sham-exposed groups should be handled during the performance of biological assays in the same manner as those in the test groups.

Similarly, animals in the unmanipulated control groups should undergo the same procedures for biological assays as the test and sham-exposed control animals. Animals in the unmanipulated control condition could be individually housed in suitable cages on racks located in animal quarters adjacent to the exposure facilities. Because of the ion depletion in the sham-exposed condition, a procedure which we consider appropriate for this condition, ideally the unmanipulated control condition should probably be included in all studies. However, this would substantially increase costs. Therefore, consideration should be given to employ the unmanipulated control groups in the experiments which involve longer exposure periods. If ion depletion or some other factor, such as feed and watering devices, cage design, air flow, noise, etc., make the facility less acceptable as living quarters for the animals, it should become apparent in the longer-term studies. Further preliminary experiments should be conducted to evaluate the extent to which the simulator modules affect such gross measures as food and water consumption and body weight changes.

3.5.3.3 Exposure Intervals and Period

For the initial evaluation a standard 18 hour exposure interval is suggested. This interval would allow access to the animals during the better part of a normal work day and would leave the animals undisturbed during the on periods of the exposure

schedule. The periods over which the exposure sessions will be administered should probably vary from 1 day to 13 weeks or more.

3.5.3.4 Magnitude of the DC Electric Field and Ion Current Density

From reports of measurements under existing dc transmission lines which are capable of up to ± 600 kV/m operation, dc electric fields in the range of 30 kV/m and ion current densities up to 200-300 nA/m^2 have been observed. Although the objectives of this program is to consider simulation of the environment in the vicinity of transmission lines capable of operating up to ± 1200 kV, this does not necessarily imply proportional increases in the dc fields and ion current densities. Thus, in development of this design values of 30 kV/m and 250 nA/m^2 have been used as a point of departure.

In that the design provides for co-manipulation of the dc electric field and ion current density, one of the first questions that arises in deciding upon exposure levels is the relative relationship between these two parameters. As noted in Section 2.2.2, our recommendation is that the same factor be applied to the dc electric fields and ion current densities in scaling upward or downward from the values of 30 kV/m and 250 nA/m^2.

It is recommended that for at least the initial series of experiments which will involve at least a single 18 hour exposure to the test conditions, the values for the lower exposure level be slightly below the preference threshold if such threshold can be established.

For the values of the higher level exposure condition in the early experiments, it is recommended that a dc electric field in the range of 150-180 kV/m and an ion current density in the range of 1400 nA/m be employed. These values are based on consideration of the enhancement factors for man and rat-sized subjects and will give a field and ion current density at the rats dorsal surface (assuming normal non-erect posture) comparable to those at the top of the head for an erect man in an ambient environment of about 30 kV/m and 250 nA/m^2.

It is further recommended that selection of values for later experiments be delayed until completion of the earlier shorter term studies.

3.5.3.5 Record Keeping

Data should be recorded in bound logbooks or on data forms which will be bound at the end of the program. Where computer assistance is used in data handling, the computer printouts should be bound and retained as part of the data file. All original data entries must be made in ink and must be signed and dated at the time of entry. Changes to original data entries must be signed, dated, and explained by the person making the change.

3.5.3.6 Statistical Analyses

For continuous variables, the statistical approach would be analysis of variance models appropriate for evaluating the significance of factors such as the intensity of exposure, the duration of exposure, and the age and gender of the test animals. Where appropriate, the models should also include provisions for evaluating the significance of first and second order interactions of these factors. Regression techniques should be used to characterize the relationships between the intensity and duration of exposures and any observed bioeffects and in some cases correlation coefficients for the relationships between two measures will have to be derived. This could include, for example, the relationship between levels of 5-HT in blood and brain and behaviorlal measures in the long term studies or correlations between two behavioral measures in the same animals.

3.5.3.7 Quality Assurance

The program must be subject to internal quality assurance reviews. Each participating division (if more than one) must have a staff with reporting responsibilities exclusive of the project management. The quality assurance unit must maintain a master schedule for the program and review critical phases of the program. A written report should be prepared after review and compliance or noncompliance to the master schedule, protocols, and standard operating procedures documented. The quality assurance unit should also spot check data records and each report except monthly progress reports.

3.6 Specific Study Methods

The "Specific Studies" discussed in this section are not the only studies to be recommended. Their selection was influenced by the foregoing literature review, by the background and experience and opinions of the authors. Comments concerning

the specific aims of the biologic tests and the evaluation and reporting methods are included but detailed protocols are not included.

The early experiments should include evaluations of relatively labile biological responses after short-term exposures to the test environments. The focus should be on the nervous system and behavior but assays of tracheal ciliary function and lung respiratory function and measurements of heart rate might also be included.

3.6.1 Short Term Exposures

For reasons explained previously we would recommend adult male rats distributed equally to two early studies. The facility should permit 138 rats (23/condition) to be exposed at once. If this was done with one replication, 46 male rats could be allocated to each of the following groups, therefore, half the animals in each group will be processed in the initial and half in the replicate test.

- Sham exposure positive
- Sham exposure negative
- High + electric field, high + ion current density
- Low + electric field, low + ion current density
- High - electric field, high - ion current density
- Low - electric field, low - ion current density

Within each exposure group of 46 rats, the following numbers might be evaluated as indicated.

- 16 rats - open-field testing followed by auditory startle testing
- 6 rats - electroencephalograms (EEG)
- 10 rats - assays of blood and brain levels of 5 hydroxytryptamine (5HT) and 5-hyroxyindoleacectic acid (5-HIAA)
- 4 rats - assays of tracheal function
- 10 rats - heart rate measurements and respiratory function tests

Two tests are recommended: One employing a single 18 hour exposure and another employing 7 days exposure of 18 hours each. Each biological assay would be performed at the end of the exposure. Each would require a total of 276 rats.

3.6.1.1 Open Field Testing

Locomotor activity in a novel environment and emotional reactivity as evaluated by defecation upon being placed in the novel environment should be evaluated by an open field test with provisions for automated monitoring of locomotor activity. Alternatively, other means of monitoring locomotor activity might be included.

3.6.1.2 Auditory Startle

These tests should employ a small enclosure chamber in which a controlled and reproducable auditory stimulus can be provided. A suitable apparatus to record the electrical analogs of the chamber displacement (Conner et al, 1970) could be employed to permit measurement of the magnitude of each startle response.

For each animal the average amplitude of the startle response is calculated for each of five two-trial blocks. To allow detection of any treatment effects on habituation of the startle response with repeated trials, "Blocks of Trials" are an added factor in the Analysis of Variance.

3.6.1.3 Neurophysiology (EEG)

As a measure of the test exposures on neural activity, pre-/and postexposure recordings of EEG activity are performed.

Detailed explanation of rationale of employing Power Spectrum Analysis from implanted electrodes appears in Section 3.4.1.

The highest exposure group should be compared to Controls by acceptable methods for this procedure. Additional animals can be tested should a sufficiently strong response dictate.

3.6.1.4 Determination of Blood and Brain Levels of 5-HT and 5-HIAA

Two methods of analysis in blood should be considered i.e., spectroflourescence and high performance liquid chromotography (HPLC). Procedures for the spectroflurometric method can be adapted from reports by Curzon and Green (1970); Krueger,

Andriese, and Kotka (1963); Sommerville and Hintenberger (1975); and Welech, Mayer, and Kawant (1972). Those for HPLC can be adapted from Sasa and Blank (1977).

Analysis of 5-HT (5-hydroxytryptamine) and 5-HIAA (5-hydroxyindoleacetic acid) in brain tissue should also be performed, consideration should be given to whether these would best be made on homogenates from whole brain or from certain brain fractions. The procedure for the extraction of the brain tissues for the above analysis is described by Curzon and Green (1970).

The analytical data obtained from both the spectrophotoflurimetric method and the HPLC procedure should be expressed as means and standard deviations for each group. Statistical significance should be examined by analysis of variance techniques.

3.6.1.5 Tracheal Bioassay

Tracheal ring explants are removed from rats in the various exposure groups, cultured, and monitored for ciliary activity and cytopathology.

A two-way analysis of variance should be used to test the hypothesis of no treatment differences for the exposure periods studied (Winter, 1971). Duncan's new multiple range test and the chi-square distribution test can be used to determine patterns of significant treatment differences in ciliary beating frequency and cytopathology (Siegel, 1956).

3.6.2 A Recommended Teratology Study

This study should evaluate the survival, growth, and morphological development of fetuses of female rats that will be exposed to the test conditions for a part of each day throughout most of gestation.

3.6.2.1 Design

Ten-week old Fischer 344 rats are recommended as breeding stock. At the end of quarantine 161 selected animals are bred and sperm positive females are assigned equally to one of seven treatment groups

- Unmanipulated or shelf control
- Sham-exposed control positive
- Sham-exposed control negative
- High + electric field, high + ion current density
- Low + electric field, low + ion current density

- High - electric field, high - ion current density
- Low - electric field, low - ion current density

The rats are exposed from day 2 of gestation to day 21.

3.6.2.2 Necropsy - Examination of Fetuses and Data Handling

Necropsies should consider pertinent enumerative and descriptive data concerning dams and fetuses such as the following:

- Number of pregnant females/group
- Percent mortality of pregnant females/group
- Maternal body weight on days 1, 8, 15, and 22 of gestation [group means and standard deviation (SD)].
- Maternal body weight change on days 8, 15 and 22 of gestation (actual weight change and weight change adjusted for the weight of the uterus, placenta, and fetuses; both weight changes calculated from the weight on day 1; group means and SD).
- Corpora lutea/dam that survives to day 22 (group means and SD).
- Implantation sites/dam that survives to day 22 (group means and SD).
- Percent early resorptions/dam that survives to day 22 using a denominator = number of implanation sites (group means and SD).
- Percent late resorptions/dam that survives to day 22 using a denominator = number of implantation sites (group means and SD).
- Percent resorbed or dead fetuses/dam that survives to day 22 using a denominator = number of implanation sites (group means and SD).
- Percent live male fetuses/dam that survives to day 22 using a denominator = number of live fetuses (group means and SD).
- Weight of live fetuses (mean and SD of litter means for each group).
- Percent incidence/litter of specific anomalies, categories of anomalies, or of anatomical variations detected in external, visceral or skeletal examinations; denominator = the number of live fetuses in the litter subjected to the specific examination procedure (group means and SD).

- Percentage of litters in each group that contain at least one dead or resorbed fetus (confidence limits are to be approximated from the binomial distribution, dams that die before day 22 are to be excluded from the calculation).
- Percentage of litters in each group that contain at least one fetus with a major malformation (confidence limits are to be approximated from the binomial distribution; dams that die before day 22 are to be excluded.
- Data from necropsy of dams that die before day 22 of gestation are summarized separately.

For quantitative variables, analysis of variance is used to determine whether there is a significant effect of exposure. Those variables which yield a significant F ratio should be further analyzed to determine which of the test groups are significantly different from the sham exposed control group (Dunnett's t test, Steel and Torrie, 1960). The individual data points in the form of the percentage of each litter that was affected in a specified manner (death, resorption, or anomalies) is subjected to the inverse sine transformation for proportions prior to analysis (Steel and Torrie, 1960). Where neither the original data points nor a transformation are appropriate for parametric analysis (e.g., percent litters with one or more affected fetuses), the chi-square test or Fisher's Test (Sieger, 1956) and Finney's (1971) prohibit analysis should be employed as appropriate.

3.6.3 Suggested Studies Employing 13 Weeks of Exposure

Those two studies could run consecutively (e.g., males then females) and involve maximum exposure periods of 13 weeks with various biological responses being sampled at interim periods during the studies. With the exception of aggression testing and 5-HT measurement, which would be performed only for males, and the reproductive parameters, the biological variables considered should be the same for both experiments -- as shown in the following schema (Figure 3-1 and Figure 3-2).

3.6.3.1 Design

A total of 161 6-week old male rats and 161 female rats of the same age should be equally divided among the seven exposure conditions or groups listed below.

Figure 3-1

13-Week Exposures

161 Male Rats

23 Rats Per Each of Seven Conditions

Body Weights (weekly)

Clinical Observations (weekly)

Cage Checks (daily)

Open Field Test (test week 4)

Opthamology Exams (test weeks 1 & 13)

Subgroup A (10 Rats)

Week 1 - Pre-exposure hematology, clinical chemistry

Week 6 - Interim hematology, clinical chemistry

Week 7 - Breed to unexposed females

Week 10- Breed to unexposed females

Week 13- Final hematology, clinical chemistry

Week 14- Necropsy examination, organ weights

Subgroup B (13 Rats)

Week 7 - Auditory startle

Week 8 - One-way avoidance test

Week 12- Aggression testing

Week 14- 5-HT, 5-HIAA (Blood and Brain)

Week 14- Sperm counts and motilities

Week 14- Tracheal bioassay (4 rats)

Figure 3-2

13-Week Exposures

161 Female Rats

23 Rats Per Each of Seven Conditions

Body Weights (weekly)

Clinical Observations (weekly)

Cage Checks (daily)

Open Field Test (test week 4)

Optthamology Exams (test weeks 1 & 13)

Subgroup A (10 Rats)

Week 1 - Pre-exposure hematology clinical chemistry

Week 5 - Check estrus cycling

Week 6 - Interim hematology, clinical chemistry

Week 11- Check estrus cycling

Week 13- Final hematology, clinical chemistry

Week 14- Necropsy examination, organ weights

Subgroup B (13 Rats)

Week 7 - Auditory startle

Week 8 - One-way avoidance test

Week 14- Hormonal assays

- Unmanipulated control group
- Sham-exposed control group positive
- Sham-exposed control group negative
- High + electric field, high + ion current density
- Low + electric field, low + ion current density
- High - electric field, high - ion current density
- Low - electric field, low - ion current density

Each exposure or control group of 23 male or female rats can be further subdivided according to the biological parameters on which they will be evaluated. Subgroup A would be composed of ten males or ten female rats and Subgroup B of 13 animals of each sex. The evaluations that are suggested for each of these subgroups are listed in the schema and described in greater detail as follows:

3.6.3.2 Exposure Interval and Period

The animals in the sham-exposed and test exposure groups should be exposed to the appropriate control or test environments for 18 hours/day, 7 days/week, for 13 weeks. Some final testing can be conducted in test week 14 but no exposures would be given during that week.

3.6.3.3 Evaluations Common to All Animals in the Recommended 13 Week Studies

Body weights should be determined once each week for all animals at the time of physical examinations throughout the exposure period. Animals found dead or moribund in daily checks should be necropsied and the organs and tissues listed in Section 3.6.3.15 below should be examined for gross abnormalities and saved. An eye examination should be performed by indirect ophthalomoscopy prior to the start exposure (test week 1) and again during the 13th week of exposure. All animals should be evaluated by the open field test as described in Section 3.6.3.12 the 4th week of the exposure period.

3.6.3.4 Interim Bleedings for Hematology and Clinical Chemistry (Subgroup A)

Blood could be collected via the sublingual plexus or orbital sinus from ten males and ten females from each test and control group during the week preceding the start of the exposure period (test week - 1) and again for the same rats during test weeks 6 and 13. The hematological and clinical chemistry parameters that should be considered are listed along with suggested applicable methods in Tables

3-11 and 3-12.

3.6.3.5 Male Reproductive Effectiveness (Subgroup A)

To evaluate reproductive functioning in males following the test exposures, ten male rats from each test and control group should be cohabited with a series of untreated females. After an appropriate period, the females are euthanized and the outcome of the periods of cohabitation evaluated.

A total of 280 untreated females should be employed as breeders. These animals should be obtained in two lots of 140 rats each and be quarantined for at least 2 weeks prior to pairing them with the test and control males in the study. The female breeders should be 11 weeks old at the start of quarantine and 13-14 weeks old at the time they are paired with the males. Excepting that they should be housed two female rats/cage, these animals should be maintained under the same conditions as described for unmanipulated control animals.

A mating period should involve cohabitation of each male twice with two different untreated females for 4 hours on each of 5 days during the "off" segments of the daily exposure schedule during tests weeks 7 and 10.

On the 12th day after the end of the mating period, the female breeders should be euthanized. The ovaries and uterus should be exposed and the following counts made:

Corpora Lueta
Live Implantations
Late Postimplantation Deaths
Early Postimplantation Deaths

For rats in which pregnancy is not evident upon unaided observation, the uterus should be removed and examined under a dissecting micorscope. If fading metrial glands are detected by this method, these would be counted and the count recorded for Total Implantations and Early Postimplantation Deaths. If no metrial glands are detected, the female would be counted as "not pregnant".

Separate analyses must be performed to evaluate the effects of the test exposures at test week 7 and test week 10. If indicated, similar analyses will be performed to evaluate the differences between the two control groups. The parameters that must be considered in the analyses are as follows:

Fertility Index
Total Number of Corpora Lueta
Total Number of Implantations
Percent Preimplantation Loss
Percent Dead Implantations
Proportion of Females with One or More Dead Implants
Proportion of Females with Two or More Dead Implants

3.6.3.6 Sperm Counts and Motilities (Subgroup B)

For a second evaluation of the male reproductive system, determinations of the number of sperm and their motilities, should be performed in test week 14 when the animals in the B subgroups are sacrificed.

3.6.3.7 Estrus Cycling (Subgroup A)

The initial evaluation of the female reproduction system will be the teratology study described in Section 3.6.2. In addition the regularity of estrus cycling will be evaluated in animals in the A subgroups of this study using a four-phase division established by examination of daily vaginal smears; diestrus; proestrus; estrus and metestrus.

3.6.3.8 Hormonal Assays (Females, Subgroup A)

Selected Hormonal Assays on the females of Subgroup A should be performed to supplement the information on the female reproductive system. Using radio immunoassay techniques the following blood levels should be determined: estradiol, progesterone, and prolactin. Since RIA techniques are being employed the following levels of corticosteroids should also be determined: cortidsterone, deoxycorticosterone and cortisone.

3.6.3.9 Endocrine Organ Weights (Subgroup A)

As one measure of the possible effects of the test environments on the endocrine system, certain organs could be weighed at the time of necropsy. These might include the adrenal, pituitary, and thyroid glands as well as the testes and ovaries. The organs should be removed, trimmed of excess fat,and weighed. Data is to be reported as group means and standard deviations for organ weights and organ weight: body weight ratios.

3.6.3.10 Auditory Startle (Subgroup B)

The auditory startle response will be evaluated in both male and female animals during test week 7.

3.6.3.11 One Way Avoidance Testing (Subgroup B)

Suitable training trials should be completed in order to evaluate escape or avoidance behavior with conditioned and unconditioned stimulus conditions. These tests will be completed in Week 8 to detect possible changes and induced deficiencies in sensory capacities or alterations in behavior.

3.6.3.12 Agression Testing (Subgroup B)

Aggression testing in treated and untreated males of Subgroup B should be completed using procedures similar to those described by Thor, Gheselli and Ward (1974). Data should be expressed as the number of attacks, initiated, the number of attacks received and the number of wins and lossess incurred by each experimental animal summarized as group means and standard deviations.

3.6.3.13 Determinations of 5-HT and 5-HIAA Levels in Blood and Brain (Series 4, Subgroup B)

Blood will be collected and the brain removed from animals in the B subgroups for Series 4 at the time of their euthansia in test week 14. Determinations of 5-HT and 5-HIAA levels in blood and in brain homogenates will be made as described in Section 3.6.1.4.

3.6.3.14 Tracheal Bioassay (Series 4, Subgroup B)

Four animals will be randomly selected from each B subgroup of Series 4 at the time they are uethanized in test week 14. Tracheal bioassays will be performed on these animals by the procedures described in Section 3.6.1.5

3.6.3.15 Necropsy Examination and Collection and Fixation of Tissue (Subgroup A)

All animals which die on test will be necropsied regardless of autolytic state. In addition, moribund animals will also be necropsied, if in the opinion of the Study Director in consultation with the pathologist, it is unlikely that they will survive another 24 hours.

Terminal body weights will be recorded immediately prior to routine sacrifice following a 17-19 hour fast. The necropsy procedure will be a thorough and systemati- examination and dissection of the animal viscera and carcass, and collection and fixation of the following tissues:

Adrenals[a]
Brain[a]
Cecum
Colon
Doudenum
Epididymis
Esophagus
Eyes
Gonads[a]
Gross lesions
Heart[a]
Ileum
Jejunum
Kidneys[a]
Larynx
Liver[a]
Lungs and mainstem bronchi
Lymph nodes:
    Mandibular
    Mesenteric
Mammary Gland
Muscle, skeletal
Nasal turbinate (anterior)
Pancreas
Pituitary[a]
Prostate
Rectum
Salivary gland
Siminal vesicles
Sciatic nerve
Skin, abdominal
Spinal cord
Spleen[a]
Sternum including marrow
Stomach[a]
Thymus
Thyroids (parathyroids)[a]
Tissue masses
Trachea
Uterus
Urinary bladder[a]

Blood and bone marrow (femur) smears should be prepared for all animals at sacrifice. Organs marked "a" will be weighed at necropsy, except for spontaneous deaths.

Wet tissues should be maintained until a determination can be made from the necropsy data and from other data collected in the project whether there are organs for which histopathologic examination might be fruitful. If such organs are identified, upon consultation with the sponsor, histopathologic examination of these organs could be added to the program plan.

3.6.4 Susceptibility of Mice to a Respiratory Infectious Agent

The animals will be 360 male and 360 female mice. Sixty mice of each sex allocated to the following exposure conditions and will be exposed for 18 hours per day for seven days.

- Sham exposure positive
- Sham exposure negative
- High + electric field, high + ion current density
- Low + electric field, low + ion current density
- High - electric field, high - current density
- Low - electric field, low - ion current density

Challenge with the infectious agent will take place following the last of the 7 exposure intervals employing *Streptococcus pyogenes* (Lancefield Group C), passaged in mice, isolated from the heart, and grown and harvested under appropriate conditons. Mortality rates and survival times are determined and compared and the percentage of animals that die during the 14-day post-infection period are evaluated by the chi-square test for group independence. Survival time of the different test groups shall be compared to that of the sham-exposed groups by the Student's t test.

3.7 Possible Directions for Future Research

A biological experimental design including proposed methods for studying the effects of the dominant components of the HVDC transmission line has been presented. The design is intended as the first approach to a broad bioeffects screen in the test species considered. It is anticipated that the results obtained will be used to guide future research. Some of the directions anticipated for future research are as follows:

- Exposure over longer periods including over two-three generations
- Examination of certain labile responses such as behavior, heart rate, respiratory functioning during short, repeated exposures.
- Dissociation of the dc electric field and ion current density components of the test environment.
- A more extensive consideration of the relationship between the magnitude of the fields and/or ion current densities and the biological responses.
- Experimental manipulation of other components of the HVDC transmission line environment such as noise and humidity.
- A more extensive probe of certain biological systems. This could be supplementation of behavioral testing with possibly more sensitive but more time consuming tests, examination of other components of 5-HT metabolism, drug interaction experiments, challenge with infectious agents other than those proposed and challenge prior to the test exposures, consideration of other components of the endocrine system, and examination of immune systems.

Adey, W.R. and Bawin, M. (Eds), Brain Interactions with Weak Electric and Magnetic Fields, Neurosc.: Res. Program Bul. 15: 1977.

Altman, G. and Lang, S. Territory choice of white mice under Faraday conditions and in electrical fields. A. Tierpsychol. 34: 337-344, 1974.

Andersen, I. Effects of natural and artificially generated air ions on mammals. Int. J. Biometeor. 16 Supp: 229-238, 1972.

Andersen, I., Vad, E. The influence of electric fields on bacterial growth. Int. J. Biometeor. 9: 211-218, 1965.

Archer, J. E. and Blackman, D.L. Prenatal psychological stress and Offspring behavior in rats and mice, Experimental Psychobiology, 4: 193-248, 1971.

Assael, M. Pfeiffer, Y. and Sulman, G.G. Influence of artificial air ionisation on the human electroencephalogram. Int. J. Biometeor. 18: 306-312, 1974.

Bachman, C.H., McDonald, R.D., and Lorenz, P.J. Some physiological effects of measured air ions. Int. J. Biometer. 9: 127-139, 1965.

Bachman, C.H., McDonald, R.D., and Lorenz, P.J. Some effects of air ions on the activty of rats. Int. J. Biometeor. 10: 39-46, 1966.

Bassett, C.A.L., Hermann, I. The effects of electrostatic fields on macromolecular synthesis by fibroblasts *in vitro*. J. Cell Biol. 39: 9A, 1968.

Bodganski, D.F., Weissbach, H., and Udenfriend, S. The distribution of serotonin, 5-hydroxytryptophan decarboxylase and monoamine oxidase in brain. J. Neurochem. 1: 272-278, 1957.

Bogdanski, D.S. and Udenfriend, S. Serotonin and monamine oxidase in brain. J. Pharmacol. Exp. Ther., 116: 7(Abstract), 1966.

Bonneville Power Administration, Transmission Line Reference Book HVDC to ± 600 kV. Palo Alto, California: EPRI. Appendix to Chap. 7 by Harrington and Kelly.

Bonneville Power Administration, op. cit., Chap. 7.

Bracken, T.D., et al. Ground level electric fields and ion currents on the celilo-sylmar ± 400 kV DC intertie during fair weather. IEEE Trans. PAS, 97: 370, 1978.

Bracken, T.D. and Furumasu, B.C. Field and ion current measurements in regions of high charge density near direct current transmission lines. Presented at Amer. Met. Soc. Conf., Issaquah, Washington, August 4, 1978.

Bridges, J.E., Biological effects of high voltage electric fields, IIT Research Institute, Project E8151 Final Report, EPRI Contract RP381-1, November, 1975.

Bridges, J.E., Becker, D.S., Preache, M.M. Biological effects of high voltage electric fields: an update. Final report to EPRI EA1123, 1: 1979.

Bridges, J.E. ad Preache, M.M. Biological influence of power frequency electric fields - a tutorial review from a physical and experimental view point IEEE, manuscript submitted, 1980.

Clark, R. A rapidly acquired avoidance response in rats. Psychono.Sci. 6: 11-12, 1966.

Comber, M.G. and Humphreys, D.R. HVDC testing at project UHV, accepted for presentation at 7th IEEE PES Conference and Exposition on Overhead and Underground Transmission and Distribution, Atlanta, Georgia, April 1-6, 1979.

Committee on Biosphere Effects of Extremely-Low-Frequency Radiations, Division of Medical Sciences, Assembly of Life Sciences, National Research Council, Biologic Effects of Electric and Magnetic Fields Associated with Proposed Project Seafarer. Washington, D.C.: National Academy of Sciences, 1977.

Connor, R.L., Stolk, J., Barchas, J., and Levine, S. Parachlorophenylalanine and habiutation to repetitive auditory startle stimuli in rats. Physiol. Behav. 5: 1212-1219, 1970.

Cooper, J.R., Bloom, F.E., and Roth, R.H. The biochemical basis of neuropharmacology. New York: Oxford University Press, 1970.

Curzon, G. and Green, A.R., Br. J. Pharmacol. 39: 653-655, 1970.

Douglas, W. W. Histamine and antihistamines; 5-hydroxytryptamine and antagonists. In L.S.Goodman and A. Gilman (Eds.) The Pharmacological Basis of Thereapeutics. New York: MacMillian Publishing Co., Inc. 590-629, Fifth Edition, 1975.

Epstein, M.A. and Ondra, G.W. The interaction of static and alternating electric fields with biological systems. IEEE Trans. on Electromag. Compatability EMC 8:45-51, 1976.

Feldberg, W. and Myers, R.D. Effects of temperature of amines injected into the cerebral ventricles: A new concept of temperature regulation. J. Physiol. 173: 226-237, 1964.

Felici, N. Sumeire, C., Carraz, G., and Bériel, H. Atmospheric ions and pollution. Does aerion depreviation have a lethal effect? RGE, 86: 501-505, 1977.

Finney, D.J. Probit Analysis, London: Cambridge University Press, 1962.

Frazier, M.J. The effect of electric and magnetic fields near HVDC converter terminal on implanted cardiac pacemakers, IIT Research Institute, Project No. E8167 Summary Report, EPRI Contract No. RP679-1-3, September, 1978.

Frey, A.H., Publication from the Institute for Research, State College, Pennsylvania, 1967.

Frey, A.H. and Granda, R.E. Human reactions to air ions. Presented at: International Conference on Ionization of the Air, American Institute of Medical Climatology, October 16-17, Philadelphia, PA, 1961.

Gilbert, G.O. Effects of negative air ions upon emotionality and brain serotonin levels in isolated rats. Int. J. Biometeor. 17: 267-275, 1973.

Goodman, L.S. and Gilman, A. (Eds.) The Pharmacological Basis of Therapeutics. New York:MacMillan Publishing Co., Inc. Fifth Edition, 1975.

Goldman, M. and Rivolier, J. Atmospheric ions and pollution. Study of the biological effects of excess negative ionization. RGE, 86:497-500, 1977.

Gualtierotti, R. The influence of ionization on endocrine glands. In R. Gualtierotti, I. H. Kornblueh and C. Siroti (Eds.) Bioclimatology Biometeorology and Aeronionotherapy. Milan: Carlo Erba Fdn., 88-92, 1968.

Guillerm, R., Badre, R., and Hee, J. Effects of light atmospheric ions on the ciliary activity of sheep and rabbit tracheal mucosa *in vitro*. C.R. Acad. Sci. 262:669-671, 1966.

Hermer, M.Z. The effect of static electric field on the heart and respiration rate in rats. Latv. Psr. Zi Nat Akad Vestis, 2: 102-106, 1971.

Hingorami, N.G. HVDC transmission - an overview. Electric Power Research Institute, January, 1978.

Holland, L. The Properties of Glass Surfaces. John Wiley and Sons, Inc., New York, 1964.

Jones, F., Effects of a positive electrostatic field on emotionally disturbed children. Dissert. Abs. 35: 75-6137, 1975.

Jouvet, M. Insomnia and decrease of cerebral 5-hydroxytryptamine after destruction of the raphe system in the cat. Advanc. Pharmacol. 6: 265-279, 1968.

Kensler, C.J. and Battista, S.P. Chemical and physical factors affecting mammalian ciliary activity. Amer. Rev. Resp. Dis. 93:93-102, 1966.

Knoll, M., Eichmeier, J. and Schön, R.W. Properties, measurement, and bioclimatic action of "small" multimolecular atmospheric ions. Adv. Electronic and Electron Physics, 19:177-254, 1964.

Knoll. M. Rheinstein, J,. Leonard, G.F., and Highberg, P.W. Influence of light atmospheric ions on human visual reaction time. Presented at: International Conference on Ionization of the Air, American Institute of Medical Climatology, Philadelphia, PA. October 16-17, 1961.

Koranyi, G. Surface Properties of Silicate Glasses., Akademiai Kiado, Publishing House of the Hungarian Academy of Sciences, Budapest, 1963.

Krivova, T.I., Lukovkin, V.V., and Uakubenko, A.V. Effect of DC electrical field on human organism. In Filippov, V.I. and Morosov, Y.A. (Eds.) Protection from the Action of Electromagnetic Fields and Electric Current in Industry. Moscow: All-Union Central Scientific Research Institute of Work Safety, 1973., (DOE translation No.TR-20).

Krueger, A.P. Some observations of the biological effects of gaseous ions Presented at: International Conference on Ionization of the Air, American Institute of Medical Climatology, Philadelphia, PA. October 16-17, 1961.

Krueger, A.P. Air Ions and Physiological Function. J. Gen. Physiol. (Commemorative Vol. for J.H. Northrop), Part 2, supplement, March 45: 233-241, 1962.

Krueger, A.P. Are air ions biologically significant? A review of a controversial subject. Int. J. Biometeor, 16: 313-322, 1972.

Krueger, A.P., Andriese, P.C. and Kotaka, S. The biological mechanism of air ion action: The effect of CO_2^+ in inhaled air on the blood level of 5-hydroxytryptamine in mice. Int. J. Biometeor. 7:3-16, 1963.

Krueger, A.P., Andriese, P.C., and Kotaka, S. Small air ions: Their effect on blood levels of serotonin in terms of modern physical theory. Int. J. Biometeor. 12:225-239, 1968.

Krueger, A.P., Andriese, P.C. and Lamprecht, S.M. The effects of inhaling non-ionized or positively ionized air containing 2-4% CO_2 on the blood levels of 5-hydroxytryptamine in mice. Int. J. Biometeor, 10:17-28, 1966.

Krueger, A.P. and Kotaka, S. The effects of air ions on brain levels of serotonin in mice. Int. J. Biometeor, 13:25-38, 1969.

Krueger, A.P., Kotaka, S. and Andriese, P.C. Some observations on the physiological effects of gaseous ions. Int. J. Biometeor, 6:33-48, 1962.

Krueger, A.P., Kotaka, S. and Reed, E.J. The course of experimental inflenze in mice maintained in high concentrations of small negative air ions. Int. J. Biometeor. 15:5-10, 1971.

Krueger, A.P., Kotaka, S., Reed, E.J. and Turner, S. The effect of air ions on bacterial and viral pneumonia in mice. Int. J. Biometeor. 14: 247-260, 1970.

Krueger, A.P. and Levine. H.B. The effect of unipolar positively ionized air on the course of coccidioidomycosis in mice. Int. J. Biometeor. 11: 279-288, 1967.

Krueger, A.P. and Reed, E.J. Effect on the air ion environment on influenza in the mouse. Int. J. Biometeor. 16:209-232, 1972.

Krueger, A.P. and Reed, E.J. Small air ions and the course of respiratory disease in mice. Abstracts Sixth Int. Biometerological Congress, Netherlands, 70, September, 1973.

Krueger, A.P. and Reed, E.J. Biological impact of small air ions. Science, 193:1209-1213, 1976.

Krueger, A.P. and Reed, E.J., Day, M.D. and Brook, K.A. Further observations on the effect of air ions on influenza in the mouse. Int. J. Biometeor. 18:46-56 1974.

Krueger, A.P. and Smith, R.F. Effects of air ions on isolated rabbit trachea. Proc. Soc. Exptl. Biol. Med. 96:807-809, 1957.

Krueger, A.P. and Smith, R.F. The effects of air ions on the living mammalian trachea. J. Gen. Physiol. 42:69-82, 1958.

Krueger, A.P. and Smith, R.F. Effects of gaseous ions on tracheal ciliary rate. Proc. Soc. Exptl. Biol. Med. 98:412-414, 1958.

Krueger, A.P. and Smith, R.F. Parameters of gaseous ion effects on the mammalian trachea J. Gen. Physiol. 42:959-969, 1959.

Krueger, A.P. and Smith, R.F. The biological mechanism of air ion action. II. Negative air ion effects on the concentration and metabolism of 5-hydroxytryptamine in the mammalian respiratory tract. J. Gen. Physiol. 44:269-276, 1960.

Krueger, A.P., Smith, R.F., Hildebrand, G.J. and Meyers, C.E. Further studies of gaseous ion action on trachea. Proc. Soc. Exptl. Bio. Med. 102:355-357, 1959.

Krueger, A.P., Smith, R.F. and Miller, J.W. Effects of air ions on trachea of primates. Proc. Soc. Exptl. Biol. Med. 101:506-507,1959.

Kusmina, T.R. The effect of inhalation of air ions on the elctrochemical properties of blood during exsanguination and recovery of cats. Int. J. Biometeor. 11:191-194, 1967.

Lott, J.R. Effects of continuous and pulsating electrical fields on brain wave activity in rats. Abst. Sixth Int. Biometeor. Cong., Netherlands, September, 1973.

Lott, J.R., McCain, H.B. Some effects of continuous and pulsating electric fields on brain wave activity in rats. Int. J. Biometeor. 17: 221-225, 1973.

Maickel, R.P., Cox. R.H., Saillant, J. and Miller, F.P. A method for the determination of serotonin and norepinephrine in discrete areas of the rat brain. Neuropharmacol. 7:275-281, 1968.

Marino A.A., Berger, T.J., Mitchell, J.T., Duhacek, B.A., and Becker, R.O. Electric field effects in selected biologic systems. Annals NY Acad. Sci. 238:435-444, 1974.

Marino, A.A., Berger, T.J., Becker, R.O., and Hart, F.X. Electrostatic field induced changes in mouse serum proteins. Experientia 30:1274-1275, 1974.

Maruvada. P.S. Corona performance of a conductor bundle for bipolar HVDC transmission at ± 750 kV IEEE Trans. PAS. 96:1872, 1977.

Mayyasi, A.M., Terry,R.A. Effects of direct electric fields, noise, sex and age on maze learning in rats. Int. J. Biometeor. 13:101-111, 1969.

Miller, M. Personal Communication, 1978.

Minkh, A.A., The effect of ionised air on work capacity and vitamin metabolism. Presented at: International Conference on Ionization of the Air, American Institute of Medical Climatology, Philadelphia, PA, October 16-17, 1961.

Mose, J.R., Fischer, G. Effects of electrostatic fields: Results of further animal experiments. Arch. Hyg. Bakteriol. 154:378-386, 1970.

Mose, J.R., Fischer, G. and Porta, J. Effects of electrostatic fields on the oxygen consumption of liver cells in mice. Arch. Hyg. Bakteriol. 154:549-552, 1971.

Moyer, K.E. Kinds of aggression and their physiological basis. Commun. Behav. Biol. 2:65-87, 1968.

Nakamura, H. Personal Communication, 1979.

Nazzaro, J.R., Jackson, D.E., and Perkins, L.E. Effects of ionized air on stress behavior. Med. Res. Engin. 6:25-28, 1967.

Petelina, V.V., Burdo, T.D. Condition of various brain regions and their interaction under the effect of static electric field. Fiziol Zh SSR Im I M Sechenova, 28:673-678, 1972.

Refshauge, C., Kissinger, P.T., Dreiling, R., Blank, L., Freeman, R., Adams, R.N., Life Sciences, 14:311, 1974.

Rheinstein, J. Statistical evaluation of the influence of atmospheric ions on the simple reaction time and on the optical moment. Presented at: International Conference on Ionization of the Air, American Institute of Medical Climatology, Philadelphia, PA, October 16-17, 1961.

Sarma, M.P, and Janischewskyj, W. Analysis of corona losses on DC transmissio lines, Parts I and II, IEEE Trans. PAS, 88:718 and 88:1476, 1969.

Sasa, S. Blank, C.L. Analytical Chemistry, 49:354-359, 1977.

Selye, H. The Physiology and Pathology of Exposure to Stress. Montreal: Acta, Inc., 1950.

Shah, K.R., Griffard, W. F., and Denbrock, F. A., HVDC transmission assessment. Proceed. Amer. Power Conf. 39: 1183-1190, 1977.

Sheppard, A.R. Biologic effects of static electric fields and air ions in relation to dc power line transmission. In T.D. Bracken (Ed.) Proceedings of the Workshop on Electrical and Biological Effects Related to HVDC Transmission. Richland, Wash.: Pacific Norwest Laboratory (PNL-3121) 3.0-3.29, 1979.

Sheppard, A.R. and Eisenbud, M. Biological Effects of Electric and Magnetic Fields of Extremely-Low Frequency. New York University Press, 1977.

Siegel, S. Nonparametric Statistics for the Behavioral Sciences. New York: McGraw-Hill, 1956.

Slote, L. An experimental evaluation of man's reaction to an ionized air environment. Presented at: International Conference of Ionization of the Air, American Institute of Medical Climatology, Philadelphia, PA. 1961.

Sommerville, B. and Hintenberger, H. Clin. Chem. Acta. 65:399-402, 1975.

Soyka, F. The Ion Effect. New York: Bantam Books, Inc., 1978.

Steel, R. G. D. and Torrie, J.H. Principles and Procedures of Statistics with Special Reference to the Biological Sciences. New York: McGraw-Hill, 1960.

Sulman, F.G., Levy, D., Lunuan, L., Pfeifer, Y. and Tal, E. Absence of harmful effects of protracted negative air ionization. Int. J. Biometeor. 22:53-58, 1978.

Swan, W.F.G. Atmospheric reactions to air ions. Presented at: International Conference on Ionization of the Air, American Institute, Medical Climatology, Philadelphia, PA, October 16-17, 1961.

Terry, R.A., Harden, D.G. and Mayyasi, A.M. Effects of negative air ions, noise sex and age on maze learning rats. Int. J. Biometeor 13:39-49, 1969.

Thor, D.H., Ghiselli, W.B., and Ward, T.B. Infantile handling and sex differences in shock-elicited aggressive responding of hooded rats. Devel. Psychobiol.,7:273-279, 1974.

Waibel, R. The influence of dc and 50 Hz electric fields on mice. Presented at: First Symposium on Electromagnetic Compatability Montreaux, Switzerland, pp. 175-176, 1975.

Walsh, R.N. and Cummings, R.A. The open-field test: A critical review. Psychol. Bull. 83:482-504, 1976.

Wehner, A. P., The clinical, scientific and technical development of electro-aerosology. Presented at: International Conference on Ionization of the Air, American Institute Medical Climatology, Philadelphia, PA, October 16-17, 1961.

Welch, K.M.A., Mayer, J.S. and Kawant, I. J. Neurochem, 19:1079-1087, 1972.

Wilson, J.G. and Fraser, F.C. (Eds) Handbook of Teratology, Vol. 1. General Principles and Etiology. New York: Plenum Press, 1977.

Winsor, T. and Beckett, J.C. Biological effects of ionized air in man. American J. Phys. Med. 37:83-89, 1958.

Worden, J.L., Some biological effects of air ionization. Presented at: International Conference on Ionization of the Air, American Institute Medical Climatology, Philadelphia, PA, October 16-17, 1961.

Wurtman, R.J. Brain monoamines and endocrine function. Neurosci. Res. Program Bull. 9:172-297, 1971.

APPENDIX A

SIMULATOR DETAIL DRAWINGS

APPENDIX A

SIMULATOR DETAIL DRAWINGS

This appendix provides detail drawings of the various components on the prototype HVDC bioeffects simulator. These drawings, along with the brief explanations provided here, should be adequate to enable the fabrication of additional simulator units.

Figures A-1 to A-3 are three views of the plenum of the simulator. The plastic dome section of the plenum was obtained from a local manufacturer of plastic skylights, who made the domes to the dimensions shown. The remaining portion of the plenum is fabricated from acrylic plastic. The air diffuser shown in the views of the plenum is a 12-inch commercial concentric ring ceiling diffuser. The diffuser has been modified by removing the outer ring, for convenience in mounting.

Figure A-4 shows the material specifications and dimensions for the air diffuser and straightening grids, which are mounted in the upper region of the corona section.

Figures A-5 and A-6 show a side and top view, respectively, of the corona chamber.

The dimensions and material used for the corona and control grids are shown in Figure A-7. The drawing of Figure A-8 is of the grid section separator. The corona and control grids are fastened to the grid section separator with nylon screws.

The glass caging section is shown as top and side views in Figures A-9 and A-10. The glass panels are butt-glued with epoxy.* After fabricating, the unit is cleaned with alcohol; then all glass surfaces are treated with dimethylsiloxane. The alcohol-based silicone compound is applied with a clean gauze. The alcohol evaporates, and the surfaces are rubbed with a clean dry gauze.

The base unit construction is shown in side and top views as Figures A-11 and A-12. Details of the leg construction are shown in Figures A-13 and A-14. Figure A-15 shows a detail of the under-the-wall feeder.

---

*A suitable epoxy is Epon 815 (Shell Chemical Co.), with 5% coloidal silica (Cabosil).

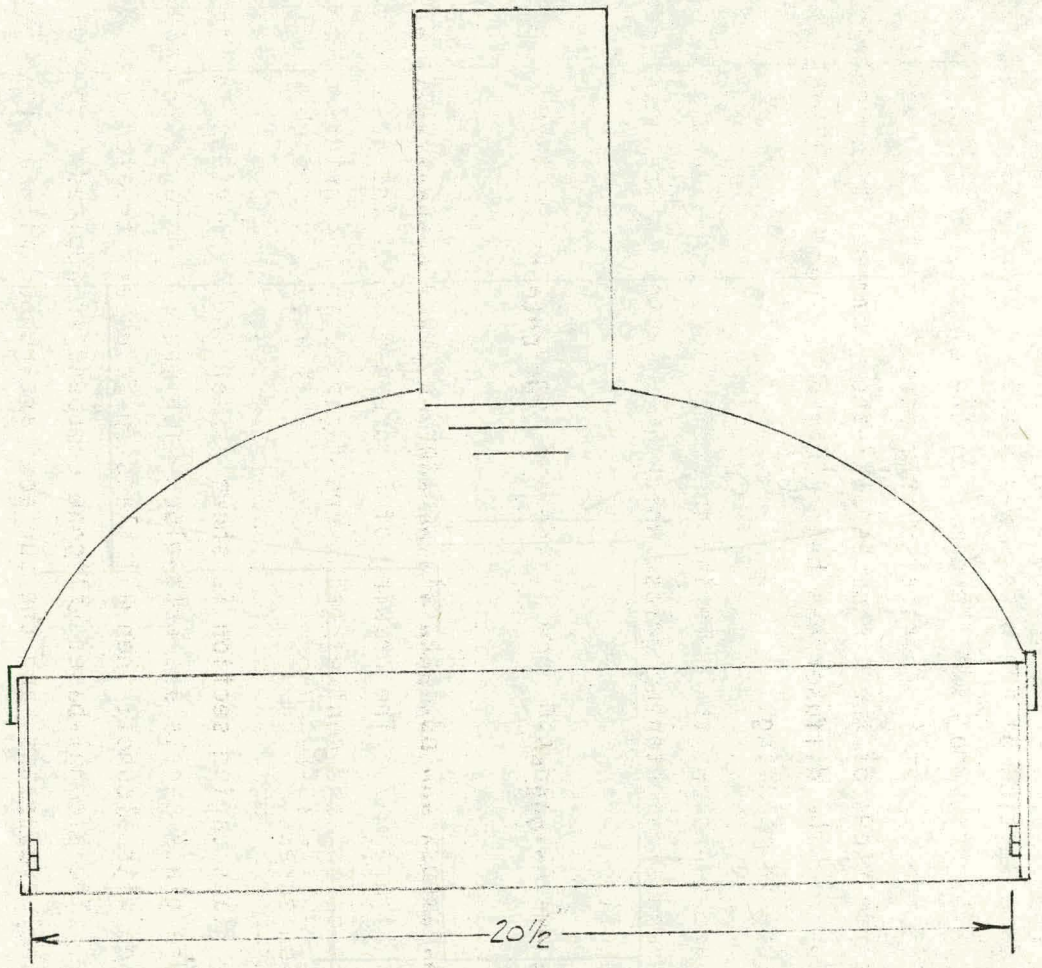

Figure A-1 PLENUM - FRONT VIEW

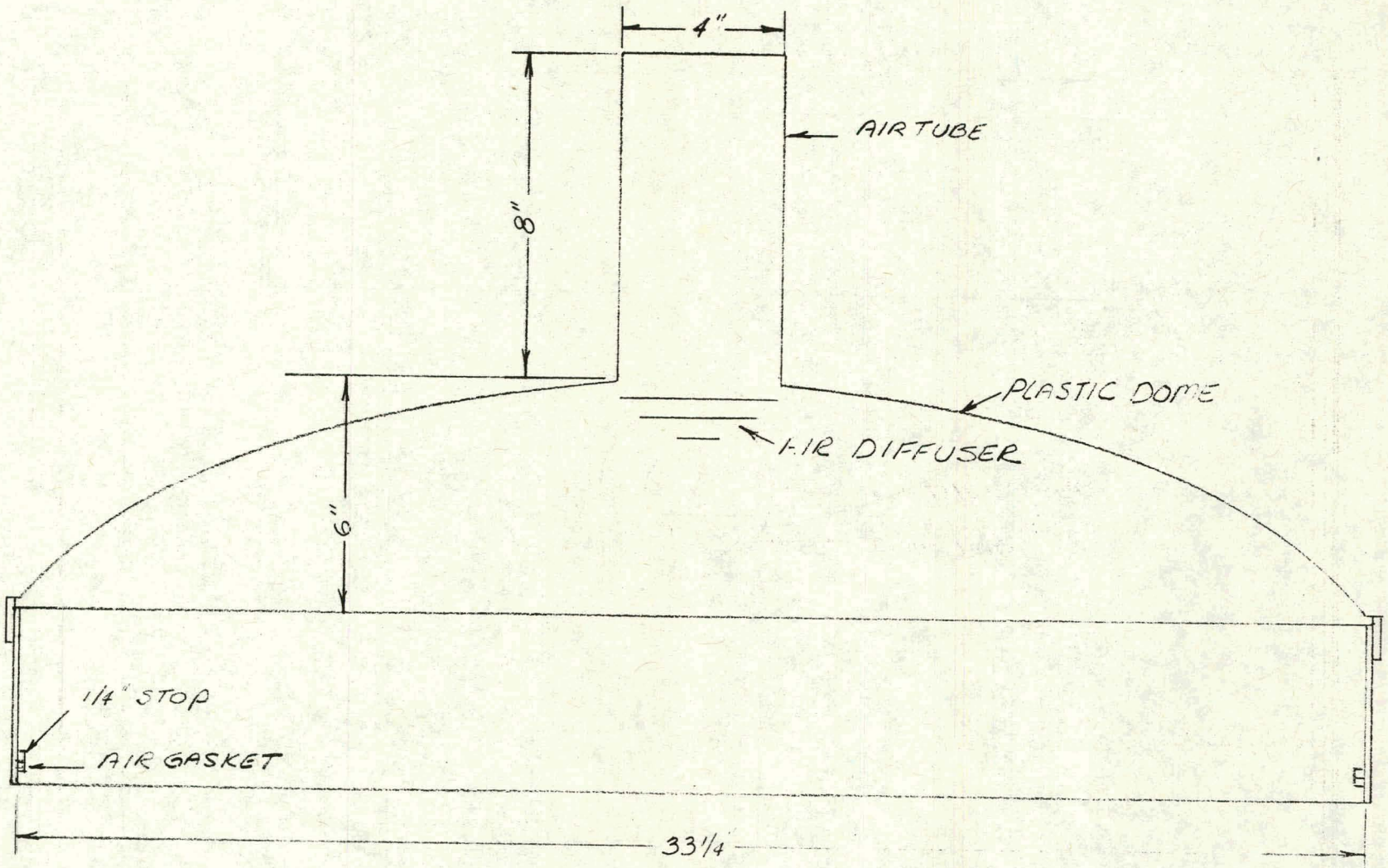

Figure A-2 PLENUM - SIDE VIEW

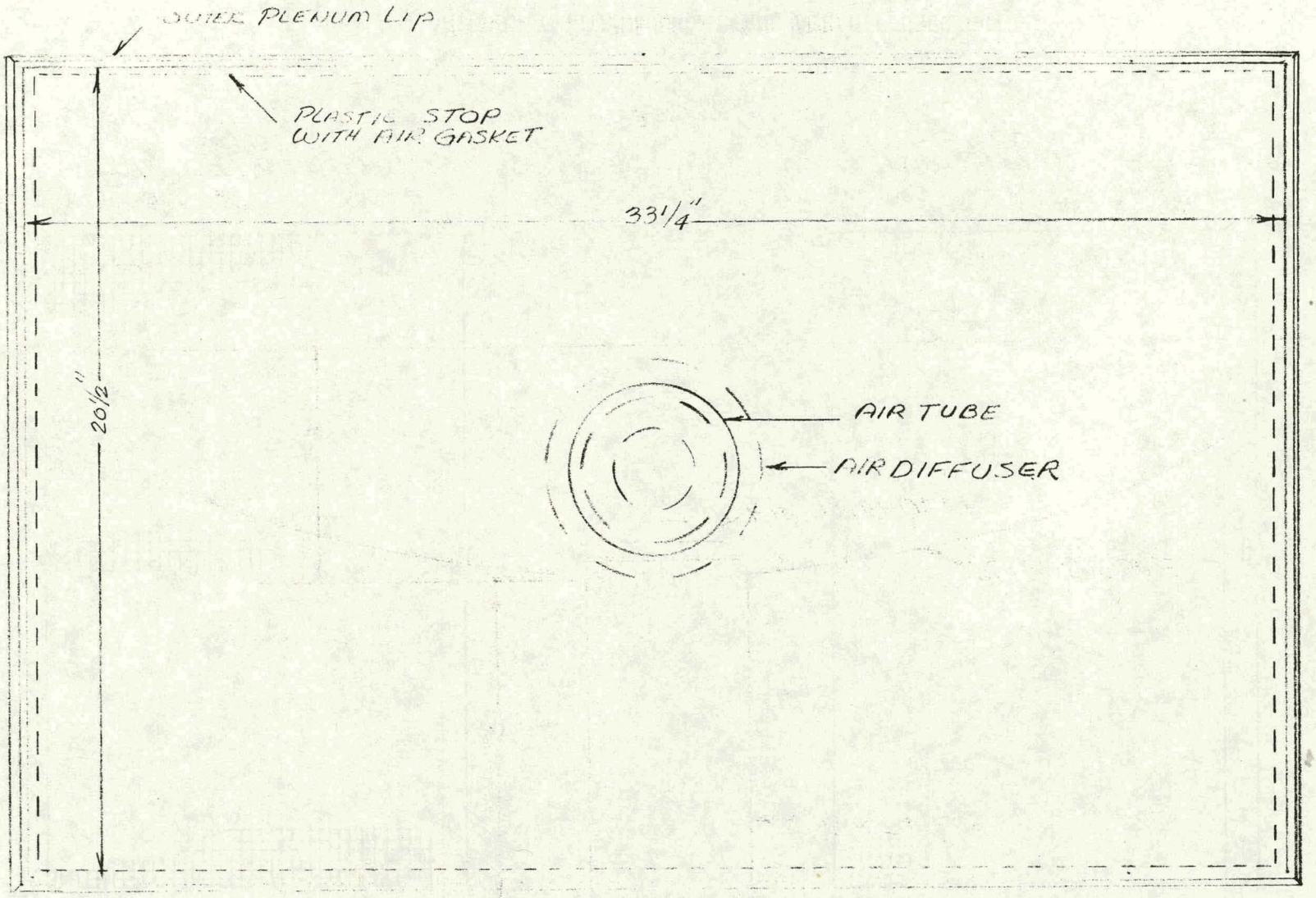

Figure A-3 PLENUM - TOP VIEW

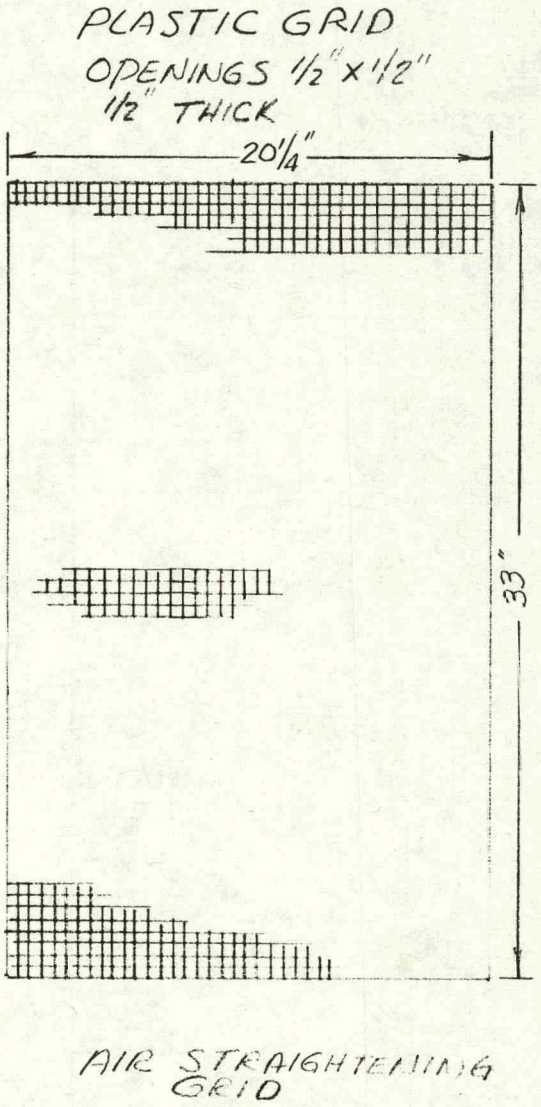

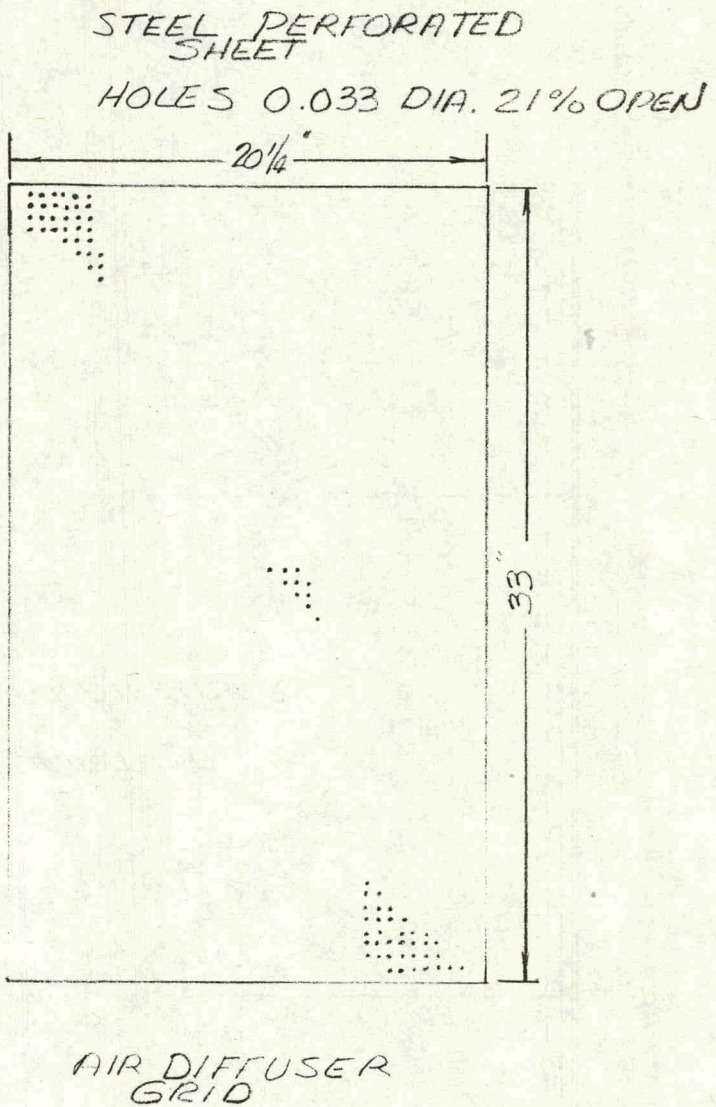

Figure A-4 AIR STRAIGHTENING GRID AND AIR DIFFUSER GRID

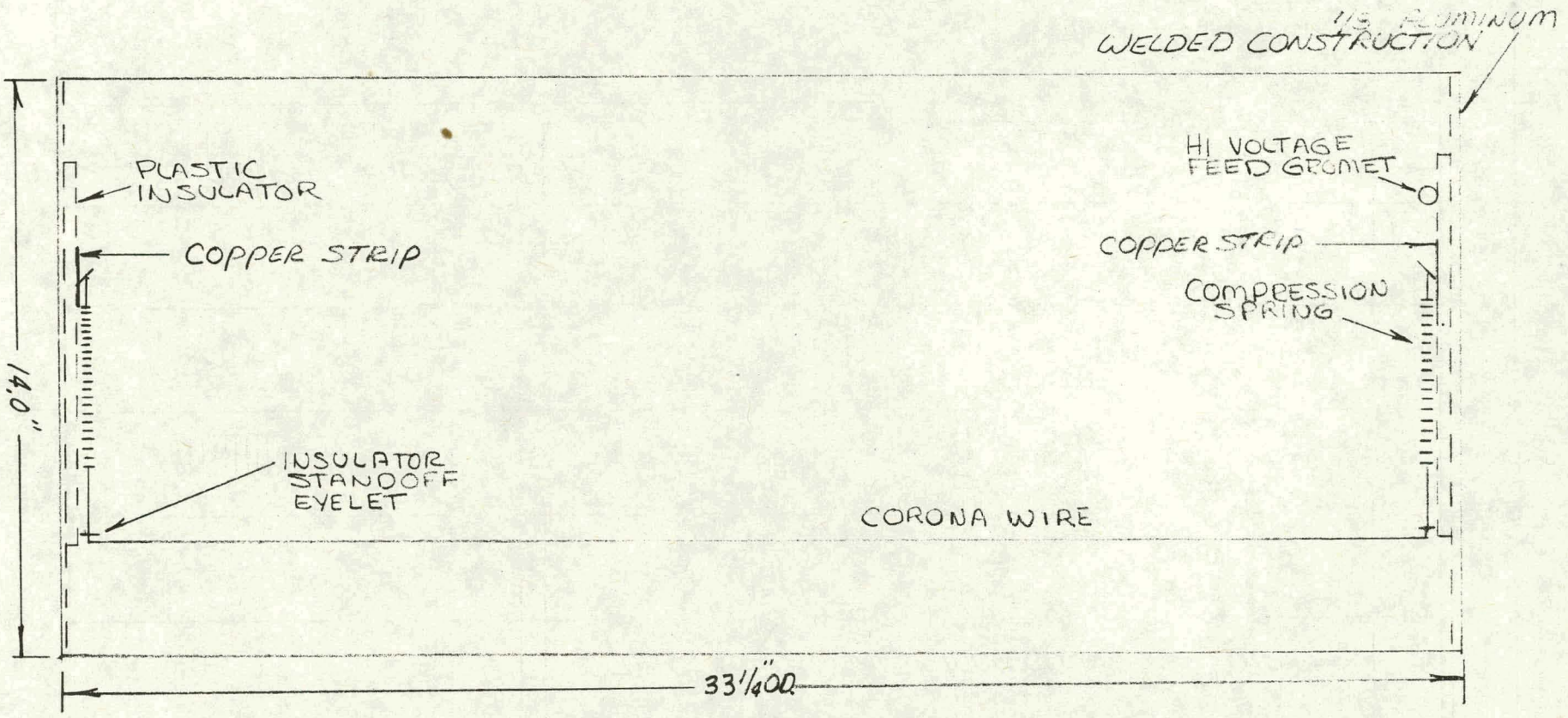

Figure A-5 CORONA SECTION - SIDE VIEW

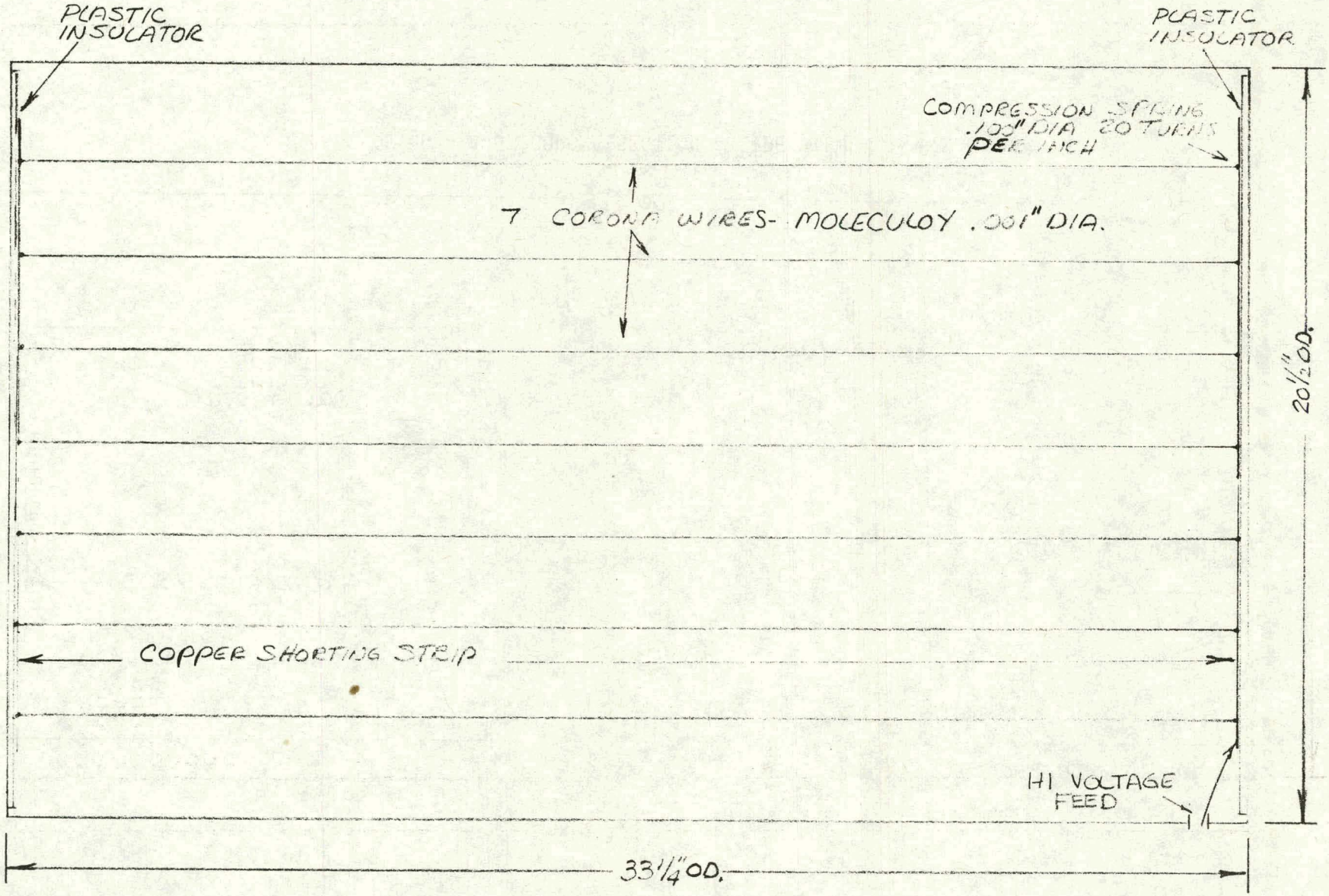

Figure A-6 CORONA SECTION - TOP VIEW

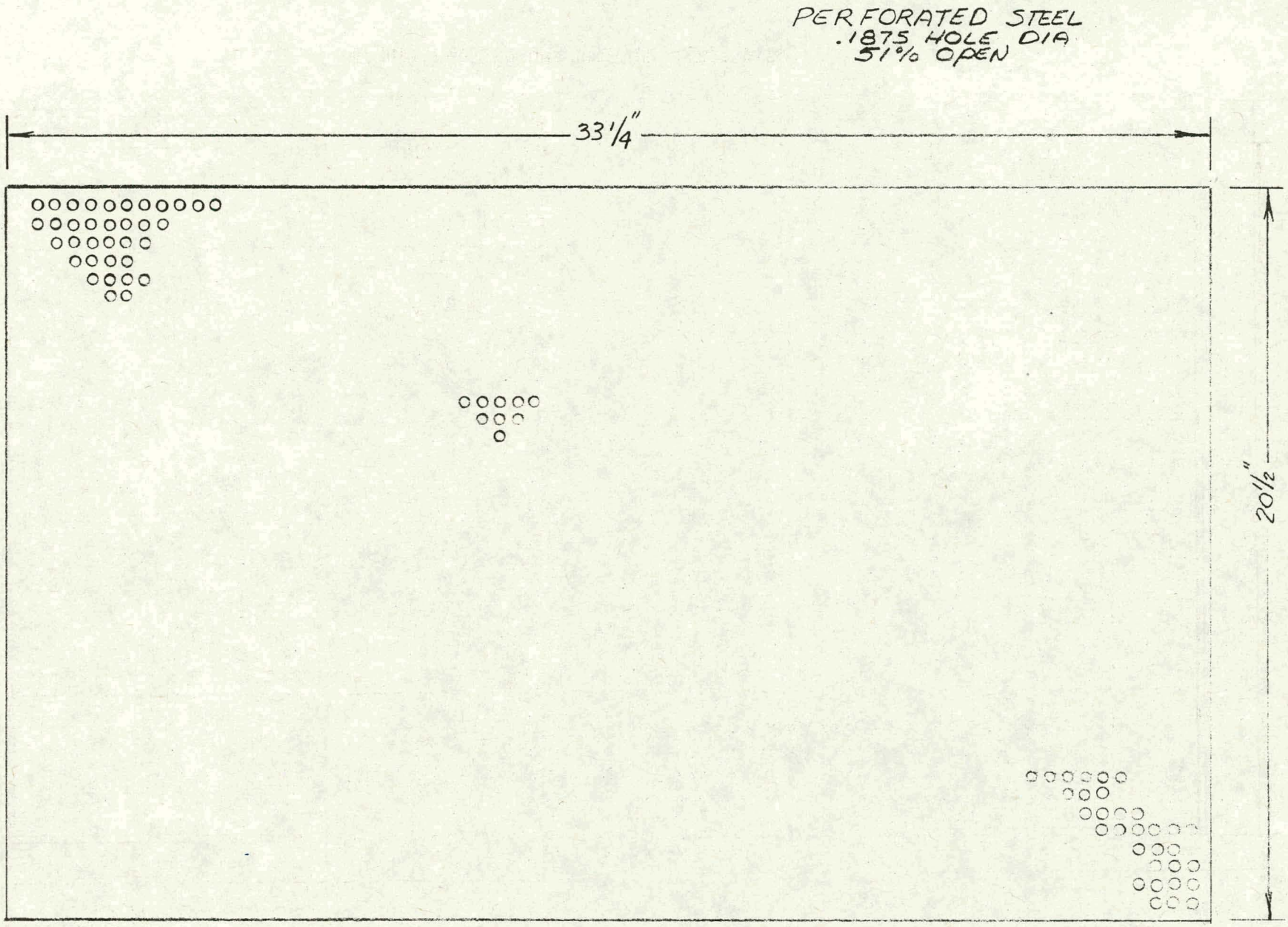

Figure A-7 CONTROL GRID AND CORONA GRID (Identical)

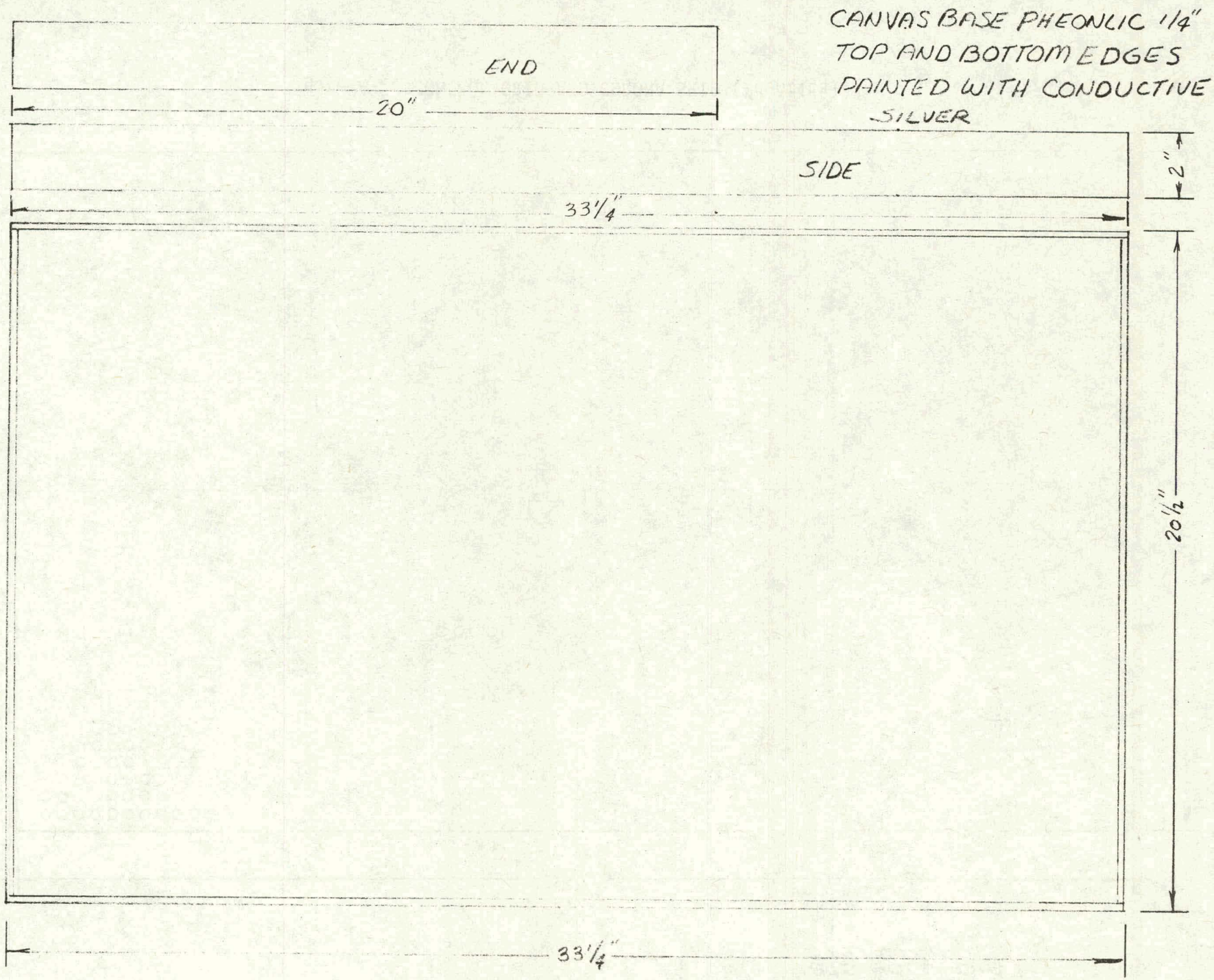

Figure A-8 GRID SECTION SEPARATOR

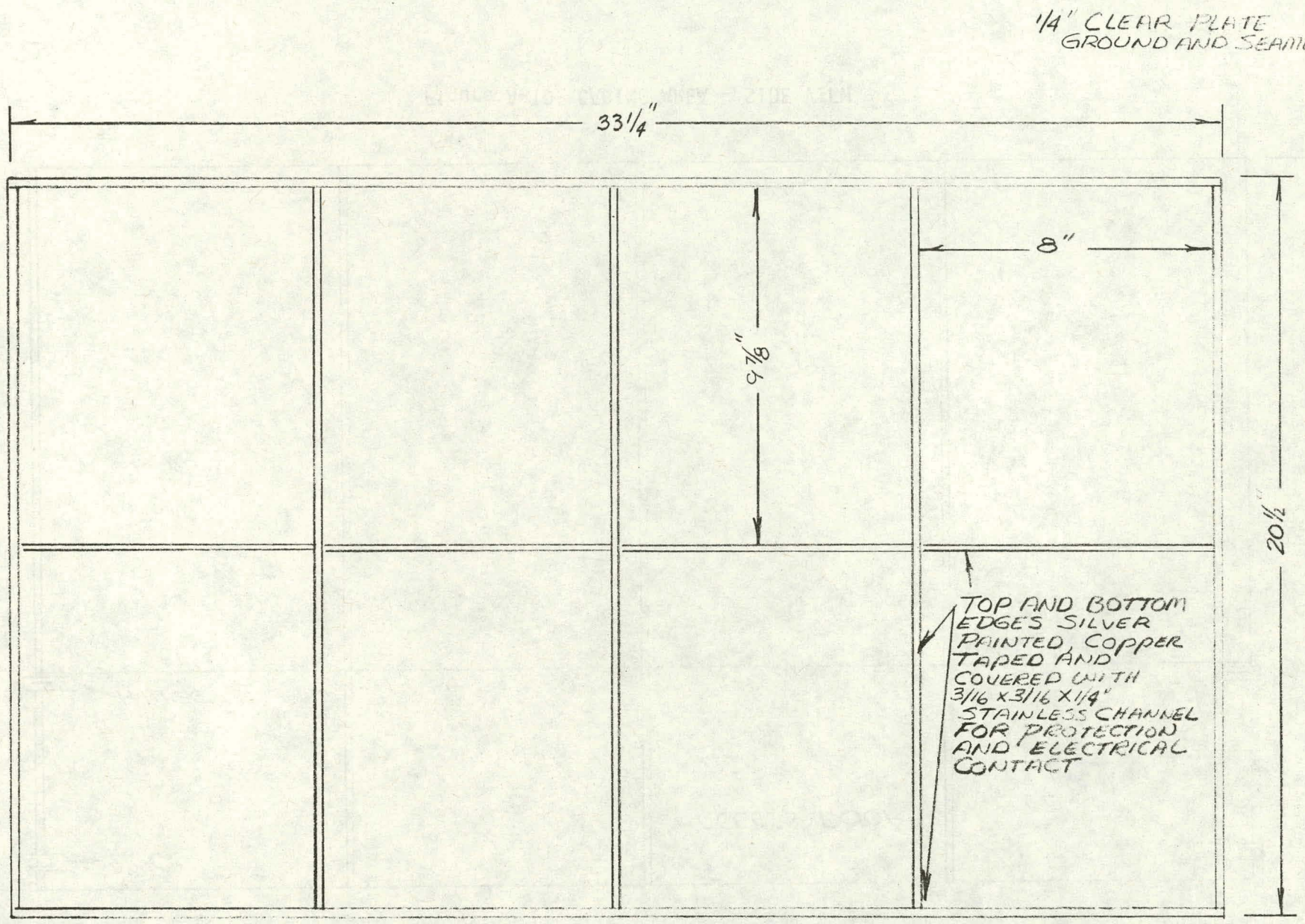

Figure A-9 CAGING AREA - TOP VIEW

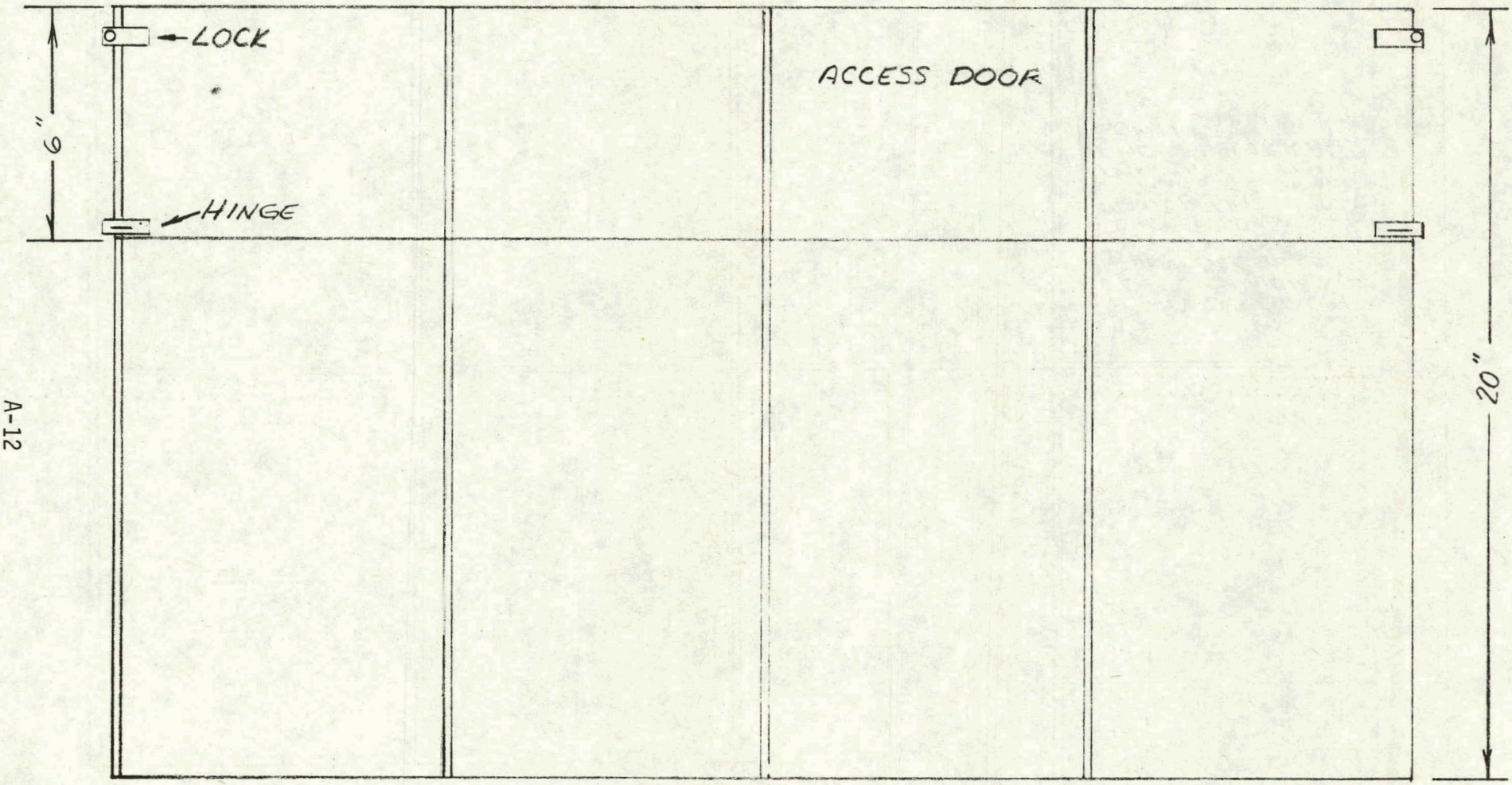

Figure A-10 CAGING AREA - SIDE VIEW

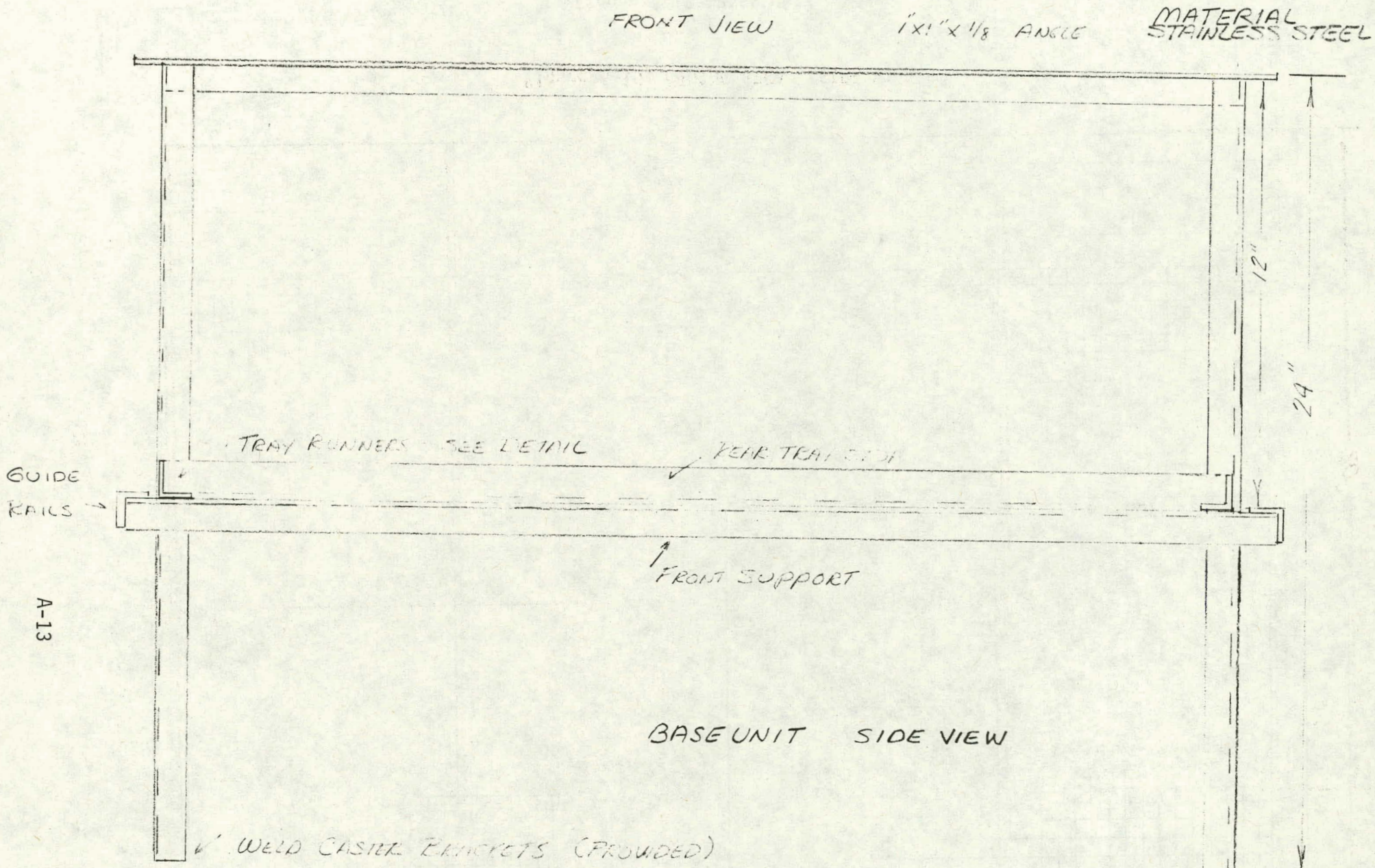

Figure A-11 BASE UNIT - FRONT AND SIDE VIEWS

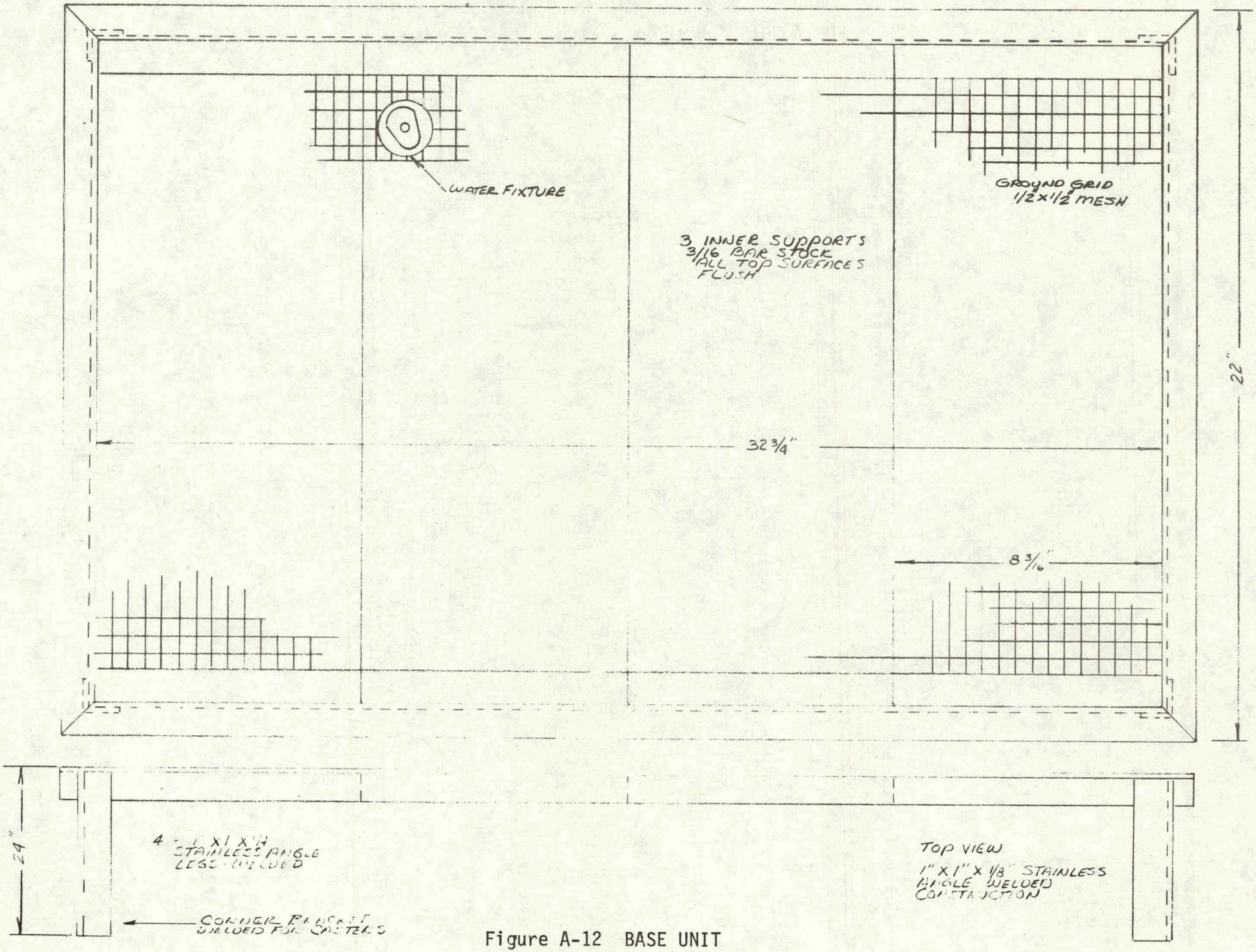

Figure A-12 BASE UNIT

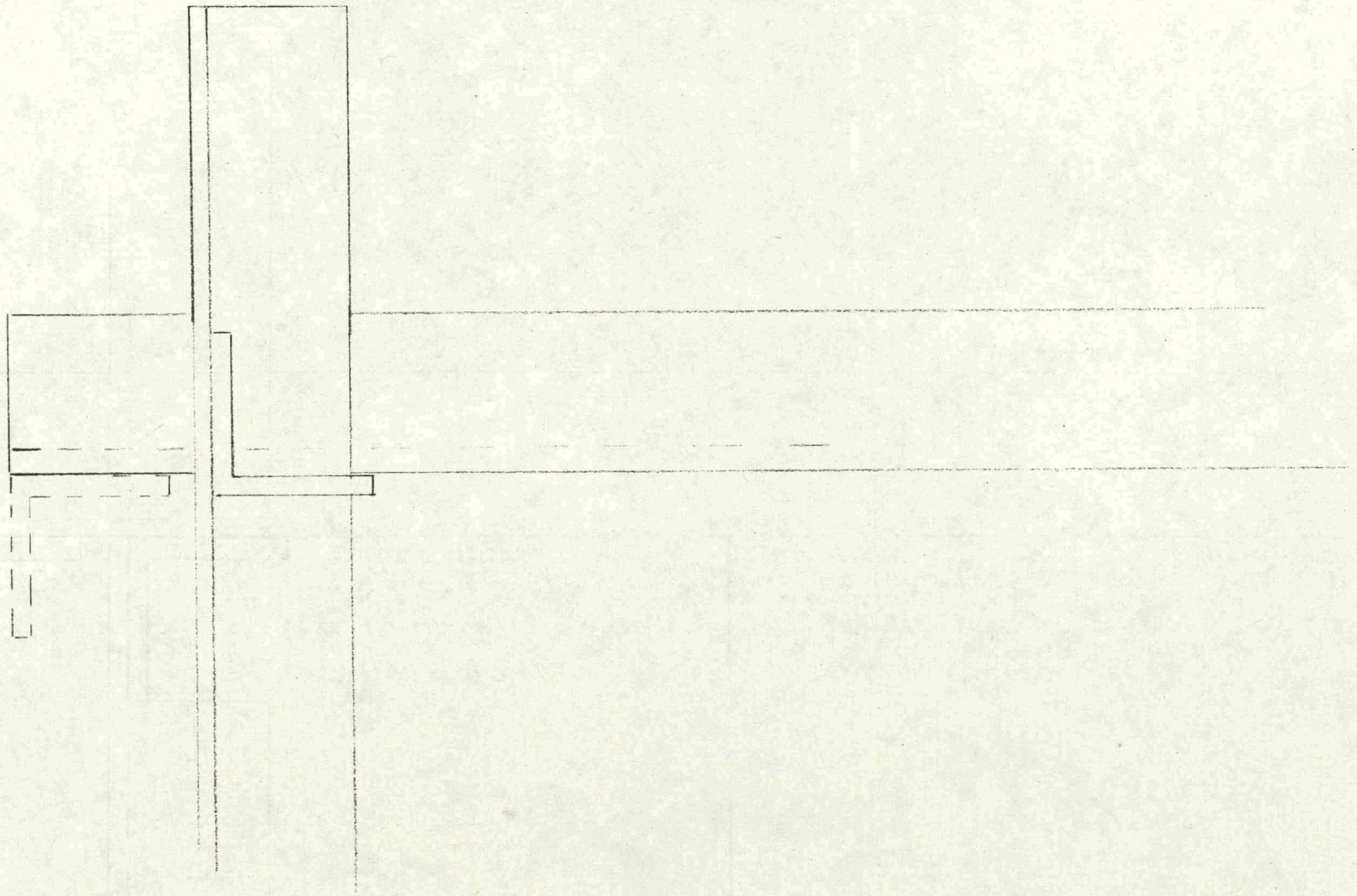

Figure A-13 BASE UNIT LEG AND TRAY DETAIL

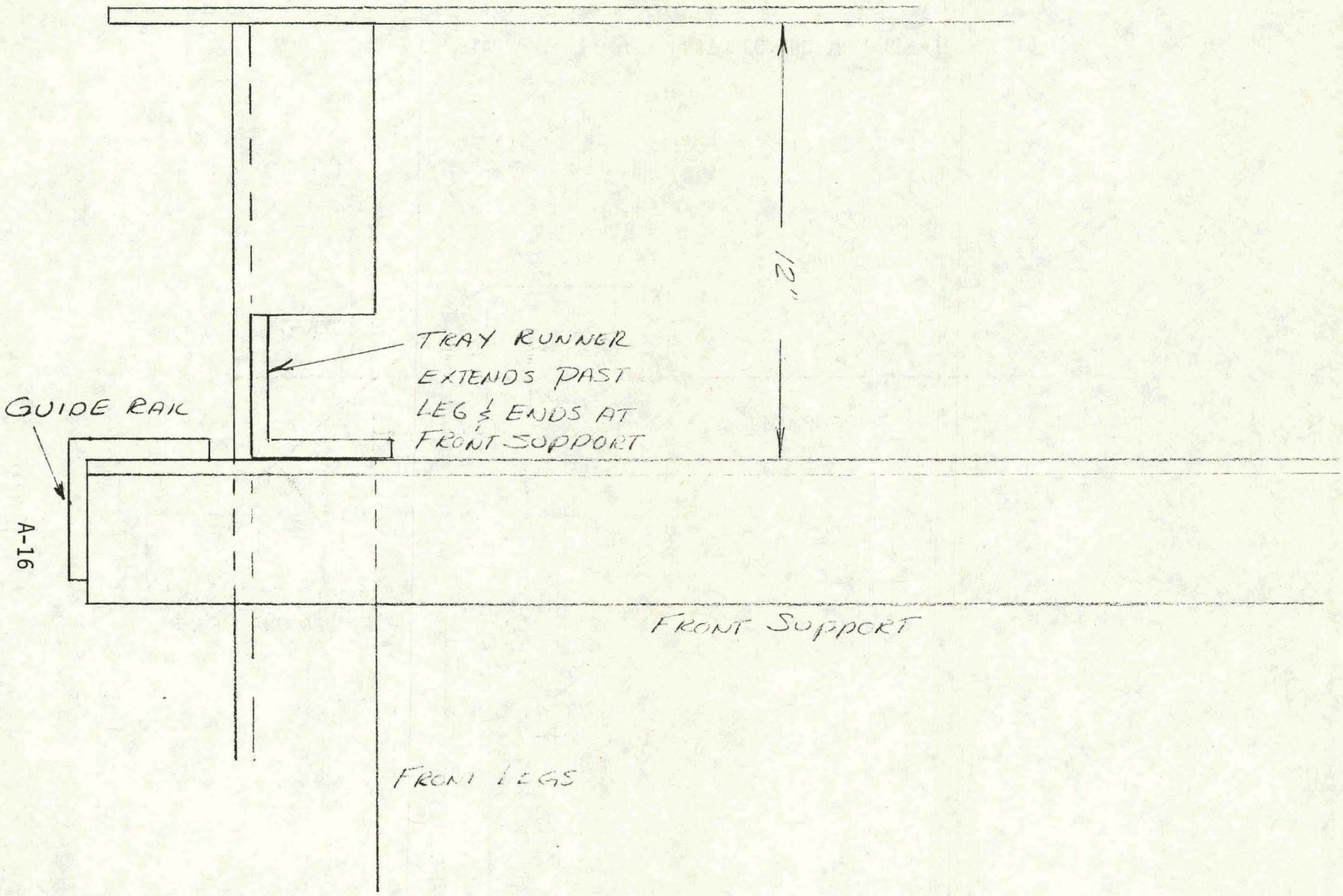

Figure A-14 BASE UNIT DETAIL - SIDE VIEW

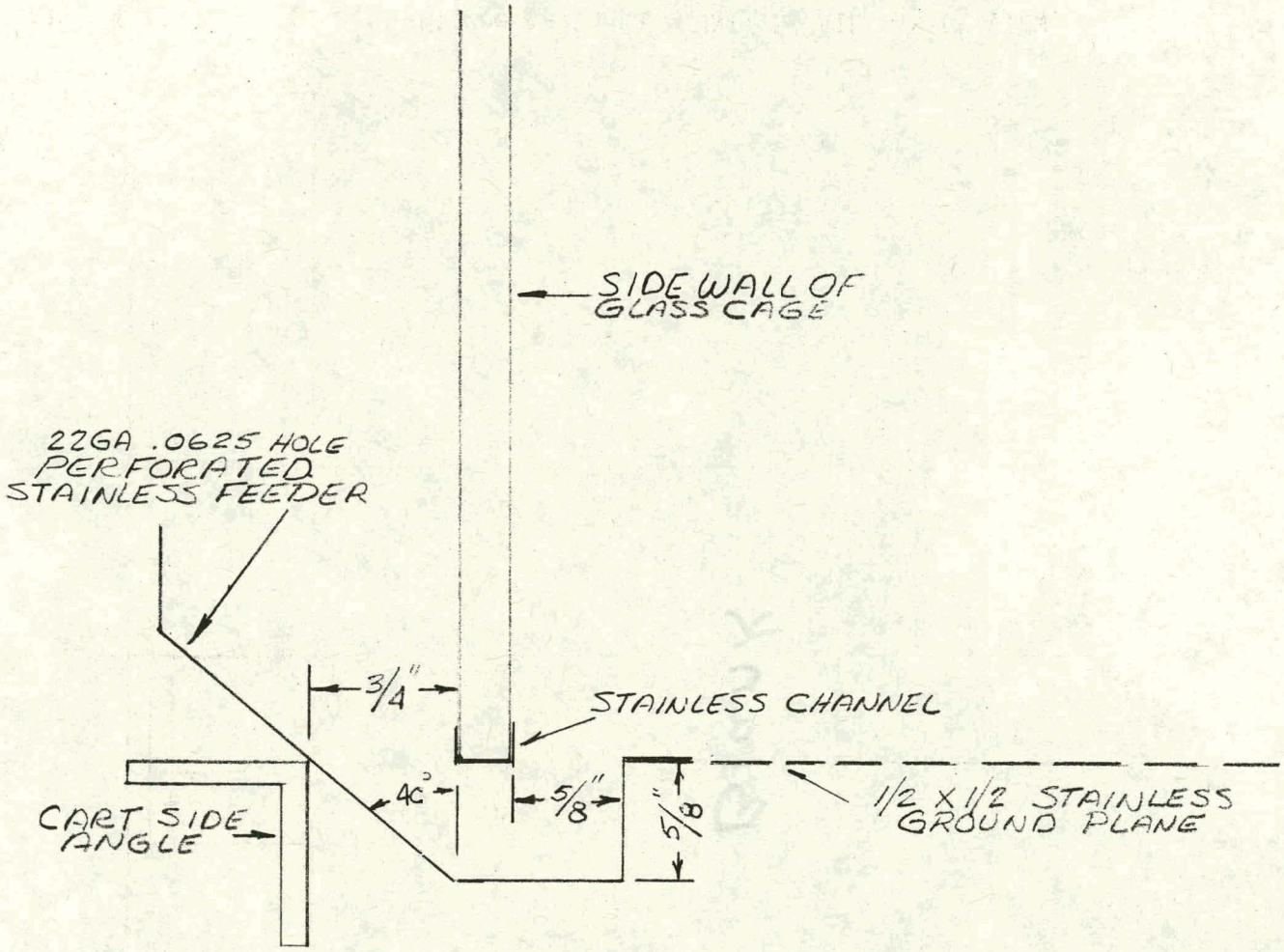

Figure A-15 FEEDER - SIDE VIEW

Blank

APPENDIX B

FABRICATION AND TESTING OF SECOND THROUGH FOURTH PROTOTYPE SIMULATORS

APPENDIX B

FABRICATION AND TESTING OF SECOND THROUGH FOURTH PROTOTYPE SIMULATORS

This Appendix describes the developmental, fabrication and testing efforts with three prototype model simulators which employed glass animal caging sections. The main text of this final report provides an overview of the simulator development effort, the basic rationale for the overall design and the performance characteristics of the final prototype. However, many of the developmental steps which led to the final simulator model have been omitted from the main body of this report for brevity, since many readers will not be interested in such detail.

The first four quarterly reports which were prepared on this program have described the work efforts performed up to the time that the second prototype model simulator was fabricated. However, the testing of the second prototype and the efforts which led to the subsequent fabrication of the third and fourth prototype have not been reported. The purpose of this appendix, therefore, is to provide a report of technical progress and results which covers the period from the Fourth Quarterly until the present.

The technical efforts performed during this period, along with the results obtained by tests performed with the prototype simulators will be described in a more or less chronological manner. This type of discussion will enable the reader to observe the performance improvements which resulted from the various design modifications which have been incorporated.

B.1 TEST METHODS

Before describing the results which were obtained with the different simulator units, the method used to evaluate simulator performance will be reviewed. The factor which appeared to be most critical in the simulator development, and which forced the most modifications to the design was the uniformity of the ion current density. We were interested in insuring a uniform ion current density environment in the animal caging area of the simulator. Both the details of the animal caging section and the corona section design have a significant effect on the ion current density uniformity. Both were modified substantially during this period in order to effect an acceptably uniform ion environment.

The ion current density was generally measured at the simulator ground grid by one of two current probes which we have fabricated. These two probes are shown in Figure B-1. The larger of the two probes has an active area of 100 cm^2. This probe was used when we were not interested in the fine details of the current, but were interested in the average ion current level in the simulator. The smaller probe shown in Figure B-1 has an active area of 10 cm^2 and was used for characterizing the ion current density uniformity within the simulator. The outside dimensions of this probe are 2 x 2 inches.

An individual animal compartment of the simulator has a floor area of 8 x 10 inches. A complete current density map of such a compartment would consist of twenty different non-overlapping positions of the smaller current probe. A current density map of the entire simulator consists of 160 different current density readings with the probe (20 readings per 8 x 10-inch compartment) moved to the different locations on the ground grid. Many full or partial "maps" were made during this period to assess the effects of various changes which were made in the simulator. The use of this small of a probe was debated during the investigation as possibly being too exacting, since it is considerably smaller than the collection area of a rat-sized animal, and is considerably smaller than the 1 m^2 probe generally used to measure the current density beneath transmission lines. However, it was felt that the acceptability of the design could not be questioned from a uniformity standpoint if adequate uniformity could be shown with such a small sized current probe.

B.2 SECOND PROTOTYPE SIMULATOR

The second prototype simulator was described briefly in the Fourth Quarterly Report. However, the salient features of the simulator will be presented here for completeness.

Figure B-2 shows a photograph of the unit, which is comprised of five functional components: plenum, corona chamber, grid section, caging area, and base. The function of each of these sections has been described in the foregoing quarterly reports and in the main text of this final report.

The second prototype differed from the first prototype in two respects. First, the corona chamber was made with aluminum walls. The corona wires were one-mil steel wires as had been previously used. These wires were arranged and mounted in the same manner as had been used for the first

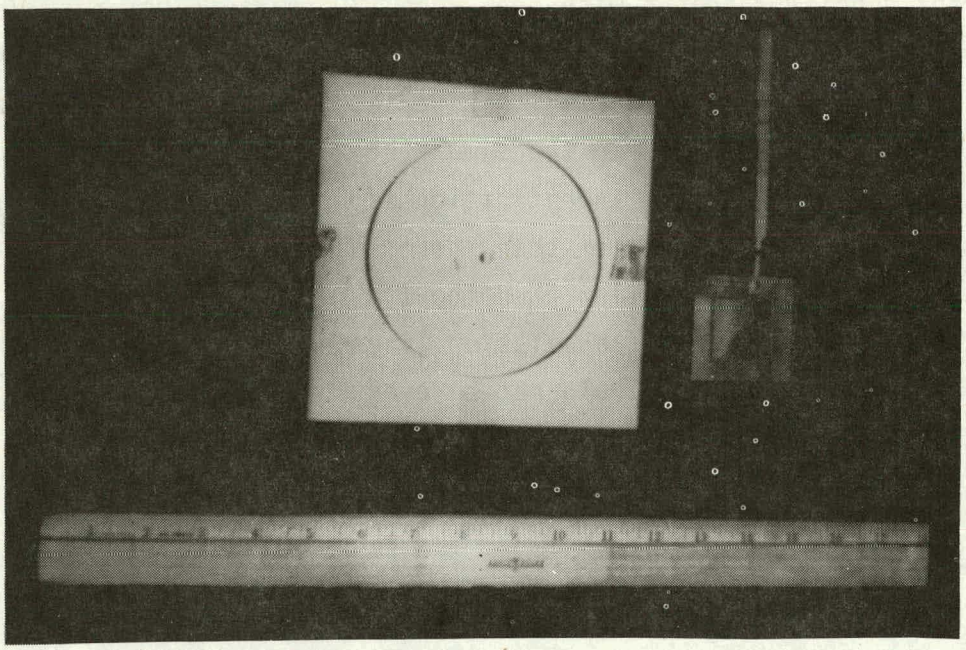

Figure B-1 ION CURRENT DENSITY PROBES

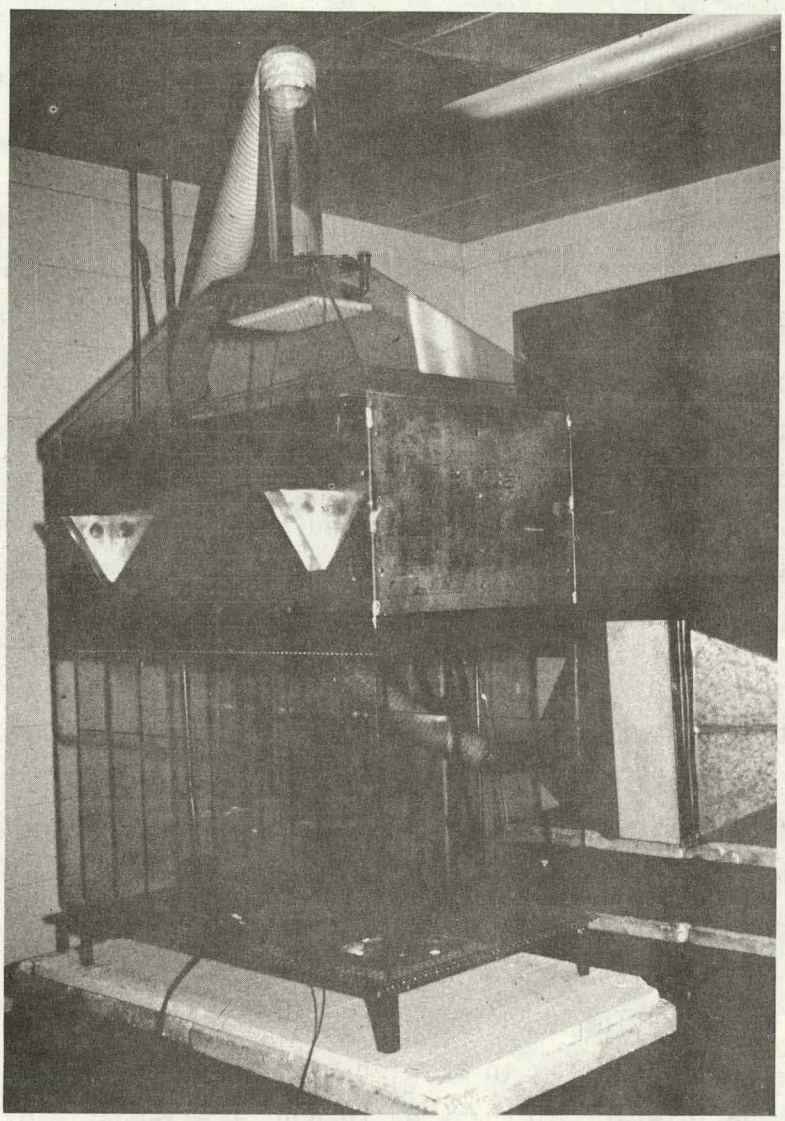

Figure B-2. PHOTOGRAPH OF SECOND PROTOTYPE SIMULATOR

prototype. Three wires were used, with one wire centered in the width of the chamber and the other two wires mounted four inches on either side of the center wire. The wires were mounted at a height of six inches above the corona grid. The wires were attached to 5/8-inch diameter copper tubes which were mounted in a horizontal position on the inside of the two end walls of the corona chamber by means of small Plexiglas standoffs. Each copper tube feed was separated from the end wall by 3/4-inch, which was an adequate distance to insure that no corona current was drawn from the feed tube to the wall at the voltage necessary to produce corona from the corona wires which were strung between the two feed tubes. Use of this corona wire arrangement had resulted in reasonable lateral uniformity in current density with the first prototype, as was indicated in Figure 8 of the Fourth Quarterly. However, it had been noted during testing of the first prototype that improvements in the feed arrangement would probably be necessary to improve the ion current density near the end walls of the simulator.

The second major change between the first and second prototype was a different animal caging section. The caging section of the second simulator was fabricated from 1/4-inch thick plate glass panels, which were glued together with epoxy. The caging area was divided into four major compartments with glass partitions. However, the small walls, which divide each major compartment into two were not included.

The long side walls of the caging section each have a removable six-inch high door at the top, for access to the animals. The long side walls do not extend clear down to the ground plane, but end 7/8-inch above the ground plane to accommodate a feeder trough. Figure B-3 shows a sketch of the planned feeder arrangement. A single animal cage mock-up of the feeder arrangement has been fabricated and tested with an animal for several weeks. The animal acclimated to the feeder with no problems, increasing in weight at the same rate as a control animal. The feeder troughs were not installed in the glass prototype unit to facilitate ease in testing with the current probe, which was inserted into the interior of the area through the feeder slot. The metalized strip on the bottom of the wall (the top of the feeder slot) was connected to ground, to provide a conduction path for the wall current-to-ground.

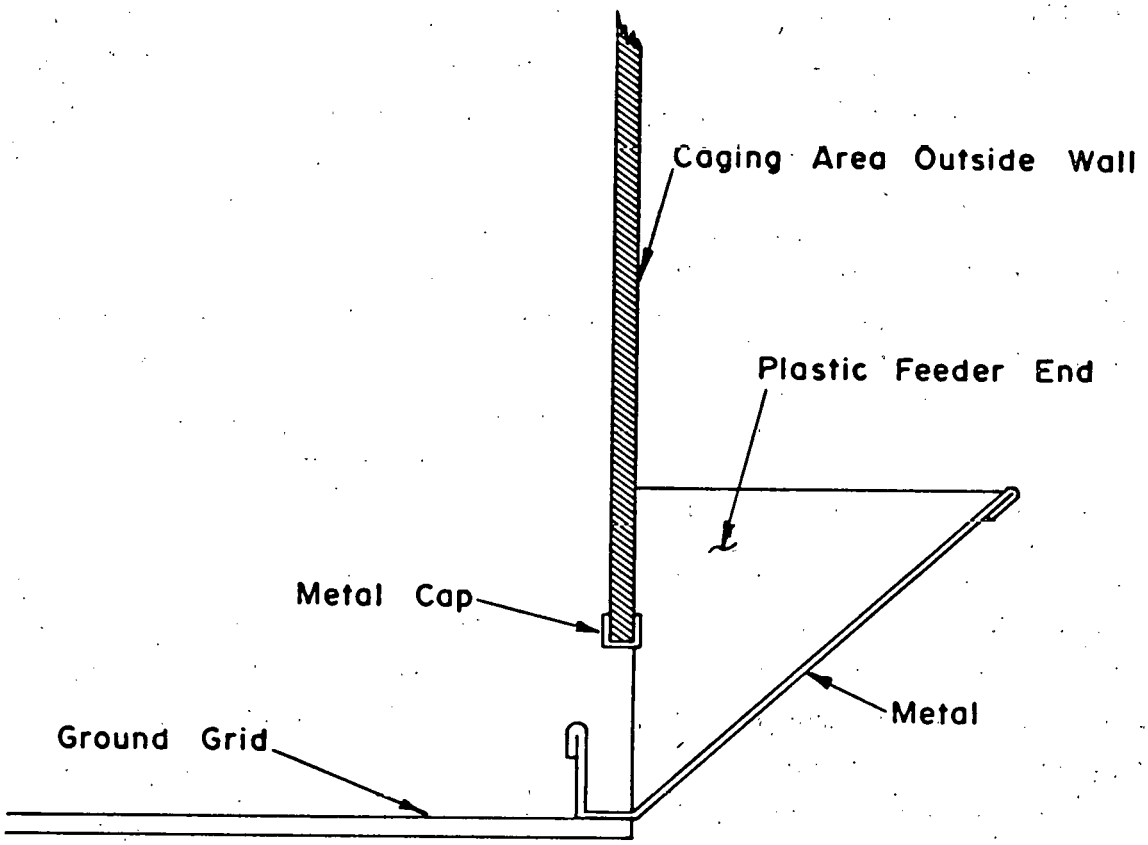

Figure B-3. PLANNED FEEDER ARRANGEMENT CUTAWAY VIEW

One of the first current density maps which was made is presented in Table B-1. The map is of three of the four compartments. Each value shown in the table is the current density in nA/m^2 at that probe position. The table depicts how the current density varies at different locations within the compartment. The positions are as looking down into the unit from above. Review of the data shown in the table shows that relative to the current density levels near the center of the compartments, the levels are down

- significantly at most corners,
- significantly at most cross walls,
- somewhat along the long outside walls.

The above data were obtained with a plate voltage of 15 kV - which should produce nominal electric fields of 30 kV/m. A corresponding electric field map was made in the same compartments as the current density map shown above. For the field map, the Monroe 225 field meter was used. In order to facilitate moving the field probe to the various locations on the ground grid, the field probe was set on top of the ground grid rather than being flush-mounted as it was intended to be used. When the probe is mounted on top of the ground grid, the fields are enhanced, thus resulting in a higher field reading than when flush-mounted. A comparison of the field meter readings flush and on top of a ground plane shows an enhancement ratio of 2.06. Therefore, the data obtained with the field meter on top of the ground grid was corrected by the above enhancement ratio to give the values shown in the map of Table B-2 for the second prototype. The field data were obtained with the ion source off. It is seen that some variability in the field was observed; however, the field variation is quite small compared to the observed variation in ion current density displayed in Table B-1.

Preliminary experimentation had been made with the first prototype with a cross wall inserted. It had been noted that ion current depressions existed at the corners, where the walls joined. Bridging the corners with thin strips of conductive adhesive copper tape resulted in some improvement. Therefore, some preliminary tests were made with the second prototype to investigate the desirability of using copper strips to force equal potentials at wall corners.

During this same period, some modifications to the corona chamber wire arrangement and feeds were also made. Tests were made with the animal section removed and with the control grid lowered to two inches above the ground plane

Table B-1

FIRST CURRENT DENSITY MAP OF SECOND PROTOTYPE

Readings in nA/m^2

150	185	180	5
175	190	195	5
175	190	200	10
175	185	190	5
195	200	200	15
190	200	205	50
175	180	185	35
125	180	190	35
90	175	175	70
80	115	135	140

40	180	185	175
70	205	210	190
55	210	210	195
55	200	190	175
85	185	185	180
105	195	190	190
80	175	180	180
75	185	190	140
80	175	180	85
85	140	150	50

10	195	185	70
45	205	200	125
70	200	210	145
70	185	180	125
60	205	190	100
55	180	180	95
60	195	180	115
60	200	195	130
65	195	200	90
75	170	170	60

Table B-2

FIRST ELECTRIC FIELD MAP OF SECOND PROTOTYPE

Values are in kV/m

29.1 29.1 31 35	35.9 34 33.5 33.5	32 30 33 35.9	
27.7 27.2 27.1 35	34 30 29.1 31	30 28.2 29.1 34	
28.1 27.2 27.1 35	36.9 30.6 29.1 34	31 28.2 29.1 35	
30 27.7 27.1 37.9	37.9 31 30 34	34 29.1 29.1 34	
31 28.1 27.1 35.9	37.9 31 30.6 35.9	33.5 29.6 29.1 34	
31 28.1 27.1 35	37.9 31 30.6 35.4	33.5 29.6 29.1 34	
31 28.1 27.1 35.4	36.9 30 30 35	33 29.1 29.1 34	
30 27.2 29.7 33	35 29.1 29.1 33	32.5 28.6 28.2 34	
29.1 27.2 27.2 32	30.6 27.2 27.7 33.5	31 28.2 28.2 34	
29.6 29.1 28.1 31	28.1 27.2 28.2 33.5	32.5 31 33 35	

in an attempt to better characterize the ion uniformity from the "source". The feed modifications and lowering the wires to 4-1/2 inches above the corona grid provided some improvement at the end walls; however, the improvement did not appear satisfactory and depressions along the side walls still existed. During this period, one end compartment (the one we called the fourth compartment) was coated both inside and out with dimethylsiloxane. For a few days after the coating, the ion current density distribution in that compartment was greatly upset. However, gradually the distribution returned to about what it had been prior to coating.

Table B-3 shows a current density mapping with the somewhat modified corona chamber and with the fourth compartment coated with silicone. It is seen that problems still existed in corners and side, and end walls.

Table B-4a and b shows a current density map of the first compartment under two conditions. The map of Table B-4a was made with 1/4-inch conductive adhesive tape strips placed horizontally as grading rings on the inside of the compartment. The strips formed complete rings around the compartment and were spaced at two-inch intervals up the walls. The map of Table B-4b is for the same compartment without the tape strips. The standard deviation of the data with tape strips of Table B-4a is 17% of the mean while for the non-stripped condition of Table B-4b, the standard deviation is about 29% of the mean. Thus, the use of tape guard rings improved the current density uniformity. Notably, the current depressions at the corners are not as severe with the tape strips.

In a similar manner, Table B-5a and B-5b compares current density maps of the fourth compartment with and without 1/4-inch wide copper tape strip guard rings.

Table B-6a is a current density map of the second compartment with the same tape guard ring arrangement. Comparison with the untaped second compartment data of Table B-3, again shows an improvement. For the map of Table B-6b, the second compartment was divided into two with a glass wall, to form two 8 x 10-inch compartments. The dividing wall was held in place with RTV and also had copper tape guard strips which made contact to the copper strips on the main compartment walls. It is seen that the addition of the compartment dividing wall depressed the current density readings somewhat in the new corners, but that the overall compartment uniformity was better than without the tape guard strips.

Table B-3

CURRENT DENSITY MAP OF SECOND PROTOTYPE
- FOURTH COMPARTMENT TREATED WITH SILICONE -

Readings in nA/m^2

4	3	2	1
55 160 140 130	140 155 165 120	50 160 195 60	65 150 110 70
85 200 200 185	190 210 200 120	80 225 220 110	85 170 160 120
95 215 205 200	185 215 230 115	95 215 225 185	140 180 175 120
105 205 205 195	160 215 220 135	120 215 215 200	175 180 170 130
125 205 195 180	135 195 210 100	105 200 195 200	175 165 170 120
125 215 200 180	120 200 220 120	100 205 200 195	170 165 170 115
110 200 195 190	95 195 205 135	130 190 200 190	160 170 165 130
80 200 205 200	70 215 220 140	155 210 210 180	150 180 175 140
20 195 190 190	30 200 205 135	145 200 205 120	100 170 165 135
10 150 135 145	10 150 160 90	155 170 180 60	45 135 135 35

Table B-4

CURRENT DENSITY MAP OF FIRST COMPARTMENT OF SECOND PROTOTYPE
WITH (a) AND WITHOUT (b) COPPER STRIP GRADING RINGS

115	140	105	95
140	155	145	115
175	165	150	130
180	185	160	130
165	170	145	135
165	175	155	135
170	175	160	125
190	180	170	140
155	170	155	130
100	130	120	100

(a)

105	125	70	85
140	160	150	110
180	170	165	120
175	165	165	130
175	175	160	130
190	170	170	125
180	180	170	135
175	180	175	135
145	180	175	50
100	140	145	10

(b)

Table B-5

CURRENT DENSITY MAP OF FOURTH COMPARTMENT OF SECOND PROTOTYPE
WITH (a) AND WITHOUT (b) COPPER STRIP GRADING RINGS

(Readings in nA/m^2)

100	125	120	110
140	160	155	145
170	165	170	150
150	170	170	145
140	150	150	135
140	165	170	140
145	160	160	145
165	160	160	145
150	155	155	150
90	110	110	110

(a)

55	160	140	130
85	200	200	185
95	215	205	200
105	205	205	195
125	205	195	180
125	215	200	180
110	200	195	190
80	200	205	200
20	195	190	190
10	150	135	145

(b)

Table B-6

CURRENT DENSITY MAP OF SECOND COMPARTMENT OF SECOND PROTOTYPE WITH COPPER STRIP GRADING RINGS (a) AND WITH DIVIDING WALL (b)

(Readings in nA/m^2)

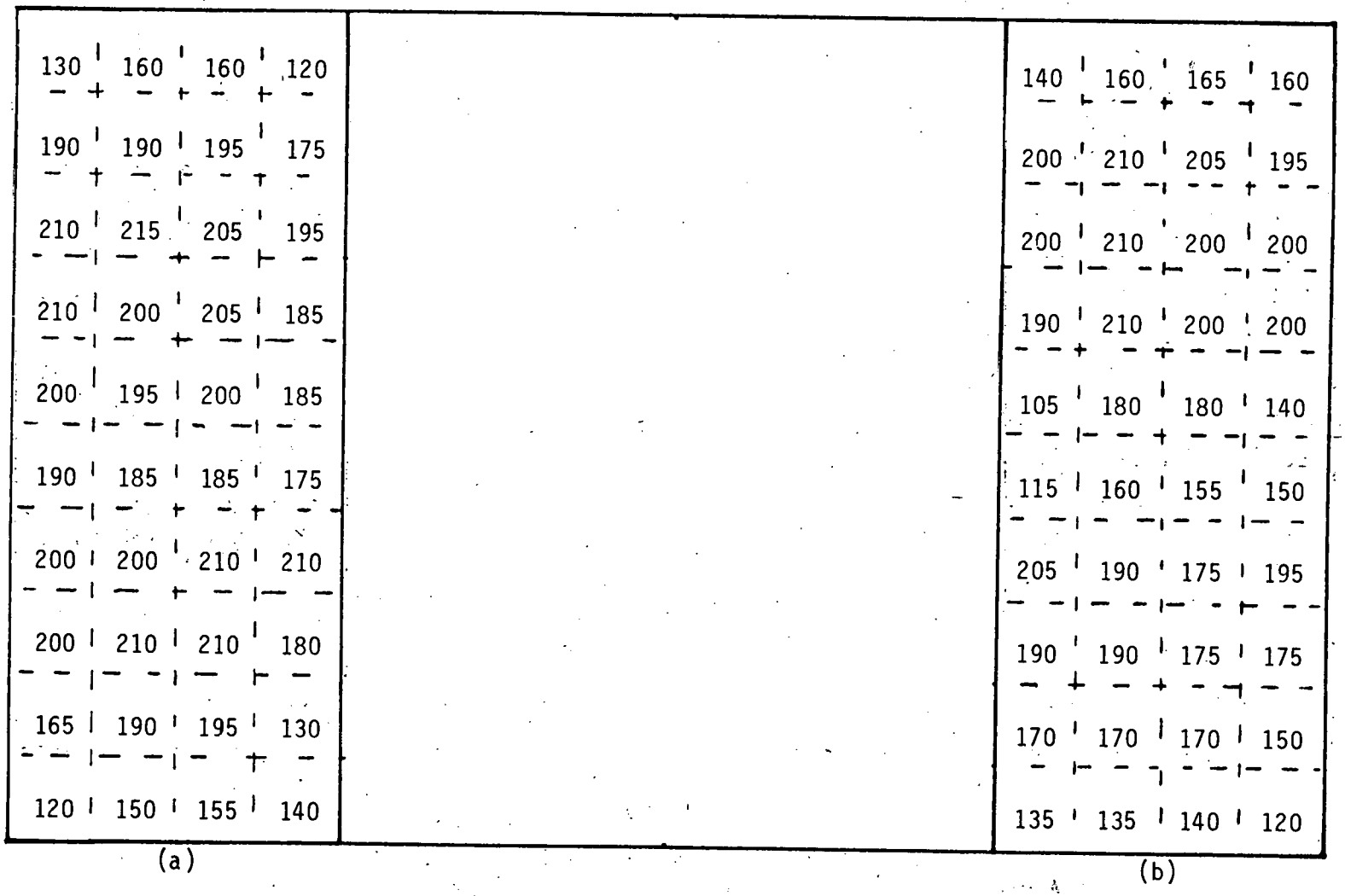

It was felt that some of the ion current density nonuniformity being observed was still due to the corona source configuration, particularly along the side walls of the chamber. Therefore, it was decided to further investigate alternate wire arrangements. It was thought that additional wires could be used without encountering severe ozone problems, since negligible levels had been observed with the three-wire arrangement since we had started using 1-mil diameter wires. Therefore, a new temporary corona wire feed and mounting arrangement was fabricated. This feed arrangement does not warrant discussion, since it was temporary, other than noting that it allowed us to easily change the number of wires used - the spacing between wires - and the height of the wires above the corona grid. Tests were made with the small current probe on the ground grid, with the control grid only two inches above the ground grid. Thus, the ion uniformity exiting from the control grid could be readily mapped. Arrangements of up to nine wires were tested; however, a reasonable compromise was seven wires which were spaced on 2.5-inch centers across the width of the chamber and at a height of 2.5 inches above the corona grid.

The seven-wire arrangement noted above, with the temporary feed, produced a quite uniform ion distribution at locations away from the end walls, i.e., the feed locations. Therefore, experimentation was conducted to determine an acceptable feed arrangement which would allow the corona source to produce uniform ion densities out to the feed-end walls.

The feed design experiments used a single corona wire, which was mounted by various means in the corona chamber at a height of 2.5 inches. The current density was probed at locations, below the control grid, which were under the wire. The probe was moved at successive positions along the wire, starting at the feed-end wall. For these tests, no caging section was used. The control grid was lowered to a height of two inches above the ground grid, so that the current density uniformity as the ions exited through the control grid could be observed. For these tests, the control and ground grids were made larger, so that they extended a few inches beyond the chamber walls, to minimize edge-effect distortions. In this manner, the effect of the wire mounting arrangement on the current density near the wall could be observed.

Figure B-4 illustrates wire mounting arrangement in the corona chamber for the start of this test sequence. A sheet of Plexiglas was fastened to the end wall of the corona chamber to prevent the metallic components of the feed from

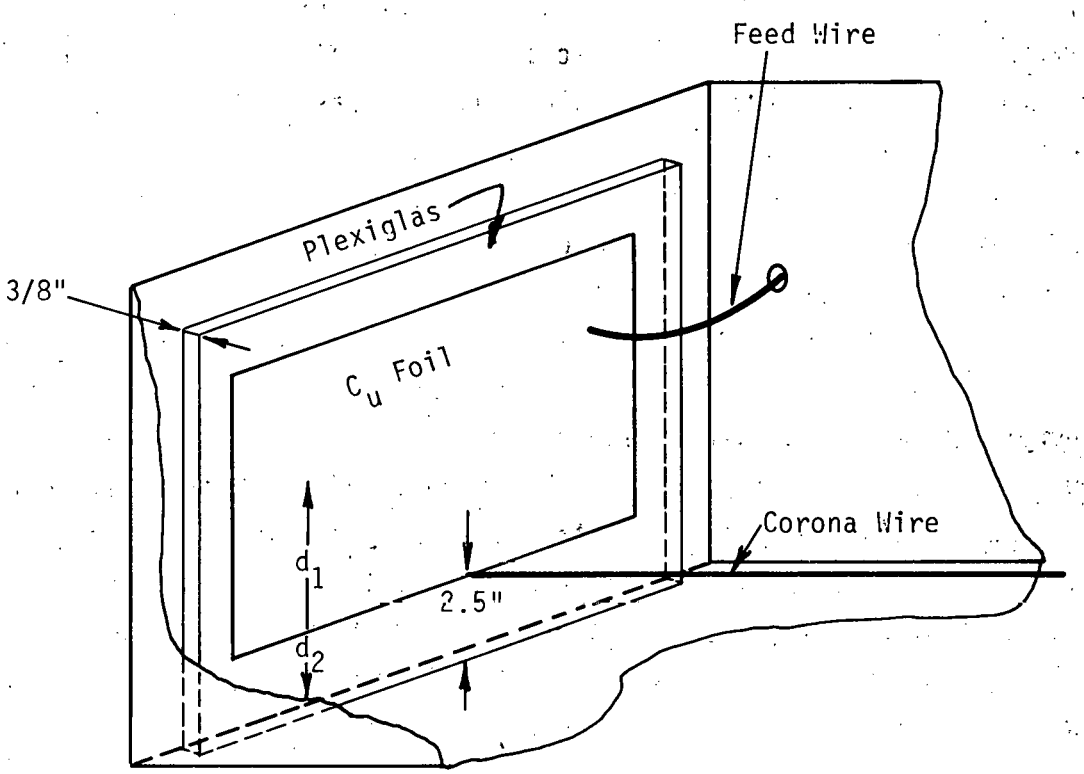

Dimensions		Current Density (nA/m^2) at Probe Center From End Wall (Inches)		
d_1	d_2	1	3	5
5"	2.5"	30 nA/m^2	170	190
3"	2.5"	30	170	190
1"	2.5"	80	170	190
1"	0.25"	140	180	195

Figure B-4 CURRENT DENSITY BELOW CONTROL GRID AS A FUNCTION OF POSITION ALONG WIRE FOR DIFFERENT FEED CONDITIONS

arcing or corona to the end wall. A sheet of copper foil was fastened to the plastic and the single corona wire was fastened near the bottom edge of the copper sheet. The data of Figure B-4 show how the current density below the control grid varied with position of the probe, as it was moved away from the wall, directly under the wire. The data are for different heights (d_1) of copper foil and for two values of d_2, the distance that the plastic extended below the corona wire, for a constant corona wire current. The uniformity became better as the height of the copper foil decreased and as the amount of plastic below the wire also decreased. From these data, it appeared that the size of the copper feed strip in the vicinity of the corona wire should be minimized, and that the plastic should not extend much below the corona wire.

Some type of feed strip was necessary to feed a common voltage to multiple wires. To minimize the influence of the fields from such a feed on the fields at the wires, the arrangement shown in Figure B-5 was made. For this arrangement, the feed strip is remote from the corona wire. The current density data shown in the figure was obtained in the same manner and with the same wire current as was used for the data of Figure B-4. It is seen that the arrangement shown provided a current density that did not vary with probe position away from the feed-end wall. The plastic between the end wall and the vertical wire run prevents this section of wire from producing corona, even though it is in close proximity to the end wall. Removal of the plastic caused excessive corona current to the end wall. Thus, from a current density uniformity standpoint, the feed arrangement shown appeared to be a significant improvement.

The feed arrangement shown was changed slightly to provide for more suitable fabrication. The glass rod was eliminated, and a small slotted plastic washer was glued to the plastic sheet at each wire position. A light spring was used to attach the vertical wire segment to the copper feed strip. The use of a spring in this location does not affect the operation, but ensures that the wires remain in tension. Figure B-6 is a photograph of the corona wire feed arrangement in one of the final prototype corona chambers which was built using this feed arrangement. Tables B-7 and B-8 compare current density measurements of the original three-wire arrangement (B-7) with the seven-wire configuration (B-8). For these measurements, no caging section was used, and the control grid, supporting the grid and corona sections, was lowered to

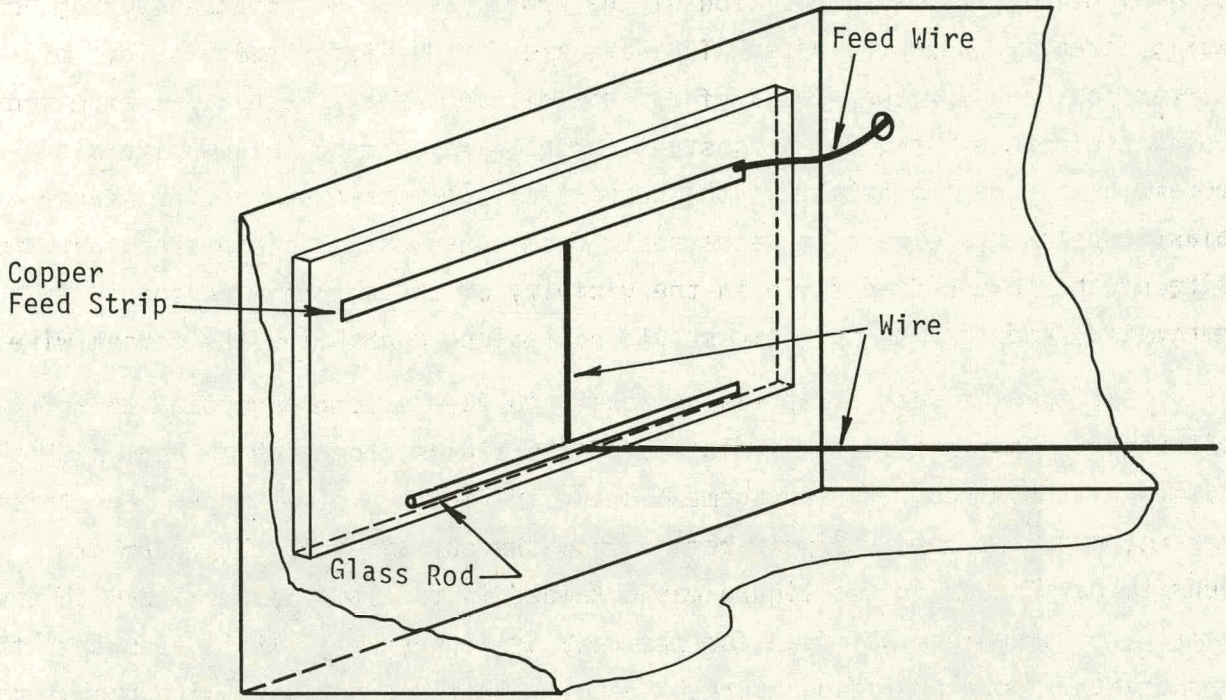

Current Density (nA/m^2) At
Probe Center From End Wall (Inches)

1	3	5
200	200	200

Figure B-5. CURRENT DENSITY BELOW CONTROL GRID
AS A FUNCTION OF POSITION ALONG WIRE

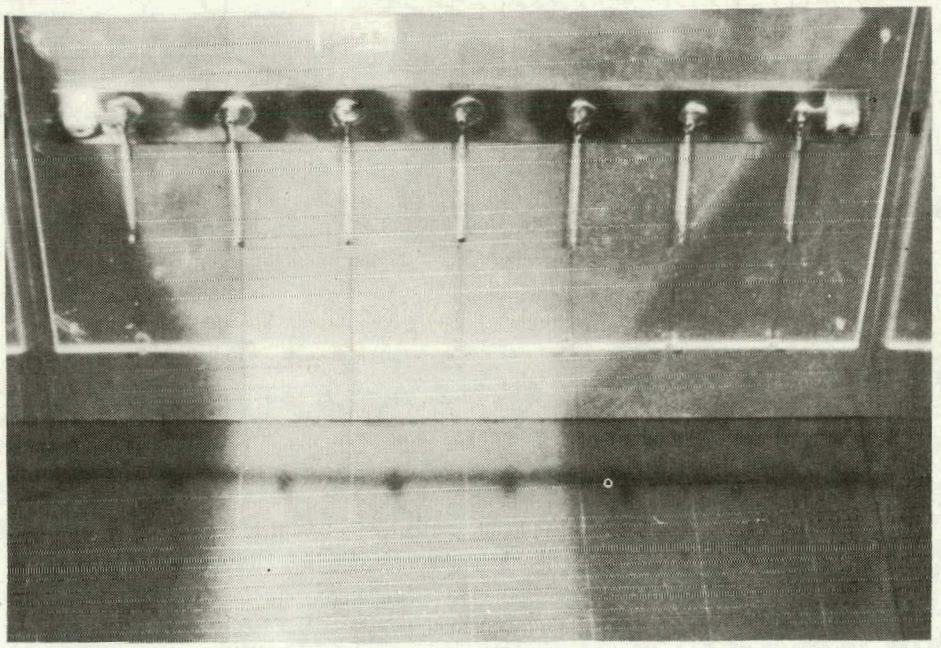

Figure B-6 VIEW OF INSIDE END WALL OF PROTOTYPE CORONA CHAMBER SHOWING METHOD OF MOUNTING AND FEEDING CORONA WIRES

Table B-7

CURRENT DENSITY AT DIFFERENT LOCATIONS FOR ORIGINAL SECOND PROTOTYPE CORONA WIRE CONFIGURATION
(Control Grid 2" Above Ground Grid)

(Test Locations Relative to Chamber Dimensions)

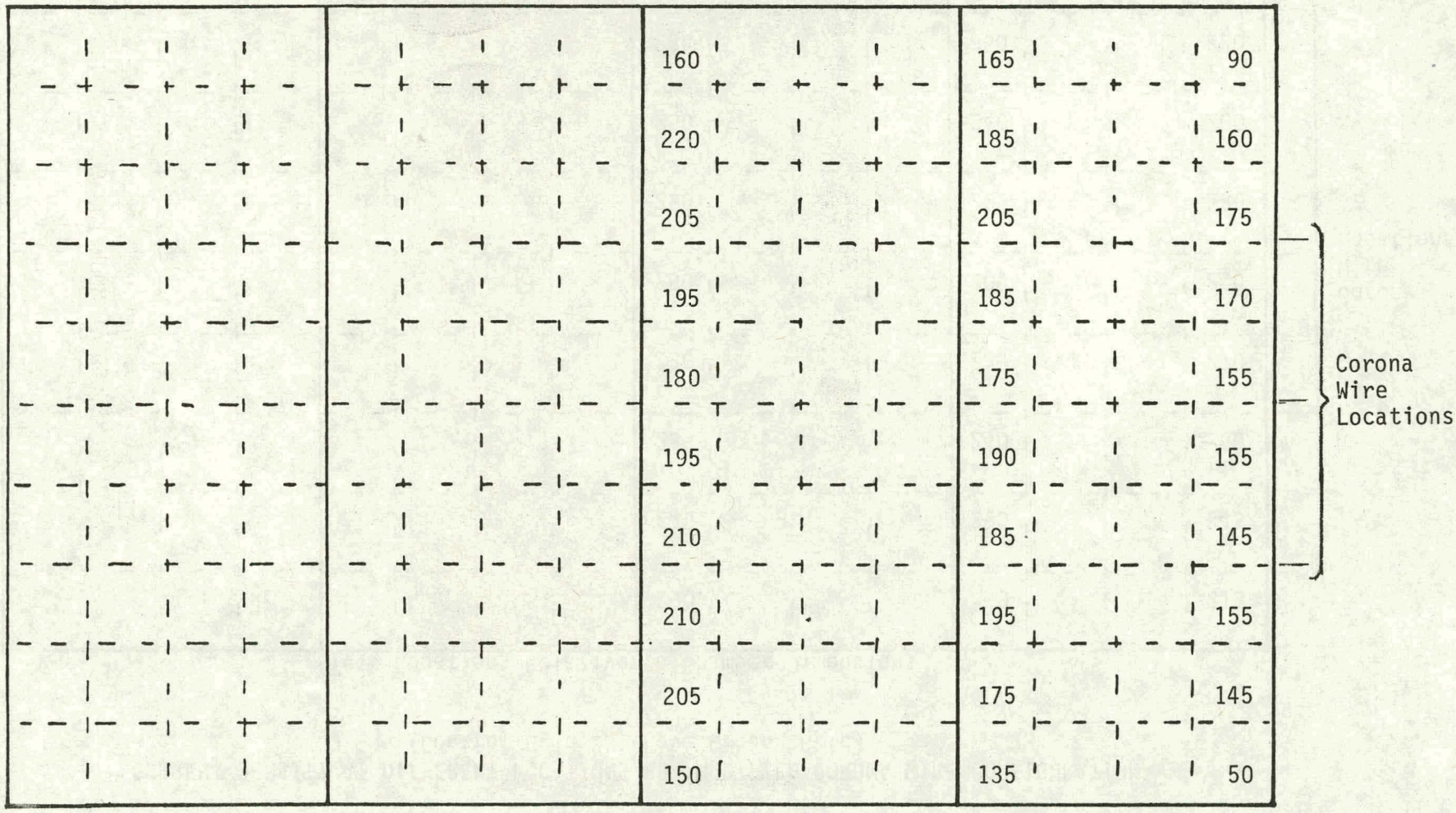

Table B-8

CURRENT DENSITY AT DIFFERENT LOCATIONS FOR MODIFIED CORONA WIRE CONFIGURATION
(Control Grid 2" Above Ground Grid)

(Test Locations Relative to Chamber Dimensions)

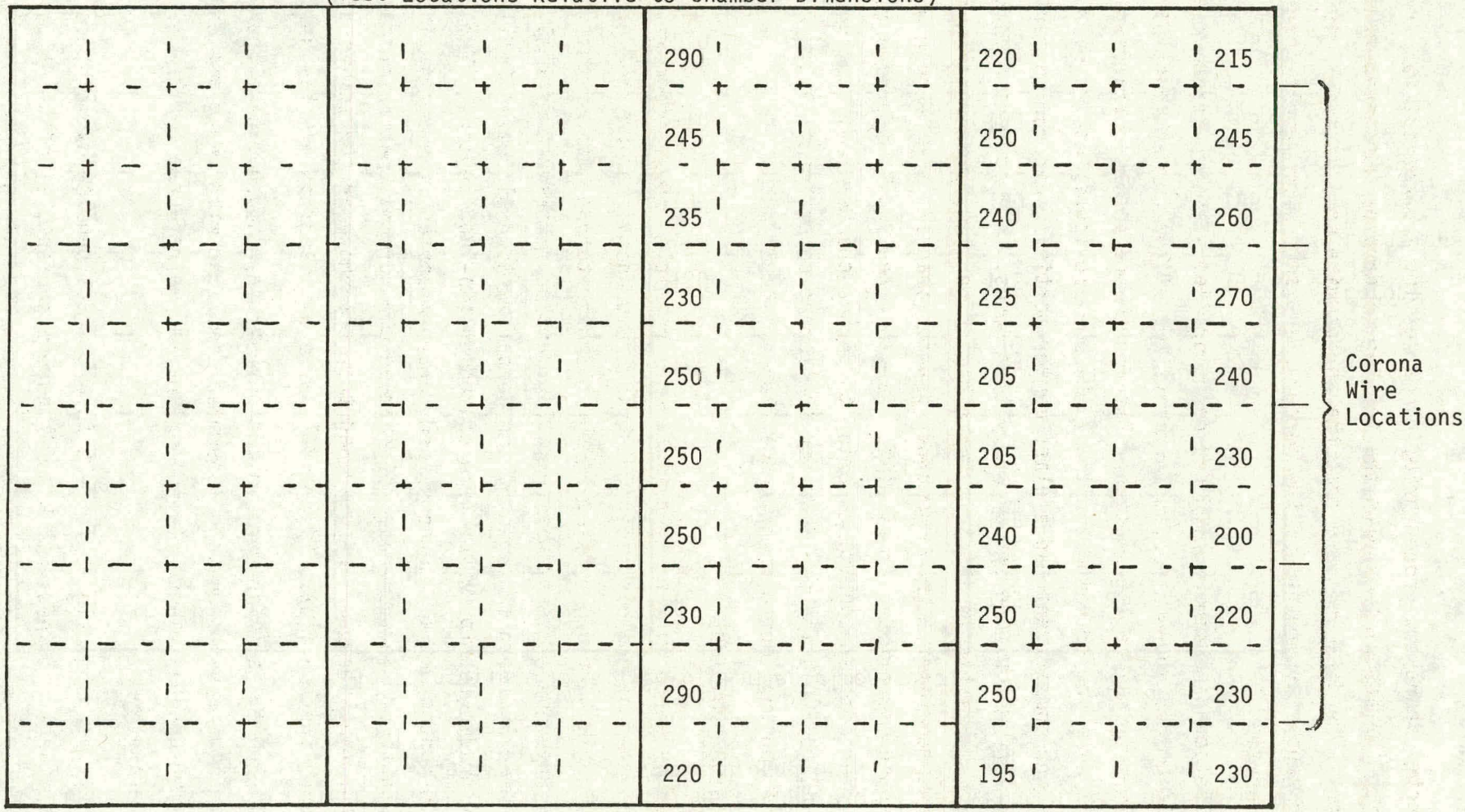

two inches above the ground grid. This testing arrangement was previously described in association with the testing to develop the seven-wire configuration. The data indicate that the corona wire modifications resulted in significant improvements at the corners, and some improvement for the side wall locations.

The corona chamber which had been modified with the seven-wire arrangement described above was used to retest two of the compartments of the second prototype animal caging section The fourth and second compartments were tested. The fourth compartment was the one previously coated with silicone. The second compartment had a glass center partition and had copper strip guard rings which were spaced every two inches. The current density map of these compartments is shown in Table B-9. The standard deviation of the fourth compartment data is somewhat greater than 17% of the mean while for the second compartment it was 14%. Previous tests of these same two compartments, for similar conditions prior to corona chamber modification, resulted in standard deviation of 16.5% for the second compartment (Table B-5b data) and 34% for the fourth compartment (Table B-6b data).

B.3 THIRD PROTOTYPE

In order to further investigate the possible improvements which might accrue from the use of grading strips, a new animal caging section was fabricated. This section, denoted as the third prototype, was of the same geometry as the previous glass prototype caging section. However, central glass partitions were included in three of the compartments. All walls had 1/4-inch wide copper grading strips which were spaced on two-inch centers. The copper strips were in contact at all corners, and were overcoated with a thin layer of epoxy. The purpose of the epoxy was to minimize the current that an animal might draw from the tape strips. Tests showed that the epoxy on the strips did not influence the ion flow. Figure B-7 shows a photograph of this unit.

The unit, as it appears in the photograph, does not have the doors in place. Figure B-8 shows the assembled simulator with the glass animal section with grading rings. As so configured, we referred to the unit as the third prototype.

The data shown in Table B-10 is a current density map of this prototype. The data were obtained with a total corona current, I_c of 50 μA, a grid voltage, V_g, of 160 volts, and a plate voltage, V_p, of 15 kV. When these data are

Table B-9

CURRENT DENSITY MAP OF TWO COMPARTMENTS OF SECOND PROTOTYPE WITH MODIFIED CORONA CHAMBER

4	3	2	1
150 185 175 150		185 185 180 180	
240 250 220 195		140 260 250 185	
270 265 250 230		200 250 250 220	
300 260 260 215		225 225 240 215	
300 275 265 225		230 240 235 180	
300 280 275 215		230 220 230 210	
290 270 300 275		200 230 230 235	
310 260 300 185		150 230 235 200	
275 260 290 220		195 230 235 180	
215 240 235 190		140 205 210 190	

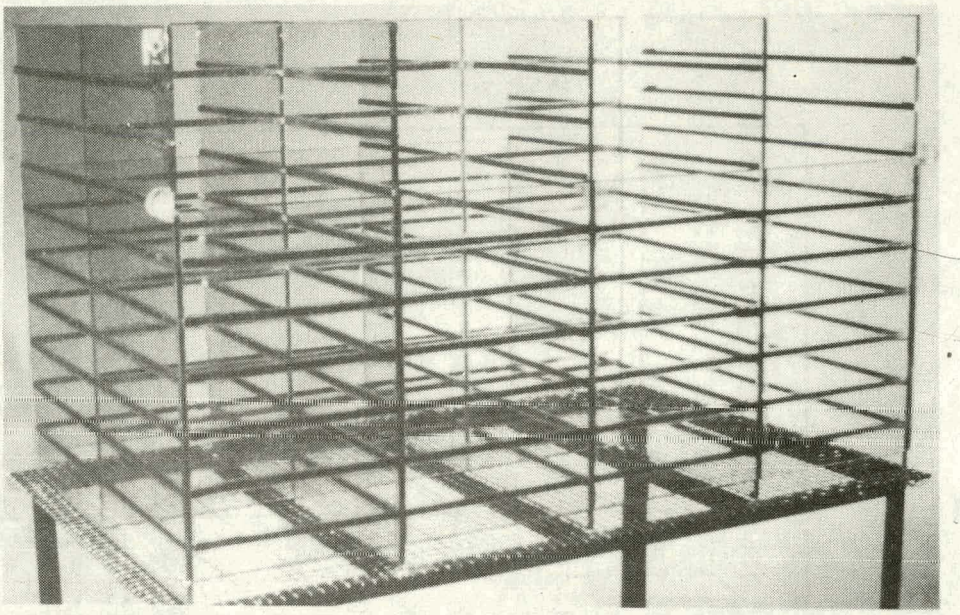

Figure B-7 PROTOTYPE CAGING SECTION WITH COPPER STRIP GRADING RINGS

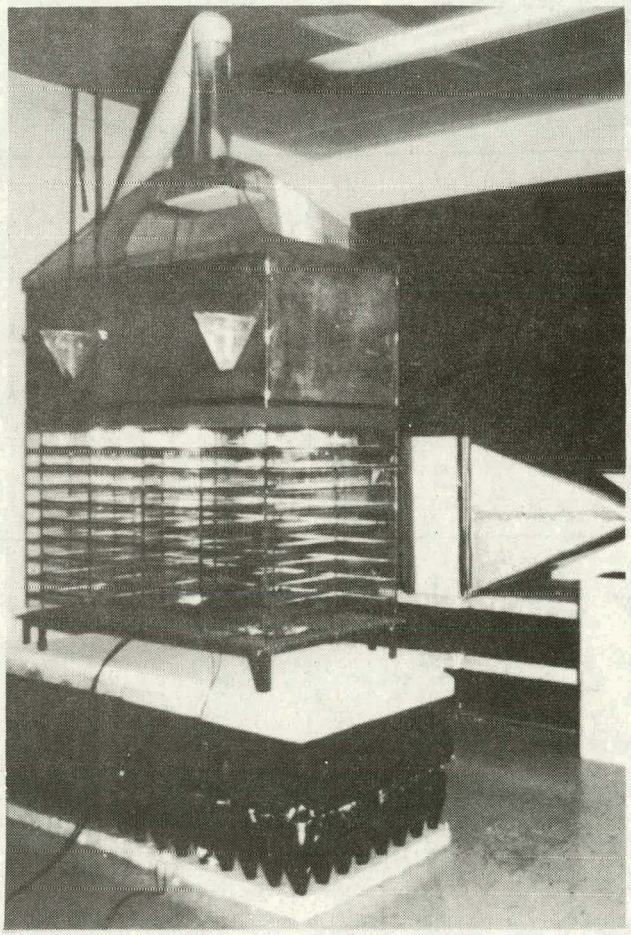

Figure B-8 THIRD PROTOTYPE SIMULATOR

Table B-10

CURRENT DENSITY MAP OF THIRD PROTOTYPE SIMULATOR

4	3	2	1
120 175 170 175	180 185 175 165	215 175 155 125	135 165 170 155
195 220 220 225	215 225 225 220	230 215 210 175	180 220 210 200
200 240 240 235	215 230 225 220	215 235 240 200	220 240 220 215
200 210 230 230	225 230 230 225	200 240 235 220	225 240 220 205
200 200 220 235	240 220 225 215	170 245 225 200	215 250 215 190
175 200 225 210	220 225 230 215	200 240 230 215	220 235 205 185
190 220 235 220	230 230 230 200	210 230 245 240	220 230 215 190
190 205 220 210	225 225 225 210	205 225 235 230	225 225 200 185
170 210 220 220	215 220 225 215	205 215 225 225	205 210 200 165
130 175 175 190	175 170 175 165	165 155 170 135	140 160 165 110
8	7	6	5

compared to that obtained with the second prototype (Table B-2), a significant improvement is seen. However, the data of Table B-2, for the second prototype, was for the condition of cleaned glass but without the application of a silicone coating. In an effort to ascertain the effects of silicone coating and compare with the use of grading rings, the second prototype was completely treated with silicone and retested. The current density map of the second prototype for this condition is shown in Table B-11.

Table B-12 compares summarized data for the graded third prototype with the silicone-treated first prototype animal caging section. The data show the mean and standard deviation in percent from the mean for each 8 x 10-inch compartment area in the two units. The third prototype had three of the four major compartments divided into two with partitions, while the second prototype had just the four major compartments without any dividers. Comparison of these data shows that the current density was somewhat more uniform in the silicone treated second prototype than for the graded third prototype. However, since the second prototype did not have as many walls, a one-to-one comparison may not be justified.

Review of the detailed current density maps of Tables B-10 and B-11 for the two prototypes, shows that the current density values were low along the feeder walls. As previously noted, the feeder side walls did not extend clear down to the ground grid. There was an opening of about 3/4 inch for the feeder trough to fit into. The bottom of the feeder wall (i.e., the top of the feeder slot) was metalized, and this metalized strip was at ground potential. Thus, both the feeder trough and the bottom of the glass wall would be at the same potential, namely, ground.

The raising of ground, by this 3/4 inch at the feeder walls, was questioned relative to the effect on the nearby current density, as sensed by the probe. An experiment was conducted using the third (graded) prototype to assess this effect. For the experiment, the metalized strip at the bottom of the feeder wall was removed from ground, and raised (with a power supply) to the potential which it should be if the wall were an ideal voltage divider. For a voltage of 15 kV across the total wall, it was calculated that the potential at the height of the feeder strip should be about 670 volts.

Table B-11

CURRENT DENSITY MAP OF SECOND PRCTOTYPE CAGING SECTION AFTER COMPLETE SILICONE TREATMENT

(Values in nA/m^2)

110 160 150 165	170 175 175 170	160 150 150 150	140 120 125 140
155 185 175 190	190 180 175 195	180 175 170 175	175 165 160 150
130 185 175 185	200 185 175 180	175 185 175 190	180 175 155 145
135 185 190 200	200 190 180 195	180 185 185 185	185 175 175 150
160 185 190 195	200 185 185 195	205 185 195 190	195 180 175 185
180 180 175 185	190 185 185 195	185 175 185 195	175 185 170 165
130 175 185 185	185 180 175 185	175 175 180 185	185 180 170 140
125 175 175 185	180 175 175 175	175 175 170 185	185 175 170 145
110 165 175 185	185 180 185 185	190 180 170 175	170 175 180 120
115 140 150 155	160 150 140 165	160 150 140 140	140 150 155 120

Table B-12

COMPARISON OF SUMMARIZED CURRENT DENSITY DATA
FOR THIRD AND SILICONE TREATED SECOND PROTOTYPES

Third Prototype

$\bar{j}$ = 164 nA/m^2 σ = 14.3%	$\bar{j}$ = 173 σ - 9.7%	$\bar{j}$ = 177 nA/m^2 σ = 15.5%	$\bar{j}$ = 162 nA/m^2 σ = 14.7%
$\bar{j}$ = 199 σ = 12.7%	$\bar{j}$ = 211 nA/m^2 σ = 10.4%	$\bar{j}$ = 210 nA/m^2 σ = 14.7%	$\bar{j}$ = 195 nA/m^2 σ - 17%

Coated Second Prototype

$\bar{j}$ = 164 nA/m^2 σ = 11%	$\bar{j}$ = 173 σ = 9%	$\bar{j}$ = 177 nA/m^2 σ = 8%	$\bar{j}$ = 162 nA/m^2 σ = 16%
$\bar{j}$ = 162 nA/m^2 σ = 13%	$\bar{j}$ = 177 nA/m^2 σ = 9%	$\bar{j}$ = 185 nA/m^2 σ = 5%	$\bar{j}$ = 170 nA/m^2 σ = 14%

With the feeder strip raised to the above potential, a current density map of the compartment which was denoted as #6 in the map of Table B-10 was made. This data is shown in Table B-13. For these data, the mean of the four data points along the feeder wall is 88% of the mean of the other data points in the compartment. For the original data on this compartment with the feeder wall grounded (from Table B-10), the mean of the four data points along the feeder wall was 77% of the mean of the other data points in the compartment. Thus, it appeared that the grounding of the feeder strip might be contributing to the nonuniformity in current density.

It was not desired to have the metalized strip at the bottom of the feeder-side wall at a potential, unless the effective voltage source impedance were very high, such that the current which could be drawn by a contacting animal would be minimal.

Various methods for forcing the feeder strip potential were considered, One of the alternatives considered was the redesign of the feeder so that the wall could extend down to the ground plane. However, before embarking on such a redesign, it was desired to perform a preliminary assessment of the potential benefits of such a change. The second prototype animal section was used to test this arrangement. To simulate the absence of a feeder slot, the second prototype animal caging section was turned upside down so that the doors were on the bottom and the feeder slots were at the top. The feeder slots were temporarily bridged with strips of glass.

With the simulator turned upside down, all of the walls were of equal height, with no discontinuities at the bottom periphery of the structure. Table B-14 presents the data from a current density map of the unit for this condition. Table B-15 presents a summary of this data, which shows the mean current density and the percentage standard deviation from the mean for each 8 x 10-inch compartment-sized area of the simulator. For convenience in moving the current probe from location to location, the glass animal section was raised about 1/4 inch off of the ground grid by use of small metallic shims.

Comparison of the data of Table B-14 for the upside-down second prototype with the prior data for this same unit right side up, which was presented in Table B-11 and summarized in Table B-12 shows that a substantial improvement

Table B-13

CURRENT DENSITY MAP OF COMPARTMENT #6 OF THIRD PROTOTYPE WITH FEEDER STRIP AT 670 V

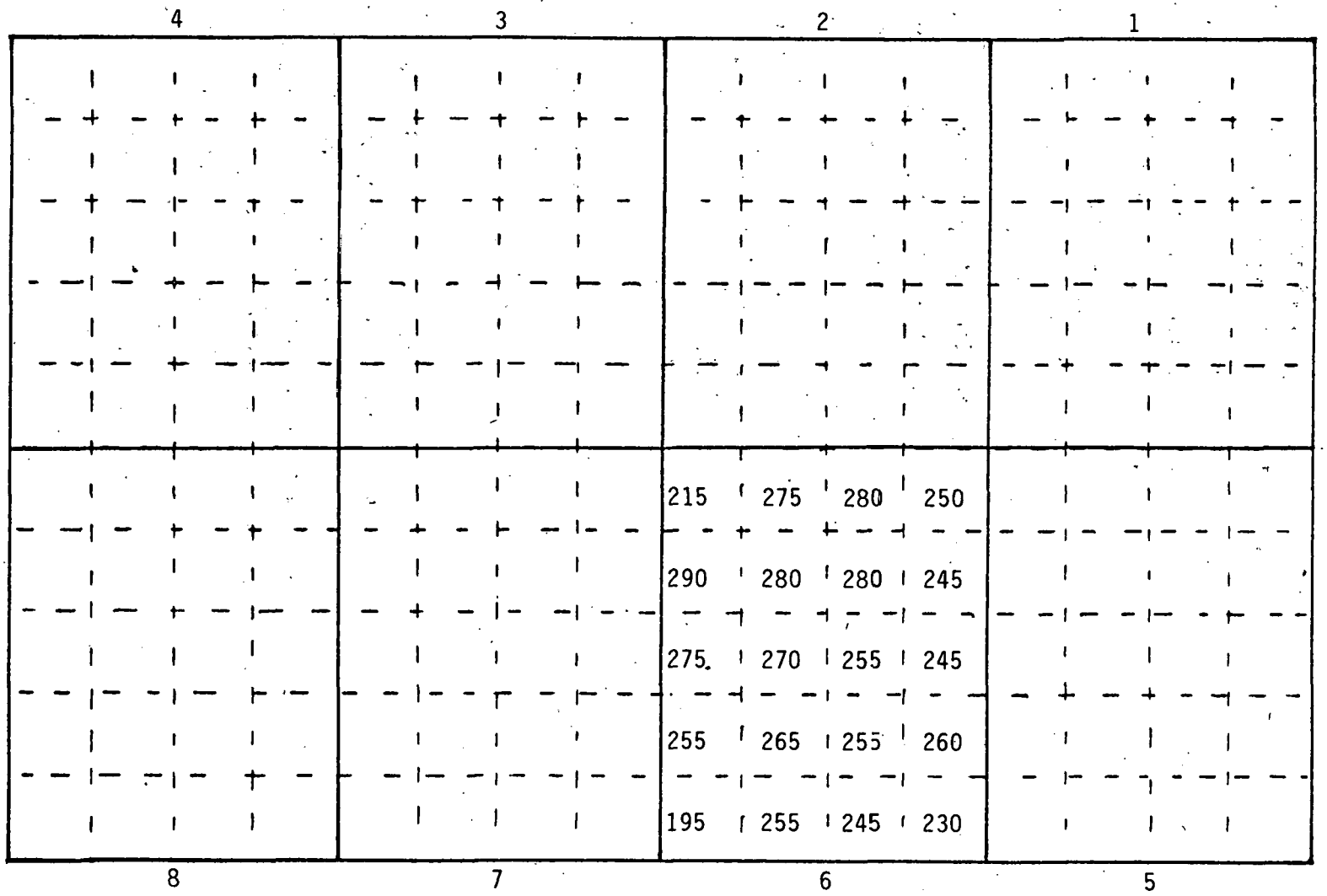

Table B-14

CURRENT DENSITY MAP OF SECOND PROTOTYPE CAGING SECTION TURNED UPSIDE DOWN - NO FEEDER SLOT

(Values in nA/m^2

170 180 190 185	180 185 200 190	185 185 180 175	175 175 175 160
175 185 195 185	180 200 200 195	190 195 185 180	175 180 185 165
170 185 190 185	175 190 185 180	170 180 185 180	165 175 175 165
170 185 190 180	185 195 195 180	185 195 200 180	170 185 175 160
185 185 200 200	200 200 200 190	190 195 190 185	175 170 170 170
185 195 200 200	200 205 215 210	195 205 210 195	180 190 190 175
180 185 185 195	200 205 205 200	190 195 195 180	180 185 175 170
180 195 185 180	195 195 195 185	180 195 195 180	175 185 175 165
170 185 190 180	185 195 190 185	185 195 185 180	175 175 180 170
175 195 205 185	180 185 200 185	190 200 190 180	160 160 165 170

Table B-15

SUMMARY OF TABLE B-14 DATA

$\bar{j}$ = 185 nA/m^2 σ = 4.7%	$\bar{j}$ = 190 nA/m^2 σ = 4.5%	$\bar{j}$ = 185 nA/m^2 σ = 4%	$\bar{j}$ = 172 nA/m^2 σ = 4%
$\bar{j}$ = 188 nA/m^2 σ = 4.9%	$\bar{j}$ = 196 nA/m^2 σ = 4.9%	$\bar{j}$ = 196 nA/m^1 σ = 4.9%	$\bar{j}$ = 175 nA/m^2 σ = 5%

was effected by eliminating the feeder slot discontinuity. For the new arrangement, the compartment-area percentage standard deviation were all 5% or less, compared with up to 16% for this same unit with the feeder slot down.

On the basis of these test results, it was decided to redesign the feeder so that the food pellets would pass under the side walls with the walls extending down to the ground grid level. Figure B-9 shows a sketch of the feeder arrangement with the bottom of the wall at ground grid level.

B.4 FOURTH PROTOTYPE

The test results presented above showed that the use of guard strips on the animal section were not necessary. It appeared that acceptable performance could be obtained with a glass animal caging section which was treated with a dimethylsiloxane hydrophobic compound and did not have discontinuities for the feeders. Therefore, a new base section, incorporating the new feeder design, and a new animal caging section were fabricated. The use of these components along with the remainder of the simulator is termed the fourth prototype.

Figure B-10 shows a photograph of the base unit with feeder chutes and watering units installed, and Figure B-11 shows a photograph of the fully assembled fourth prototype simulator. The animal section is divided into eight compartments and has hinged doors for animal access. All surfaces of the glass caging section have been treated with the silicone hydrophobic compound.

Table B-16 presents a current density map of the fourth prototype simulator. A summary of this data in terms of the means of the compartment current densities and the standard deviations as a percentage of the compartment means is shown in Table B-17.

These data were taken with the completely assembled prototype simulator. The feeder troughs and watering units were in place; the animal caging unit was setting flush on the ground grid; the air plenum was installed and supplied with approximately 35 cfm of air through a HEPA filter. The total corona current for this test was 50 μA and the control grid to ground potential, V_p, was 16 kV, thus producing a nominal electric field of 32 kV/m. It is felt that the data of Tables B-16 and B-17 show that this prototype provides a very acceptable current density uniformity over the entire exposure area of the simulator.

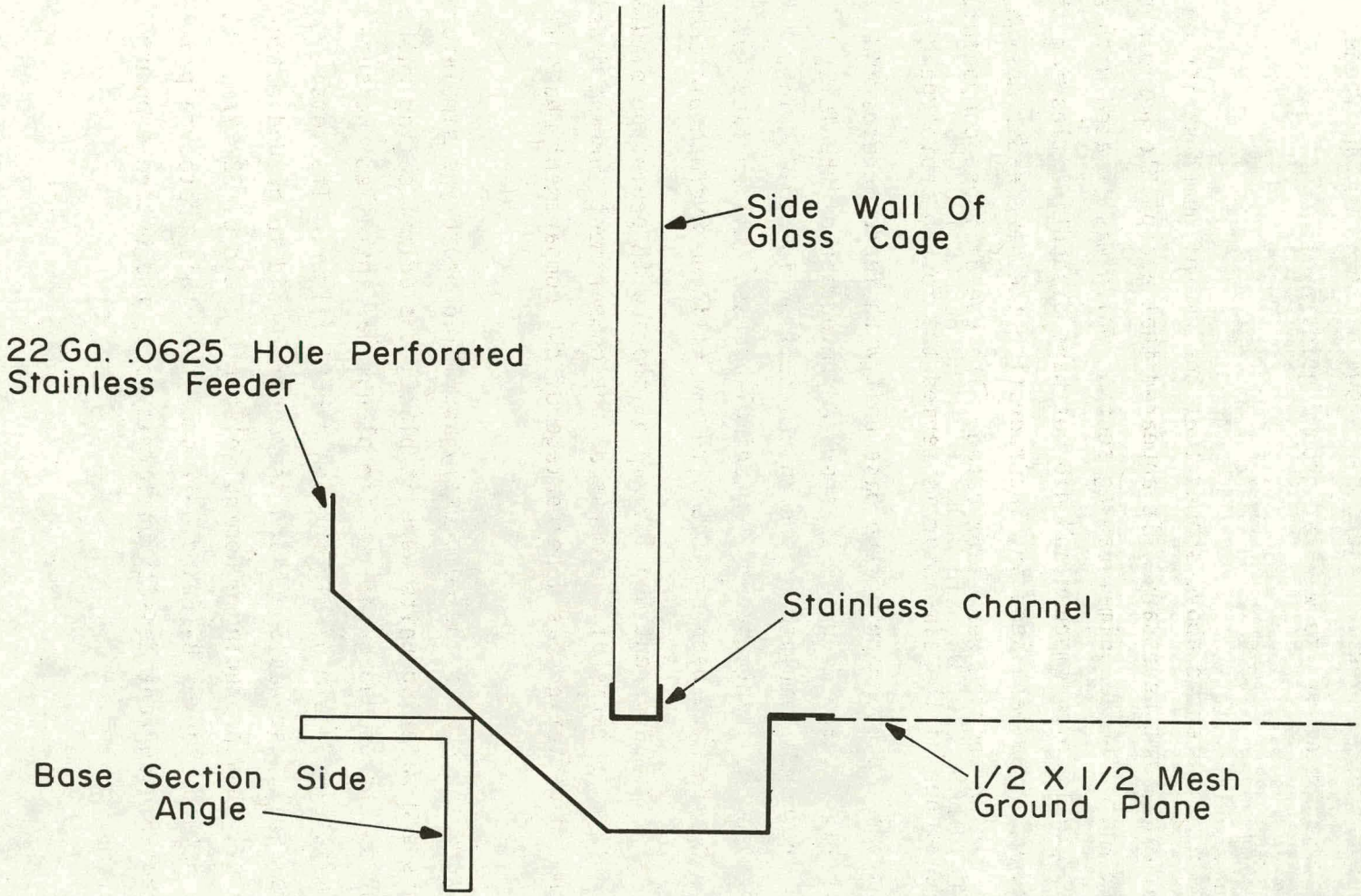

Figure B-9 UNDER THE WALL FEEDER CHUTE SKETCH

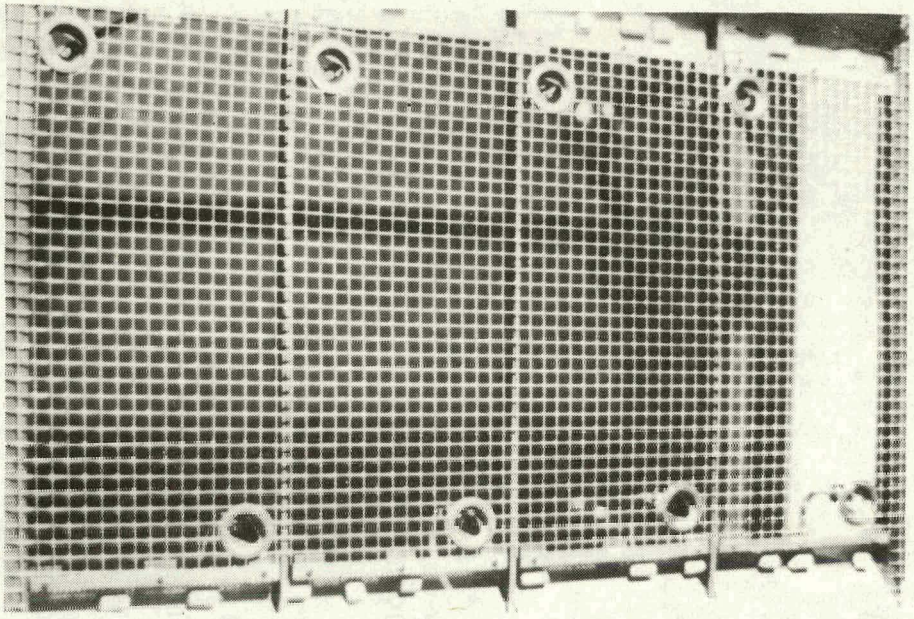

Figure B-10 BASE SECTION WITH UNDER-THE-WALL FEEDER TROUGHS

Figure B-11 FULLY ASSEMBLED FOURTH PROTOTYPE SIMULATOR

Table B-16

CURRENT DENSITY MAP OF FOURTH PROTOTYPE SIMULATOR

(values in nA/m^2)

220 230 225 215	230 220 230 230	220 225 225 235	225 220 225 215
235 235 240 225	235 230 235 245	235 235 235 235	240 245 230 230
230 235 230 230	230 230 235 235	230 225 235 235	230 235 220 230
225 230 235 230	225 225 220 235	220 230 230 225	225 225 200 225
210 225 235 225	215 210 220 225	225 220 220 225	220 215 195 210
185 190 195 220	200 220 220 225	230 220 220 220	225 220 215 210
195 195 205 210	210 205 235 230	220 215 225 225	225 225 225 230
195 195 210 210	215 210 230 225	225 220 230 225	235 235 225 230
215 215 225 210	230 225 235 235	245 235 225 235	240 240 230 235
185 200 205 215	210 220 225 225	235 235 230 230	225 225 215 210

Table B-17

SUMMARY CURRENT DENSITY DATA FOR FOURTH PROTOTYPE SIMULATOR

$\bar{j}$ = 220 nA/m^2 σ = 3.3%	$\bar{j}$ = 228 nA/m^2 σ = 3.6%	$\bar{j}$ = 228 nA/m^2 σ = 2.6%	j = 223 nA/m^2 σ = 5.4%
$\bar{j}$ = 204 nA/m^2 σ = 5.7%	$\bar{j}$ = 222 nA/m^2 σ = 4.6%	$\bar{j}$ = 227 nA/m^2 σ = 3.2%	$\bar{j}$ = 226 nA/m^2 σ = 3.9%

Figure B-12 shows a pen recorder trace of the output voltage from a Keithly picoammeter sensing the output from the 10 cm^2 current probe which was on the ground grid in one of the compartments. The trace shown is just a segment of a longer trace made for an overnight test of the simulator. The vertical scale of the trace is labeled in terms of current density in nA/m^2, and the chart speed was 10 min/cm. This data was obtained with air supplied to the simulator, and shows the stability of the ion current density with time.

Figure B-13 compares the audible noise spectrum in the simulator with and without 50 μA of corona current supplied to the corona wires. Air was being supplied to the chamber for both of the recorded noise spectra. To obtain these measurements, a B&K 4136 1/4-inch condenser microphone was inserted into the chamber through the ground grid. The microphone was pointed upward and the tip of the microphone was approximately two inches above the ground grid. The microphone output was fed through a B&K 2209 sound level meter to a Spectral Dynamics Model 310C Real Time Analyzer and a Model 3026 Ensemble Averager. The processing bandwidth was 150 Hz. As can be seen from the two spectra of Figure B-12, noise which is attributable to the corona could be measured. This audible noise level is virtually imperceptible. However, since it will be present for test simulators, it should also be produced in the simulators which are used to house sham-exposed subjects. Since the simulator design enables the various desired exposure environments to be established with a fixed value of corona current (in the range of 50 μA), the audible noise spectrum should be a constant for different exposure environment levels.

The fourth prototype simulator has been tested to quantify the ozone levels in the animal section. The test was made using a Dasibi Model 1003AH Ozone Monitor, which operates on the principle of ultraviolet light absorption by ozone. The unit has a range of 0.000 to 1.000 PPM, with a quoted accuracy of 3%. The functioning of the monitor was checked with a Dasibi 1501 UV ozone source prior to the testing. The air in the simulator was sampled through a 4-foot length of teflon tubing, which was inserted through the ground grid. The inlet to the sampling tube was approximately one inch above the ground grid, and the tube was parallel to the simulator air flow direction.

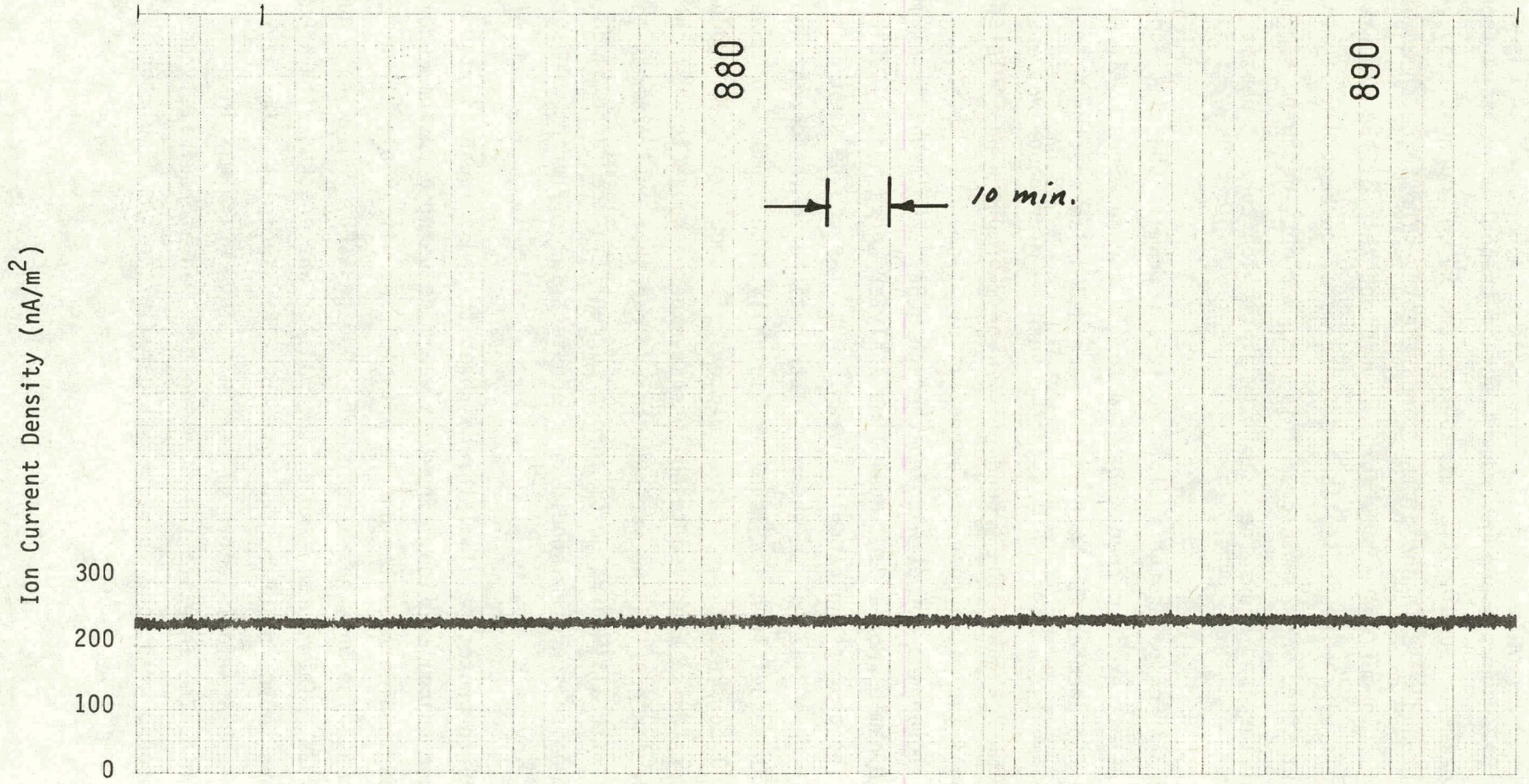

Figure B-12 ION CURRENT DENSITY VS. TIME FOR FOURTH PROTOTYPE SIMULATOR

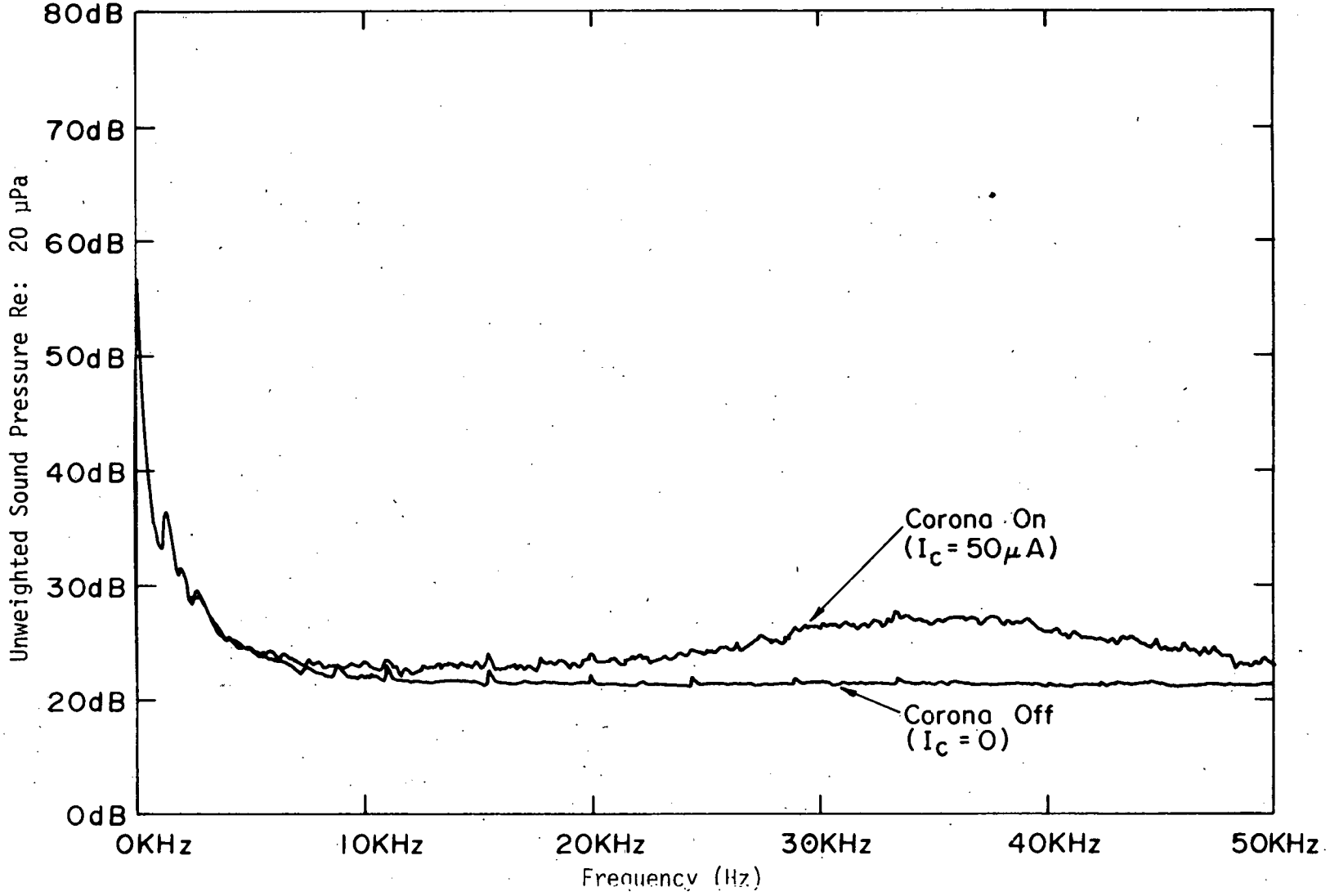

Figure B-13 ACOUSTIC SPECTRUM WITH AND WITHOUT CORONA

For this ozone test, the corona current, I_c, was 50 μA; the nominal electric field was 32 kV/m and the ion current density was adjusted to be 300 nA/m^2. The simulator was supplied with HEPA filtered air flow at approximately 35 cfm. The ozone monitor was fed to a chart recorded which was calibrated for a display sensitivity of 10 ppb per cm. The monitor and simulator were operated for a period of approximately 100 minutes. During this period, no detectable ozone level was observed. After this run, the sampling tube was removed from the simulator interior and was situated to sample the air outside but near the simulator, with the simulator operating parameters as noted above. A twenty-minute sampling for this condition also indicated no detectable ozone. The incidence of nonmeasurable ozone indoors in Chicago during the winter time is not unusual, and provides an ideal situation, since it is not necessary to subtract the ambient from the desired measurement.

An electric field map has been made in one of the compartments of the fourth prototype. The map was made for the same simulator operating parameters that was used for the current density map of Table B-16. For these measurements, the Monroe 225 field probe was set on top of the ground grid and moved to 20 different locations within the 8 x 10-inch compartment, in an analogous manner to a current density map. The standard deviation of the 20 measurements was 4.5% of the mean. The minimum field sensed was 8% below the mean, while the maximum field was 9% above the mean. These measurements are quite cumbersome to make within the assembled simulator. The deviations noted are probably worse case, and contributed to by the difficulty in ensuring that the probe face is normal to the vertical. It has been noted that when the electric field probe is on top of the ground plane, several percent change in reading results from the probe face being a few degrees off the horizontal.

The information that has been presented in this appendix provides a rather detailed overview of the developmental steps leading to the final, or fourth, prototype HVDC bioeffects simulator. Significant performance improvements have accrued in progressing from the second to the fourth prototype. The test results which have been presented in the foregoing paragraphs are felt to adequately demonstrate the suitability of this simulator design for use in biological testing of small animals to HVDC environments.

APPENDIX C

ANIMAL PREFERENCE TEST

APPENDIX C

ANIMAL PREFERENCE TEST

An animal preference test was conducted to determine if test animals would exhibit a preference when given the choice between a space in which a field and ion environment was established, or a space in which negligible fields and ion levels were present. A special simulator was fabricated for use in these tests. This simulator was comprised of two modules, each of which was similar in design to the prototype simulator unit.

This appendix provides a description of the enclosure designed for the preference tests. Also described are the electrical characterizations which were made on the simulator prior to animal testing; the physical arrangement for the test; and the procedures followed during the animal test sequence. A summary of physical data taken during the preference tests is presented. Information is also presented on the animals used and their care during the test sequence. Also presented in this Appendix is an analysis of the data taken on animal location within the simulator during the preference tests. The animal location data were photographically recorded and analyzed after the test.

1. TEST ENCLOSURES FOR ANIMAL PREFERENCE TEST

1.1 General Description of Simulators

The animal preference tests employed two HVDC environment simulators, which were mounted onto a common base unit. The two simulators were of the same basic design as the final prototype simulator which has been described in the main text of this report, although these simulators differed from the prototype in some details.

Figure C-1 shows a plan view and front view sketch of the preference test simulator arrangement. The two simulators, designated as A and B, were physically the same, and were comprised of an animal caging section, a grid section, a corona section and a plenum section. These simulators were the same as the prototype simulator previously described, with the exception of the animal caging section and the base section. As seen in the sketch of Figure C-1, the two simulators were separated by a passage, or tunnel through which the animals could move from one simulator to the other. The separation distance between simulators was twelve inches, which was chosen to prevent corona on the exterior of the simulators, due to their difference in potential, and close proximity to each other.

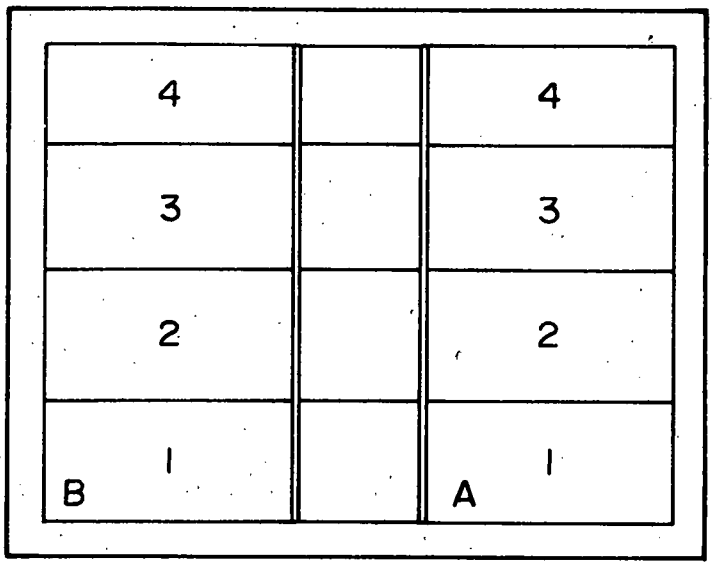

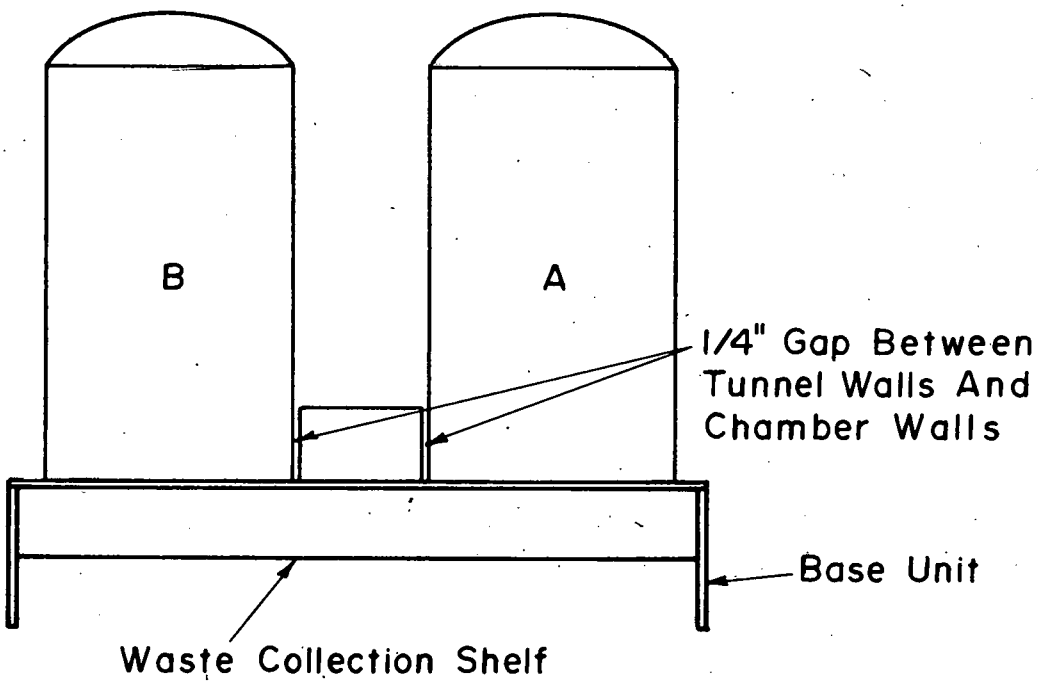

Fig. C-1 PLAN AND FRONT VIEW SKETCH OF PREFERENCE SIMULATOR

The base unit of the preference test simulator supported both individual simulators. The base unit was fabricated from angle iron. Bar stock supports which ran the width of the base unit were placed at the location of the animal enclosure walls and provided support for the simulator units. The top surface of the base unit was covered with 1/2" x 1/2" hardware cloth. This hardware cloth mesh top served as the ground grid and floor of the simulators. This mesh provided a grid for the animals to stand on; provided for the free exit of the simulator air flow; and allowed the animal waste to fall through to the waste collection shelf below. There were no feeding or watering provisions in the preference test base unit, since each animal test was for only 45 minutes.

The animal caging sections of the preference test simulator were made of glass, as for the prototype simulator. However, the preference test animal section was divided into only four compartments, as shown in Figure C-1. The overall dimensions of the preference animal caging sections were the same as the prototype; therefore, each animal compartment was 8" x 20". For the animal tests, one compartment in each simulator was reserved for field and ion current density measurements; thus, three compartments were available for animals.

The preference simulator animal caging sections were fabricated with one, rather than two, animal access door. The door was the top six inches of the long outside wall of each simulator. The animals had access from one simulator chamber to the other through a tunnel between the two simulators. The long inside wall of each animal chamber, which faced the opposite simulator, extended down to two inches from the ground plane, thus leaving a two-inch opening through which the animals could pass from the chamber into the tunnel which separated the two chambers.

Two different tunnel configurations were used to separate the two simulator units. The first sixteen preference trials employed a tunnel which had a two-inch height. This tunnel was divided into four sections by walls which were coplanar with the simulator chamber interior walls. Thus, the animals in a given compartment in chamber A were constrained to having access to the same compartment in chamber B. The tunnel did not contact the walls of the two simulator chambers. The tunnel walls were separated from the chamber walls by a gap of approximately 1/4" as is shown in Figure C-1. The tunnel walls were made of glass, as were the chamber walls. However, a removable plastic lid was placed on top of the tunnel. This top could be removed for placing the animals

into the tunnel at the start of each test. Several plastic pegs were glued to the tunnel top. These pegs protruded into the tunnel for the purpose of discouraging the animals from lying in the tunnel.

During the first sixteen preference trials, it was observed that the animals tended to spend a significant portion of time in the tunnel rather than in either one of the two chambers. It was felt that the low height of the tunnel was an inducement for the animals to prefer the tunnel over either chamber. Therefore, for the second sixteen preference trials, a new tunnel, or center section, was fabricated. This second tunnel section was made of plastic, had 12-inch high walls, and did not have a top. Figure C-2 is a photograph showing an overall view of the simulator with the second tunnel. The movie camera used to record animal location in the simulator is seen in the foreground. Figure C-3 is a closer view showing the second connecting tunnel structure.

As noted above, one wall of each simulator did not extend down to the ground plane, but was cut short by two inches to provide access from one simulator chamber to the other by the animals. Discussion of the field and ion uniformity problem with the prototype simulator, which has been presented in Appendix B of this report, has provided evidence that uniformity problems were introduced due to feeder slots in the bottom of the prototype simulator chamber walls. It was anticipated that some field and ion uniformity problems would also be encountered with the preference test chambers, due to the cutting short of the chamber walls to provide animal access from one chamber to another. Testing of the preference test simulators showed that the animal access slots did introduce field and ion current density nonuniformity. Various alternate treatments of these slots were investigated. It was found that the nonuniformity was minimized when a conductive adhesive backed copper tape strip was placed along the bottom of this short access wall, and grounded to the ground grid. Therefore, the preference tests were conducted with the top of the animal access slots in the chamber walls grounded. As will be shown later, this arrangement resulted in somewhat lower fields and ion current density within an excited preference simulator, for positions very near the access wall.

1.2 Simulator Biasing and Control

The simulators for the preference test were biased for field and ion control in a different manner than typically was employed during the prototype

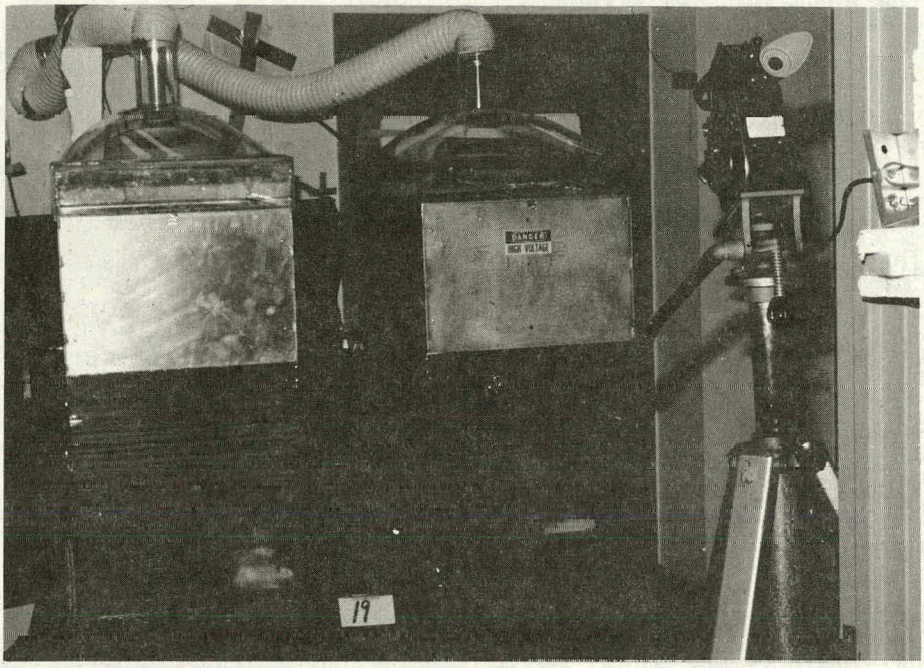

Figure C-2 PHOTOGRAPH OF PREFERENCE TEST SIMULATOR

Figure C-3 PHOTOGRAPH OF TUNNEL AREA

simulator development. A single power supply was used to create the desired HVDC environment conditions within a given preference test simulator. The preference testing employed three levels of simulated environment. In addition, a control condition, for which negligible field and ions were present in the animal caging section, was used. The power supply biasing arrangement differed, depending on whether a simulator was in the "control" condition, or whether an intended field or ion environment was produced.

Figure C-4 shows schematically the single power supply bias arrangement for producing a HVDC test environment in a simulator. The output from the high voltage supply is connected to the corona wire feed. When the supply is at voltage, corona current flows from the corona wires due to the potential developed between the wires and the corona grid and corona chamber walls. The majority of this corona current flows through the control grid bias resistor, R_g, and the field bias resistor, R_f, due to ions being collected by the grid and chamber walls. A small percentage of the ion current flows through the space between the corona and control grids, and into the animal housing section between the control and ground grids. Once the free ions enter the animal housing section, they move under the influence of the exposure field and terminate on the ground grid.

The electric field in the animal exposure chamber is caused by the corona current flowing through the field bias resistor, R_f. The current flow through R_f causes a potential between the control grid and the ground grid. The current through the field bias resistor is determined by measuring the voltage, V_f, across a 100-kΩ resistor that is in series with the field resistance, R_f. The value of R_f is selected to produce the desired field in the animal exposure chamber, for the desired corona current. As in the prototype simulator, typically a total corona current of 50 μA was used. In the conduct of the preference tests, three values of R_f were used, thus giving three field levels. The values of R_f used were: 350 MΩ; 800ΩM ; and 1600 MΩ. These resistance values, along with the exposure chamber plate separation and a 50-μA field resistor current, correspond to field levels of approximately 32 kV/m, 79 kV/m and 158 kV/m, respectively.

As in the prototype simulator, the voltage across the grid section (between the corona grid and the control grid) controls the ion current density in the animal exposure chamber. For the present bias arrangement, the grid voltage is produced by the corona current flowing through the grid bias resistor, R_g.

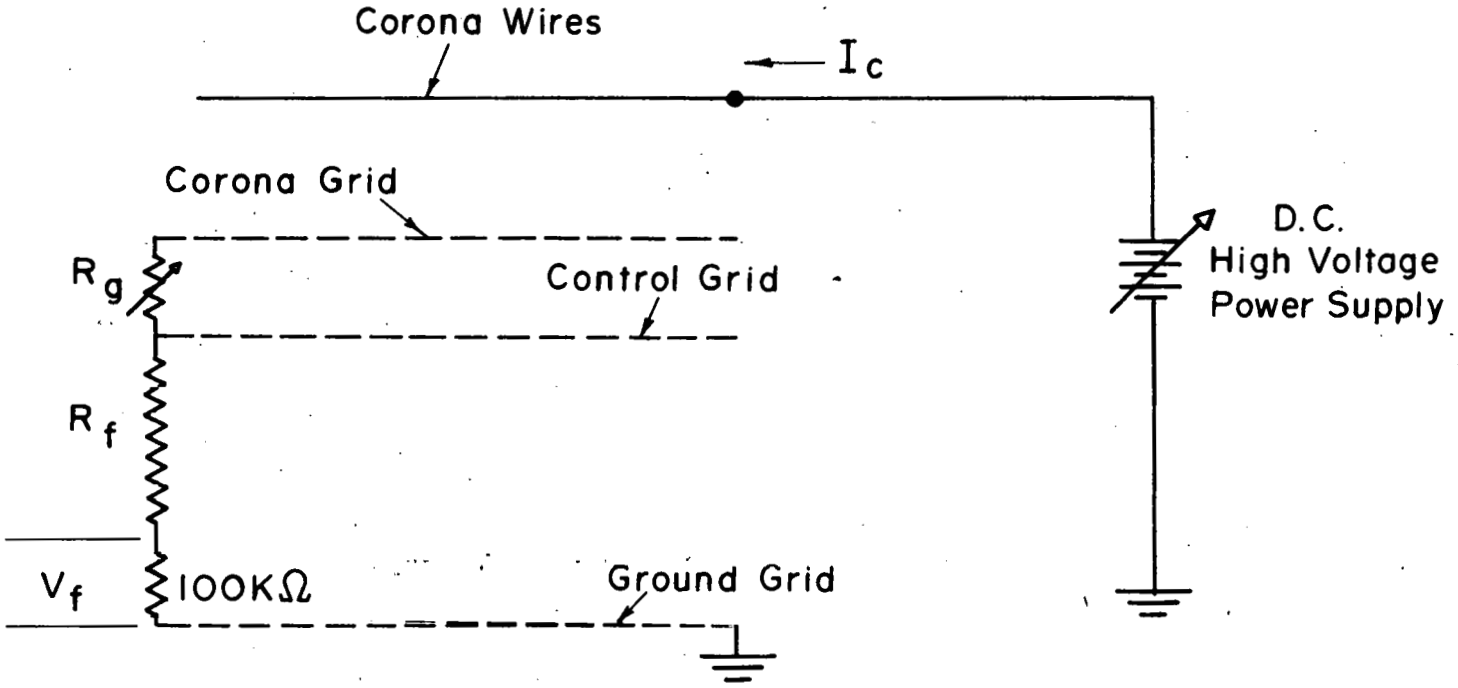

Fig. C-4 BIAS ARRANGEMENT FOR PRODUCING, HVDC ENVIRONMENT IN SIMULATOR

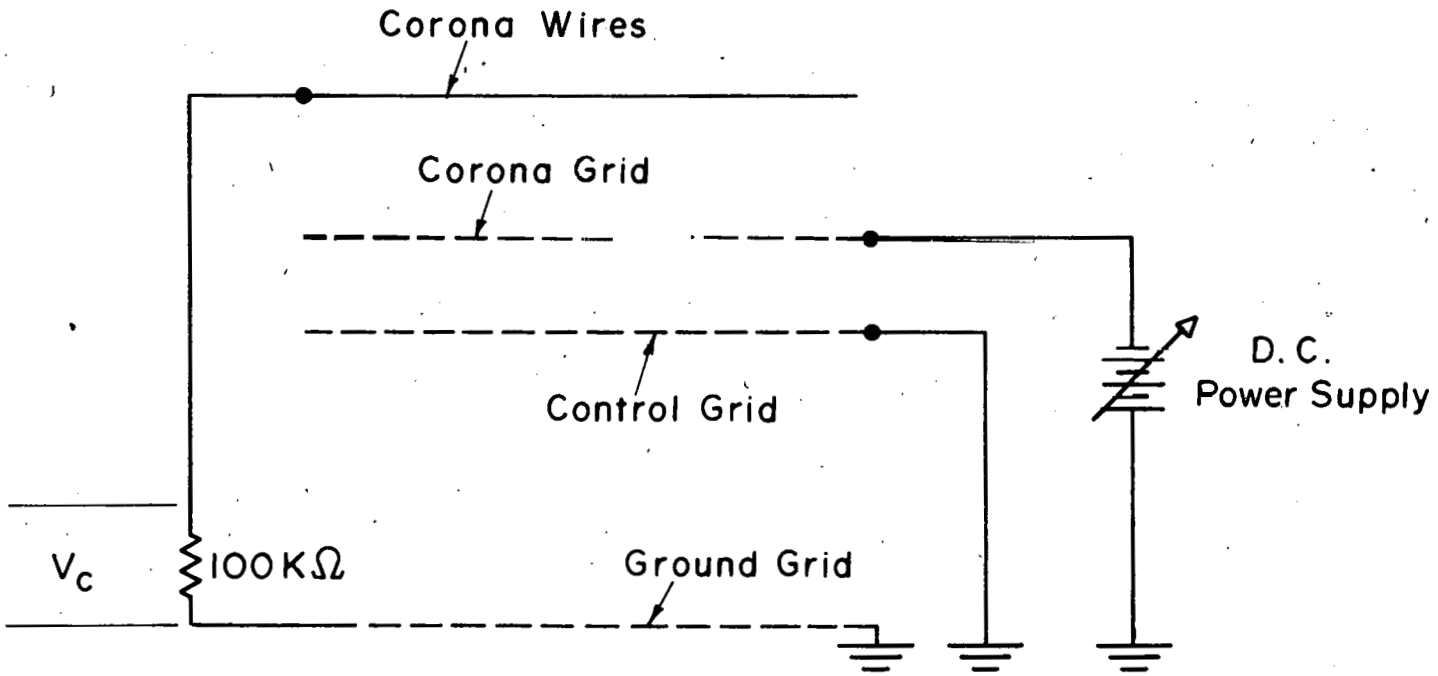

Fig. C-5 BIAS ARRANGEMENT FOR PRODUCING CORONA CURRENT IN "CONTROL" SIMULATOR

Physically, R_g was a potentiometer which could be adjusted in value to produce the desired ion current density in the animal exposure chamber. The ion current density is determined by measuring the output from a 100 cm^2 current sensing probe located on the ground grid of the chamber.

When a simulator chamber was used as a "control", the bias arrangement was different than that described above for use in the "test" condition. When used as a "control", it was desired that the chamber produce the same polarity and magnitude of corona current as the other chamber, when the other chamber was operated in one of the HVDC environmental "test" conditions. This procedure was felt to be desirable to ensure that any acoustic noise produced by the corona wires in the "test" chamber would also be produced in the "control" chamber. Figure C-5 shows schematically the bias arrangement for producing corona current in a "control" simulator. The power supply polarity shown in Figure C-5 will produce positive ions, as will the arrangement shown in Figure C-4. Thus, the two bias arrangements shown in Figures C-4 and C-5 are "test-control" complements for positive ions. Reversal of the power supply in both figures will result in negative ions.

The "control" bias arrangement is intended to result in negligible fields and ions in the animal exposure chamber, but with the same acoustic noise as an "at environment" test simulator. From Figure C-5, the control grid is shown to be directly connected to the ground grid, thus preventing dc fields from being developed in the animal exposure chamber. In the same figure, the negative output from the power supply is seen to be connected to the corona grid. Since the corona wires are grounded (through 100 kΩ), to the ground grid, the wires are positive relative to the corona grid and positive ions will be produced. The corona current is measured by sensing the voltage developed across the 100-kΩ resistor in the corona wire feed wire. The wires can be driven to the same corona current level used to produce HVDC test environments (typically 50 μA).

For the arrangement shown in Figure C-5, the power supply voltage appears between the corona grid and the control grid. The control grid is positive with respect to the corona grid. Due to the polarity of the grids, the positive ions that enter the region between the corona grid and the control grid, are repelled back to the corona grid by the field in the inter-grid space. The strong field in the grid region prevents ions from moving down into the animal caging section of the simulator for this bias arrangement, even though the corona produced by the wires is the same as for a simulator which is used to establish HVDC test environments.

2. ENVIRONMENTAL CHARACTERIZATIONS

2.1 Overview and Summary

Prior to the conduct of animal preference tests, using the simulator arrangement described above, a variety of tests were performed to quantify the various physical environments that the animals would be exposed to. Tests were conducted to characterize the uniformity of the ion current density and electric field intensity in both simulator units used for the preference experiment. These uniformity characterizations were made for three different exposure levels, which were in the range of those used for the preference experiment. Measurements were also made in a chamber when it was operated in the "control" condition to check the absence of fields and ions.

Measurement of the air ion concentration in the room was made to insure that no corona was forming on the exterior surface of the simulators when they were raised to the highest voltage used in the preference experiment. Audible noise measurements were made in each simulator to ensure that this environment was the same for both "test" and "control" conditions. Light level measurements were made at several locations within each simulator, to ensure that the lighting intensity was similar in each simulator, so that this factor would not influence an animal preference choice.

The following paragraphs present a description of the procedures employed in these various measurements, as well as their results. However, as a summary of these measurements, it can be stated that other than the intended variable (the field and ions) all measured physical factors, were very similar in the two simulator chambers. Thus, based on these measurements and their results, the animals should not be expected to show a preference for one chamber over the other due to the physical factors investigated.

2.2 Preference Simulator Electric Fields and Ion Current Density Uniformity

After fabrication of the preference test simulator units, measurements were made to determine the variation in field and ion current density levels as a function of position within the animal housing section. Since one long wall of each chamber did not extend down to the ground grid, to allow animal access to the chamber from the tunnel area between simulated inits, it was anticipated that some field and ion nonuniformity would exist along this wall.

Preliminary tests showed that nonuniformities in the ion current density existed and were a function of how the bottom edge of the animal access wall was treated. These preliminary tests indicated that the ion current density at the ground grid was more uniform when the bottom edge of the open access wall was metalized (with copper tape) and grounded, than when left floating. No significant improvement was observed when the metalized strip at the bottom edge of the animal access wall was extended to run completely around the outside periphery of the chamber, in effect forming a complete contacting peripheral guard ring at a height of two inches from the ground grid. Therefore, a conductive adhesive copper tape strip was placed at the bottom of the access wall of each chamber and grounded to the ground grid.

Ion current density and relative electric field maps were made for both of the preference test simulator chambers, for three levels of field and ion current density. The excitation levels used in the mapping were in the range of the three exposure levels later used for the preference testing.

Similar procedures were used to take this mapping data as had been used for obtaining mappings of the prototype simulators. Current density and electric field readings were made on a 2" x 2" matrix of positions within the floor space area of each animal compartment of the simulators. Since each animal compartment of the preference simulator had an 8" x 20" floor area, forty data points were obtained for a 2" x 2" matrix mapping of the compartment.

The current density readings were obtained with the same current probe used for other mappings. The probe has an active area of 10 cm^2 and outside dimensions of 2" x 2". The probe was moved to successive contiguous locations on the ground grid, and the current output from the probe was monitored with a Keighly 610A. The power supply voltage, as well as the simulator bias resistor values remained fixed during the current density mapping of a simulator.

A mapping of the relative electric field level was made on the same 2" x 2" matrix as for the current density mappings. For these measurements, a Monroe 225 electric field meter was used. The probe head was set on top of the ground plane at the different measurement locations; therefore, the measurements are not absolute, but provide an indication of the field variation from location to location. The field measurements were made for the same power supply setting and simulator bias resistor settings as for the current density measurements. The simulator had an air flow of approximately 35 cfm for these measurements.

With reference to Figure C-4, the following procedure was used to establish the environments for these measurements. Measurements were made at low, medium, and high field levels, using field resistors (R_f) of 320, 800 and 1600 megohms, respectively. The power supply was adjusted to produce a 50 μA current through the field bias resistor, R_f, by measuring with a Fluke Model 8030 digital multimeter a 5 volt (V_f) drop across the 100 kΩ resistor which was in series with R_f. With the 10 cm^2 current probe in the center of one of the compartments, the grid resistor was adjusted to produce a current density reading that was in the desired range.

Measurements at all three excitation levels, for both simulators, showed the same trends. Tables C-1 and C-2 show the current density levels obtained from mapping the two simulators at the highest excitation level. Tables C-3 and C-4 show the electric field maps for the simulators at the same excitation condition. The field levels shown in these tables are the field meter readings divided by a factor of two. A test with the field probe both on top of the ground and mounted flush with the ground had shown that the meter indicated a reading which was a factor of 2.06 higher for the on top of ground condition. The tabulated values provide an indication of how the fields vary for the different locations shown. However, these values should not be taken as an accurate indication of field level. The intent here is to show the field variation which results from the slot in the bottom of the tunnel access wall.

Both the current density and field is seen to decrease within four inches of the animal access wall. Some depression in the current density is also noted within two inches of the outside wall which is opposite to the access wall. This is illustrated in Figure C-6, which provides a summary of Tables C-1 and C-2 data.

Each point on a curve of Figure C-6 was obtained by averaging the sixteen measurements along the long dimension of the simulator, at a given distance from the tunnel access wall. There are ten measurement points across the narrow dimension of the unit. The ten longitudinal means were then normalized with respect to the mean of all 160 current density measurements within the simulator for the given excitation condition, for plotting in Figure C-6. Figure C-6 shows a curve for each of the two simulator modules.

TABLE C-1

CURRENT DENSITY MAP OF "A" UNIT OF PREFERENCE SIMULATOR FOR "HIGH" EXCITATION CONDITION
(Values in nA/m^2)

4				3				2				1			
750	800	950	875	950	925	910	950	975	900	800	700	850	800	800	800
1250	1200	1300	1350	1400	1250	1260	1350	1350	1325	1325	1450	1475	1425	1325	1275
1200	1160	1220	1375	1275	1275	1260	1450	1350	1350	1350	1400	1550	1375	1325	1300
1250	1050	1200	1225	1150	1175	1200	1250	1350	1225	1350	1425	1480	1250	1250	1275
1100	1050	1120	1225	1150	1250	1200	1225	1325	1325	1325	1400	1325	1325	1225	1150
1020	1100	1120	1250	1200	1175	1125	1050	1050	1250	1300	1375	1125	1300	1225	1125
1200	1125	1160	1325	1350	1260	1225	950	1025	1200	1450	1450	1150	1275	1100	1100
1000	875	1050	1100	1150	1050	1100	800	900	1100	1100	1200	1050	1075	950	925
870	825	875	875	900	950	850	500	550	1000	925	1100	900	975	875	800
650	600	625	600	700	625	625	350	350	725	650	750	575	660	625	500

Tunnel Wall

TABLE C-2

CURRENT DENSITY MAP OF "B" UNIT OF PREFERENCE SIMULATOR FOR "HIGH" EXCITATION CONDITION
(Values in nA/m^2)

1	2	3	4
620 600 860 950	1020 850 950 950	950 780 950 950	850 950 900 850
1260 1150 1250 1250	1300 1250 1160 1300	1230 1300 1220 1330	1350 1350 1320 1300
1150 1150 1250 1400	1250 1300 1200 1300	1230 1260 1250 1300	1400 1410 1230 1350
1300 960 1150 1120	1250 1100 1120 1300	1230 1250 1250 1380	1360 1250 1150 1240
1150 1000 1100 1250	1150 1030 1160 1300	1200 1230 1220 1300	1240 1250 1150 1160
1100 1000 1100 1200	1220 1050 1200 1200	1250 1160 1220 1410	1240 1250 1150 1050
1150 1160 1140 1230	1160 1100 1150 1230	1200 1160 1270 1350	1360 1100 1100 1000
1000 940 1050 1050	1060 1000 930 1000	1000 1050 1020 1150	1200 1050 940 840
800 800 850 850	850 900 800 900	820 820 900 950	1000 900 860 700
450 600 600 650	680 600 600 680	620 620 650 620	650 600 575 500

Tunnel Wall

TABLE C-3

ELECTRIC FIELD MAP OF "A" UNIT OF PREFERENCE SIMULATOR FOR "HIGH" EXCITATION CONDITION

(Probe on Top of Ground Grid. Meter Reading Divided by 2, in kV/m)

1				2				3				4			
200	190	190	190	190	190	190	190	190	190	190	190	190	190	190	177
190	172	175	180	190	175	175	185	190	175	175	180	190	175	175	185
180	170	170	180	190	170	170	185	190	172	172	180	190	170	170	185
180	167	170	180	185	170	170	182	190	170	170	180	185	170	170	182
177	165	167	180	182	167	170	182	185	170	170	180	182	167	170	182
177	165	167	177	180	167	167	180	182	167	170	180	180	167	167	180
175	160	165	175	177	165	165	177	180	165	165	175	175	165	165	177
175	152	150	170	177	160	160	170	175	160	160	165	175	160	160	170
155	142	145	155	160	147	150	157	165	150	152	157	160	147	150	157
127	110	115	122	122	117	120	125	135	130	130	132	125	117	120	125

Tunnel Wall

TABLE C-4

ELECTRIC FIELD MAP OF "B" UNIT OF PREFERENCE SIMULATCR FOR "HIGH" EXCITATION CONDITION

(Values in kV/m)

1				2				3				4			
180	180	180	177	192	182	180	180	185	177	180	180	190	182	180	170
180	170	172	180	195	175	175	177	185	170	172	180	187	175	170	170
180	170	172	177	190	170	172	175	185	170	170	175	185	170	170	170
182	170	170	175	185	170	170	175	185	170	170	172	185	170	170	165
185	167	170	177	180	170	170	172	185	170	170	175	182	170	167	162
180	165	167	175	177	165	167	170	185	175	167	170	180	165	165	160
172	162	162	170	175	162	165	167	180	175	165	167	177	162	162	160
165	155	155	165	167	155	160	160	175	157	160	162	170	152	155	155
152	142	140	150	155	145	148	150	162	145	147	152	157	145	145	145
112	110	100	112	125	107	110	120	120	112	117	125	122	115	112	120

Tunnel Wall

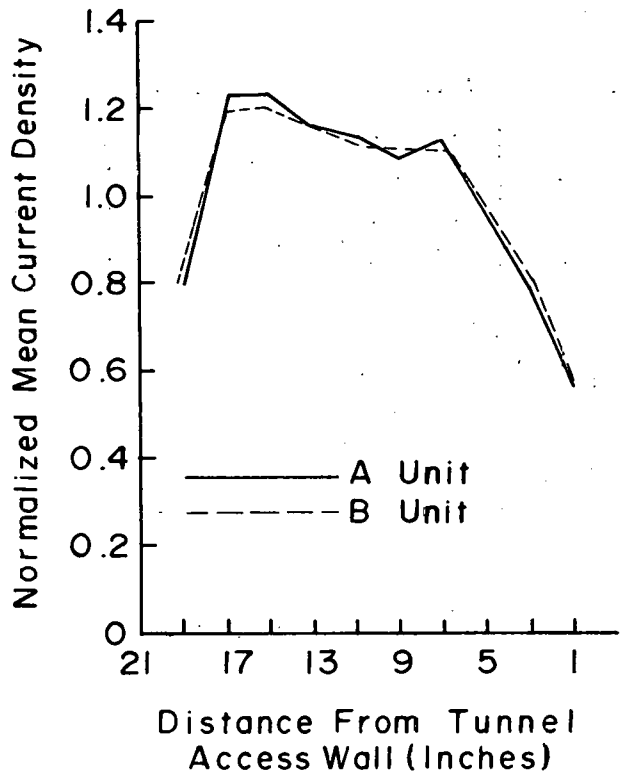

Fig. C-6 NORMALIZED MEAN CURRENT DENSITY PROFILE ACROSS PREFERENCE SIMULATOR WIDTH FOR HIGH LEVEL TEST CONDITION

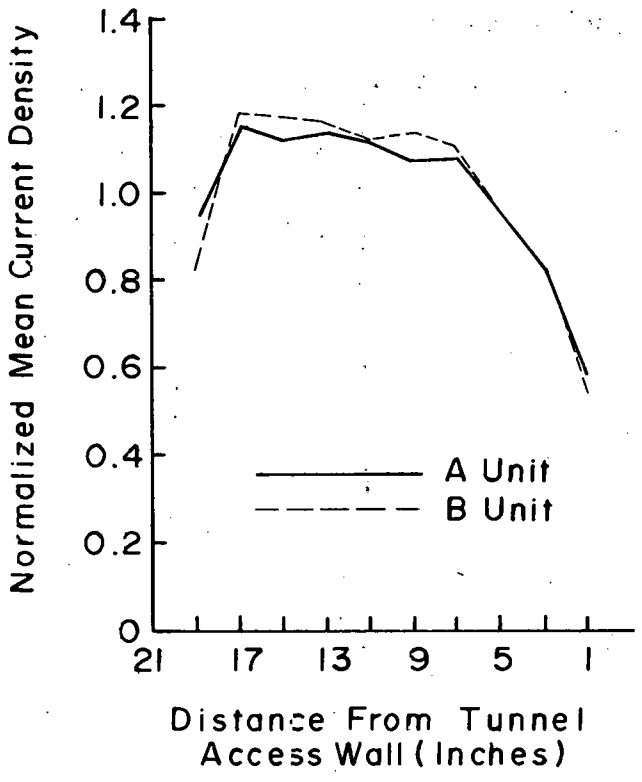

Fig. C-7 NORMALIZED MEAN CURRENT DENSITY PROFILE ACROSS PREFERENCE SIMULATOR WIDTH FOR LOW LEVEL TEST CONDITION

For comparison with Figure C-6, Figure C-7 presents normalized mean current density profiles, for the two simulators, which were obtained at the low excitation level used. The current density for the low excitation condition was approximately 250 nA/m^2. It is seen that these normalized current density profiles are very similar to those presented in Figure C-6 for the high level excitation case. Thus, it is seen that with respect to electric field and ion current density uniformity, the two preference test simulators gave comparable results. It is also seen that the uniformity of the current density was virtually independent of the environment level established in the simulator.

2.2 Control Condition Environment

The "control" condition was established by use of the bias arrangement shown in Figure C-5. For this bias arrangement, corona current flows through the corona wires, as in the test condition. The corona current was set to be the same as for the "test" bias conditions, i.e., 50 μA. The control grid was shorted to the ground grid so that no potential was developed across the animal caging section. With this arrangement, measurements have shown that no electric field can be sensed in the animal chamber with the Monroe 225 electric field meter on its most sensitive scale, i.e., $\bar{E} < 100$ V/m. The shorting of the control grid to ground causes the full power supply voltage to appear between the corona grid and the control grid. The polarity of the bias across the grid section is such to inhibit ions from flowing into the animal caging section from the corona chamber.

Use of the current probe in a chamber with "control" condition bias indicated a negligible ion current density level. However, it was felt that a better assessment of the ion environment within the "control" chamber could be provided by using an ion counter.

A Wessix Model Mark IV ion counter was used to make these measurements. The ion counter was mounted below the ground grid. A hole was cut in the ground grid to enable the air intake of the ion counter to protrude slightly into the simulator through the ground grid. Measurements were made with the ion counter polarizing voltage at -200 volts.

Measurements of the current from the ion counter allows the ion density to be determined from the relationship

$$N = \frac{I_w}{ev\ A} \qquad \text{(C-1)}$$

where

N = ion density in ions/cm^3

e = electron charge - 116 c 10^{-19} coulombs

v = air velocity through ion counter

= 75 cm/sec (quoted by mfgr.)

A = area of ion counter collection plates = 49 cm^2

I_w = the ion current collected by the ion counter.

With the ion counter mounted as above, the electrical bias to the simulator "off", and normal air flow through the simulator, the negative current from the ion counter was 1.05 x 10^{-13} amperes. From Eq. C-1, this current corresponds to an ambient negative ion density within the simulator of $N = 180$ ions/cm^3.

After this ambient reading was obtained, the simulator was "control" biased with a total corona wire current of 50 μA. After a period of approximately five minutes, the ion counter current stabilized at 1.1 x 10^{-13} amperes, which corresponds to about $N = 190$ ions/cm^3. Thus, the ions produced in the corona chamber of the "control" biased simulator had a negligible effect on the ion count in the animal exposure section of the simulator.

The adjacent simulator module was then biased at the "high" negative condition, while the module with the ion counter remained in the negative control bias condition. The environment in the "high test" condition simulator was a current density and field of approximately 1200 nA/m^3 and 150 kV/m, respectively. The current from the ion counter in the "control" simulator gradually increased over a period of several minutes, and finally stabilized at $I_w = 2.2 \times 10^{-13}$ amperes, which corresponds to an ion density of 375 ions/cm^3. The voltage to the "test" simulator was subsequently removed. The ion current in the "control" biased simulator gradually decreased and, after ten minutes, was 240 ions/cm^3. Thus, it appears that the operation of a "test" chamber which is adjacent to a control chamber results in some increase in the ion density of the "control" simulator. However, the ion density in the control simulator was still well within the range which is considered as normal for an ambient environment.

As a comparison, the simulator in which the ion counter was mounted was biased in the "low" negative test condition. The ion current density was adjusted for 250 nA/m^2, as measured with the 100 cm^2 current probe. The field for this bias condition had previously been measured, with the Monroe 225 field meter mounted flush with the ground plane (through the hole in which the ion counter was mounted), to be 36 kV/m. For this condition, the current from the ion counter was 0.78×10^{-10} amperes, which corresponds to an ion density of $N = 1.33 \times 10^5$ ions/cm^3, by use of Eq. C-1.

This ion density can also be estimated from the current density and the electric field from the relation

$$N = \frac{10^{-6} j}{ekE} \qquad \text{(C-2)}$$

where

N = ion density (ions/cm^3)

j = current density (A/m^2)

e = electron charge (1.6×10^{-19} coulombs)

E = electric field intensity (V/m)

k = ion mobiling (m^2/Vs).

The ion mobility is typically taken to be in the range of 2×10^{-4} m^2/Vs. Using this value of k and the above current density and field levels, the ion density determined from Eq. C-2 is $N = 2.17 \times 10^5$ ions/cm^3. This value of ion density is a factor of 1.6 larger than that determined above by use of the ion counter for the "low" test bias condition.

The discrepancy between the ion density as determined by the ion counter and the field and current density for the "low" test condition was not investigated. The principal reason for employing the ion counter was to establish that the ion density for the "control" bias condition was negligible with respect to that of the "test bias condition. From this standpoint, the possible error of almost a factor of two in the ion counter reading does not appear of great consequence. The "control" simulator ion density, with the adjacent simulator biased at the "High" test condition (a worst case) is a factor of 350 less than the ion density in the "low" test condition, based on measurements with the ion counter. Thus, these tests show that the method used to bias the "control" simulator provides

an adequate suppression of the ions that exist in the corona chamber of the "control" biased unit. The reason for biasing the "control simulator is to produce the same acoustic environment as for the "test" condition. The comparison of the acoustic environment in the "test" and "control" conditions is presented in the following section.

2.3 Acoustic Measurements

Measurements that were made during the development of the prototype simulator showed that measurable acoustic noise was produced by the corona wires. Therefore, it was planned to use the bias arrangement shown in Figure C-5 to excite the corona wires of a "control" simulator the same as for a "test" simulator, without producing a field or ion environment in the simulator. It was reasoned that under these conditions the "control" simulator acoustic noise would be the same as for a "test" simulator. Prior to the conduct of the preference tests, acoustic measurements were made in the simulator to ensure that the noise for the "control" and "test" bias conditions were similar.

The measurements were made with a B&K 2209 precision sound level meter and a B&K 16B octave filter set. Readings were made of the unweighted sound pressure levels, in dB, relative to 20 μPa. Readings were taken in each octave band from 31.5 Hz to 31.5 kHz. The measurements were made with the complete preference test simulator located in the same location which was used for the animal preference testing. The microphone (a B&K Model 4133 one-half inch diameter condenser mike) was inserted into a simulator through the mesh of the ground grid, from underneath. The second animal compartment from one end was arbitrarily selected for use in the measurements in each simulator module. The mocrophone was mounted near the center of the compartment. The barrel of the microphone was vertical and the sound inlet pointed upward and was at a height of approximately one inch above the ground grid.

Figure C-8 shows preliminary measurements without electrical excitation of the simulator. Shown in this figure are three curves: one shows the meter readings for the instrument noise level; the second shows the levels obtained in the (A) simulator module for ambient conditions, i.e., no electrical excitation or air flow; the ambient in the other module was within 1 dB of these readings except in the 250 and 500 Hz octaves, where the second module was 2 dB lower than that shown, and in the 31.5 Hz octave where the (B) chamber was 4 dB higher than that shown. The third curve of Figure C-8 shows the readings made

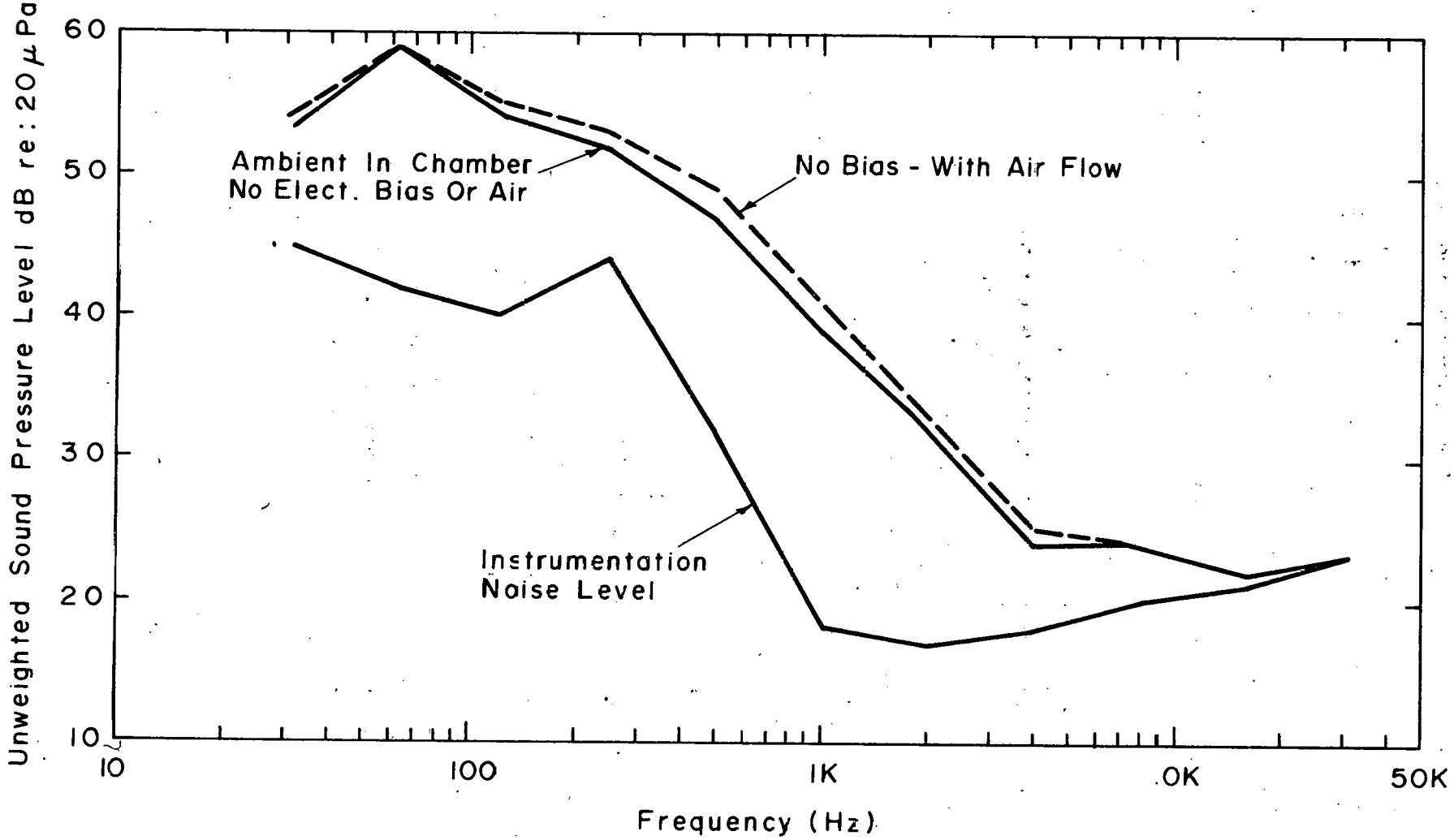

Fig.C-8 OCTAVE BAND BASELINE ACOUSTIC NOISE LEVEL MEASUREMENTS

with air flow through the chamber. It is seen that adding the air flow increases the sound level by about 1 dB over most of the band.

Figure C-9 shows the acoustic spectral levels obtained when this simulator was operated in the positive and negative control condition. These conditions are denoted by + C and - C, respectively, on the figure. The magnitude of the total corona current was 50 μA for each of these cases. It is seen that the acoustic noise spectrum for positive ions is nearly identical to the ambient with air flow for all octave bands below 16 kHz. The positive ion corona noise is noticeably above the ambient in the 16 kHz and 31.5 kHz bands, but only by one or two dB.

The "control" negative corona acoustic noise is seen to be measurably greater than the ambient with air and the positive corona noise for frequencies of 4 kHz and above. In the highest octave band tested, the negative corona noise was 11 dB greater than with no corona.

The curves of Figure C-10 compare the acoustic noise of the other simulator module, when it was operated at both polarities with "test" condition bias at the highest excitation level used for the preference tests. The curves are designated by + H and - H to indicate positive and negative corona at the highest field conditions used for the preference tests. For these tests, the bias arrangement of Figure C-4 was used with a field resistor R_f = 1600 megohms. The total corona wire current for these tests was 50 μA, as it had been for the tests of the "control" condition of Figure C-9.

Comparison of the + H curve of Figure C-10 with the + C curve of Figure C-9, or the - H curve with the - C curve, shows that the acoustic noise within the two simulator modules is the same when they are operated at the same corona conditions. The acoustic noise spectra for negative corona has higher level components at the higher frequencies than for positive corona. Since the noise spectra were different for the two polarities of the corona, both positive and negative "control" conditions were employed in the preference tests.

2.4 Light Levels

In preparation for the animal preference testing, light level measurements were made within the two simulator modules. The purpose for light level characterizations was to ensure that the light intensity was substantially the same in both simulator units. If the light levels were the same in both simulator

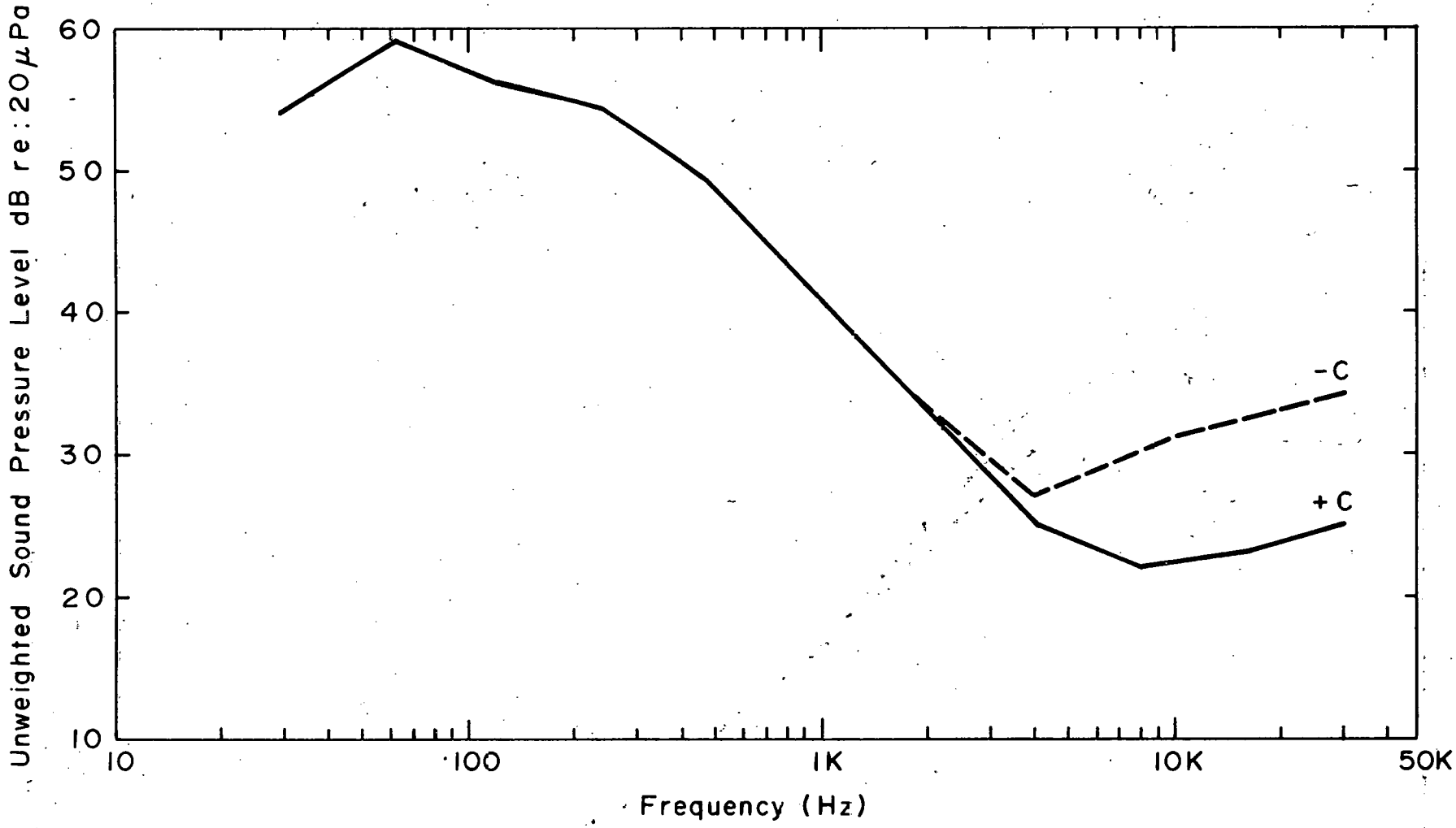

Fig. C-9 OCTAVE BAND ACOUSTIC NOISE LEVELS IN CHAMBER A WHEN OPERATED AS "CONTROL"

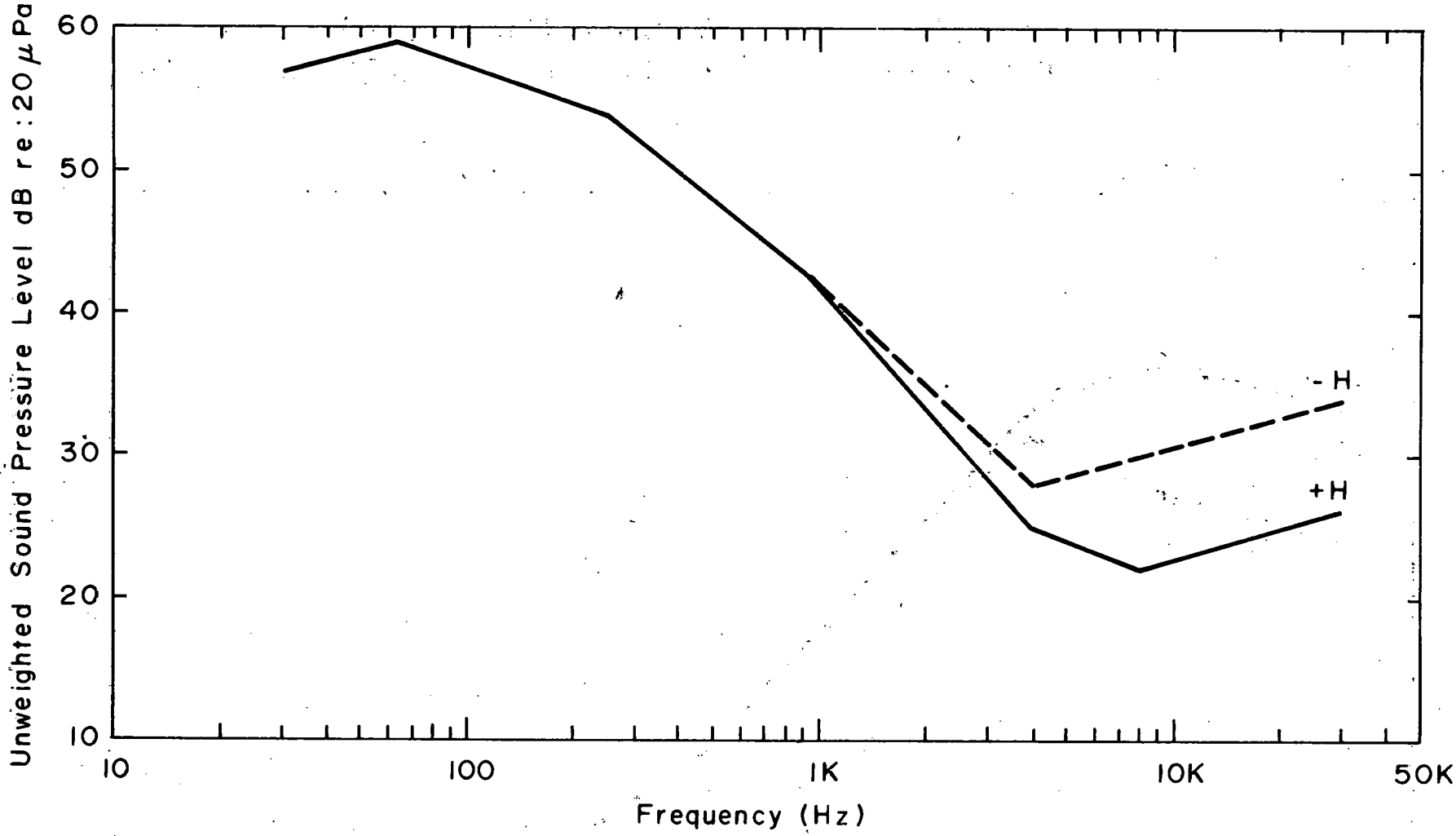

Fig. C-10 OCTAVE BAND ACOUSTIC NOISE LEVELS IN CHAMBER B WHEN OPERATED AT HIGHEST "TEST" CONDITION

modules, then the animals should not exhibit a preference which might be keyed to differences in light illumination.

The light level measurements were made with the simulator located where the preference tests were conducted. The measurements were made with a Weston Model 603 light meter. During initial measurements, the position of the simulator within the room and the location of fluorescent tubes in the overhead lighting fixture was adjusted to produce an illumination which was similar for both simulator chambers. Light level readings were made at three locations within each of the three animal areas of each simulator. The readings were made at the ground grid level within the animal compartment. Readings were obtained in the center, near the tunnel access wall, and near the opposite outside well of each animal compartment.

Figure C-11 presents a plan view sketch of the preference simulator upon which is recorded the light level readings at the approximate locations where the readings were made. The light levels indicated in Figure C-11 are in foot candles.

It can be seen from Figure C-11 that for each animal compartment, the light intensity was higher near the interconnecting tunnel wall than near the outermost wall. However, the variation in light intensity is very similar in both simulator chambers. Thus, it is not expected that an animal would show a preference of one simulator over the other based on light intensity. It will be noted that light intensity measurements were not taken in the fourth compartment of the preference simulator. This chamber was used for the placement of current density probes during the animal preference Tests. Thus, animals were not placed in this compartment.

2.5 Field and Ion Current Density Combinations for Preference Testing

During the conduct of the preference tests, one of the two simulators was in the control bias condition; the other simulator was in the test bias condition. The control simulator was always at the same polarity as the test chamber. In the test sequence, the choice of which chamber was "test", its polarity and its excitation level was randomized. Four excitation levels for the "test" chamber were used. These were denoted "Control", "High", Medium", and "Low" conditions. For all conditions, "Control", or "High", "Medium", or "Low" test, of either polarity, the total corona wire current was adjusted to be 50 μA.

B Simulator			Tunnel	A Simulator			Compartment
							4
8	8	11		12	10	9	3
6.5	7.5	12		12	9	7	2
7.5	8.5	12.5		12	9	8	1

(readings in ft candles)

Figure C-11 LIGHT INTENSITY READINGS IN PREFERENCE TEST SIMULATOR

A Monroe 225 field meter was used to measure the fields in the center of the fourth compartment of each simulator (the compartment of Figure C-11 in which light readings were not taken). The field measurements were made with the field probe mounted in a cutout in the ground grid so that the probe was flush with the ground grid. Measurements of the field were made for both polarities, for all three field bias resistors. That is, 1600 megohm for the "High" condition, 800 megohm for the "medium" condition, and 320 megohm for the "low" condition. In each case the current through the field bias resistor was set at 50 μA. The ion current density was set by adjusting the control grid bias potentiometer, to produce 1200 nA/m^2 for the "high" condition, 650 nA/m^2 for the "medium" condition, and 250 nA/m^2 for the "low" condition, as measured with the 100 cm^2 current probe. Table C-5 presents the electric field intensity that was measured for the above conditions.

The electric fields within the simulators were not measured during the conduct of the animal preference test, since the electric field probe produces a quite loud audible tone due to the vibrating plunger. The field is established by the field bias resistance value, the current flow through the resistance, and the ion current density. The current through the field bias resistor was always set to 50 μA for all test conditions of the animal preference tests. The current density at the center of the fourth compartment of the "test" simulator was measured with the 100 cm^2 current probe which was placed on the ground grid. A "dummy" current probe, which consisted of a brass plate with the same dimensions as the current probe, was placed on the ground grid in the center of the fourth compartment of the "control" simulator, to visually simulate the current probe located in the "test" simulator.

3. DESCRIPTION OF PHYSICAL ARRANGEMENT FOR ANIMAL PREFERENCE TESTING

The preference testing setup used three adjacent rooms in the Life Sciences facilities at IITRI. The general physical arrangement is shown in the plan view sketch of Figure C-12. The location of the major items used in the testing are shown on this sketch.

The preference test simulator was located in the center room of the three room complex. The power supplies, the air blower and HEPA filter, as well as the instrumentation used to monitor the simulator bias currents and the ion current density were located in the west-connecting room. This room served as

Table C-5

FIELD INTENSITY AT GROUND GRID
IN CENTER OF FOURTH COMPARTMENT

Bias Condition	Field Intensity kV/m Simulator	
	A	B
High +	144	146
High -	146	152
Med +	84	84
Med -	86	84
Low +	35	34
Low -	36	36.5

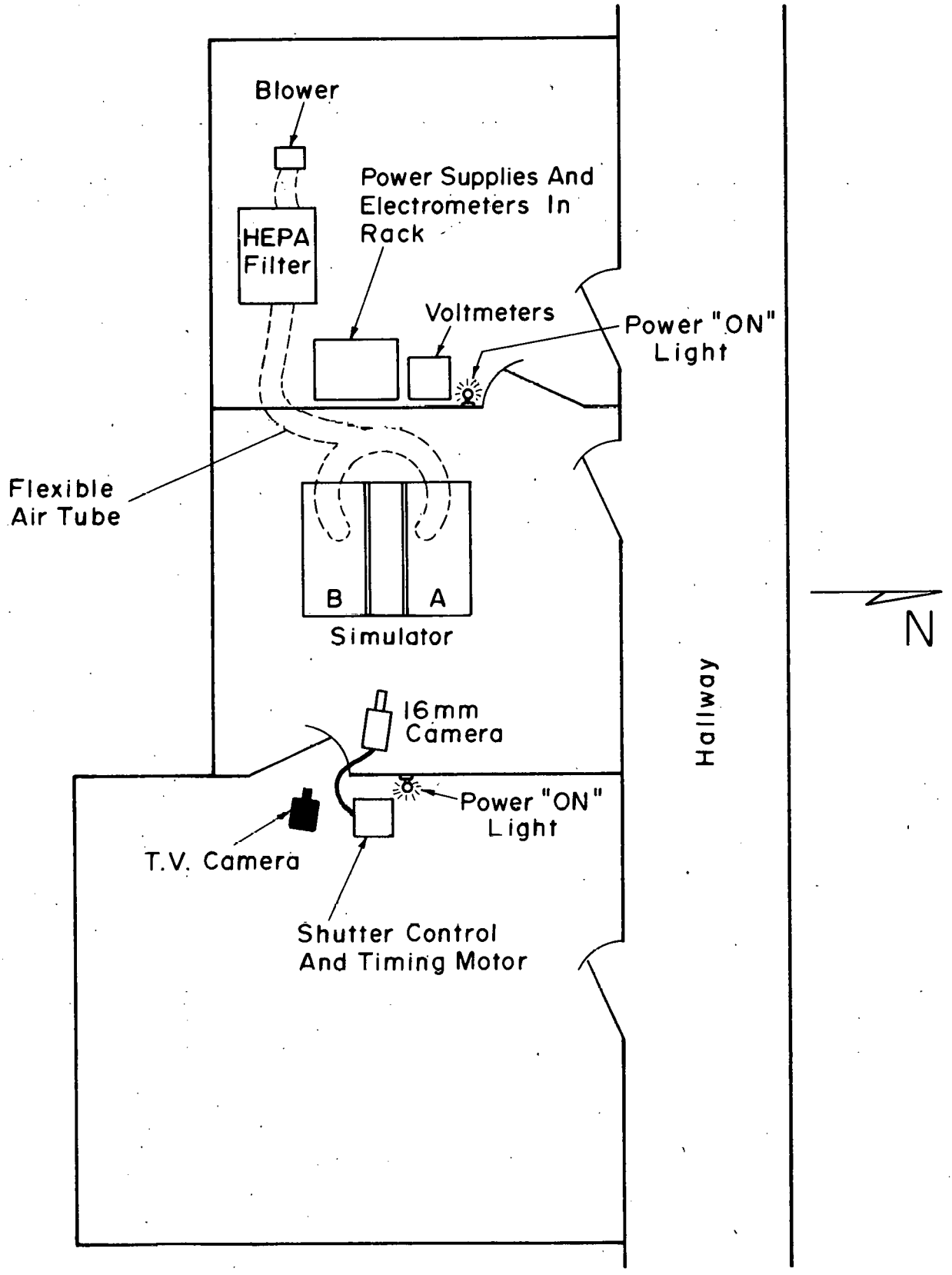

Fig. C-12 SKETCH OF PHYSICAL ARRANGEMENT FOR ANIMAL PREFERENCE TEST

the control room for the tests. The east-connecting room was used to locate the camera control equipment as well as a TV camera and recorder.

A 16-mm movie camera was located in the center room with the simulator. The movie camera was set for single framing and was controlled by a solenoid and motor driven cam arrangement which was located in the east-connecting room. The movie camera exposed a single frame every fifteen seconds during the animal tests. A counter which was located in the control room accumulated the number of exposed frames in a given test. By this arrangement, the location of the animals within the simulator at fifteen-second intervals was recorded on film. The film was used for post-test analysis of animal location during the test sequence.

A television camera and recorder were also located in the east-connecting room for selected tests. The TV camera was mounted on a tripod to view the simulator chamber through a window in the closed door between the center and east rooms.

During the normal course of the preference tests, except when the TV camera was being used, personnel were only located in the "control" room. The doors from the center and east rooms, which led to the hallway, were locked, and the other two doors of the center room were closed. The window in the door between the center room and the control room was translucent, with the exception of a small area through which the simulator and animals could be viewed. When primary power was applied to the power supplies, flashing red lights were activated in both the control room and in the east-connecting room.

The filtered air from the HEPA filter was conducted through a four-inch flexible tubing. This tubing was routed from the control room into the center room through a hole located near the ceiling of the common wall between the two rooms. The air to the two simulator plenums was fed through equal lengths of flexible tubing connected to a tee in the main air supply line.

The high voltage lines from the power supplies were RG-8/U coaxial cable, which were run through the hole in the wall between rooms with the air supply tubing. The ground shield of the cable was cut back approximately four feet from the end of the high voltage cable which was attached to the simulators. The cables which were used to monitor the ion current density probe and the simulator currents were run along the floor and underneath the door between the control room and the center room.

Two power supplies were used, one for each simulator model. The "test" simulator, either the A or B chamber, was supplied by a Spellman Model RHR100-PN100/RCP/LL144, 100-kV power supply. The "control" simulator was fed with a Sorensen Model 1030-20, k0-kV power supply.

4. METHODS FOR PREFERENCE TESTS

4.1 Animals

Ninety-six male Fischer 344 rats (Charles River, Wilmington, MA) were used in the preference testing. The animals were 5 weeks old at the time they were received and 21-22 weeks old at the time the tests were conducted. Prior to testing they were housed three rats/cage in polycarbonate cages (19 x 10.5 x 8 in) on a bedding of hardwood origin (Absorb-dri). Food (Purina Lab Blocks) and tap water were available for ad libitum consumption except during the test period when no food or water was provided. Animal rooms were maintained at a temperature and relative humidity of approximately 75° F and 40%, respectively. A light-dark cycle of 14 hr light: 10 hr dark was employed with the onset of light occurring at 6:00 A.M.

Prior to testing the animals were weighed and checked for signs of unhealthiness. Those selected for testing appeared to be in good health and weighed between 244 and 393 g. (mean ± standard deviation = 323 ± 23 g.).

4.2 Experimental Groups

The animals were randomly assigned (12 rats/conditon) to eight experimental conditions which differed as to the choices available to the animal in the preference testing apparatus. These conditions or choices were as follows:

Negative Polarity	Positive Polarity
Control vs Control (C-)	Control vs Control (C+)
Low vs Control (L-)	Low vs Control (L+)
Medium vs Control (M-)	Medium vs Control (M+)
High vs Control (H-)	High vs Control (H+)

The low, medium, and high designations refer to the levels of dc electric fields and the ion current densities in the test side of the preference testing apparatus. Nominal values were as follows:

Low - 35 kV/M, 250 nA/m^2
Medium - 84 kV/M, 650 nA/m^2
High - 145 kV/M, 1200 nA/m^2

The control conditions on control sides for groups tested at positive and negative polarities differed in the current polarity used to excite corona wires as described above. Where the choice was control vs control, one side or the other of the test apparatus was designated as the "test" side for purposes of data tabulation. Each of the eight experimental groups were subdivided so that for half the animals in each group, the test side was the left side of the apparatus and for the remaining animals the test side was the right side of the apparatus.

4.3 Testing the Preference Response

Basically a preference trial or run sequence involved setting the desired field and ion conditions for the run, placing three animals in the apparatus, and recording their position in the apparatus with single-frame photography at 15-sec intervals for a period of 45 min. The details of the procedures for a single run are included in the instructions prepared for the personnel who conducted the tests (Table C-6). Periodically during a run, the animals were observed through a window in the door between the test room and the room where the instrumentation was located. There was no systematic recording of these observations but notes were made on general appearance of the animals or unusual behaviors. Certain physical data were also recorded in connection with each run. These included recording of wet and dry bulb temperature measurements with a psychrometer (Model PP100, Environmental Technology Corp.) prior to and at the end of each run. Relative humidity was later derived from these readings with the aid of psychrometric charts. Ion current density was monitored during the test runs with the 100 cm^2 current probe and electrometer (Kiethyl Model 610A) with output to a strip chart (Hewlett Packard 7155B) in order to provide a permanent record of current density vs time.

For a given run the condition of the three separate sections of the apparatus, one allocated for each of three animals that were tested simultaneously, were the same with respect to the ion current density and the electric field. Thus, for a given trial or run, the three animals tested in that run were all from the same experimental group. The animals could see each other during the preference test period but were physically separated by the glass walls of the apparatus.

The preference test runs were administered over a 10-day period in two series of 16 runs each. The runs were conducted between the hours of 8:00 A.M. and 5:00 P.M. In each series of 16 runs, the 8 experimental conditions listed above occurred twice. The order in which they occurred was decided by a random process and is shown in Table C-7. Each animal was tested for one 45-min period. Thus, between

TABLE C-6

INSTRUCTIONS FOR PREFERENCE TEST SEQUENCE

The following steps will be performed for each numbered test condition. The data sheet, which will require data entries to be recorded, provides the key to the test conditions. Each test condition is assigned a number from 1 to 32. The tests will be performed in numerical sequence. Since the test conditions have been randomized with respect to polarity, excitation level and selection of which of the two chambers is to serve as the control condition, successive numerically-designated tests may require the change of more than one variable.

After identification of the excitation level "high-medium-low or off" and polarity for each chamber "A;B", corresponding to the test number:

(1) Set Polority of Power Supplies.

a) the 10-kV, supply is set to the opposite polarity that is designated for the test;

b) the 100-kV Spellman is set to the same polarity as is indicated for the test condition on the data sheet when a "high-medium-low" excitation condition applies. When the test condition requires the "control-control" condition, the 100-kV supply is also set at the opposite polarity indicated by the test condition.

(2) Power Supply Connection.

a) Connect the output of the 10-kV supply to the outside corona box connection of the chamber that is designated as the "control".

b) Connect the output of the 100-kV supply to the corona wire feed to the chamber which will be excited to the "high-medium-low" condition. If both chambers are to be "control", connect the 100-kV supply output to the corona box connection of the chamber that is not connected to the 10-kV supply.

(3) Field Resistor Connection.

a) For the chamber designated as "control", connect the "short circuit" jumper between the control grid and ground. If both chambers are control, place the control-grid to ground short on both chambers. Record "0" in the field resistor column of the data sheet for the appropriate chamber.

b) Select the 1600-, 800-, or 320-megohm resistor string to correspond to the "high-medium-low" excitation condition, respectively. Install the resistor string from the control grid to ground grid, with the 100 k tap at the bottom. Connect the VDM input leads across the 100 kilohm resistor. Record the field resistor value used on the data sheet.

c) For the chamber(s) designated as "control", connect the corona wire feed to ground through 100 k. Monitor the voltage developed across this resistor (proportional to the total corona wire current) with a second DVM.

(4) Control Grid Bias.

a) The chamber(s) designated as "control" have no resistive jumper across the grid section.

b) For the active or "test" chamber, place the grid bias potentiometer across the grid section.

(5) Ion Monitoring Instrumentation.

a) Locate the 100 cm^2 current probe in the center of the fourth compartment of the test chamber and the "dummy" probe in the "control" simulator fourth compartment. Connect the current probe output to an electrometer which is set to the same polarity as the test condition. The current scales to be used for the different excitation level conditions are:

Excitation	Electrometer Scale
"Low"	3×10^{-9}
"Medium"	1×10^{-8}
"High"	3×10^{-8}

The electrometer output feeds a paper tape recorder. Zero both the electrometer and the recorder on the appropriate scale. Switch electrometer to the 1-volt scale and connect electrometer to dc voltage. Adjust voltage for full-scale electrometer reading, then adjust recorder gain for full-scale recorder reading. Reconnect lead from current probe and reset electrometer to appropriate current scales. Record run number and current scale on recorder chart paper.

(6) Camera.

a) Reset frame counter to zero.

b) Wind camera.

c) Check footage counter to insure at least ten feet of film left.

d) Check view to insure that it was not disturbed during winding.

e) Close viewfinder.

(7) Record simulator room wet/dry bulb temperature on data sheet in experiment start column. Place card which identifies run number on simulator.

(8) Bring "test" simulator up to voltage and set bias resistor string current at 50 μA. Adjust grid bias potentiometer to produce appropriate current density for test condition. "H" = 1200 nA/m^2, "M" = 650 nA/m^2, "L" = 250 nA/m^2. Secure power supply. Measure value of grid potentiometer and record on data sheet.

(9) Place animals in chamber tunnel and record time when last animal placed. After animals are situated, leave room and close door.

(10) Turn on 10-kV supply and raise voltage until "control" chamber current (monitored by DVM across 100 k to ground in corona wire feed) is 50 μA (5 volts) across 100 k. Record resistor voltage on data sheet.

(11) Turn on 10-kV supply and raise voltage to produce 5 volts across 100 k in field resistor string. Record resistor voltage on data sheet.

(12) Turn on camera and chart recorder (J current monitor) and record time on data sheet. Note: After placing animals into chamber (Step 8) complete Steps 9 through 11 without delay.

(13) During the test:

a) monitor the two resistor voltages. These voltages are not anticipated to change; however, if they do, make slight power supply adjustments to bring the voltages back to the reference values.

b) observe animals and observe the pen recorder trace. Make note of any unusual animal behavior observed and note any observed changes in ion current density that may be related to animal movements.

(14) The animal test is completed when the camera frame counter accumulates to 185. When this occurs, shut off camera and record time on data sheet.

(15) Turn off power supplies.

(16) Re-enter animal test room:

a) read and record wet/dry bulb temperature;

b) remove animals from simulator.

(17) Follow Steps 1 through 16 for next test condition.

Table C-7

EXCITATION CONDITION FOR PREFERENCE TEST SEQUENCE

	Run Number	Simulator A (Right Side)	Excitation Condition B (Left Side)
S	1	C -	C -
	2	C -	L -
E	3	C +	C +
R	4	C +	C +
I	5	H -	C -
	6	C +	M +
E	7	H +	C +
S	8	C +	H +
	9	C +	L +
1	10	L +	C +
	11	L -	C -
	12	C -	M -
	13	C -	C -
	14	M -	C -
	15	C -	H -
	16	M +	C +
			*
S	17	L +	C +
	18	M +	C +
E	19	C +	M +
R	20	C -	H -
I	21	C -	L -
	22	M -	C -
E	23	C +	L +
S	24	C +	C +
	25	C -	M -
2	26	L -	C -
	27	C -	C -
	28	H +	C +
	29	C +	H +
	30	H -	C -
	31	C +	C +
	32	C -	C -

*Tunnel Modifications were made after the first 16 runs. (see Section C 1.1)

the two series each experimental condition occurred four times. This yielded, for each experimental condition, 12 sets of approximately 180 photographic frames which could be scored for the location of the animals in the apparatus.

4.4 Scoring and Analysis of Preference Test Data

Scoring was performed by personnel who knew the purpose of the experiment but had not been involved in conducting the test. At the time of scoring the data sheets were numbered or labeled only with the run number which was taken from the photographic record of the run. Thus, the personnel responsible for scoring did not know the experimental condition associated with the run.

For scoring, the photographic record of the run was projected with a single frame projector and for each frame the location of each animal was checked as being the left compartment, the right compartment, the center (tunnel) of the apparatus, or indeterminable. The instructions with respect to scoring criteria were as follows:

> "Score an animal as being in the left compartment or right compartment if any part of the body other than the tail can be seen in the compartment."
>
> "If no part of the body other than the tail can be seen in either the left or right compartments and the animal can be seen, score the animal as being in the center compartment."
>
> "If for one or more frames you cannot distinguish the animal from the background sufficiently well to score, check the space in the indeterminable column."

If the record included more than 180 frames for a run, only the first 180 frames were considered. For three runs, the record was short by five or fewer frames and due to problems with focusing during some of the early runs, there were a few frames where the position of one or more animals could not be discriminated and were scored as indeterminable. However, for all animals there were at least 172 scorable frames and for most animals 180 frames could be scored.

After scoring was completed, for each animal the number of frames the animal was scored as being in the center of the apparatus or in the "test" side of the apparatus was summed for 15 min segments (60 frames) and for the entire run (180 frames). For control vs control runs, the "test" side was that side of the apparatus which had been randomly selected as such prior to conducting the tests. For

statistical analyses these counts were converted to percentages using the number of scoreable frames for 15 min segments of the run or for total run as the denominator.

The data were summarized as the average percentage of frames for each group spent in the test side or in the center of the test apparatus. Group means were derived for percentages based on both run segments (15 min or 60 frames) and on total run time. For testing statistical significance of differences in the percentage of time spent in the test side, analysis of variance techniques were applied (Winer, 1962). Where the total run time was considered and polarities analyzed separately, the analysis of variance was a single factor mode. In considering run segments, either a two-factor or three-factor model was applied. The two factor (field-ion levels x run segment) analysis was employed when the data for positive and negative polarities were considered separately. The three factor (polarity x field-ion level x run segment) analysis was employed when both polarities were considered in a single analysis.

5. PREFERENCE TESTING RESULTS AND DISCUSSION

5.1 Physical Data

Table C-8 shows the temperature and relative humidity at the start of each test run. The temperature change during the period of a run, in general, was less than one degree, except for Run 18 in which the recorded temperature decreased 3° from start to finish of the run and Run 20 in which the recorded temperature decreased by 2°. The mean temperature over all runs was 75° F and the relative humidity was 20%.

Figure C-13 shows a typical pen recorder trace of the current density sensed on the 100 cm^2 current probe during one of the preference tests. It will be noted that several rapid changes in current density sensor output level are indicated on the trace. These occurrences, in general, were noted when an animal reared to the vertical position. These changes in current density sensor output are believed to be due to displacement currents which result from rapid fluctuations in the electric field when the animal stands up.

TABLE C-8

TEMPERATURE AND RELATIVE HUMIDITY AT START OF EACH TEST

Test No.	Temperature F°	R.H.
1	76.5	10
2	76.0	12
3	75.0	14
4	75.5	20
5	75.0	20
6	75.0	21
7	77.0	15
8	75.0	20
9	77.0	23
10	76.0	20
11	77.0	22
12	76.0	18
13	76.5	19
14	76.0	20
15	76.0	20
16	75.0	24
17	77.0	33
18	77.0	28
19	74.0	33
20	74.0	31
21	76.0	30
22	73.0	20
23	74.0	18
24	75.0	16
25	75.0	18
26	75.0	16
27	75.0	16
28	75.0	16
29	75.0	16
30	70.5	19
31	71.0	19
32	71.0	20

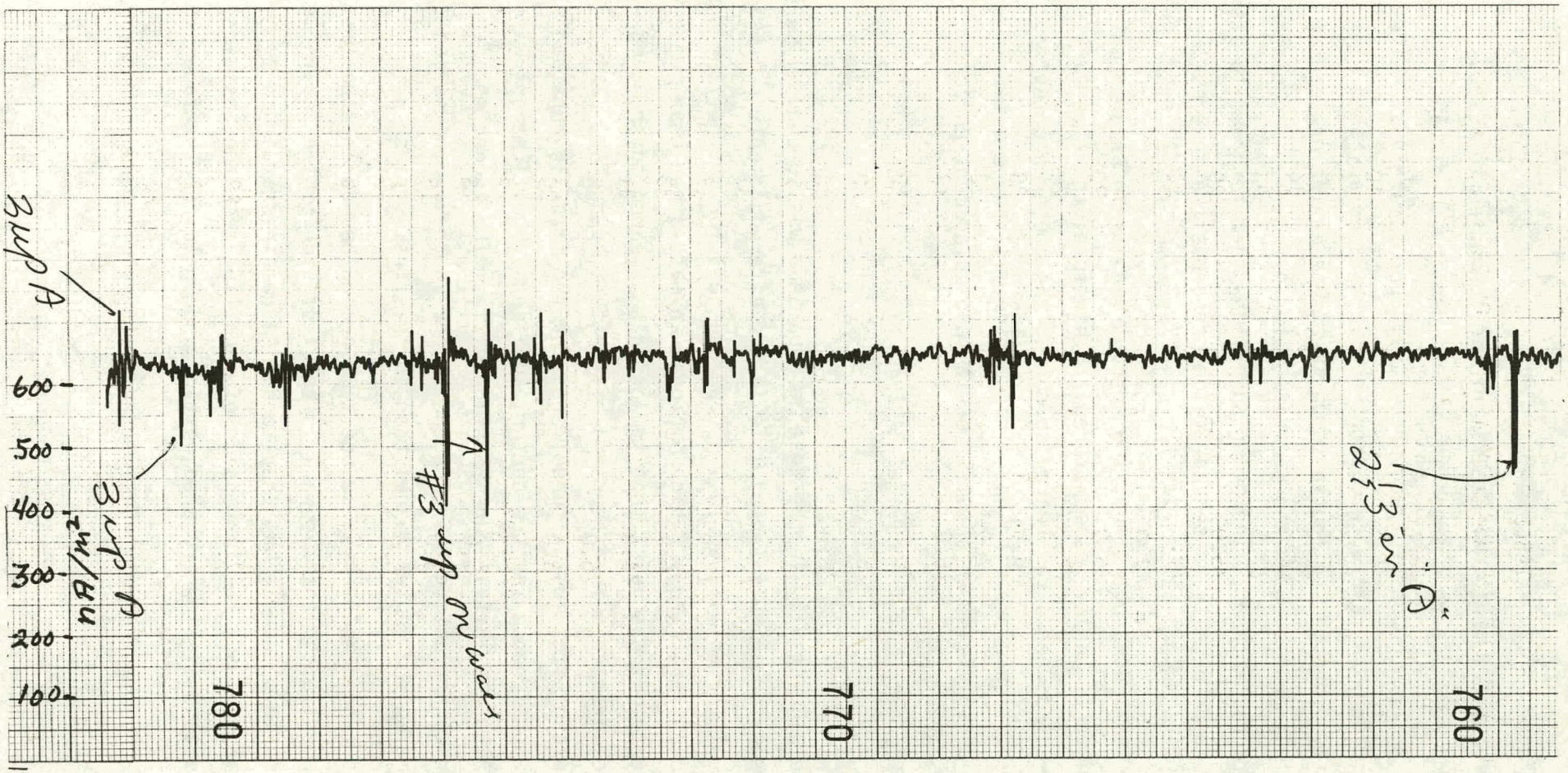

Run #22 61CB on 1 x 10^{-8} Scale
Chart Speed 1 min/cm

Figure C-13 PEN RECORDER TRACE OF ION CURRENT DENSITY FOR REPRESENTATIVE ANIMAL PREFERENCE TEST

After the animal preference tests, an experiment was conducted to assess whether these fluctuations were due to changes in current density or displacement currents. For this test, a copper foil-covered tube, approximately the size of an erect rat was fabricated. A reference current density was established with the 100 cm^2 current density probe in the fourth compartment, as in the preference tests. The power supply was then secured and the "simulated erect rat" was placed in the center of the third compartment. The power supply was then returned to its original setting. The current density as sensed by the probe was the same as before the "simulated rat" had been placed into the adjacent compartment. Thus, the presence of an erect "rat" does not affect the current density in an adjacent compartment (where the current density was monitored). Therefore, the time-varying current which was observed when a rat reared up during the preference tests must have been due to the motion of rearing up. This motion will cause a time-varying change in the electric field, which will result in displacement current being induced into the current probe.

5.2 General Observations

In general, the overall activity in the testing apparatus was somewhat limited but appeared to be greater for animals tested late in the afternoon. After a brief exploratory period many of the animals would lie down and rest for most of the test run. In some of the pretest trial runs (which employed animals other than those included in the experiment), it was noted that the animals appeared to spend more time in the center tunnel area than in either end of the test apparatus. This observation prompted the use of pegs in the tunnel area for the first 16 runs and since this did not abolish the preference for the center, additional modifications were made to the tunnel prior to the last 16 runs (Section C1.1). The second modification was also unsuccessful in counteracting this tendency since in the second series some groups averaged more time in the center tunnel than in the first series.

Many of the animals tended to rear up at one time or another during the test run. When this occurred while the animals were in the test side of the apparatus under the high excitation level condition, they tended to remain standing but a very brief period of time and gave the impression of recoiling from the position. Often such animals would assume a low crouched postion and would rub the face area with its paws.

5.3 Preference Response

Despite the occurrence of behaviors which appeared to observers as a fairly strong indication that rats could detect the presence of the high level field and ion condition, excitation level had no statistically significant effects on the time rats spent in the test side of the preference apparatus. This was true whether the data were analyzed in terms of 15-min run segments (Table C-9, Figure C-14) or in terms of total run time (Table C-10, Figure C-15). Most groups, regardless of polarity or excitation level, tended to decrease the time spent in the test side after the initial 15 min as indicated by the significant F ratios for "run segment" obtained for both polarities (Table C-9b) and in the three factor analysis (Table C-9c). The general pattern was a decrease in time spent in the test side between the first and second run segments and little or no change thereafter. The exceptions to this pattern were groups tested at low levels of field and ions. At this level animals tested at a positive polarity, decreased, then increased the time spent in the test side, whereas with a negative polarity, no change was observed until the third segment.

Considering the total run time (Figure C-15), it should be noted that when percent time spent in the test side of the apparatus was plotted as a function of the field strength, positive and negative polarities yielded very similarly shaped curves. Faced with a lack of statistical significance we do not wish to place too much emphasis on this similarity, however, it it possible that these curves are illustrative of a trend that might be statistically demonstratable with larger group sizes or repeated testing of the same groups of animals over several days.

The tendency to decrease time in the test side of the apparatus over run segments was also reflected in an increase in the time spent in the center tunnel. This in fact appeared to be the preferred location after the first few minutes of the run. This tendency was noted during the conduct of the experiment. The basis for this preference is not clear. Several possibilities exist. The center compartment was shorter than the end compartments and rodents generally prefer smaller, more snug areas. Alternatively, the audible noise associated with corona generation or the direct air input in the end compartments may have been contributing factors. It might be noted, however, that the 35 cfm rate of air flow was not perceptible to an experimenter with his hand held in the animal exposure area.

Table C-9a

PERCENT FRAMES SPENT IN THE "TEST" SIDE OF PREFERENCE APPARATUS FOR 15-MIN RUN SEGMENTS (GROUP MEANS ± STANDARD DEVIATION)

Excitation Level of Test Side	Negative Polarity Run Segment 1 Mean+SD	2 Mean+SD	3 Mean+SD	Positive Polarity Run Segment 1 Mean+SD	2 Mean+SD	3 Mean+SD
Control	28±26	21±30	15±26	29±32	15±28	11±25
Low	30±32	31±40	25±36	29±30	18±27	31±43
Middle	33±30	25±30	20±29	28±27	18±31	18±29
High	26±30	14±29	10±28	16±17	3±5	4±7

Table C-9b

ANALYSIS OF VARIANCE TABLES FOR TWO FACTOR ANALYSES

Source of Variation	Negative Polarity Sums of Squares	df	Mean Square	F	Positive Polarity Sums of Squares	df	Mean Square	F
Between Ss	108712	47			84787	47		
A (Excitation Level)	2905	3	968	0.40	6707	3	2236	1.26
Ss within groups	105807	44	2405		78080	44	1775	
Within Ss	23153	96			24087	96		
B (Run Segment)	3378	2	1689	7.78*	3878	2	1939	9.07*
AB	636	6	106	0.45	1350	6	225	1.05
B x Ss within groups	19139	88	217		18859	88	214	

Table C-9c

ANALYSIS OF VARIANCE TABLE FOR THREE FACTOR ANALYSIS

Source of Variation	Sums of Squares	df	Mean Square	F
Between Ss	195128	95		
A (Polarity)	1629	1	1629	
B (Excitation Level)	9097	3	3032	1.45
AB	515	3	172	0.08
Ss within groups	183887	88	2090	
Within Ss	47240	192		
C (Run Segment)	6419	2	3210	14.86*
AC	837	2	419	1.94
BC	1470	6	245	1.13
ABC	516	6	86	0.40
C x Ss within groups	37998	176	216	

*p<.05

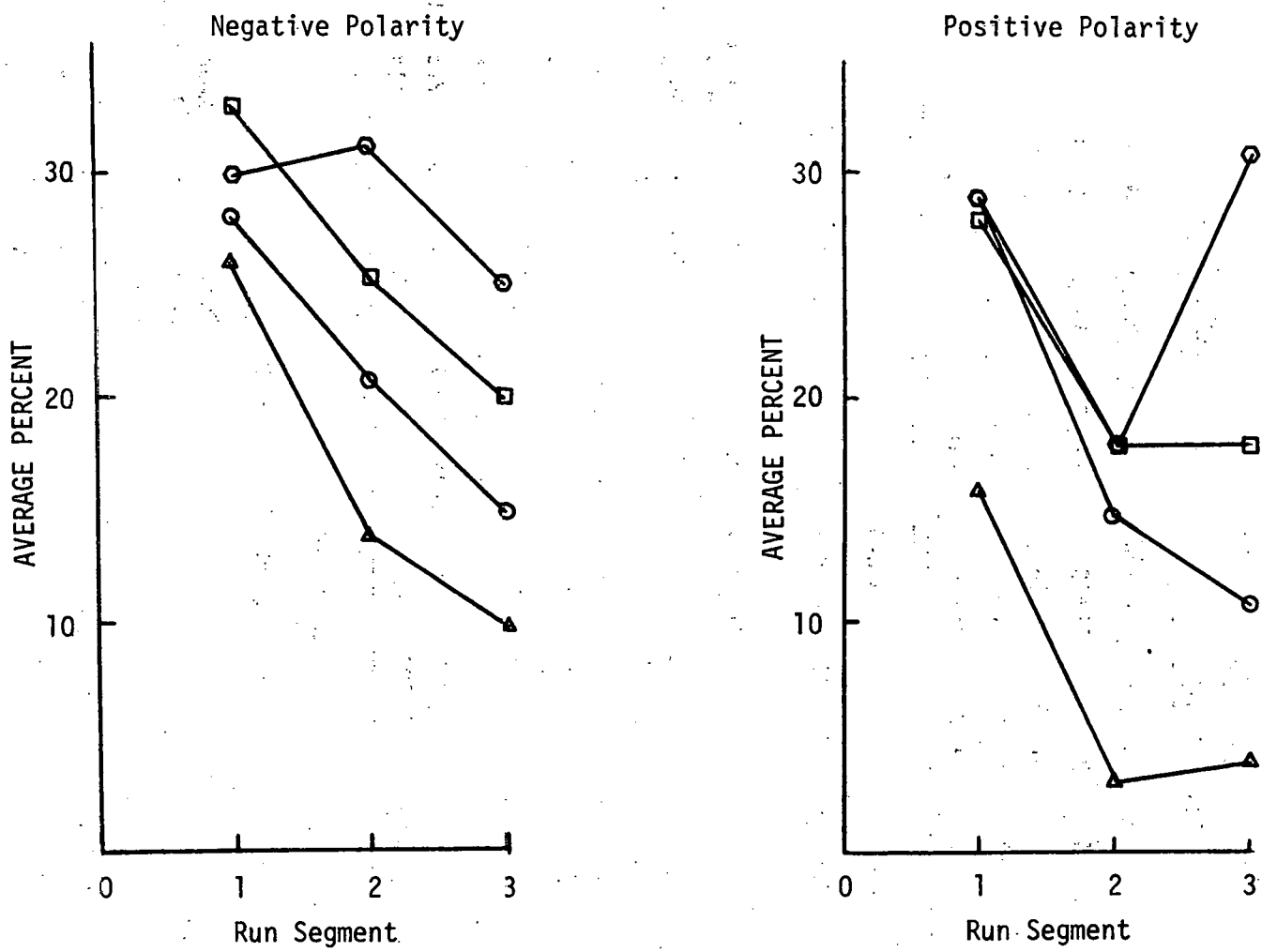

Fig. C-14 Average Percent Frames Spent in the Test Side of Preference Apparatus for 15-min Run Segments

Legend: O-Control, ○-Low Excitation Level, □- Middle Excitation Level, Δ-High Excitation Level

Table C-10a

PERCENT TIME SPENT IN THE TEST SIDE OF PREFERENCE APPARATUS FOR THE TOTAL RUN TIME (GROUP MEANS ± STANDARD DEVIATION)

Excitation Level	Negative Polarity Mean ± SD	Positive Polarity Mean ± SD
Control	21±21	19±26
Low	29±36	26±28
Middle	26±27	21±29
High	17±27	8±8

Table C-10b

SINGLE FACTOR ANALYSIS OF VARIANCE TABLE

Source of Variation	Negative Polarity Sums of Squares	df	Mean Square	F	Positive Polarity Sums of Squares	df	Mean Square	F
Excitation Level	990	3	330	0.41	2201	3	734	1.24
Error	35301	44	802		26060	44	592	

Table C-10c

TWO FACTOR ANALYSIS OF VARIANCE TABLE

Source of Variation	Sums of Squares	df	Mean Square	F
A (Polarity	552	1	552	0.79
B (Excitation Level)	3021	3	1007	1.44
AB	170	3	57	0.08
Error	61362	88	697	

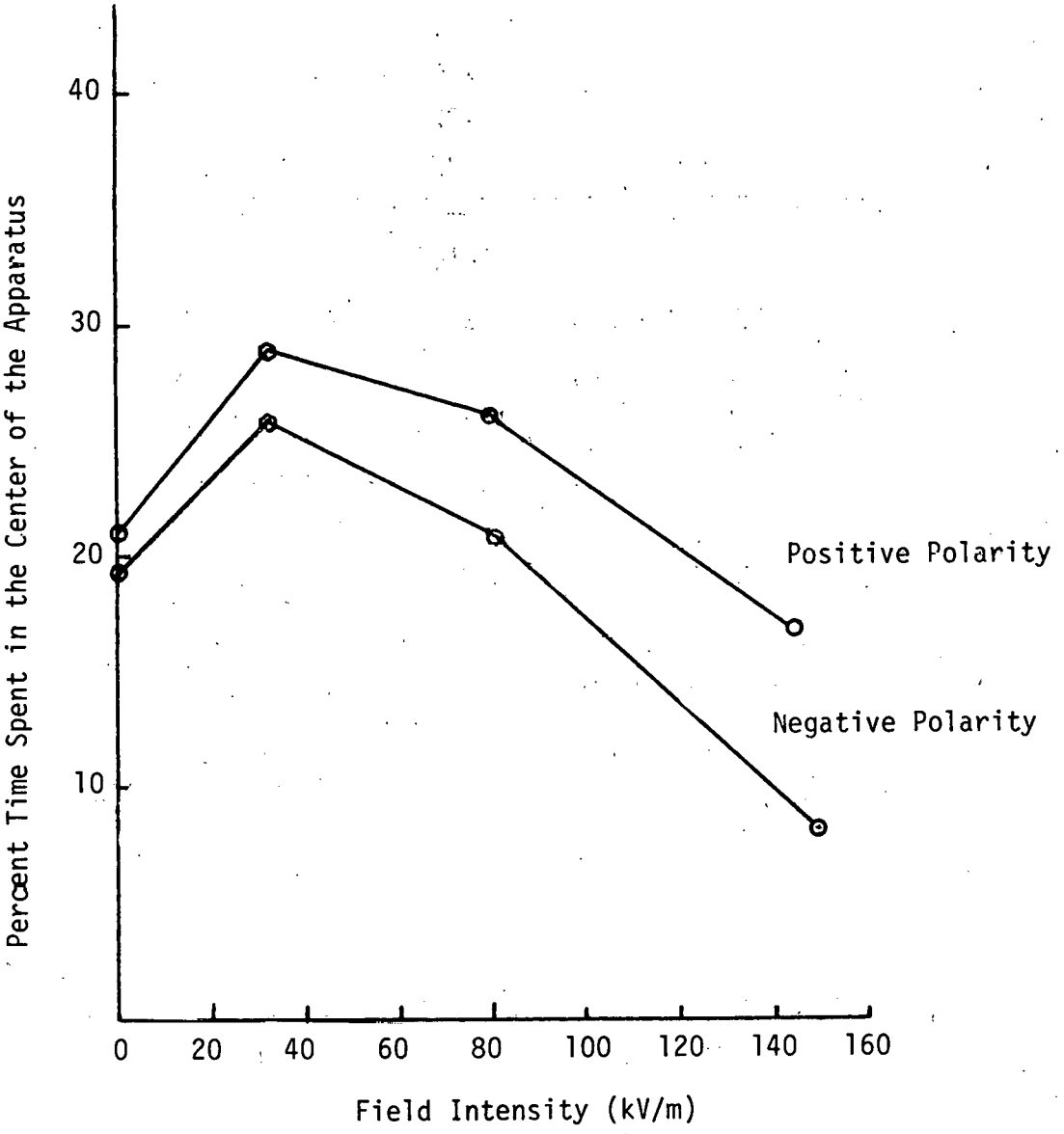

Fig. C-15 Percent Time (frames) Rats Were in the Center of the Test Apparatus for the Total Run Time.

For groups tested at a positive polarity, excitation level was a significant factor in determining the preference for the center of the apparatus (Table C-11b). However, this was not a straight forward relationship. The graphs of these data indicate that animals tested at the highest excitation level spent the most time in the center of the apparatus and the least amount of time was by animals in the middle excitation level group (Figure C-16). The Neuman-Keuls procedure for comparing pairs of means was applied to the six possible comparisons of excitation levels averaged across run segments (Winer, 1962, Table C-11c). Only the high excitation and middle excitation levels were significantly different from each other and none of the excitation levels differed significantly from controls.

To summarize, the preference experiment yielded no strong statistical support for an interpretation that rats preferred or avoided the field and ion experimental conditions. Observational data suggested that when standing erect rats could perceive the high excitation level condition but this has not been documented on an animal by animal basis. There appeared to be trends suggesting that at the low and middle excitation levels, rats were more likely to remain in the test side of the apparatus than they were at the high excitation level or under control conditions. This is suggested in the similarly-shaped curves obtained for positive and negative polarities for time spent in the test side as a function of field strength (Fig. C-15) and in the significant difference obtained for excitation level in the amount of time spent in the center of the test apparatus (Table C-11b). However, considering the high within group variability seen through the study, at best this should be accepted as a working hypothesis and not as a firm conclusion.

We think the procedures developed for preference testing are in general workable but could be improved by certain revisions or additions. These would include further attempts to reduce the bias toward the center compartment which may be even stronger than indicated due to the use of scoring criteria which operated against detecting this bias. These attempts could perhaps include expansion of the center tunnel to the same size as the end compartments, enclosing the end walls of the apparatus with an opaque material to reduce the greater feeling of spaciousness in the end compartment, and/or providing an air flow comparable to that in the end compartments in the center tunne. Other revisions or additions to the testing procedure might include the use of younger animals, testing of both sexes, an

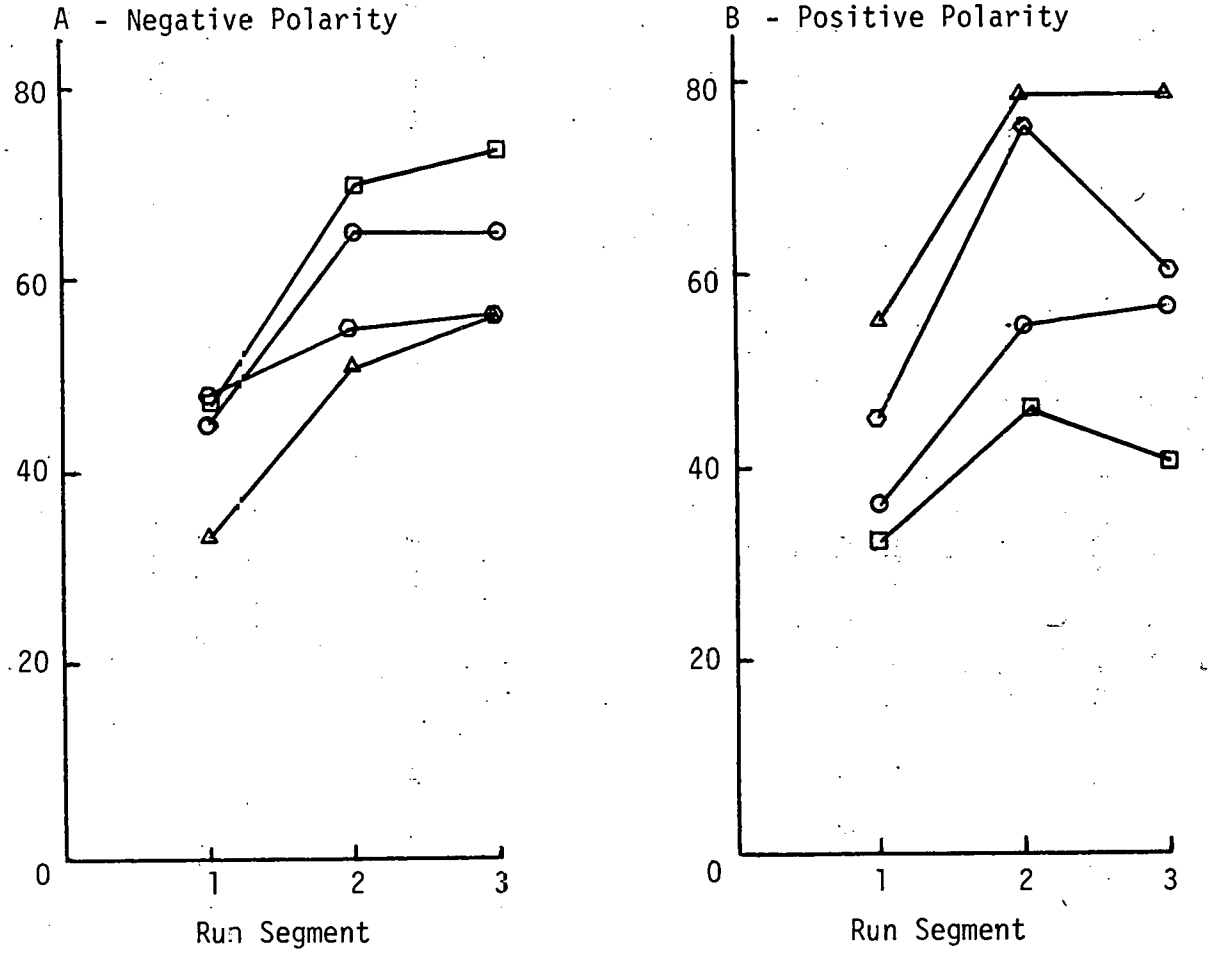

Fig. C-16 Average Percent Frames Spent in the Center of Preference Apparatus for 15-min Run Segments

Legend: O-control, ○ -Low Excitation Level, □-Middle Excitation Level, Δ High Excitation Level

TABLE C-11a

PERCENT FRAMES SPENT IN THE CENTER OF PREFERENCE APPARATUS FOR 15-MIN RUN SEGMENTS (GROUP MEANS ± STANDARD DEVIATION)

Excitation Level of Test Side	Negative Polarity Run Segment 1 Mean±SD	Negative Polarity Run Segment 2 Mean±SD	Negative Polarity Run Segment 3 Mean±SD	Positive Polarity Run Segment 1 Mean±SD	Positive Polarity Run Segment 2 Mean±SD	Positive Polarity Run Segment 3 Mean±SD
Control	46±25	65±34	65±39	37±25	55±39	57±40
Low	48±35	55±40	57±39	45±23	75±27	60±37
Middle	47±20	69±30	73±27	33±16	46±40	41±37
High	34±30	52±41	57±49	56±26	78±31	78±35

TABLE C-11b

ANALYSIS OF VARIANCE TABLE

Source of Variation	Negative Polarity Sums of Squares	df	Mean Square	F	Positive Polarity Sums of Squares	df	Mean Square	F
Between Ss	85606	47			82935	47		
A (Excitation Level)	4721	3	1574	0.86	18936	3	6312	4.34*
Ss within groups	80885	44	1838		63999	44	1455	
Within Ss	92591	96			86703	96		
B (Run Segment)	10470	2	5235	5.70*	11150	2	5575	6.65*
AB	80792	88	918		1713	6	286	0.34
B x Ss within groups					73840	88	839	

TABLE C-11c

TABLE OF ORDERED MEANS AND DIFFERENCES FOR NEWMAN-KEULS COMPARISONS OF PAIRS OF MEANS FOR FACTOR A (EXCITATION LEVEL)

Excitation Level	Middle	Control	Low	High
	Means (Averaged Across Run Segments)			
	40	50	60	71
	Differences Between Means			
Middle	--	10	20	30*
Control	--	--	10	20
Low	--	--	--	11

*p<.05

increase in group size, and repeated testing of the same animals. With respect to the latter, it may be easier to detect a preference once the initial exploratory activity has habituated, by testing the same animal over several days at different excitation levels. This would of course still require that some means of reducing the preference for the center tunnel be effected.

Finally, to fully document the observation of detection of the test condition when the rat is in the erect position, we would suggest video monitoring thoughout each test run and recording each time an animal stands erect the nature of the behavior that follows.

*U S GOVERNMENT PRINTING OFFICE: 1980 341-060/325

United States
Department of Energy
Washington, D.C. 20585